THE METABOLOMIC RESPONSE TO SEVERE THERMAL INJURY AND THE IMPACT OF AGE

By

CHRISTOPHER MICHAEL FRANCIS WEARN

A thesis submitted to

The University of Birmingham

for the degree of

DOCTOR OF PHILOSOPHY

Institute of Inflammation and Ageing
College of Medical and Dental Sciences
University of Birmingham
August 2017

Abstract

Severe thermal injury results in a profound hypermetabolic response and is associated with increased morbidity, mortality and delayed rehabilitation of burn survivors. Serum ^{1}H-NMR metabolomics was used to examine early global metabolic changes in the response to severe thermal injury (>15% TBSA) in young adults (16-64 years) and older adults (<15% TBSA). Early changes in the metabolome reflected hypoxic metabolism, hyperglycaemia, increased ketogenesis, peripheral lipolysis and increased energy production in both cohorts. Early metabolic profiles from the young adult group were used to construct OPLSDA models that could discriminate with high accuracy between outcome groups. Models from 0-24hrs serum samples predicted survival (AUC 0.92), whilst models from 24-96hrs samples predicted Multiple organ failure (MOF) (AUC 0.92) and sepsis (AUC 0.89). Untargeted LC-MS metabolomics was applied to study the longitudinal changes in the serum metabolome after severe thermal injury in 13 young adults, from admission until 6-months post-injury. Univariate ANOVA analysis revealed significant changes in 432 metabolite features, affecting 35 distinct classes, representing global metabolic disturbance. Changes in 300 lipid metabolite features may represent a 'lipid storm' in serum after severe thermal injury. Novel areas of metabolism and metabolites were identified as putative biomarkers warranting further targeted study.

Acknowledgments

Firstly, I'm extremely grateful for all financial support received during the project from Queen Elizabeth Hospital Birmingham, The Scar Free Foundation Charity and the Royal College of Surgeons of England for a one year Research Fellowship grant allowing to me complete a third year of research.

I'd like to thank every member of staff within the Birmingham Scar Free Foundation Burns Research Centre who helped design, set-up and run the SIFTI study. Thank you to all the research nurses in the Burns and Trauma research teams who worked tirelessly collecting samples and data over the 3 years of the study, including Amy Bamford, Sarah Reavenall and Sarah Ryles. Amy, thanks for working so hard and for putting up with me for 3-years and the pain of those CRF booklets. Thank you to our collaborating teams at Birmingham Children's Hospital (Miss Yvonne Wilson, Sister Clare Thomas, Lisa Charles, Sarah Payne, Federica D'Asta), St Andrew's Burns Centre in Chelmsford (Professor Peter Dziewulski and Helen Gerrish) and at the McIndoe Burns Centre, Queen Victoria Hospital in East Grinstead (Mr. Baljit Dheansa and Simon Booth). SIFTI certainly opened my eyes to the challenges and rewards that can be found in collaborating across the country. This is certainly a positive way forward for Burn care research in the UK.

My supervisors, Professor Janet Lord and Professor Naiem Moiemen, have inspired me in their respective fields and encouraged me a few years ago to progress my MD project into a PhD. They have mentored and advised me all along the way, thank you. Dr. Warwick Dunn and Dr. Stephen Young have been fantastic in helping to

design and run the metabolomics experiments, I am also grateful to you both for all the many data analysis tutorials. Thank you Ricardo Di Guida and Dr. William Allwood in Dr Dunn's research group who were fantastic in helping to prepare samples and running the LCMS analyses. Thanks to Dr Martin Fitzpatrick (Young Group) for the NMR analysis tutorials.

Thanks also to Dr. Paul Harrison for those 'post-it note' ideas discussions. For all your help in the lab and for being such an entertaining group - Hema Chahal, Hannah Smith, Dr. Jon Hazeldine, Dr. Peter Hampson, Robert Dinsdale and Dr. Ashleigh Philp.

Most importantly of all, thank you to all the injured patients and their families at all four research centres who agreed to take part in the research and willingly attended hospital for study visits long after discharge. Without your participation, none of this research would have been possible.

To my wife, Rowan and daughters Isabelle and Rose.
Thank you for all your help, support and positivity that kept me going through the difficult times.

Contents

List of Figures

List of tables

List of abbreviations

2-HB	2-Hydroxybutyrate
3-HB	3-Hydroxybutyrate
3-HPPA	3-(3-Hydroxyphenyl)-3-hydroxypropanoic acid
ABA	American Burn Association
ABSI	Acute Burn Severity Index
ACCP	American College of Critical Care Physicians
ACTH	Adrenocorticotrophic hormone
ADH	Anti-diuretic hormone
AF	Atrial fibrillation
ALI	Acute lung injury
ANS	Autonomic nervous system
APACHE II Score	Acute Physiology and Chronic Health Evaluation II Score
APCI	Atmospheric pressure chemical ionisation
ATP	Adenosine triphosphate
AUROC	Area under the receiver operating characteristic curve
AVP	Arginine vasopression
BMR	Basal metabolic rate
BOBI	Belgian Outcomes in Burns Index
BP	Blood pressure
BSEP	Bile-salt export pump
BSI	Blood stream infection
CARS	Counter anti-inflammatory response syndrome
CCI	Chronic critical illness
CE	Capillary electrophoresis
CID	Collision induced dissociation
CLP	Caecal ligation and puncture
CNS	Central nervous system
CoA	Coenzyme-A
COP	Colloid osmotic pressure
COPD	Chronic obstructive pulmonary disease

COX	Cyclo-oxygenase
CRF	Case report form
CRH	Corticotrophin releasing hormone
CSHA	Canadian Study of Health and Ageing
CTL	Cytotoxic T-lymphocyte
CVP	Central venous pressure
CVVH	Continous veno-venous haemofiltration
DAG	Diacylglycerol
DAMPs	Damage associated molecular patterns
DG	Diacylglycerols
DHA	Docosahexaenoic acid
DHEA	Dehydroepiandrosterone
DHEAS	Dehydroepiandrosterone sulfate
DM	Diabetes mellitus
$DMSO_2$	Dimethyl sulfone
dsDNA	Double-stranded DNA
DTH	Delayed type hypersensitivity
EPA	Eicosopentanoic acid
ESI	Electrospray ionisation
ETC	Electron transport chain
FA	Fatty acyls
FDR	False discovery rate
FFA	Free fatty acid
FID	Free induction decay
FT	Fourier transformation
FT-ICR	Fourier transform ion-cyclotron resonance
G-CSF	Granulocyte colony stimulating factor
GC	Gas chromatography
GL	Glycerolipids
GP	Glycerophospholipids
HAS	Human albumin solution
HDAC	Histone deacetylase

HDU	High-dependency unit
HDU	High-dependency unit
HES	Hospital Episode Statistics
HILIC	Hydrophilic interaction liquid chromatography
HIV	Human Immunodeficiency Virus
HLA-DR	Human leukocyte antigen-antigen D related
HMDB	Human metabolome database
HMR	Hypermetabolic response
HO-1	Heme-oxygenase-1
HPA	Hypothalamic-pituitary adrenal axis
HSL	Hormone sensitive lipase
HTG	Hepatic triglyceride
HTN	Hypertension
IBID	International Burn Injury Database
ICU	Intensive Care Unit
IDO	indoleamine 2,3-dioxygenase
IFN-λ	Interferon-gamma
IGF-1	Insulin-like growth factor-1
IGFBP-3	Insulin-like growth factor binding-protein-3
IHD	Ischaemic heart disease
IL	Interleukin
IL-1RA	Interleukin-1 receptor antagonist
IMCL	Intramyocellular lipids
IP3	D-myo-inositol-1,2,6-triphosphate
IQR	Interquartile range
IRS-1	Insulin receptor substrate-1
KNN	*k*-nearest neighbours algorithm
LA_{50}	Lethal Area 50
LBM	Lean body mass
LC	Liquid chromatography
LFT	Liver function test
LMWH	Low-molecular weight heparin

LOS	Length of stay
LOX	Lipo-oxygenase
LPS	Lipopolysaccharide
LT	Leukotriene
LV	Latent variable
LX	Lipoxin
LysoP	Lysoglycerophospholipids
MALT	Mucosal associated lymphoid tissue
MAP	Mean arterial pressure
MCP-1	Monocyte chemoattractant protein – 1
MDT	Multi-disciplinary Team
MG	Monoacylglycerols
MMA	Methylmalonate
MMP	Matrix metalloproteinase
MODS	Multiple organ dysfunction syndrome
MOF	Multiple organ failure
mRNA	Messenger RNA
MRP-3	Multi-drug resistance associated protein-3
MS	Mass spectrometry
mtDNA	Mitochondrial DNA
MUFA	Monounsaturated fatty acid
MWCO	Molecular weight cut-off
NAA	Non-essential amino acid
NADH	Nicotinamide adenine dinucleotide
NADPH	Nicotinamide adenine dinucleotide phosphate
NBR	National Burn Repository (US)
NETs	Neutrophil Extracellular Traps
NK-cell	Natural killer cell
NMR	Nuclear magnetic resonance
NMR	Nuclear magnetic resonance
NO	Nitric oxide
NOESY	Nuclear Overhauser Effect Spectroscopy

NPV	Negative predictive value
OFA	Oxidized fatty acid
OGTT	Oral glucose tolerance test
OPLSDA	Orthogonal partial least squares discriminant analysis
PA	Glycerophosphates
PAF	Platelet activating factor
PAMPs	Pathogen associated molecular patterns
PC	Principle component
PC	Glycerophosphocholines
PCA	Principle components analysis
PE	Glycerophosphoethanolamines
PGC-1β	PPARλ coactivator 1β
PGE	Prostagandin-E
PGP	Glycerophosphoglycerols
PI	Glycerophosphoinositols
PICS	Persistent inflammation immunosuppression catabolism syndrome
PLSDA	Partial least squares discriminant analysis
PPAR	Peroxisome proliferator-activated receptor
PPM	Parts per million
PPV	Positive predictive value
PQN	Probabilistic Quotient Normalisation
PR	Prenol lipids
PRR	Pattern recognition receptor
PS	Glycerophosphoserines
PUFA	Polyunsaturated fatty acid
QC	Quality control
QEHB	Queen Elizabeth Hospital Birmingham
QQQ	Triple quadrupole
REE	Resting energy expenditure
RF	Radiofrequency
rHGH	Recombinant Human Growth Hormone

ROC	Receiver operator characteristic
ROS	Reactive oxygen species
RPLC	Reverse phase liquid chromatography
RSD	Relative standard deviation
RT	Retention time
SAM	Sympathetic-adrenal-medullary
SCCM	Society of Critical Care Medicine
SFA	Saturated fatty acid
SIFTI	Scientific Investigation of biological pathways Following Thermal Injury
SIRS	Systemic inflammatory response syndrome
SMR	Standard metabolic rate
SNS	Sympathetic nervous system
SOFA	Sequential organ failure assessment score
SP	Sphingolipids
SPM	Specialised pro-resolving mediator
SSD	Silver sulfadiazine
ST	Sterol lipids
SVD	Singular value decomposition
TAG	Triacylgylcerol
TBSA	Total Body Surface Area
TCA	Tri-carboxylic acid
TG	Triglyceride
TG	Triacylglycerols
Th	T-helper cell
TLR	Toll-like receptor
TMSP	2,2,3,3-tetradeuteropropionic acid
TNF	Tumour necrosis factor
TOBSY	Total through bond correlation spectroscopy
TOF	Time-of-flight
TPR	Total peripheral resistance
TTR	Time-to organ Recovery

TX	Thromboxane
UHPLC	Ultra-high performance liquid chromatography
UTI	Urinary tract infection
UUN	Urinary urea nitrogen
VIP	Variable importance projection
VLDL	Very low-density lipoprotein

Chapter 1: Introduction

Chapter 1: Introduction

1.1 Epidemiology

Burn injury is one of the most devastating forms of trauma, which has long lasting physical, psychological and social consequences for victims. Worldwide burn injury remains a significant problem, with 11 million people sustaining burns severe enough to seek medical attention annually and the incidence is ranked 4th among all injuries, higher than the combined incidence of TB and HIV infection (1). Data from the World Health Organisation (WHO) suggests that burn injuries result in 195,000 deaths globally each year (WHO burns factsheet 2012). In the UK, an estimated 175,000 people attend emergency departments annually for burn injures (2) and data from the National Hospital Episode Statistics database (HES) suggests the annual admission rate has continued to increase since 2002 with over 11,000 admissions in 2010 (3).

The age groups at highest risk for sustaining a thermal injury are the very young and the very old. A recent study of UK hospital admissions has shown that the <5-year olds and ≥85 year olds experience the highest incidence of burn injury (figure 1) (3). The higher susceptibility of young children to burns is related to their inquisitiveness, lack of appreciation of danger and decreased ability to escape from it (4). In the UK and Europe, just under half of all patients admitted with severe burn injury are children and children under the age of 5 years account for 50-80% of all childhood burns (2,5).

Another high-risk group for burn injury is the elderly population, defined as people aged 65 years and above. The elderly are more susceptible to sustaining burns and injury than younger adults due to increased frailty, visual impairment, age-related

deteriorations in judgment and co-ordination and changes in cognition and balance (1). Improvements in medicine over the last half-century have resulted in an increase in the average life span in the western world of 30 years. This is reflected in the increasing proportions of elderly people sustaining burn injuries; a recent analysis of the US National burn repository showed a rise in the number of patients admitted with burns over the age of 55 years from 11.2% in 1991 to 15.4% in 2003 (6). Similarly in Europe, the proportion of patients with severe burns that are elderly has increased from 10 to 16% (5).

In terms of aetiology, flame burns account for almost 60% of injuries followed by scalds and then contact burns in Europe (5). Data from the US National Burn Repository (NBR) mirrors this pattern with flame burns accounting for 44% of admissions, Scalds 33% and contact 9% (7). Electrical, chemical and radiation burns are less common. The aetiology pattern does vary with age group and in the paediatric population, scalds predominate accounting for 60-75% of burn admissions (7). In the elderly, flame burns are most common followed by scalds and the majority of injuries occur in the home (55.6%) (6). This is in contrast to younger adults, where burns are usually sustained due to work related incidents or activities outside of the home (8). Overall, there is a male preponderance in burn admissions; in the USA 70% of burn related admissions are male (7). In the UK, the incidence of burns is higher in males than females in all age groups except the 5-9 year olds and the ≥85 year olds (3).

1.2 Outcomes and complications

Outcomes following burn injury can be divided into short term outcomes, those that are important during hospitalization and longer term outcomes which impact on the burn survivors quality of life and functioning in society once discharged from hospital. Historically burn injury was associated with very poor outcomes and many patients succumbed to shock from the initial injury and those that survived this died later from infectious complications and sepsis (9). Fortunately, outcomes following severe burns have improved in recent decades (Figure 1) due to a combination of advances in critical care medicine, early burn wound excision and coverage, blood conserving surgery and creation of dedicated burn multi-disciplinary teams (MDT) (10). In the western world, children with burns to >95% of their total body surface area (TBSA) survive over 50% of the time (11).

1.2.1 Mortality

Mortality is now a less relevant outcome following burns in children, however it remains an important outcome in adults with major burns (>20% TBSA) and the elderly burn patient regardless of burn size (Figure 1). There are three major influencing factors on burn mortality: age, total burn size (TBSA %) and the presence of inhalation injury (Ryan et al., 1998, Klein et al., 2014). Indeed, many composite mortality prediction models include these as variables (Tobiasen 1982; Ryan et al., 1998; Belgian Outcomes in Burn Injury Study Group 2009). It has been demonstrated that there is a gradual monotonic effect of age on burn mortality until the age of approximately 50 years with an inflection point somewhere between 50 and 60 years (12). In the same study looking at outcomes in the Glue grant consortium cohort and

National Burn Repository data, there is a monotonic effect of burn size on mortality until a TBSA of 70% is reached (12). At the Birmingham Burn Centre there is a long history of analyzing and publishing burn mortality data since the 1940's when J.P. Bull first developed the calculation of the lethal area 50 (LA_{50}) approach using probit analysis (13). The LA_{50} is the burn size (TBSA %) at which there is a 50% mortality rate. The most recent publication shows the continuing improvements in the LA_{50} over the last 65 years of burn treatment in Birmingham (14).

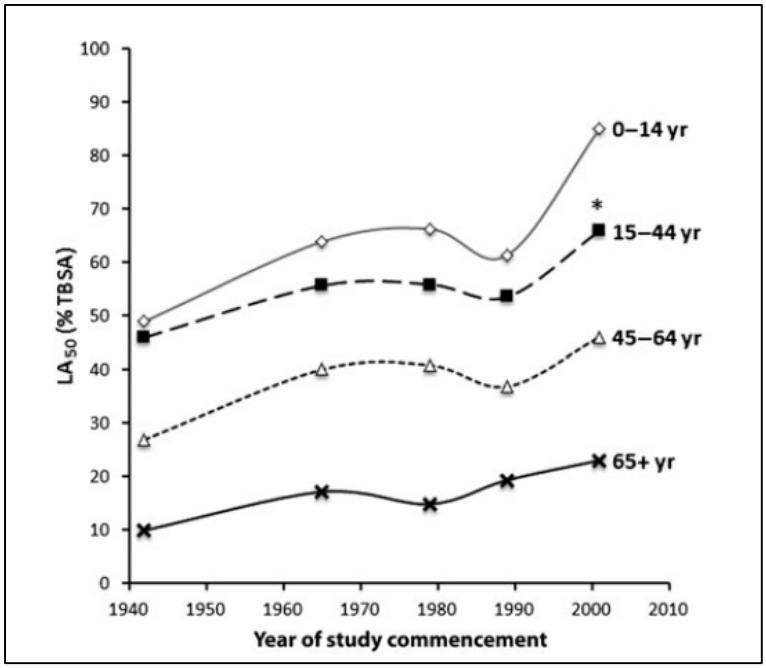

Figure 11-1. Plot of the lethal area 50 (LA50) for 4 different age groups treated at the Birmingham Burns Centre 1940-2010 (Taken from **(14)**

As can be seen in figure 1, the LA_{50} demonstrates an inverse relationship with age ranging from the children with an LA_{50} of 85.1% to the elderly with an LA_{50} of 23.1%. Another important finding of this study was that survival gains were found to be least in the elderly group, as can be seen by the relatively small change in LA_{50} over the last 70 years.

1.2.2 Length of stay (LOS)

The continual improvements in burn survival have led to a shift in focus towards other outcome measures and length of stay (LOS) is an important and easy to measure short term outcome that can be used to compare burns services. The LOS gives an indirect measure of morbidity and complications and has been shown to correlate with aesthetic and functional outcomes as well as the healthcare costs (15). A recent systematic review highlights that age and TBSA are the strongest predictors of LOS so must be taken into account in risk adjustment (15). It has been highlighted that the total LOS is a poor measure of resource utilization and that the LOS in specific levels of care (Intensive care unit (ICU), high dependency unit (HDU) or ward) allows better estimation of resource consumption (16).

1.2.3 Infection and sepsis

The skin forms an important physical and immunological barrier to potential invading micro-organisms and a burn injury represents a complete loss of skin epidermal integrity and consequently patients with burn injury are susceptible to wound colonisation with bacteria and fungi. This colonisation, in the presence of the avascular burn eschar, puts burn injured patients at high risk of wound infection (17). In addition, there is disruption of normal gut barrier integrity, facilitating translocation of bacteria and absorption of bacterial endotoxin (18). This together with the host of documented defects in innate and adaptive cellular immunity post-burn, means that the severely injured burn patient is highly susceptible to infections which increase mortality and morbidity and prolong recovery and hospitalisation. Patients with severe burn injury are susceptible to a whole host of nosocomial acquired infections

including wound infection, pneumonia, blood stream infection (BSI), urinary tract infection (UTI) and vascular catheter related bloodstream infections. The most recent prospective data from the US Glue grant cohort of adults and children with burns >20% TBSA demonstrates the very high incidence of nosocomial infections after severe burn. In this study, 71% of the adult cohort and 68% of the paediatric cohort experienced nosocomial infections and burn wound infection was the commonest cause in each group (19) (table 1.1).

	Adults (n = 300)	**Children (n = 241)**
All nosocomial infections (%)	70.7	67.6
Wound infection (%)	52.3	93.8
Pneumonia (%)	47.7	10.4
Blood-stream infection (%)	28.3	15.8
Sepsis (%)	10.3	2.9

Table 11-1. Incidence of nosocomial infections and sepsis in adult and paediatric cohorts of the US glue grant Host Response to Injury Study. Data adapted from **(19)**.

Sepsis is the deleterious host response to infection and may lead to septic shock, multiple organ failure (MOF) and death. A systematic review of epidemiology studies of burn injured patients has highlighted that there is higher incidence of sepsis in cohorts of burn intensive care patients (28-51%) as compared to cohorts of non-burn trauma patients and other populations of intensive care patients. The same study also showed that the mortality rate from sepsis is higher in cohorts of burn injured patients compared to these other groups, ranging from 28-65% (20). In a study of autopsy reports from 144 burned children a shift was seen in leading cause of death from respiratory failure in the 1990's to sepsis in the 2000's, with 54% of deaths

being due to sepsis (21). In a UK study of autopsy reports, the leading cause of death was MOF with 54% of these cases being secondary to sepsis (22).

One of the major challenges in the field of sepsis research is defining the condition with either clinical or laboratory parameters. The ACCP/SCCM sepsis definitions are the most widely used internationally and are based on the systemic inflammatory response syndrome criteria (SIRS) (Table 3) and have been recently updated (23). These criteria are however, not especially useful in patients with severe burns since many patients will persistently meet the SIRS criteria due to their hyperdynamic circulation and hyperthermia related to their endocrine stress response. To try to tackle this issue, a group of US burn physicians from the American Burn Association (ABA) met in 2007 and developed a consensus group of sepsis trigger criteria which included 6 items and higher threshold values for temperature and heart rate (table 2). One retrospective analysis evaluated the diagnostic utility of these criteria and found that devised scoring system was poorly predictive of bacteremia as a surrogate marker of sepsis (24). This led the group to develop their own modified sepsis trigger criteria which outperformed the ABA trigger criteria, again in terms of predicting bacteremia (AUROC 0.775 vs. 0.619) (25). The importance in being able to recognize sepsis earlier is earlier treatment and therefore improved outcomes. A large multi-centre study of patients with septic shock demonstrated the importance of early recognition, with decrease in survival rate by 7.6% for every hour delay in administering antibiotics (26).

1.2.4 Multiple organ failure (MOF) / Multiple organ dysfunction syndrome (MODS)

Multiple organ failure (MOF) or Multiple organ dysfunction syndrome (MODS) is clinically defined as when two or more organs fail either in parallel or sequentially. The terms MOF and MODS are often used interchangeably in the critical care literature; although the term MODS has been recommended by the ACCP/SCCM, this has not been universally accepted. MOF was a syndrome that emerged in the 1970's as advances in critical care medicine meant patients began to survive single organ failure. It was initially studied as a final common pathway to death in association with sepsis but it became clear in the 1980's that it occurring following trauma and surgery in the absence of infection (27). A number of theories as to the underlying pathophysiology of MOF have been proposed including: gut barrier dysfunction and bacterial translocation (28), flow-dependent oxygen consumption (29) and the two-hit hypothesis of initial inflammatory hits priming the immune system for subsequent development of late systemic inflammation and MOF (30) (see section 1.4.1). During the 1990's, post-injury MOF was found to display a bimodal phenomenon with >60% of MOF occurring as a late onset rather than early post-injury, but recent studies suggest this late peak has disappeared (31).

A number of scoring systems have been developed to quantify the severity of MOF including the Marshall MODS score (32), the Denver Post-injury multiple organ failure score (33) and the Sequential Organ Failure Assessment (SOFA) score (34). The Marshall and SOFA scores ascribe scores to 6 organ domains according to the degree of failure (Pulmonary, Renal, Hepatic, Cardiovascular, Haematologic,

Neurological). The Denver score simplified this to 4 domains by excluding the platelet count and neurological assessment and showed equal performance to the Marshall score in validation studies (33). The US host response to injury study adopted the Denver Score to define MOF outcomes and found within their severe burn injury cohort, 26.7% of adults and 27.8% of children developed MOF (19). In a UK study of autopsy findings in patients with severe burns, it was found that MOF was the leading cause of death (71% of cases) and over half of cases were secondary to sepsis (22).

1.3 Pathophysiology of the burn wound

Cutaneous burn injury can be caused by a variety of mechanisms including thermal injury from flame, contact with hot objects or radiated heat. Other mechanisms include chemical injury, electrical injury, friction and freezing. Burns are classified according to depth, size in terms of total body surface area (TBSA) burnt and anatomical location. Depth is internationally classified on a I-III scale but an anatomical classification is more practically useful. Superficial burns (Grade I) occur from sun exposure, scalds and flash injuries, involve the epidermis only and are expected to heal within 7 days. Superficial partial thickness burns (IIa) are typically from scalds and involve the epidermis and superficial (papillary) dermis and usually heal within 2 weeks by primary intention (regeneration). Deep partial thickness (IIb) burns involve the deeper (reticular) dermis and may take 3-6 weeks to heal and healing may be associated with abnormal scarring. Full thickness burns (III) are often due to flame, electrical or contact injury and will not heal by primary intention and require skin grafting for timely healing (35).

Thermal injury to the skin results in cell death due to the denaturation of proteins and a loss of plasma membrane integrity. The duration of exposure and the temperature of the heat source is important as cell necrosis occurs after 1 hour at a temperature of 45°C but only 1 second at 69°C ((10) – chapter 10). In 1953, Douglas Jackson described that there are three distinct concentric zones of injury within a burn wound (figure 2). Centrally there is *zone of coagulation* consisting of irreversibly necrosed tissue and peripherally there is the *zone of hyperaemia*, which is characterized by increased perfusion and usually heals without intervention. In between these two zones is the *zone of stasis*, which contains a mixture of viable and non-viable cells, capillary vasoconstriction and ischaemia (36). This zone has the potential to progress to complete cell death but with good resuscitation and wound care this zone has the potential to heal without surgical intervention (10,35).

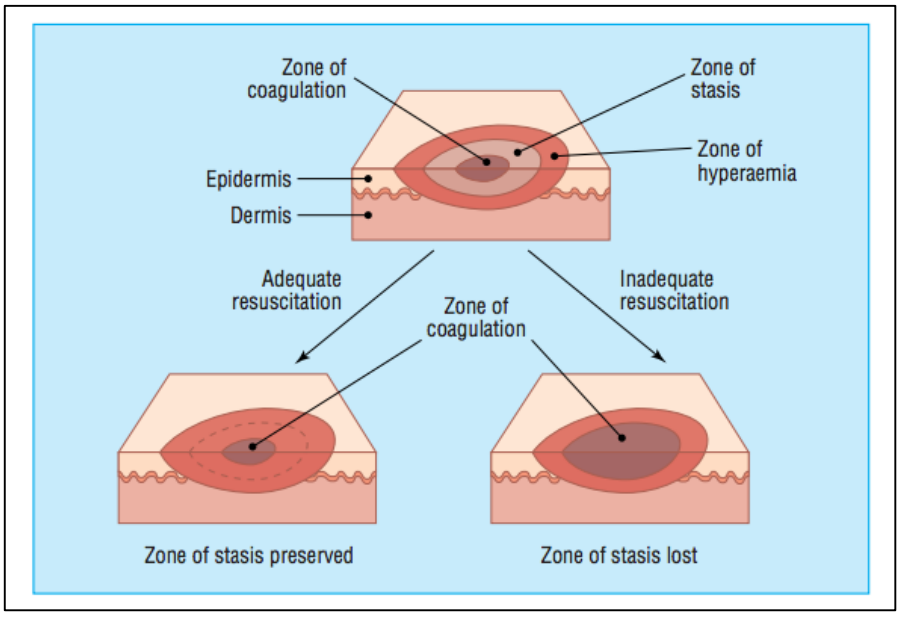

Figure 11-2: Jackson's 3 Zones of burn injury (Taken from Hettariatchy & Diewzulski, ABC of burns 2004. **(37)**.

1.4 Inflammatory response to severe thermal injury

The definition of a severe burn in the literature is variable, but it is known that burns affecting over one third of the TBSA result in a complex systemic pathophysiological response in humans (38). This systemic response includes systemic inflammation, an endocrine stress response and hypermetabolism which results in a hyperdynamic circulation, increased body temperature, increased oxygen consumption, increased CO_2 production, glycolysis, proteolysis, lipolysis and futile substrate cycling (39-41). These responses are common to other major trauma and sepsis, however the response after severe burns is both more profound and more prolonged (42,43). There is increasing evidence that both the magnitude of the initial inflammatory insult and the duration of ongoing inflammation determine patient outcomes after burns and trauma.

1.4.1 Immune-inflammatory paradigms following injury

Inflammation is the reaction to tissue injury and is a tightly regulated and localised acute host response necessary for haemostasis, protection against invading microorganisms and the initiation of wound healing and repair mechanisms. However, severe tissue injury as seen in patients with multiple trauma or severe burns results in a massive release of inflammatory mediators into the circulation resulting in a complex system wide activation of the immune system with deleterious effects on a multitude of organ systems. The clinical manifestation of this response is termed the Systemic Inflammatory Response Syndrome (SIRS) and occurs in other conditions such as sepsis, ischaemia reperfusion injury and pancreatitis (44). The concept of SIRS came from a desire to better understand systemic inflammation in

trauma and surgical patients with no evidence of infection, previously termed ‘sepsis syndrome’. A consensus conference between the American College of Chest Physicians (ACCP) and Society of Critical Care Medicine (SCCM) in 1992 resulted in the emergence of the definitions of 1) SIRS, defined by clinical criteria (table 2), 2) sepsis – SIRS in the presence of documented infection and 3) Multiple organ dysfunction syndrome (MODS) – organ dysfunction in the presence of SIRS (44).

	SIRS criteria	Parameters
1	*Body temperature*	>38°C or <36°C
2	*Heart rate*	>90 beats per minute
3	*Respiratory rate*	> 20 breaths per minute
4	*White cell count (leukocyte)*	>12,000 per uL or <4000 per uL or >10% immature band forms

Table 11-2: Systemic inflammatory response syndrome (SIRS) criteria. A score of ≥2 is required for a diagnosis of SIRS. **(45)**

After the introduction of the concept of SIRS in the 1990’s, it was not long after that Polly Matzinger proposed the ‘danger model’, which gave an explanation for the development of SIRS in the absence of infection. This model proposed that the immune system is more concerned with damage than recognition of self or non-self and thus responds to alarm signals from damaged tissues in the same way as to an infectious pathogen (46). We now know that tissue injury, for example trauma, results in release of danger signaling molecules, also termed ‘alarmins’ or ‘damage associated molecular patterns (DAMPS)’ and that these can activate the innate immune system through receptors on immune cells such as the toll-like receptors (TLR) (47). Prior to the emergence of these concepts, it has long been known that following trauma and burns, a period of immunosuppression arises during which patients are susceptible to the development of infections and sepsis (48). This

phenomenon was later coined the ‘compensatory anti-inflammatory response syndrome’ (CARS) (49). The SIRS/CARS model of the response to injury or sepsis suggested that the initial pro-inflammatory SIRS phase is followed temporally by a period of immunosuppression or CARS, characterized by anti-inflammatory cytokine production (e.g. IL-10) and defects in adaptive immunity. It was also felt that during the CARS phase, patients are susceptible to subsequent episodes of SIRS and CARS from a ‘second hit’, e.g. surgery, infection or sepsis, which are responsible for adverse clinical outcomes (Figure 3a).

This SIRS/CARS paradigm began to be questioned when a study in a murine model of sepsis showed simultaneous production of pro and anti-inflammatory cytokines in response to the insult (50). More recently, work from the US host-response to injury Glue grant program, demonstrated that following severe blunt trauma and burns, pro- and anti-inflammatory gene expression is simultaneously increased in circulating leukocytes (51). They propose a new immune-inflammatory model for the response to trauma, stating simultaneous pro and anti-inflammatory responses (Figure 3b). The study also showed no evidence of ‘second inflammatory hit’ associated with later complications, only differences in the size and duration of the transcriptional reorganization between patients with complicated and uncomplicated outcomes. In summary, the model proposes that the initial magnitude of both the pro-inflammatory and anti-inflammatory responses and the time to resolution is important in determining patient outcomes after major trauma and burn injury.

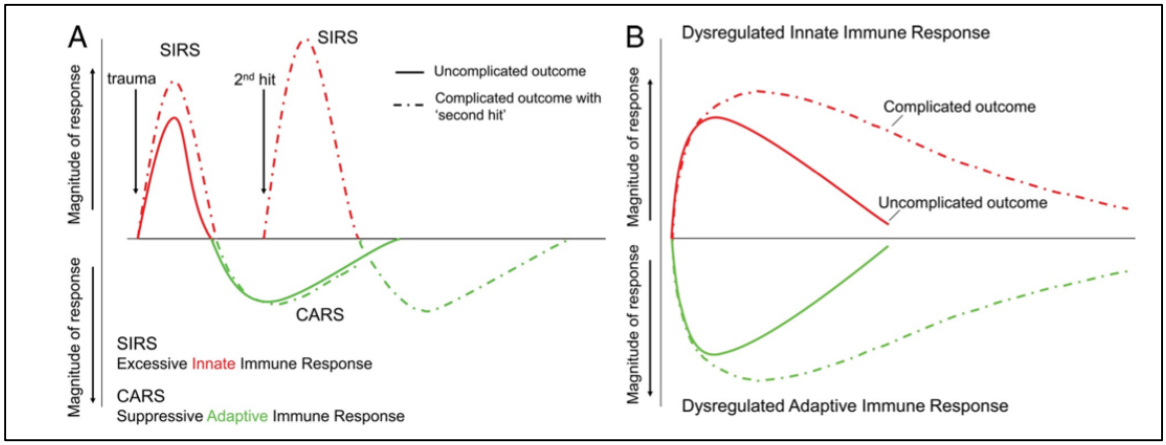

Figure 11-3. Models of inflammation after injury. a) Long held paradigm of the immune-inflammatory response following trauma showing pro- followed by anti-inflammatory processes. b) New model proposed by Xiao et al. based on gene expression profiling of circulating leukocytes in trauma and burns patients suggesting concurrent SIRS/CARS immediately post-injury. *Taken from Xiao et al. 2011. A genomic storm in critically injured humans. JEM 208:2581-2590* **(51)**.

More recently a group from Florida have proposed another model to explain the prolonged ICU stay seen in some critically ill patients. They introduced the term 'persistent inflammation catabolism syndrome' (PICS) to describe the phenotype of patients who survive their initial inflammatory insult but reside in the ICU for many weeks needing organ support and experiencing nosocomial infections, progressive protein catabolism with loss of lean body mass and failure to regain muscle strength (figure 4) (52). More recently they have utilized genomic microarray data from severe blunt trauma patients to show that patients with complicated outcomes exhibit gene expression changes consistent with persistent defects in adaptive immunity and increased inflammation (53). This clinical syndrome has not yet been studied in a population of thermally injured patients.

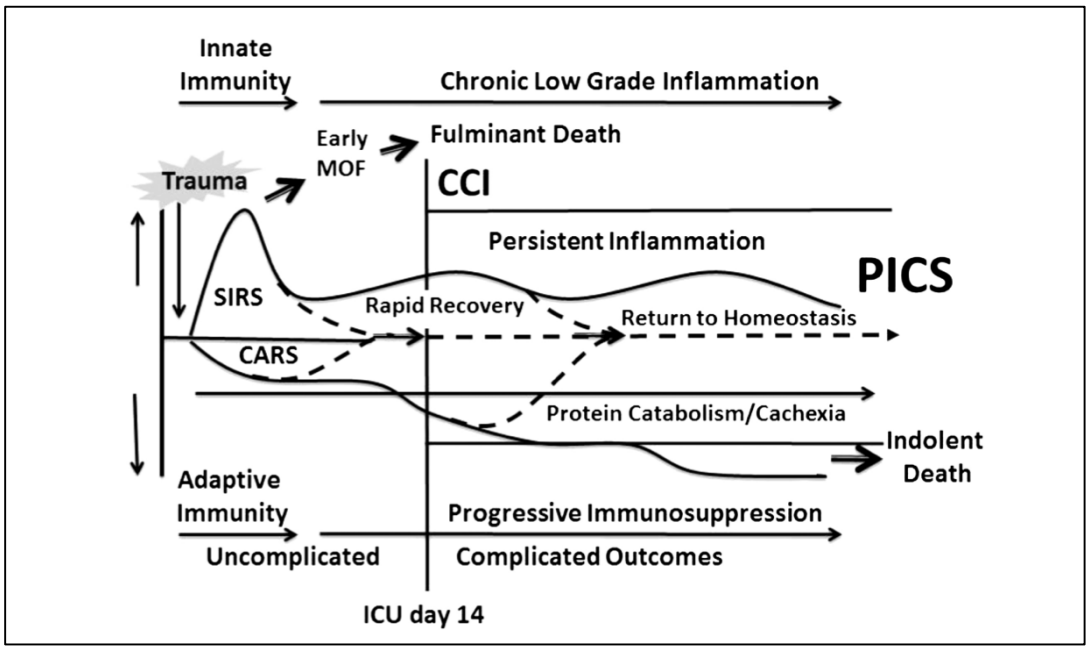

Figure 11-4. New proposed model of the human immune-inflammatory response to traumatic injury incorporating concepts of SIRS, CARS, chronic critical illness (CCI) and PICS.*Taken from Vanzant et al., Persistent inflammation, immunosuppression and catabolism syndrome after severe blunt trauma. J Trauma Acute Care Surg. 76: 21-30* **(53)**.

1.4.2 Cytokines and chemokines

Pro-inflammatory cytokines, chemokines and non-cytokine inflammatory mediators are the primary mediators of SIRS. Non-cytokine mediators include platelet activating factor (PAF), eicosanoids (e.g. leukotrienes, prostaglandins) and complement C3a and C5a (10). Cytokines play important regulatory roles in immune and inflammatory responses, affecting lymphocyte proliferation, cell survival, cell differentiation, antigen presentation or cell trafficking (54). They can be broadly classified as either pro or anti-inflammatory and subclass of cytokines are the chemokines which act as chemo-attractants to recruit immune cells to their site of release.

Early studies of circulating cytokines in burn injury focused on individual cytokines and demonstrated elevations of Interleukin-1 (IL-1) (55-57),, IL-2 (58) , IL-6 (59-61) and IL-8 (62). Tumour necrosis factor-α (TNF-α) is a classical pro-inflammatory cytokine produced primarily by cells of the monocyte, macrophage lineage and promotes endothelial cell permeability, neutrophil release from the bone marrow, enhances their recruitment to the site of injury and promotes phagocytosis. It also promotes activation of T-helper (Th), promotes fever and the production of acute phase proteins on the liver and promotes catabolic metabolism including muscle breakdown and lipolysis (63). Although elevated levels have been demonstrated in septic shock (64), studies in trauma and burn injured patients have yielded conflicting data. Several studies have shown a relationship between elevated circulating TNF-α and shock, MODS and mortality (65,66) but others have found no relationship to prognosis and outcome following burn injury (55,56).

The Interleukin-1 cytokine family, have also been studied as markers of SIRS and includes IL-1α, IL-1β and IL-1 receptor antagonist (IL-1RA) plus other more recently discovered members, IL-18, IL-33, IL-36 and IL-37 (67). IL-1 (IL-1α and IL-1β) is a pro-inflammatory cytokine and is produced by a wide variety of cell-types including monocytes, macrophages, lymphocytes, NK-cells and keratinocytes. It has some similar effects to TNF in that it induces other pro-inflammatory cytokine release and contributes to the catabolic response to injury (63). IL-RA is anti-inflammatory, through its action as a biologically inactive competitive ligand for IL-1 receptor, with early studies showing poor correlation with measures of illness severity such as the Acute Physiology and Chronic Health Evaluation (APACHE) II score, an inverse

relationship to burn size and lower levels in non-surviving patients (55). In contrast, one study demonstrated higher levels in non-survivors and those who developed infections (57).

The pro-inflammatory cytokine IL-6, more than any other cytokine, has stood the test of time as a reliable marker of inflammation and elevations in circulating levels have been demonstrated after elective surgery, trauma and burn injury (68). IL-6 is inducible in nearly every human tissue and cell type but the most important source is from mononuclear phagocytic cells (69). IL-6 is induced by other pro-inflammatory cytokines including IL-1 and TNF-α. Akin to TNF-α, it also induces pyrexia and activates hepatic production of acute phase proteins but also promotes differentiation of B cells and T-cell proliferation (63). It also has anti-inflammatory properties, being able to inhibit the synthesis of IL-1 and TNF-α and stimulate the synthesis of IL-1 receptor antagonist (IL1-RA) (70). Guo et al., showed that IL-6 is elevated on the first day after burn injury, peaks on the sixth day and remained elevated for 21 days post-burn (60). Circulating IL-6 also correlates with the size of the burn injury (61,71), the presence of inhalation injury (72) and adverse outcomes include lethal sepsis (73), and death (61,74).

The most widely studied chemokine in burn injury is IL-8 (CXCL-8). It is a neutrophil chemo-attractant and circulating levels have consistently been shown to be profoundly elevated after burn injury, with higher and persistently elevated levels in larger burns (75), non-survivors (74) and patients with MOF and sepsis (62). IL-8 mediated recruitment of neutrophils also appears to be important in the pulmonary

inflammation caused by burns and smoke inhalation (72). Another chemokine found to be elevated in severe burn injury is monocyte chemoattractant-1 (MCP-1) which plays a pivotal role in monocyte recruitment during infection and inflammation, being induced in a range of tissues by TNF-α, IL-1 and endotoxins (76).

IL-10 is produced by activated monocytes/macrophages, sub-populations of T and B-cells and keratinocytes and has pleiotropic effects, regulating a range of pro-inflammatory processes. It can inhibit the production of cytokines TNF-α, IL-6, IL-1 and Interferon-γ, stimulate monocytes to produce IL-RA and inhibit effector functions of macrophages, T-cells and NK cells (77). Circulating levels correlate with the development of sepsis in trauma patients (78) and in burns patients peak levels are predictive of ICU mortality (79). In addition to higher early peak levels of IL-10, non-survivors of burn injury and survivors with sepsis appear to have persistently elevated levels compared to survivors and non-septic survivors respectively (79,80). Similarly, IL-1RA levels correlated with burn size, area of full thickness burn and serum CRP and the development of infectious complications (57) and mortality (81).

The most recent studies to study cytokine production following thermal injury have shown that SIRS and the cytokine storm differs between adults and children (82) and between surviving and non-surviving major paediatric burn patients (74). The same group have shown in a large cohort of children with burns >30% TBSA that a severe burn induces an inflammatory and hypermetabolic response that persists for up to 3 years post injury (42). All of these recent studies, point to IL-6, IL-8, MCP-1, GCS-F and IL-RA as the most important cytokines in terms of prognosis of outcome. It is

apparent that across the vast swath of burn cytokine response literature there are inconsistencies and this may relate to differences in measurement, heterogeneity of patient populations and the presence of genetic polymorphisms within cytokine genes which effect treatment response (83,84). To date, monotherapies targeting reduction of individual cytokines as well as approaches to global reduction of pro-inflammatory cytokines such as continuous veno-venous haemofiltration (CVVH) have been unsuccessful in treating systemic inflammation and sepsis. Future therapies need to take account the complex balance of these pleiotropic mediators in order to confer outcome benefit after severe injury.

1.4.3 Damage associated molecular patterns (DAMPS)

The concept that the immune system is not simply concerned with distinguishing 'self' from 'non-self', but rather to detecting signals that indicate danger to cells was proposed by Matzinger in her 'Danger hypothesis' (46). Innate immune cells recognise and are activated by the presence of pathogenic organisms through the detection of highly conserved motifs called Pathogen Associated Molecular Patterns (PAMPs). PAMPs are recognised by Pattern Recognition Receptors (PRRs) and include a vast array of different molecules including Peptidoglycan, endotoxin, flagellin and double-stranded RNA (dsRNA) (85). These same PRRs, such as Toll-like Receptors (TLRs), also recognise self-derived molecules that are released during tissue stress or injury and necrotic cell death and are termed Damage Associated Molecular Patterns (DAMPs). In healthy tissues, DAMPs are hidden from PRRs either by compartmentalisation within cells (intra-cellular DAMPs) or sequestration in the extra-cellular matrix (ECM) (extra-cellular DAMPs) (86). DAMPs released from

injured tissues are therefore able to generate innate immune responses through the same signalling pathways as PAMPs. These highly conserved molecules are very heterogeneous and have a normal physiological role but signal danger or damage in their 'DAMP role' when become exposed to PRRs.

DAMPs can be broadly grouped according to their normal physiological location: 1) Nuclear DAMPs e.g. Histones, genomic DNA, High Mobility Group Box-1 (HMGB-1); 2) Cytosolic DAMPs e.g. adenosine triphosphate (ATP), heat shock proteins (HSPs), uric acid crystals, S100 proteins; 3) Mitochondrial DAMPs e.g. mitochondrial DNA (mtDNA), formyl peptides and 4) Endoplasmic reticulum (ER) DAMPs e.g. Calreticulin (87). A classical DAMP is HMGB-1, a DNA chaperone that is expressed in most cell types and acts as a DAMP when its becomes extra-cellular. This can occur passively after necrotic cell death but not programmed cell death (apoptosis) or can be actively secreted by stressed cells (88). It has a range of actions depending upon its redox state and which PRR it binds e.g. in its reduced state, it can bind to RAGE (receptor for advanced glycation products) and induce cell migration and autophagy or in its disulphide state it can bind to TLR-4 to induce cytokine and chemokine release by immune cells (87).

Within the field of injury research, DAMPs have become the link between tissue injury and systemic inflammation in the absence of infection. Studies of HMGB-1, showed that in patients with severe blunt trauma (Injury severity score (ISS)>15), levels increased 30-fold after injury (89). The levels of HMGB-1 have been shown to correlate with ISS and mortality (90). More recently, there has been attention focused

on mitochondrial derived DAMPs (mtDAMPs). It makes logical sense, that mitochondrial derived molecules can act as DAMPs, since they hypothesised to originate from alpha-protobacteria which lived in eukaryotic cells in a symbiotic relationship. They therefore have retained some clues to their bacterial ancestry, including methylated CpG repeats in their genome and formylated peptides (91). In *in vitro* studies, mtDAMPs, which include mtDNA, ATP, cytochrome c and formyl peptides, activate and produce functional changes in neutrophils (47). Murine *in vivo* studies demonstrated that injection of DAMPs into mice resulted in a SIRS phenotype with priming of circulating neutrophils and associated organ damage (92). In clinical studies, Zhang *et al*. have shown that following blunt human trauma, mtDNA is released into the circulation at level several thousand-fold higher than control subjects. They also showed that mtDAMPs were able to activate PMNs in a dose-dependent manner through TLR-9 signalling pathways and that they caused systemic inflammation and organ injury when administered to healthy rats (47).

Within the field of burn injury, mtDAMPs have been shown to activate $\lambda\delta$ T-Cells *in vitro,* increasing their expression of Toll-like receptors (TLRs) 2 and 4 and production of pro-inflammatory cytokines (93). In a murine burn injury model, mtDAMP administration increased systemic inflammation and led to an acute lung injury (ALI) phenotype (94). The same group have also found in patients with inhalation injury and burn injury that early elevations in the DAMPs hyaluronic acid and dsDNA in bronchial lavage specimens were associated with subsequent positive bacterial respiratory cultures (95).

1.5 Immune dysfunction following thermal injury

It has long been known that following extensive thermal injury and other forms of major trauma there is a period of immunosuppression. The innate immune system is immediate acting but in a relatively broad and non-specific fashion. Its main role is the rapid recognition of widely conserved components of infectious agents and damaged tissue, leading to destruction or removal using a variety of mechanisms. Another important role is to activate the adaptive immune system, whose responses are more delayed but highly antigen specific (96). Both arms of the immune response are affected by trauma. The key cellular components of the innate immune response are neutrophils, macrophages and dendritic cells. The actions of the adaptive immune system are mediated by T and B-lymphocytes (T cells and B cells), which have a large repertoire of antigen-receptors to recognize pathogens. The following section focuses on the impact of thermal injury on neutrophils, one of the main effector cells of the innate immune system. The effects of thermal injury on other immune cells are summarized in table 3.

1.5.1 Neutrophil dysfunction following thermal injury

Neutrophils are a critical element of the innate immune system, providing a rapid response to bacterial and fungal pathogens. To perform these tasks, they armed with an array of functions including chemotaxis, phagocytosis, generation of reactive oxygen species (ROS), degranulation and production of Neutrophil Extracellular Traps (NETs). Numerous studies have demonstrated defects in most of these functions following burn injury and early immunological studies established a link between infection and reduced bactericidal activity of neutrophils (97). This

depressed bacterial killing action has been demonstrated with *staphylococcus aureus* for more than 150 days post burn (98).

The first functional defect identified in neutrophils post-burn was in chemotaxis, the process of migrating towards chemoattractant molecules produced at a site of infection or injury. Warden et al showed that defective chemotactic indices correlated with burn size and that measurements taken after 72hrs were predictive of mortality (99). More recent studies using microfluidic devices have demonstrated that human neutrophil motility is depressed as early as 24hrs after burn injury and that the degree of migration speed (chemokinesis) inhibition correlated with severity of injury (100). The same group employed the devices to show neutrophil directionality was impaired in a rat burn model and restoration of this defect using Resolvin D2 conferred increased survival following a septic insult (101). More recent human studies have identified a spontaneous neutrophil migration phenotype from blood samples that were taken during episodes of sepsis in patients with severe burns (102). The consequences of these defects would not only represent reduced ability to deal with pathogens but also increased potential for neutrophils to migrate into and damage healthy tissues, contributing to organ dysfunction (103).

Microbicidal functions of neutrophils may be classified as oxygen dependent and oxygen independent and microbe killing is most efficient when phagocytosed within a membrane bound phagosome. Oxygen dependent killing involves the NADPH oxidase dependent generation of reactive oxygen species (ROS) such as hydrogen peroxide, superoxide anion and nitric oxide. Oxygen independent mechanisms involve release of numerous proteins, contained within granules, into the

phagosomes, including the defensins, cathelicidins, protegrins, cathepsin-G, lysozyme and lactoferrin (104).

Immune cell Type	Immune defects associated with thermal injury
Innate immunity	
Neutrophil	Depressed bacterial killing (98) Defective chemotaxis (99) Inhibited chemokinesis (100) Spontaneous migration phenotype during sepsis (102) Decreased superoxide burst/ROS production (105) Reduced phagocytosis of opsonized bacteria (106) Reduced FCRλIII receptor expression (107) Increased CD11b expression, reduced CD16 expression (108) Increased IL-10 production (109)
Monocyte	Initial monocytosis (110), monocytopaenia in non-survivors and septic patients (111) Shift in differentiation of myeloid progenitors towards monocytopoiesis (112) Impaired chemotaxis (113) Impaired phagocytosis (114) Reduced CD47 expression in sepsis and MOF (115) Reduced HLA-DR expression delayed recovered associated with sepsis and mortality (116-118)
Macrophage	Initial hyperactivity – increased production of TNF, IL-6, IL1 and PGE-2 (119) Increased initial TLR-2 and TLR-4 expression and reactivity to LPS (120,121) Increased late production of IL-10 (121) Impaired phagocytic activity (123)
Dendritic cell (DC)	Reduced numbers of circulating DCs, prolonged in septic patients (124) Reduced expression of HLA-DR reduced up to 4 weeks post-injury (125), reduced expression in patients developing sepsis (118) Decreased T-cell stimulatory capacity of dermal DCs and Langerhan's cells (126)
Adaptive immunity	
T-lymphocyte	Impaired delayed hypersensitivity type response (127) Impaired in-vitro lymphoproliferative response to mitogens Defective cytotoxic T-lymphocyte (CTL) function (128,129) Reduction in CD4+ T-Helper (Th) cells, greater in sepsis (130) Increased apoptosis (131) Decreased production of Th1- associated cytokines (IFN-γ, IL-12), increased production of Th2 cytokines (IL-4, IL10) (132) Increased regulatory T-cell activity (T-Reg) (133)
B-lymphocyte	Decreased expression of activation marker CD25 (134) Suppression of antigen-specific antibody production (135) Impairment of IgM synthesis (136) Impairment of clonal expansion and proliferation (136)

Table 1-3. Summary of innate and adaptive cellular immune defects demonstrated following thermal injury

Studies in human burn injured patients have shown decreased neutrophil oxidative capacity, early after injury and a return to normal function at 3.5 months post-injury (105). Reduced phagocytosis of opsonised bacteria has been shown with a positive correlation to burn size (106) and this could be related to changes in phagocytosis receptor expression e.g. FCRλIII receptor (107).

1.5.2 Ageing and the immune-inflammatory response to injury

Older adults are at increased risk of sustaining burn injuries (137) and experience much poorer outcomes for a given burn injury size compared to younger patients. They are also more likely to experience significant morbidity from infectious complications such as pneumonia and sepsis (138), contributing to increased mortality and greater length of stay in hospital. A number of contributing factors have been proposed to explain poorer outcomes in this group, including co-morbid disease (139), frailty (140) and thinner skin resulting in deeper thermal injury (141). There is also increasing interest in investigating the age-related changes in immune function, termed immunesenescence and its role in outcomes after injury in the older adult (142). Immunesenescence encompasses age-associated changes in the composition, phenotype and function of innate and adaptive immunity. It also includes inflammaging, a low level chronic inflammatory state, defined by elevated circulating levels of pro-inflammatory cytokines such as IL-6 and reduced levels of anti-inflammatory cytokines such as IL-10 (Wei et al 1992, Stowe et al 2010, Bartlett et al 2012). The key innate immune defects associated with ageing have been recently reviewed (143) and include decreased neutrophil phagocytosis, chemotaxis and NET formation and decreased phagocytosis, ROS production and IL-6 and TNF-

α production by monocyte/macrophages. Age-related functional deficits have also been demonstrated in Natural killer (NK) cells and DCs.

It is hypothesized that immunesenescence in older patients leads to increased susceptibility to infectious complications and altered responses to the injury itself, leading to worse outcomes. To date, studies to test this notion have been limited to animal studies. A murine burn model, utilizing a 15% TBSA scald injury, demonstrated worse survival in aged mice, impaired delayed type hypersensitivity (DTH) response and significant elevations in circulating IL-6 levels compared to younger mice (144). Further work from the same group, showed a greater shift in the cytokine profile from Th1 to Th2 in aged mice after burn injury and this could be partially recovered using oestrogen replacement (145). This has not yet been followed up in human studies, but work on other types of injury, including hip fracture have shown further reduction in neutrophil function, specifically ROS generation, induced by the injury (Butcher et al 2005). Subsequent studies by the same group revealed that patients who develop depression after hip fracture had a range of immune dysfunction including reduced neutrophil function (Duggal at eal 2014). Clearly, further research is needed to fully explore the role of immunesenesence in determining outcomes in older patients with burn injury.

1.6 The Metabolic and Endocrine Response to thermal injury

1.6.1 The 'Ebb and Flow' hypothesis

Surgery, infection, trauma, burns and haemorrhage all result in an endocrine stress response accompanied by profound changes in metabolism that parallel the

inflammatory response. Cuthbertson, in the 1930's, was the first to identify that patients enter a catabolic state after trauma and described the post-injury metabolic response as a two-phase phenomenon. There is an immediate 'ebb phase', a 24-48hr period of depressed metabolic activity, reduced oxygen consumption, reduced cardiac output, hyperglycaemia and peripheral vasoconstriction. This phase is followed by a 'flow-phase' during which metabolic activity, nitrogen excretion and oxygen consumption increase, typically within the first 5 days post-injury (146).

1.6.2 Burn shock

Since these earlier descriptions of 'ebb and flow' phases, the ebb phase can also be termed 'Burn shock', an acute period characterized by profound reductions in cardiac output which can be depressed for as long as 48hrs (147). In the face of the reduced cardiac output, arterial pressure is maintained through increases in total peripheral resistance (TPR) (148) and redistribution of blood flow to the brain, heart and the liver (149). The underlying pathophysiology behind burn shock is complex and multi-factorial but it has been demonstrated that severe burn injury results in systemic endothelial dysfunction and increases in capillary permeability with resultant protein loss into the interstitial space (150). This in turn results in significantly decreased colloid osmotic pressure (COP) allowing fluid to escape into the interstitial space giving rise to hypovolaemia and tissue oedema (151). If the resultant hypovolaemia is not corrected promptly, hypotension and inadequate tissue perfusion ensues (10). There is much evidence that the metabolic disturbance during the burn shock phase is secondary to reductions in blood flow, with fluid resuscitation restoring decreased metabolic rate (152) and preventing a reduction in oxygen consumption (153).

Improvements in the acute care and fluid resuscitation of severely burn injured patients, with consequent improvements in early survival has led to a shift in focus to the 'Flow phase' of the burn response (154).

1.6.3 The 'hypermetabolic response' to thermal injury

The metabolic response to burn injury is similar to that seen after other forms of trauma and critical illness; however, the magnitude and duration of the response is far greater (155). This profound metabolic disturbance has been termed the hypermetabolic response (HMR) and is characterized by increased metabolic rate (measured as resting energy expenditure (REE), a hyperdynamic circulation, altered temperature regulation and a number of biochemical defects resulting in hyperglycaemia and an overall catabolic state (10). The magnitude of the HMR is proportional to the size of the burn injury (71) and is influenced by the age of the patient (156) and the mechanism of the burn injury (157). The presence of inhalation injury in children with severe burns appears to have little influence on indices of hypermetabolism (158). The relationship between REE and burn size is curvilinear, with patients with <10% TBSA burns having close to normal predicted values and those with >40% TBSA burns having greater than twice the normal predicted values (159). In a large study of children with >30% TBSA burns, the REE at thermal neutrality was shown to be 140% of predicted on admission, reducing to 130% at full wound healing and 120% at 6-months post-injury (38). More recent studies from the same group have shown the HMR to persist for longer than previously appreciated, with evidence of hypermetabolism at 3-years post-injury in children with >30% TBSA burns (42).

1.6.4 The Endocrine stress response

The metabolic response to thermal injury is clearly complex and multiple mediators have been implicated in initiating and driving the response. To date, endotoxin, tumour necrosis factor α (TNFα), platelet activating factor (PAF), the cytokines IL-1β and IL-6, arachidonic acid metabolites, neutrophil adherence complexes, reactive oxygen species (ROS), nitric oxide (NO), the complement system and the coagulation cascades have all been implicated in driving this response (159). In addition to inflammatory mediators released from the site of injury, tissue damage and pain triggers impulses along afferent neurons, which ascend to the hypothalamus and brain stem of the central nervous system (CNS). These signals stimulate the 'stress response' or 'fight-or-flight' system that is composed of the sympathetic-adrenal-medullary (SAM) axis and the hypothalamic-pituitary adrenal (HPA) axis. These highly conserved responses facilitate both increased mental awareness and elevated metabolic and cardiovascular activity in readiness for a rapid increase in muscular work.

1.6.5 The Sympathetic-adrenal-medullary (SAM) axis

The SAM axis comprises the sympathetic nervous system (SNS) and the adrenal medulla. The SNS is one arm of the autonomic nervous system (ANS) and consists of neurons with cell-bodies within the CNS (pre-ganglionic fibres) and neurons that project outside the CNS to the viscera (post-ganglionic fibres). Injury, pain, anxiety, hypotension, hypothermia, hyperthermia and psychological stressors result in hypothalamic activation of the SNS with release of noradrenaline from sympathetic nerve endings and release of adrenaline from the adrenal medulla resulting in

tachycardia, increased cardiac output and changes in carbohydrate, lipid and protein metabolism (160) . In addition, neurons arising in the locus ceruleus in the brainstem release noradrenaline within the brain to increase alertness and attention (161).

Severe burn injury results in profound SNS activation which is directly proportional to burn size (162,163). Levels of urinary noradrenaline and adrenaline increase 10-fold and 4-fold, respectively, after severe thermal injury in children. The duration of the stress response to thermal injury is prolonged with urinary levels of cortisol, noradrenaline and adrenaline levels being elevated for 36 months, 24-months and 18-months respectively (42). In addition to the cardiovascular and visceral changes, catecholamines have been demonstrated to influence some of the key metabolic changes that characterize the HMR, including increased REE (164,165), glycogenolysis (166), gluconeogenesis (166) and lipolysis (165,167-169). The prolonged SNS activation may also contribute to immune dysfunction post-burn, with evidence from murine studies that noradrenaline modulates bone marrow myelopoiesis after burns sepsis (170) and that depletion of noradrenaline in bone marrow influenced the functional phenotypes of bone marrow derived macrophages after burn injury and burn sepsis (171).

1.6.6 The Hypothalamic-pituitary-adrenal (HPA) axis

The HPA axis comprises the hypothalamus, pituitary gland and the adrenal gland and is the other key component of the stress response. The paraventricular nuclei (PVN) of the hypothalamus are stimulated to release both corticotrophin releasing hormone (CRH) and arginine vasopressin (AVP or anti-diuretic hormone, ADH). CRH

then acts upon the anterior pituitary (AP) to stimulate release of adrenocorticotrophic hormone (ACTH), which in turn drives production of cortisol from the adrenal cortex. Cortisol is a catabolic glucocorticoid hormone with pleiotropic effects on metabolism, immune function, endocrine function and the cardiovascular system (172). In the context of the stress response, cortisol is geared towards mobilizing energy substrates, particularly glucose through increased gluconeogenesis in the liver, inhibition of peripheral uptake and utilisation of glucose.

Following severe burn injury in children, urinary and serum cortisol levels are elevated 8-10 fold and remained elevated about control levels for up to 36 months post-injury (42). Glucocorticoids have been shown to contribute to the wide-ranging effects on metabolism during the flow phase of hypermetabolism following thermal injury. They contribute to hyperglycaemia through increasing rates of gluconeogenesis (173,174) and glycogenolysis in the liver via opposing the anabolic effects of insulin (175) and stimulation of glucagon secretion (176,177). Corticosteroids are also associated with increased REE (178-180), skeletal muscle proteolysis (181-184), increased liberation of free fatty acids (FFA) from adipose tissue (185) and abnormal bone metabolism (186). In addition, corticosteroids increase hepatic protein synthesis to generate elevated levels of acute phase proteins (174) and gluconeogenic enzymes. They also contribute to post-burn immunosuppression and have been shown to reduce lymphocyte numbers (187) and suppress neutrophil function (188) and monocyte/macrophage activity (189).

The adrenal androgens, Dehydroepiandrosterone (DHEA) and dehydroepiandrosterone sulfate (DHEAS) are also affected by severe burn injury and have been shown to be at low levels for 4-weeks post-burn (Lephart et al., 1987). The relationship of these finding in relation to patient outcomes is unclear but studies in elderly hip fracture patients show that the cortisol:DHEAS ratio was increased in compared to age-matched controls and young patients with similar orthopaedic trauma. The study also reported that a higher cortisol:DHEAS ratio was associated with increased incidence of infection in the first 6-weeks post injury and that in vitro the suppression of neutrophil function by cortisol could be overcome by co-incubation with DHEAS (190).

1.6.7 Increased resting energy expenditure post-burn

The standard or basal metabolic rate (SMR/BMR) is defined as basal metabolism under standardized conditions of fasting, immobility, thermal-neutral environmental temperature (26-33°C) (40). The SMR represents two-thirds of the total daily energy expenditure and therefore is a key determinant of daily nutritional requirements. In critically ill patients, the REE is a more practical indirect measure of SMR derived from measurements of oxygen consumption [Vo_2] and carbon dioxide production [Vco_2] using indirect calorimetry.

A hallmark of the post-burn hypermetabolism, is increases in REE with studies showing a 25% TBSA burn injury results in metabolic rates 118-210% above that predicted by the Harris-Benedict equation (191). In children with burns >40% TBSA, the REE compared to predicted BMR at thermal neutrality is 180% on admission,

150% at full wound healing, 140% at 6 months, 120% at 9 months and 110% at 12 months (41). The same group subsequently published data on a much larger cohort of children with >30% TBSA burns showing persistence of this elevated resting metabolic rate even up to 2 years post-burn (42). This elevated oxygen consumption is due to increased energy expenditure in organs and tissues and following burn, in particular the liver and skeletal muscle (192).

A series of stable isotope studies have shown increases in substrate oxidation which matches the increases in energy expenditure with 132% increases in fatty acid oxidation, 33% increases in glucose oxidation and 41% increases in protein oxidation (193). The same study revealed significant alteration in ATP consuming metabolic pathways including protein turnover, gluconeogenesis and urea production. In addition, increases in substrate cycling were demonstrated following thermal injury, with 450% increases in glycolytic-gluconeogenic cycling and 250% increases in triglyceride-fatty acid cycling which contributes to thermogenesis and increased energy expenditure (194). Substrate cycles exist when opposing non-equilibrium pathways are active concurrently and consume ATP to produce heat without net changes in the amount of substrate or product. These ATP consuming processes have been calculated to account for only 57% of the increase in REE post-burn and the remainder has been hypothesized to due to increased Na^{+}-K^{+}-ATPase activity and increases in proton leakage across the mitochondrial inner membrane (40). Until recently evidence to support this theory has been lacking, but a group from Galveston, Texas has shown that in severely burned children with hypermetabolism, skeletal muscle mitochondria show a more thermogenic phenotype with two thirds of

mitochondrial respiration being devoted to thermogenesis (195). The molecular basis for this alteration in mitochondrial physiology is currently under investigation but this is felt to be an adaptive response to maintain thermoregulation in the context of major skin loss.

1.6.8 Post-burn hyperglycaemia and insulin resistance

The inflammatory and stress hormone milieu after severe burn injury, with increased levels of circulating catecholamines and glucagon, results in altered glucose metabolism and hyperglycaemia. This aspect of metabolic dysfunction is particular pertinent since both early hyperglycaemia and continued hyperglycaemia post-burn is associated with increased mortality (196,197) and higher plasma glucose levels are associated with more graft losses (198) and higher incidence of sepsis (196).

Post-burn hyperglycaemia is due to: 1) increased glucose production, via gluconeogenesis and glycolysis; 2) Loss of the normally suppressive action of exogenous glucose on endogenous glucose synthesis; 3) Reduced rates of glucose uptake and utilization due to insulin resistance (199). Even though glucose delivery to the peripheral tissue is actually enhanced, there is no proportional increase in glucose oxidation to match (192). Hepatic glucose synthesis is augmented by the increased availability of gluconeogenic substrates, namely glycerol from lipolysis in adipose tissue ((168) and 3-carbon amino acids, mainly alanine, from skeletal muscle proteolysis. The amount of lactate liberated from skeletal muscle is far greater than that normally present, so the additional source is likely to be through transamination of muscle pyruvate through degradation of other muscle branched chain amino acids

(200). In addition, there is significant glucose flux directed towards the burn wound where fibroblasts, endothelial and immune cells utilize glucose via anaerobic oxidation to yield lactate which is then converted back to glucose in the liver via gluconeogenesis (201). This cycling of lactate to the liver, conversion to glucose and anaerobic metabolism back to lactate is termed the Cori cycle.

Under normal healthy conditions, post-prandial elevations in serum glucose stimulate the release of insulin from the pancreatic β-cells, this mediates peripheral uptake of glucose in skeletal muscle and adipose tissue and suppresses hepatic gluconeogenesis to restore homeostasis. Within the first week post-burn, insulin stimulated glucose uptake by tissue is 50% reduced in severely burned children compared to healthy controls (202). In children with burns >40% TBSA, although blood glucose levels returned to normal levels within 6 months, peripheral insulin resistance was still present for up to 3-years post-injury (203). The molecular mechanisms underlying post-burn insulin resistance are being unravelled with post-insulin receptor signaling defects being identified. Catecholamines attenuate insulin-stimulated glucose uptake by reducing translocation of the GLUT-4 glucose transporter to the cell surface membrane in both muscle and adipose tissue (204,205). Muscle biopsy studies of burned children taken in the flow-phase (day 7) revealed impaired Insulin Receptor Substrate-1 (IRS-1) at its tyrosine binding site and inhibition of AKT (206). Wolfe and colleagues have identified an association between muscle and liver mitochondrial oxidative dysfunction, altered lipolysis rates and impaired insulin signaling affecting insulin-mediated inhibition of hepatic gluconeogenesis and peripheral glucose uptake (173,194,206,207). Pro-

inflammatory cytokines influence post-burn hyperglycaemia both indirectly, via induction of stress hormones and directly (TNF, IL-6 and MCP-1) via modulation of the insulin signaling pathway (208-210).

1.6.9 Lipid metabolism

Burn injury results in profound increases in lipolysis in adipose tissue with hydrolysis of triacylglycerol (TAG) into free fatty acids (FFAs) and glycerol and this has been attributed to elevated levels of catecholamines, in particular β-2 adrenergic stimulation. Indeed, lipolysis is consistently reduced in burn injured patients treated with beta-adrenergic blockers (169,194). However, this increased availability of FFAs is not matched by a sufficiently increased utilization via beta oxidation to generate ATP. In starvation states, lipids are the most physiologically desirable source of energy as they constitute more than 80% of the fuel stores and fatty acids can be readily metabolized by most tissue types. Indeed, in the non-stressed starvation state, 90% of FFAs undergo oxidation but following burn injury this figure is 30% (199). The remainder of FFAs are involved in futile cycling from breakdown of muscle and adipose TGs into FFA and then subsequent re-esterification back to triglycerides (TG) or very-low density lipoprotein (VLDL) in the liver (211). This cycling is a result of two simultaneous activities of catecholamines: 1) Stimulation of hormone-sensitive lipase (HSL) which facilitates lipolysis in adipose tissue and 2) Up-regulation of re-esterification in the liver (154).

What are the consequences of this deranged lipid metabolism for the severely burn injured patient? Firstly, the increased peripheral lipolysis and recycling of fat through

the liver, in combination with no proportional increase in beta-oxidation, leads to increased storage of TG in hepatocytes. This is compounded by low VLDL secretion which is unresponsive to increases TG synthesis (212). Pathological and spectroscopic studies of burned children have shown that by 1-week post-burn, hepatic TG (HTG) was increased 3-5 fold above normal (213-215). This fatty infiltration of the liver has been shown to be associated with increased incidence of infection, sepsis and poor outcome (216). A prospective study of severely burned children has shown profound hepatomegaly occurs post-injury, with liver size being 185% of predicted at 1 week and peaking at 2 weeks but with increased size for up to 12 months. This was associated with prolonged liver dysfunction as measured by hepatic protein synthesis for 12 months post-injury (217). Both hepatomegaly and hepatic steatosis were associated with increased mortality in a rat 40% TBSA burn model (218). In a recent study, children with severe burns were stratified into three lipid metabolism groups according to plasma levels of FFA and TGs. The group with elevated TGs demonstrated significantly increased liver size over the first month. Moreover the study also highlighted that this group of patients had significantly worse outcomes in terms of mortality, MOF and LOS in the ICU (219).

As discussed previously, patients with major burn injury develop significant peripheral insulin resistance, leading to hyperglycaemia and its associated complications including increased skin graft loss and sepsis (196,198). Studies in type 2 diabetes mellitus (T2DM) have implicated derangements in lipid metabolism and mitochondrial dysfunction in the development of insulin resistance and there is some evidence to suggest similar mechanisms are at play following burn injury (207). Indeed, animal

studies carried out by Cree and colleagues have shown that following burn injury the basal palmitate oxidation rate is reduced by 50% during hyperinsulinaemia and that palmitate oxidation correlated with the degree of insulin sensitivity suggesting the two are related (220). Initial hypotheses were that reduced fatty acid oxidation was related to the inhibition of carnitine palmitoyltransferase enzymes (CPT) 1 or 2, which are required for combining palmitate with carnitine allowing translocation across the mitochondrial membrane. However, the group found that mitochondrial oxidation of both glucose and palmitate was reduced, suggesting more generalized mitochondrial dysfunction (221).

The molecular mechanisms linking altered lipid metabolism and insulin resistance post-burn remain elusive. One area of focus has been on increased levels of intramyocellular lipids (IMCL), which have been shown to be associated with insulin resistance in healthy humans (222,223) and offspring of type 2 diabetic patients (224). Using in-vivo and ex-vivo proton NMR spectroscopy, Astrakas et al., showed that IMCLs accumulate in murine myocytes following burn injury and this was associated with apoptosis and mitochondrial dysfunction (225). The same group went on to show in their murine burn model that IMCL levels correlated significantly with elevated plasma FFAs. In the same animals, significant downregulation of gene expression of Glut4, Insulin receptor substrate-1 (IRS1) and peroxisome proliferator-activated receptor coactivator-1β (PPARλ coactivator-1β or PGC-1β) were observed. PGC-1 coactivators plays a critical role in glucose, lipid and energy homeostasis and PGC-1β is an upstream regulator of the IRS-1 gene. The authors of the study conclude that IMCLs are a useful metabolic biomarker post-burn, in particular of

insulin resistance. They hypothesise that PGC-1β is a potential link between increased plasma FFAs, accumulation of IMCL and altered insulin signaling leading to insulin resistance post-burn. More recent IMCL research suggests that elevated IMCL levels are not sufficient alone to disrupt insulin signaling, however the specific composition of the IMCL lipid droplets may be more important as they may yield toxic lipid signaling metabolites. Such metabolites that have been implicated in the development of insulin resistance include long-chain acyl CoAs, diacylglycerol (DAG), phosphatidic acid and ceramides (226).

1.6.10 Protein-amino acid metabolism

The composition of the human body may be divided into the fat containing component, or fat mass and the non-fat containing component, or lean body mass (LBM), comprising 25% and 75% of the human body weight respectively. Protein makes up 20% of the LBM component and the majority (60%) of the protein content is found within skeletal muscle (227). During health there is a dynamic relationship between whole body protein breakdown and protein synthesis resulting in a net protein balance (228). In contrast to fat, which serves as our major energy store, there are no intracellular stores of amino acids, rather they are all incorporated into functional proteins. During non-stressed prolonged starvation, metabolic adaptations in tissues result in a switch from glucose as the major fuel to fatty acids and ketone bodies, thus limiting protein degradation and loss of function (229). The severity of loss of LBM in chronic illness and malnutrition states correlate with increased morbidity and mortality with just 10% loss of LBM resulting in impaired immunity and increased susceptibility to infection and 40% resulting in death (Table 4.) (199,230).

Lean body mass (% loss)	Complication	Mortality (%)
10	Impaired immunity, increased infection	10
20	Decreased wound healing, failure to wean	30
30	Too weak to sit, pressure sores, pneumonia	50
40	Death, usually from pneumonia	100

Table 11-4: Complications arising due to catabolism and loss of lean body mass (LBM) (Assuming

Burn injury results in a shift of net protein balance in favour of breakdown leading to skeletal muscle catabolism and loss of LBM with the consequences of immune suppression and impaired wound healing (231), growth disturbance for up to 2-years in children (232), delayed rehabilitation and increased mortality (233). Clinical parameters that influence the degree of skeletal muscle catabolism include increasing burn size, admission weight, time to burn wound excision, the extent of hypermetabolism and the presence of sepsis (234). Studies using isotope tracer labelled amino acids have demonstrated that burn injury brings about significant increases in skeletal muscle protein synthesis by 50%, but this is outstripped by protein breakdown which is increased by 83% (235). The same studies also showed that despite a hyperdynamic circulation and increased delivery rate of amino acids, the muscle transmembrane amino acid uptake was reduced by 50-63%. However, outwards transmembrane transport was elevated in burn patients, facilitating their export to be delivered to other tissues (235).

Is this protein catabolism a maladaptive or useful response to injury? It is hypothesized that the mobilization of amino acids from skeletal muscle protein post-

injury is an adaptive response with the goal of providing amino acid substrates for wound healing (Figure 5.) (228). Evidence to support this comes from a study in which 10 patients with >40% TBSA burns were subjected to assessment of protein kinetics, using tracer labelled phenylalanine, in skeletal muscle, burn wound and skin. They demonstrated that there was a net release of amino acid from muscle but a net uptake by the wound. Moreover, protein synthesis rates were higher in the wound compared to unburnt skin and skeletal muscle (236). In addition to this, skeletal muscle catabolism may play a role in providing amino acid substrates, such as alanine, for hepatic gluconeogenesis. The rate of alanine appearance in the blood is twice that of healthy controls in children with severe burns (237).

Skeletal muscle protein catabolism post-burn, persists well beyond the time of wound closure and in a cohort of children with >40% TBSA burns. Hart et al., showed that whole body and cross-leg nitrogen balance was profoundly negative with concomitant loss of LBM at 6 and 9 months post injury, long after wounds had fully healed. Between 9 and 12 months post-injury, LBM increased, protein breakdown decreased and protein balance improved (41). These data could be used to argue against the wound protein accretion model, however it is possible that there are ongoing protein requirements for scar remodeling or perhaps this aspect of metabolic dysfunction simply persists in the presence ongoing inflammation and endocrine dysfunction that has been demonstrated for a long as 3 years post-burn (42).

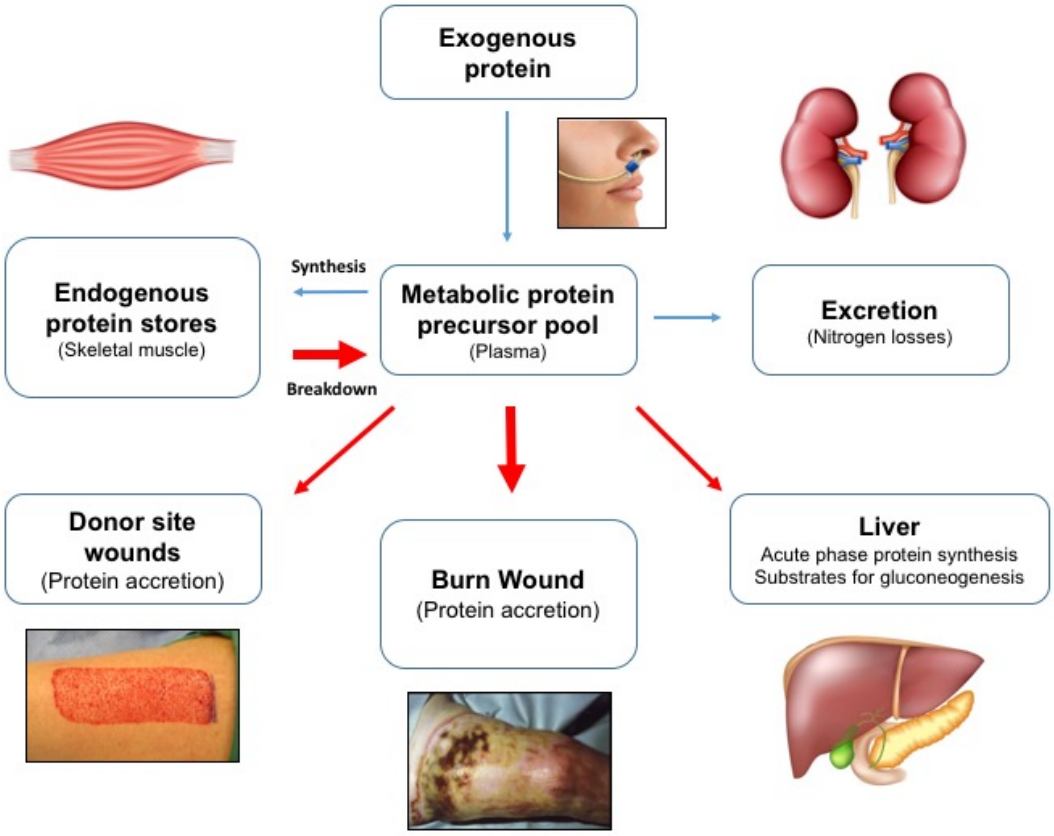

Figure 11-5. Proposed theory for redistribution of protein with flux from skeletal muscle to the burn wound, donor sites and liver. Adapted from Porter et al., 2013 **(228)**.

1.6.11 Other consequences of the HMR for the burn patient

It is clear that the hypermetabolic response to thermal injury is complex and involves a number of areas of metabolism and a range of different tissues. In addition to the profound effects on protein, lipid and glucose metabolism other organ systems affected by post-burn hypermetabolism include the heart, liver, haematopoietic system, immune system and bone metabolism. Longitudinal studies have shown in burned children heart rates, cardiac output, cardiac index remained significantly elevated above control ranges for 12 months (42). In the same study, ultrasound scanning revealed that hepatomegaly occurs with an average 75% increase in liver size compared to healthy controls. Fatty liver infiltration has been demonstrated in

burn victims as autopsy and is associated with increased incidence of sepsis and mortality (216). Bone and mineral metabolism is also impaired with hypoparathyoidism, hypocalcaemia, hypophosphataemia and compromised vitamin D metabolism (238).

1.6.12 Modulation of the HMR

Severe thermal injury thus results in a profound and prolonged inflammatory and hypermetabolic response, which although aimed at wound healing and recovery from the insult, may have deleterious effects contributing to adverse outcomes and mortality. There has therefore been a strong focus within burn care research, on trying to ameliorate the hypermetabolic response. Strategies to achieve this include prevention of infection and sepsis, early excision of the burn eschar and wound closure, nutritional support, environmental warming to thermal neutral temperature (28-33°C) and various pharmacotherapies (192). Drug treatments studied to date include: beta-adrenergic blockade with propranolol (239-241); the use of Oxandralone, a testosterone analogue (242-244); insulin (245); recombinant human growth hormone (rHGH) (246,247); Insulin-like Growth factor-1 (IGF-1) (248); Insulin–like Growth Factor Binding Protein-3 (IGFBP-3) (249); Fenofibrate (250) and ketoconazole (251). Undoubtedly, these pharmacological and non-pharmacological interventions may have contributed to improved outcomes after severe burn injury, however none have been shown to completely abolish the response. Further research is needed to unpick the complex nature of the post-burn response and identify new therapeutic targets.

1.7 Metabolomics to study thermal injury

1.7.1 Systems biology

Systems biology is a holistic approach to the scientific study of complex biological systems and aims to provide qualitative and quantitative descriptions of their emergent properties (252). Rather than studying changes in individual genes or molecules, this approach looks simultaneously at all changes across the whole interacting network of molecules of functional genes, mRNA transcripts and proteins. This global approach is making advances in a number of human diseases and the US Glue grant Host Response to Injury program has already given us new insights into the complexity of the human response to blunt trauma and thermal injury (51). Biomarkers can be utilized to predict, prognosticate, diagnose and monitor disease and systems biology is now at the forefront of molecular biomarker discovery. Biomarkers are also essential tools in the current drive to develop truly individualized healthcare approaches that have the potential to revolutionize the practice of medicine and improve outcomes from the treatment of disease.

1.7.2 What is Metabolomics?

Metabolites are low molecular weight (typically <1.5kDa) organic or inorganic biochemicals that participate in metabolic reactions and are either synthesized or consumed. They are typically not proteins, but include small peptides and are sub-divided into polar (e.g. amino acids, carbohydrates) and non-polar metabolites (e.g. fatty acids, glycerophospholipids). They may be endogenous or be derived from microorganisms in addition to xenobiotic, dietary and other exogenous sources (253).

Metabolomics is a relatively recent addition to the 'omics' family and its aim is to seek a full quantitative description of all the low molecular weight metabolites in a biological system. The metabolome can be thought of as the full complement of all metabolites in a system or biofluid and is further sub-categorised into the endometabolome (intra-cellular metabolites) and the exometabolome (extra-cellular metabolites) (252). Metabolomics also encompasses the study of changes in the metabolome in response to biological stimuli or genetic modification (254).

The metabolome falls farthest downstream of genetic variation and the processes of gene transcription, protein translation and post-translational modification (Figure 6). It is therefore the most sensitive and dynamic indicator of the true functional state (phenotype) of a biological system and takes into account the influences of diet, lifestyle, drugs, environment and disease. Although there are fewer human metabolites (>6500) when compared to the 25,000 functional genes in the genome and the 1 million proteins in the proteome, to say metabolomics is easier to apply is an oversimplification (252). Advances in the chief analytical platforms used to conduct metabolomics experiments, Nuclear Magnetic Resonance (NMR) spectroscopy and mass spectrometry (MS), has meant that analysis times are measured in minutes and that per sample costs are relatively lower than genomics or proteomics.

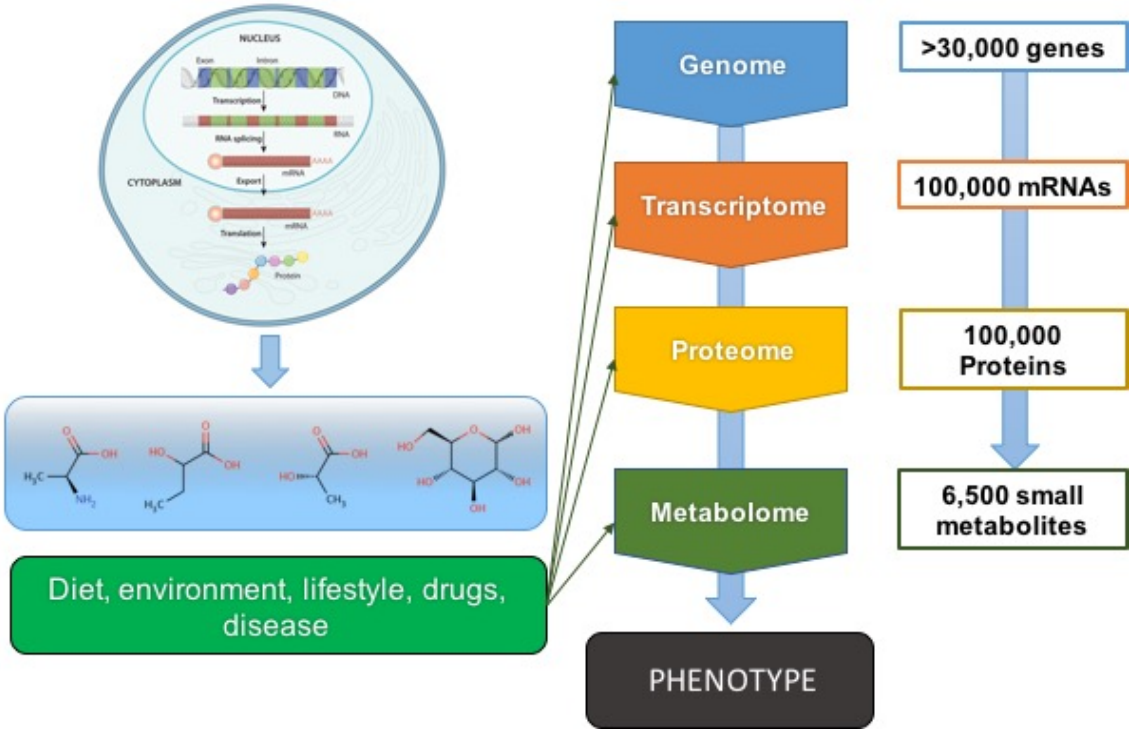

Figure 11-6. Metabolomics is downstream of other complex biological processes influencing phenotype and takes into account influences of diet, environment, lifestyle, drugs and disease on all levels.

1.7.3 Experimental strategies

Metabolomics studies may be either hypothesis generating or hypothesis testing in their approach. If there is limited metabolite data available for a particular organism or disease state for example, then an *a priori* hypothesis cannot be made regarding the importance of specific metabolites. In this situation, an untargeted (discovery phase or inductive) metabolomics strategy is employed. In the study of human disease, such strategies aim to identify either a single biomarker, a panel of biomarkers or identify new biological information which can give insight into pathophysiological mechanisms (254). Untargeted metabolomics is also called metabolic profiling and is a holistic approach is used to obtain the greatest coverage of the metabolome. In this approach, sample preparation must maximize the yield of

a broad range of metabolites from different classes and advanced analytical instrumentation is needed to measure, typically thousands, of metabolites in each sample. It is accepted that in order to obtain data on a vast number of metabolites from different parts of the metabolic network, there must be some compromise on precision and accuracy. With current technology, this means that metabolomics data is typically semi-quantitative, allowing relative differences in measured responses (rather than concentrations) to be detected (252).

If there is prior information regarding important metabolites or metabolite classes in a disease, which may have been gained from a discovery phase study, then a targeted metabolomics approach may be used. In this strategy, a much smaller number of metabolites, which may be related in terms of class or pathway or measured with a high degree of accuracy. Sample preparation is tailored to the metabolite class of interest e.g. glycerophospholipids to maximize their yield whilst filtering out as many other metabolites as possible. In order to obtain the highly accurate quantitative data, internal chemical standards are used where available. With the recognised difficulties in performing discovery phase studies, semi-targeted approaches have also been developed. In these studies, sample collection, preparation and analysis is geared towards generation of highly accurate semi-quantitative or quantitative data for up to 400 metabolites (255). The advantage here is being able to move more quickly towards translational research but the trade-off of this approach is loss of potentially relevant biological information through less comprehensive coverage of the metabolome.

1.7.4 Study Design and Metabolomics Workflow

The study design of a metabolomics study will depend on the research questions and whether an untargeted or targeted study is most appropriate. Sample collection is a vital part of any metabolomics study and care must to be taken to ensure that samples are collected at the same time of day for every sample, to avoid influences of diurnal variation in metabolism (256). Samples should be collected in identical blood/urine collection tubes and all plasticware and reagents involved in sample handling and preparation should be identical throughout the study. Blood samples should be processed into serum or plasma as soon as possible after collection and stored at -80°C. Sample preparation varies depending on the analytical method to be employed, but generally protein containing samples require a deproteinisation step, using either organic solvents or ultra-centrifugation (254). An important consideration in MS based metabolomics is the use of Quality Control (QC) samples to control for instrument variation across runs. This is particularly important if large numbers of samples are being run in different batches. In untargeted studies, it is impossible to provide internal standards for all metabolites for QC purposes. Instead, the use of pooled QC samples, which contain an aliquot of every sample in a run is recommended. The pooled QC sample is useful to condition the analytical system, to allow signal correction for drift, to assess reproducibility within the experiment and allow data integration from multiple batches (254).

After sample analysis, the next steps in the metabolomics pipeline or workflow is data processing and metabolite annotation using commercially or freely available databases such as the Human Metabolome Database (HMDB) (257). In order to

identify which metabolites are important to the research question, groups are compared using multivariate statistical modelling techniques designed for very large datasets and such as Principle Components Analysis (PCA) and Partial Least Squares Discriminant Analysis (PLSDA). Putative biomarkers highly weighted in these models can then undergo further confirmatory identification using spectral databases, MS/MS fragmentation data or spike in experiments. It has been recommended that following discovery phase biomarker studies, study validation is undertaken with an independent sample set. Candidate biomarkers emerging from these studies are then tested in a cohort validation study with larger numbers of subjects (n=>1000), but using targeted assays (252).

1.7.5 Metabolomics analysis platforms

The two most commonly employed analytical platforms in metabolomics are mass spectrometry (MS) and Nuclear Magnetic Resonance (NMR) spectrometry.

1.7.5.1 Nuclear Magnetic Resonance (NMR) Spectroscopy

The principle behind Nuclear Magnetic Resonance (NMR) is certain nuclei (^{1}H, ^{13}C, ^{14}N and ^{31}P) demonstrate non-zero magnetic moments. This means that when placed in a magnetic field, these nuclei absorb electromagnetic energy in the radio wavelength range and then re-emit this at the same frequency. The frequency of this absorption is dependent on the strength of the magnetic field, the type of atomic nucleus and the nearby electronic environment surrounding the nucleus. The most commonly used type of NMR in metabolomics is ^{1}H-NMR due to hydrogen being present in most organic metabolites and the very high abundance (99.98%) of the ^{1}H isotope (258). During a ^{1}H-NMR experiment, samples are placed in glass tubes in

between two powerful superconducting cryomagnets which bring all protons within the sample into alignment. A radiofrequency (RF) pulse signal is transmitted into the sample, which is absorbed by protons, altering their magnetization vector. After the pulse the vectors return to equilibrium, emitting their absorbed RF energy and this is known as free induction decay (FID) which can be measured by a detector. This signal is transformed into a frequency using Fourier Transformation (FT) and each proton in an organic molecule has a unique frequency or chemical shift which is measured in parts per million (ppm) units (254). A typical ^{1}H-NMR spectrum is shown in Figure 7 and is a plot of chemical shift on the *x*-axis and signal intensity on the *y*-axis. The area under the NMR spectral peaks is directly proportional to the molar concentration of the protons within each compound and highly accurate concentrations can be calculated by adding an internal chemical standard such as Trimethylsilyl-propanoic acid **(**TMSP) or 4,4-dimethyl-4-silapentane-1-sulfonic acid (DSS) (259).

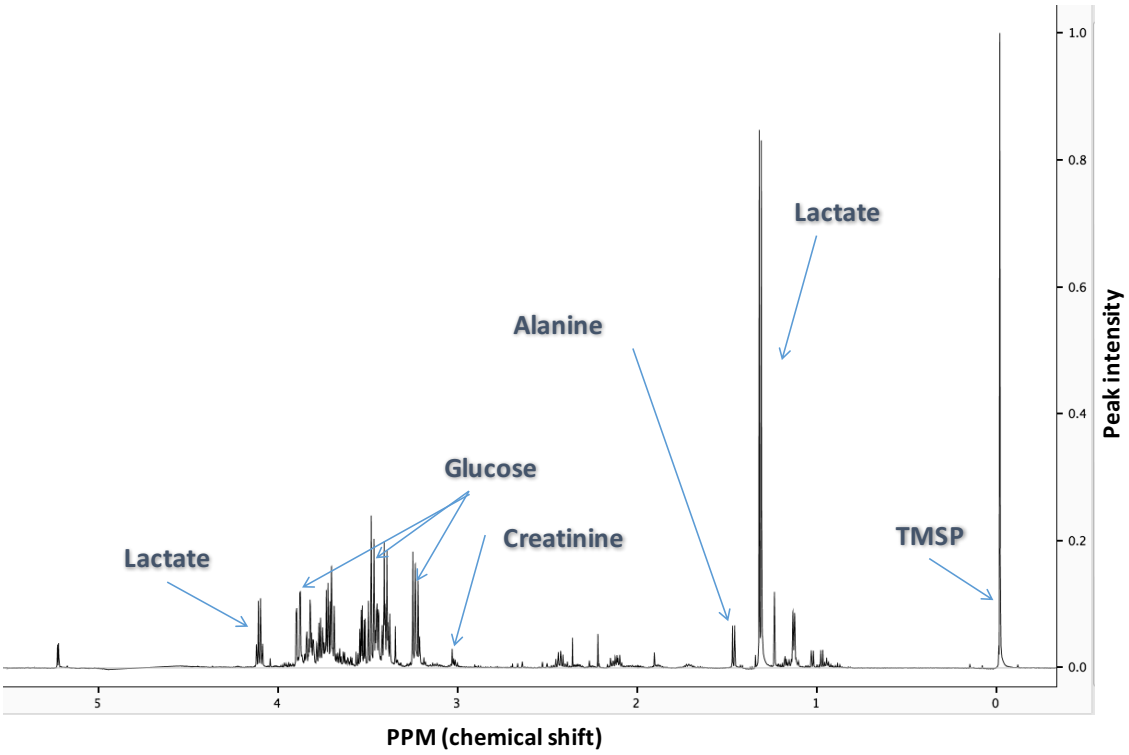

Figure 11-7. Typical ^{1}H-NMR spectrum of a serum sample with key spectral peaks annotated.

1.7.5.2 Mass spectrometry

In simple terms, mass spectrometry (MS) measures the mass-to-charge ratio (*m/z*) of positively or negatively charged ions formed from the analytes of interest. In the field of metabolomics, samples are often complex mixtures of metabolites, necessitating the coupling of MS to a chromatographic separation technique such as liquid chromatography (LC), gas chromatography (GC) and capillary electrophoresis (CE). Liquid-chromatography mass spectrometry (LC-MS) is the most widely used method in metabolomics studies due to its ability to separate a broad range of metabolites, provide quantitative and structural information and achieve ρg/mL sensitivity (260). LC allows separation of metabolites based on the rate at which they elute from a solid stationary phase within a liquid mobile phase. The stationary phase is a chromatography column packed with particles through which is passed the sample

and the mobile phase solvent. The polarity of molecules is related to their structure and electron charge distribution and this property determines how they interact with the stationary and mobile phases. The differing affinities of molecules for the two phases determines how fast they will transit through the column, which is termed their retention time (RT). Dependent on the classes of metabolites of interest different column chemistries can be applied to improve their resolution and reduce peak widths.

The most commonly applied column chemistries are reversed-phase (RPLC), which employ a non-polar stationary phase (e.g. C_{18}) and mobile phase solvent which is aqueous, allowing greatest retention of non-polar metabolites (261). The mobile phase can be either of constant composition (isocratic) or the composition may be varied during the separation (gradient elution) which improves resolution for complex mixtures (262). One of the main issues with RPLC is that polar metabolites, such as organic acids or amino acids, are relatively poorly retained and are not well resolved. To tackle this, Hydrophilic Interaction Chromatography (HILIC) is increasingly being used in metabolomics studies, increasing the coverage of the metabolome, particularly the urine metabolome (261). HILIC utilizes a hydrophilic stationary phase with gradient elution running from less polar organic solvents to increasingly aqueous solvents, thus increasing retention of polar analytes (263).

In standard LC, a number of key factors influence the resolving power of the technique including: column length and diameter, particle size, stationary and mobile phase chemistry and temperature (252). Advances in the field of liquid

chromatography in the 1970's led to the development of High Pressure Liquid Chromatography (HPLC), which combined high pressure pumps with stronger columns (264). Further developments led to the introduction of Ultra-High Performance Liquid Chromatography (UHPLC) with enhanced separation, greater resolution and faster analysis times. UHPLC combines sub 2 μm particle size, short length columns and improved instrumentation capable of withstanding high pressures up to 15,000 psi (265).

In addition to the various options for the coupled chromatography methods above, there are a multitude of MS instrument designs. The key aspects of the MS workflow are an ion source which generates charged species from the sample metabolites and a mass analyser in combination with a detector to accurately measure the mass of each ion species. The exact combination used will depend on the sample type (fluid, tissue etc.), the desired mass resolution, accuracy and analysis speed. Ion sources for fluid samples include Electrospray Ionisation (ESI) and Atmospheric Pressure Chemical Ionisation (APCI). ESI is the most commonly used source in LC-MS metabolomics and samples are generally analysed in both positive and negative ion modes to optimize results for different metabolite sub-classes (261). The commonly used instruments for metabolomics studies include Quadrupole (Q), Triple Quadrupole (QQQ), Time-of-flight (TOF), hybrid Q-TOF and ion-trap instruments. The QQQ and Q-TOF instruments are advantageous in being able to perform MS/MS experiments to gain additional structural information for biomarker elucidation (266). In such experiments, intact ions can be fragmented using collision induced dissociation (CID) and their mass analysed improving accuracy of metabolite

identification (262). Ion trap MS instruments are extremely high resolution and are able to trap and accumulate ions of low abundance to permit MS or MS^n analyses. Two ion traps most useful in metabolomics studies are the Penning trap, used in Fourier Transform Ion-cyclotron Resonance (FT-ICR) (267) and the Orbitrap, invented by Makarov (268).

1.7.5.3 Comparison of NMR and MS for metabolomics

MS and NMR are able to analyse a range of sample types including biofluids and tissues in-vivo or ex-vivo. GC-MS extends the capability to gas analysis, useful for example in breath analysis. NMR has a number of advantages as an analytical platform for metabolomics. It is highly reproducible allowing cross instrument and inter-lab studies to be performed. It provides highly accurate quantitative measurement of a broad range of metabolites with the use of a single internal standard. Its sensitivity is not affected by the hydrophobicity or pKa of samples and provides large amounts of structural information for compounds. NMR is non-destructive to the sample, allowing multiple replications of experiments and has relatively quick sample preparation and data acquisition. In MS the sample is destroyed during analysis and interacts with the instrument causing response variation during runs. It is therefore vital to include quality control (QC) procedures to adjust for this variability.

In untargeted studies MS has a number of advantages over NMR which has lower resolution so is most useful to detect the most abundant metabolites in samples. MS

provides increased coverage of the metabolome, being able to detect a large mass range from 20 – 1500 Da and typically identify hundreds to thousands of metabolites per sample compared to <100 by NMR. Advances in NMR probe technology, higher frequency instruments and 2D-NMR techniques are however increasing the sensitivity of this technique (252). The compromise of increased metabolome coverage is less accurate quantification of metabolites, in untargeted analyses data are typically semi-quantitative offering only relative concentrations. For accurate quantification in MS, internal standards are required for each metabolite of interest.

1.7.6 Metabolomics studies of thermal injury

Metabolomics approaches have been used to study burn injury and to date at total of four studies have used untargeted strategies. The first study was published in 2009 by Righi and colleagues, who applied a novel solid state NMR technique called adiabatic Total through Bond Correlation Spectroscopy (TOBSY) to study metabolic changes in a murine hind-limb burn model (269). In this study mice were subjected to a 5% TBSA hind-limb burn and underlying muscle and contralateral healthy muscle was harvested 3-days post-injury. They demonstrated elevated levels of intra-myocellular lipids (IMCLs) in muscle from burned mice consistent with known TAG-FFA cycling and lipolysis following burn injury. They also showed elevated levels amino acid anti-oxidants, glutathione, taurine, hypotaurine, which they speculate is related to increased mitochondrial stress and ROS production post burn. Other findings of the study include elevated glycine, phosphocreatine and ceramide in muscle tissue from the burned limb, the latter being an apoptotic second messenger, possibly reflecting burn induced muscle apoptosis. Watanabe and colleagues in

2011, aimed to use NMR metabolomics to study post-burn muscle metabolism in an *in vitro* myotube model (270). The study focused on muscle tissue metabolic responses to inflammatory cytokines (TNF-alpha and IFN-gamma) and the effects of intervention with des-acyl ghrelin. It is thus difficult to evaluate whether these findings are relevant to the complex systemic inflammatory and hypermetabolic response that occurs in-vivo following burn injury.

Human metabolomics studies of thermal injury have been lacking until the recent publication of a ^{1}H-NMR metabolomics study from a group in China (271). This study analysed blood samples from a cohort of 21 patients with severe burns (mean burn size 77% TBSA) and used multivariate analysis techniques to compare changes in the plasma metabolome with data from just 3 healthy volunteers. The study identified 12 metabolites significantly discriminating between burn injured subjects and controls and the most significant of these were α-ketoisovaleric acid, 3-methylhistidine and β-hydroxybutyric acid. Despite some experimental flaws in the study and no attempt to correlate changes in the metabolome with the outcomes of their study group, the study shows the potential of metabolomics as an approach to study burn injury.

Only one study has used metabolomics as an approach to the study of sepsis post-burn. Liu and colleagues used UPLC-Q-TOF MS metabolomics with the aim of identifying a biomarker panel diagnostic of sepsis in a rat 30% scald injury model (272). Caecal ligation puncture (CLP) was used as a model of polymicrobial sepsis. They performed metabolomics analysis of plasma samples and used multivariate analysis techniques to compare four groups: sham injury, burn injury, sepsis and

combined burn and sepsis. Univariate analysis showed a total of 9 metabolites that were significantly elevated in groups compared to sham injury. The most promising sepsis biomarker metabolites from the study were uracil and nitrotyrosine, both being elevated in sepsis and sepsis/burn injury but not elevated in burn injury alone. There have been no human metabolomics studies specifically looking at sepsis in the context of burn injury, but a number of studies have been published recently using the approach to study human sepsis. These studies have been conducted in neonates (273), children (274), adults with trauma (275) and adults with pneumonia (276-278). Metabolomics approaches have shown promise in identifying candidate biomarkers in the diagnosis of human septic shock (279,280) and in predicting mortality from human sepsis (277,281,282).

1.8 Summary and Thesis aims

Survival following severe burn injury has improved significantly over the last 70 years (283) and some argue survival gains have plateaued (284), though mortality in older patients remains stubbornly high. There is now an increasing shift towards focusing on reducing morbidity and other complications of burn injury. Adults and children with >20% TBSA burns are still experiencing high rates of infection and multiple organ failure (285) and sepsis remains a significant problem with high mortality (286). A step change is required to push improvements in burn care further and to improve the prognosis for older burn patients. Recent systems biology and omics based studies are just starting to increase our understanding of the complex systemic response to injury (51). The hypermetabolic response to injury and subsequent immuneparesis is responsible for a significant part of the morbidity associated with major burns and current treatments cannot fully ameliorate these effects. In order to

develop more effective therapies, for this profound disturbance of metabolism and immunity, new holistic approaches are needed to gain new insight. Metabolomics is one approach that is ideally suited to look at global changes in metabolism following thermal injury and reveal clinically useful diagnostic and prognostic biomarkers. No studies to date have used this technique to study the early post-burn response in relation to outcomes and to look at longitudinal changes weeks to months post-injury. The technique is also an important tool in the armamentarium to identify novel sensitive and specific biomarkers of disease and these are so desperately needed to improve the early recognition of sepsis in the burn injured patient.

The aims of this thesis are therefore to:

1. Determine the impact of age on clinical outcomes for burn injured patients via a retrospective analysis of outcomes and epidemiology of a population of older burn injured patients admitted to our regional burns centre;
2. Investigate the early changes in the metabolome following thermal injury in young and old adults with severe burns and their association with clinical outcomes;
3. Investigate the key longitudinal changes in the metabolome following severe thermal injury in young and old adults to identify new biological information regarding the metabolic response to thermal injury;

Chapter 2: Outcomes of burn injury in the elderly

Chapter 2: Outcomes of burn injury in the elderly

2.1 Introduction

The United Nations estimate that the proportion of the world population aged over 60 years will triple to reach two billion by 2050 (287). In the UK, the proportion of the population aged >65 years is currently 17 % and it is predicted that this will rise to 23 % by 2035. Moreover, the 'oldest old', those 85 years and over, are the fastest growing group with a projected two-and-a-half-fold increase in size of this age group to 3.5 million by 2035 (288).

An increasingly ageing population will have substantial global implications on health care systems and burn care provision. The elderly are particularly susceptible group to sustaining burn injury due to impairments in judgment, co-ordination, balance and reaction times together with reduced ability to escape from harm . Following their injury, lower physiological reserves and co-morbid disease may complicate their management and recovery [4]. Age itself is a major prognostic factor after burn injury. After controlling for percentage total body surface area (TBSA) burned and the presence of inhalation injury, it is a powerful independent predictor of mortality [5-7]. Age has therefore been included in most prognostic scoring systems of burn survival [8-11]. Elderly patients, who survive their injury, experience significantly increased morbidity, particularly from infectious complications such as pneumonia [12]. They are more likely to stay in hospital longer, are discharged back home less often and an age dependent increase in the use of post-hospitalization resources has been shown [13-14].

Survival following burn injury has improved in recent decades due to advances in burn care; including resuscitation; early excision and wound closure; nutritional support; skin substitutes; and modulation of the hypermetabolic response [15]. However, improvements in survival are lagging behind in the elderly [15-19]. Prior to embarking on a prospective study investigating the pathophysiology of the response to burn injury in elderly patients, we wanted to explore the demographics, epidemiology and outcomes of a recent cohort of such patients. We previously published a small cohort of elderly burn admissions admitted between 1999 and 2003, which showed an observed mortality rate of 34.9 % [20].

The aim of this study was therefore to:

1) Determine admission demographics and outcomes of a recent cohort of elderly patients admitted to the Birmingham Burn Centre with burn injury.

2) Compare epidemiological data and outcomes for elderly burns admissions during the 2004-2012 period with the previously published cohort.

2.2 Materials and methods

2.2.1 Study Group

Patients aged 65 years and above admitted to the Birmingham Burns Centre with acute burns from 1st January 2004 to 31st December 2012 were identified from the International Burn Injury Database (IBID) and Hospital Episode Statistics (HES). Between January 2004 and June 2010, all patients were admitted to the Burns Centre based at Selly Oak Hospital, Birmingham, UK. For the remainder of the study, patients were admitted to the Burns Centre at its location in the new Queen Elizabeth Hospital Birmingham (QEHB), Birmingham, UK. Patients admitted with non-

cutaneous burns, skin-blistering conditions and those with no medical notes available for review were excluded. Additionally, patients in whom a comfort care decision was made within 24hrs of their admission were excluded from the analysis. The exclusion criteria for the study group was identical to that used in the previously published cohort of elderly burn patients treated between 1999-2003 [20].

2.2.2 Patient management

The aspects of patient management described below have not changed between the two study periods. However, during the second period of study, clinical guidelines were formalized for the treatment of inhalation injury, nutritional support, blood product transfusion and thromboprophylaxis. The fluid resuscitation calculation employed was the Parkland formula (4mLs/kg/% TBSA) for all patients with burns ≥15 % TBSA, however in cases where there was a history of cardiovascular disease, balanced fluid resuscitation was initiated at 2mLs/kg/% TBSA. Invasive central venous pressure and arterial blood pressure monitoring was utilized for all patients requiring fluid resuscitation. Target urine output was 0.5ml/kg/hr.

Decisions regarding excisional surgery were made once a full medical history was obtained from informants and a review by a Consultant anaesthetist specializing in burn care. Patients with full thickness burns who were deemed unsuitable for surgical excision in the first two weeks post-injury were treated with daily topical application of silver sulfadiazine (SSD)/cerium nitrate. The goal of this approach is to maintain a dry adherent eschar until the patient has been medically optimized for excisional surgery. Inhalation injury was primarily diagnosed on clinical grounds if there was history of entrapment in a house or industrial fire or explosion in an enclosed space together

with clinical signs e.g. carbonaceous sputum, respiratory symptoms and signs and change in voice [21]. However, patients requiring mechanical ventilation had further confirmation of the diagnosis by fibre-optic bronchoscopy according to the minimum presence of carbonaceous deposits and erythema within the bronchi [22]. All decisions regarding the withdrawal of active care were made by a minimum of two Consultants, at least one being a Consultant Burn surgeon.

2.2.3 Data collection and statistical analysis

Data on patient demographics, burn injury details, co-morbidities, timing of surgery, complications and outcomes, including length of stay (LOS) and in-hospital mortality was extracted from the medical notes and IBID. The revised Baux score [8], Abbreviated Burn Severity Index (ABSI) score [10], Belgian Outcomes in Burn Injury (BOBI) [11] score were calculated for each patient along with a Canadian Study of Health and Aging (CSHA) Clinical Frailty Scale score [23]. Data was collated in a Microsoft® Excel® spreadsheet (Microsoft® Corporation, Redmond, WA) and statistical analysis was performed using PASW Statistics version 18 (SPSS Inc., Chicago, Illinois, USA). Data was obtained from the previously published 1999-2003 cohort [20] and comparisons were made with the current data set.

The lethal area 50 (LA_{50}), a measure of burn survivability for the TBSA at which there will be 50 % mortality, was calculated using both probit analysis and logistic regression analysis as previously described [15]. In brief, probability unit (probit) analysis uses data on a dichotomous outcome and one or more explanatory variables to predict the outcome probabilities based on the assumption that their

probits are linearly related to the values of the explanatory variables. The logit of a probability *p* is the value of log (*p*/1-*p*). Binary logistic regression analysis uses data on a dichotomous outcome and one or more explanatory variables to predict the outcome probabilities based on the assumption that their logits are linearly related to the values of the explanatory variables. A single logistic regression analysis, with age and TBSA burn as continuous explanatory variables, was performed. To enable valid comparisons with previous data this study follows the format of previous studies produced by this group.

Categorical variables were compared using Fisher's exact test and continuous non-parametric variables were compared using a Mann-Whitney U-test. To assess the effects of age, TBSA and inhalation injury, we constructed multi-variable logistic regression analysis models. Odd ratios were also calculated using these models. Data is presented as medians and interquartile ranges (IQR) unless stated. Statistical significance was considered at a probability of p-value <0.05.

2.3 Results

2.3.1 Demographics

A total of 250 patients aged 65 years and above were admitted during the study period. After 22 exclusions (12 patients had a burn injury that was deemed non-survivable and medical case notes were unavailable for 10 patients) case-notes were reviewed for the remaining 228 patients (116 males and 112 females) (Figure 2.1). Females were significantly older than males (80.6 years vs. 76.9 years, p=0.047), but there was no significant difference in burn size. The extracted data is summarized in Table 2.1. Co-morbid disease was present in 185 patients on admission (Figure 2.2a)

and the median CSHA Clinical Frailty Scale score was 3.5 (IQR 3-4). The most common mechanism of injury was by flame (40%) followed by scald (26%) and contact (17%) (Figure 2.2b).

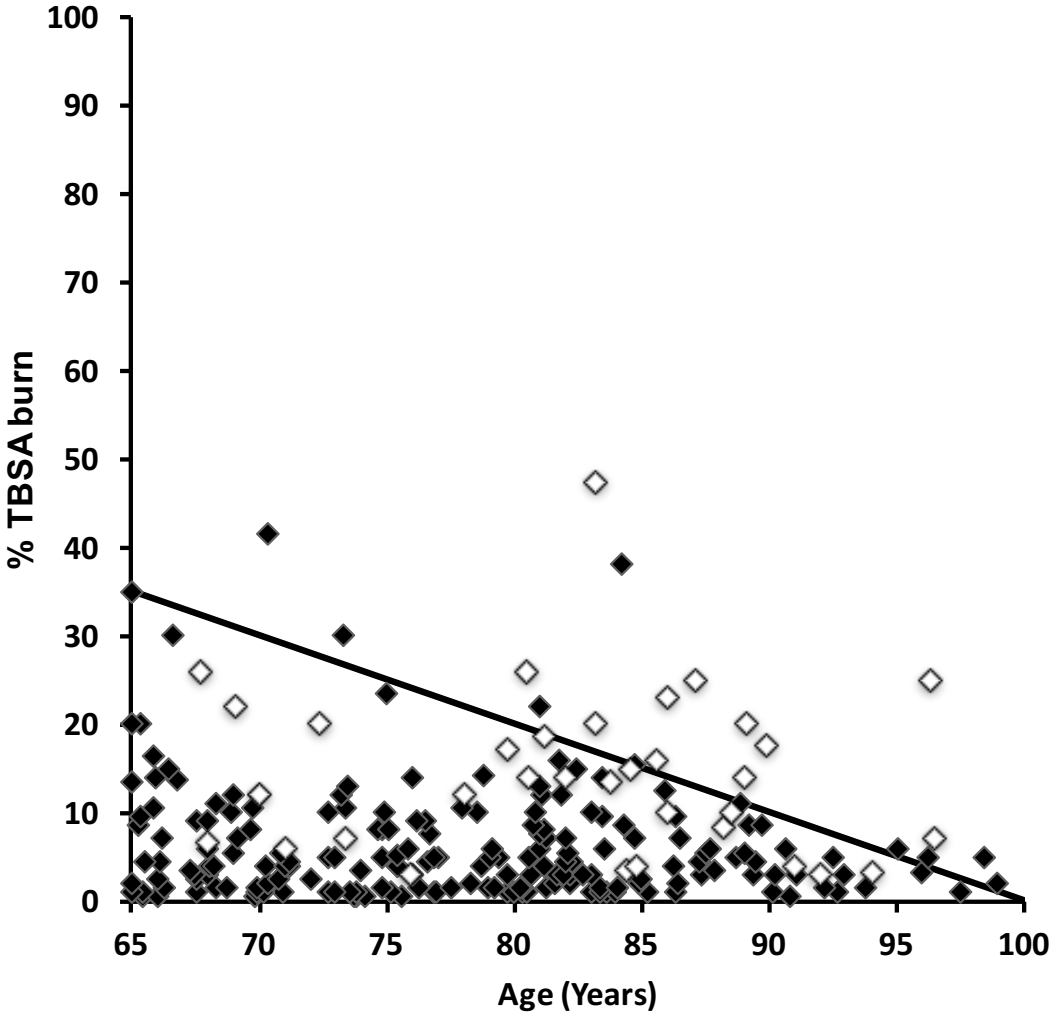

Figure 2-1. Scatter plot of percentage total body surface area (TBSA) burn versus age for elderly burn injured patients admitted during the study period. Black markers represent survivors and white markers represent non-survivors. Solid black line indicates the patient age + percentage total body surface area burn = 100.

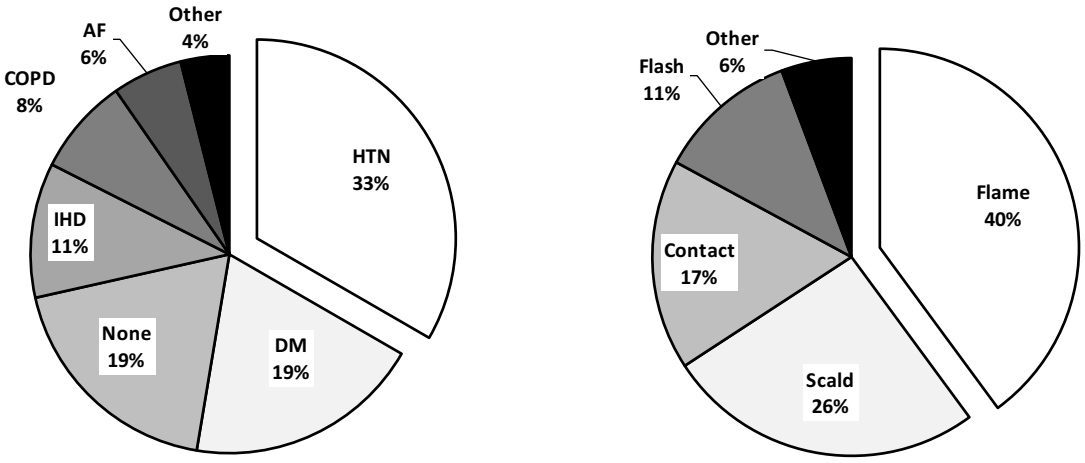

Figure 2-2 (a) Recorded co-morbidities and (b) aetiology of burn injury in elderly burn patients admitted from 2004-2012. HTN = hypertension; DM = diabetes mellitus; IHD = ischaemic heart disease; COPD = chronic obstructive pulmonary disease; AF = atrial fibrillation.

Parameter		**1999-2003**	**2004-2012**	***P-value***
Number of patients	n	63	228	
Male	n (%)	28 (44)	116 (51)	0.395
Age	years	81 (74-87)	79 (71-84)	0.095
TBSA	%	7 (5-11)	5 (2-10)	<0.001
Co-morbidities	%	87	81	0.35
Inhalation injury	n (%)	9 (14)	29 (13)	0.833
ABSI score	/18	7 (6-8)	7 (6-8)	0.753
BOBI score	/10	3 (2-3)	3 (2-3)	0.900
Revised Baux score	*	91 (83-97)	86 (78-96)	0.021
Surgery	n (%)	30 (48)	113 (50)	0.887
Time to 1° excision	days	6 (4-10)	5 (2-8)	0.046
SSD/CN dressings	n (%)	18 (28)	62 (27)	0.874

Table 2-1. Comparison of admission characteristics, surgical treatment and length of hospital stay (LOS) between the two cohorts 1999-2003 and 2004-2012. All values are medians with inter-quartile ranges (IQR), or proportion as a percentage in parentheses. TBSA = total body surface area; ABSI = abbreviated burn severity index; BOBI = Belgian outcome in burn injury; SSD/CN = Silver sulfadiazine/Cerium nitrate; * = Age + Percent Burn + 17 $^{\$}$ ($^{\$}$If Inhalation Injury = Yes)

2.3.2 Outcomes in the study group

The observed mortality for the study group was 14.9 %. Using probit analysis, the LA_{50} for the study group was 26 % TBSA (95% CI 17-89 %). The highest mortality (50%) was seen in patients with burns >20% TBSA. Mortality was lower in the surgically treated group compared to those that were managed non-surgically. Of the 192 survivors living independently pre-injury, 70 % were discharged successfully back home, 15 % were transferred to other hospitals to complete their care and the remainder required intermediate or higher level care. Complications occurred in 26 % of patients with 129 recorded complications in total: the most common being pneumonia (11 %) and urinary tract infection (6 %).

Parameter		**1999-2003**	**2004-2012**	***P-value***
LOS survivors	days	17 (7-33)	12 (4-30)	0.094
LOS survivors/% TBSA	days	3.1 (1.0-5.7)	2.4 (1.3-5.2)	0.987
Mortality				
Overall	n (%)	22/63 (34.9)	34/228 (14.9)	0.001
Burn TBSA 0-5%:	n (%)	1/19 (5.3)	6/121 (5.0)	1.000
Burn TBSA 5-10%:	n (%)	6/27 (22.2)	7/52 (13.5)	0.350
Burn TBSA 10-20%:	n (%)	11/12 (91.7)	14/41 (34.1)	<0.001
Burn TBSA >20%:	n (%)	4/5 (80.0)	7/14 (50.0)	0.338
Surgical mortality	n (%)	7/30 (23.3)	13/113 (11.5)	0.135
Non-surgical mortality	n (%)	15/33 (45.5)	21/115 (18.3)	0.003

Table 2-2. Comparison of outcomes between 1999-2003 and 2004-2012 cohorts. LOS = Length of stay; TBSA = Total body surface area

The commonest causes of death were respiratory failure, pneumonia and sepsis (Table 2.3). Non-survivors were significantly older, had a larger overall TBSA and a greater proportion sustained inhalation injury compared to the survivors (Table 3). There was an association between increased TBSA and mortality with the OR increasing for each successive TBSA group (Figure 2.3). As well as this, the mortality was higher in the inhalation injury group (52 %) than in the non-inhalation injury group (10 %; $p<0.001$). Using the same multivariate model, inhalation injury was associated with an OR of 10.8 (95% CI: 3.8-30.8). Almost equal numbers of patients underwent surgical management (n=113) with excision and skin-grafting compared to non-surgical management (n=115), which are summarized in Table 4. The LA_{50} values calculated for the age-groups 65-74 years, 75-84 years and over 85 years, showed an inverse relationship to age as expected (Figure 2.4).

Primary cause of death	**n**	**%**
Respiratory failure	10	29
Pneumonia/chest sepsis	9	26
Sepsis other	4	12
Multiple-organ failure	2	6
Major burns	2	6
Acute renal failure	2	6
Unknown	2	6
Cardiac failure	1	3
Myocardial infarction	1	3
Perforated duodenal ulcer	1	3

Table 2-3. The reported cause of death in elderly burn admissions 2004-2012.

Parameter		Survivors	Non-survivors	*P-value*
Number of patients	n	194	34	
Male:female	n:n	99:95	17:17	
Age	years	77 (70-83)	84 (77-89)	0.001
TBSA	%	5 (2-9)	14 (7-20)	<0.001
BSA:FT	%	1 (0-3)	7 (0-14)	<0.001
Inhalation injury	n (%)	14 (7)	15 (44)	<0.001
ABSI score	/18	7 (6-7)	8 (7-9)	<0.001
BOBI score	/10	3 (2-3)	2 (2-3)	0.620
Revised Baux score	*	84 (76-93)	103 (96-112)	<0.001
Patients treated surgically	n (%)	100 (52)	13 (38)	0.193
Injury to excision	days	5 (2-8)	3 (1-6)	0.759

Table 2-4: Comparison between burn survivors and non-survivors in the 2004-2012 cohort. All values are medians with inter-quartile ranges (IQR), or proportion as a percentage in parentheses. TBSA = total body surface area; BSA:FT = body surface area: full thickness; ABSI = abbreviated burn severity index; BOBI = Belgian outcome in burn injury.

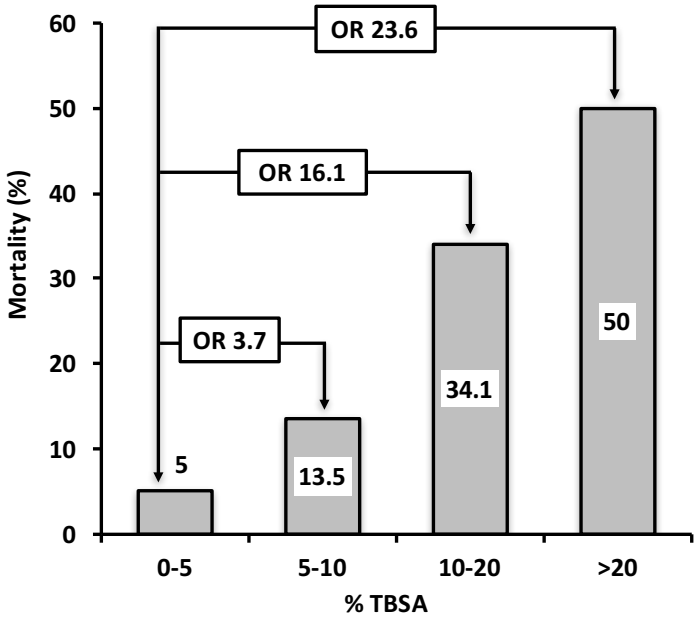

Figure 2-3. Observed mortality rate stratified by burn size group (percentage TBSA). Odds ratios of mortality (OR) calculated by multi-variable logistic regression as compared to the smallest burn-size group. TBSA = total body surface area.

Parameter		Surgical	Non-surgical	*P-value*
Number of patients	n	113	115	
Age	years	75 (69-83)	81 (74-86)	<0.001
TBSA	%	7 (3-12)	4 (2-7)	<0.001
BSA:FT	%	2 (1-4)	0 (0-2)	<0.001
Co-morbidities	%	84	85	0.856
No. co-morbidities	n	2 (1-3)	2 (1-3)	0.086
Inhalation injury	n (%)	16 (14%)	13 (11%)	0.556
ABSI score	/18	7 (6-8)	7 (6-7)	0.007
BOBI score	/10	3 (2-3)	3 (2-3)	0.676
Revised Baux score	*	85 (78-96)	88 (78-97)	0.427
Mortality	%	11.5	18.3	0.193
LOS	days	17 (9-35)	7 (2-14)	<0.001
LOS/% TBSA	days	2.8 (1.7-5.5)	1.5 (0.8-4.0)	<0.001

Table 2-5. Comparison of burns patients treated surgically compared to non-surgical management 2004-2012 cohort. All values are medians with inter-quartile ranges (IQR), or proportion as a percentage in parentheses. TBSA = total body surface area; BSA:FT = body surface area: full thickness; ABSI = abbreviated burn severity index; BOBI = Belgian outcome in burn injury; LOS = length of stay.

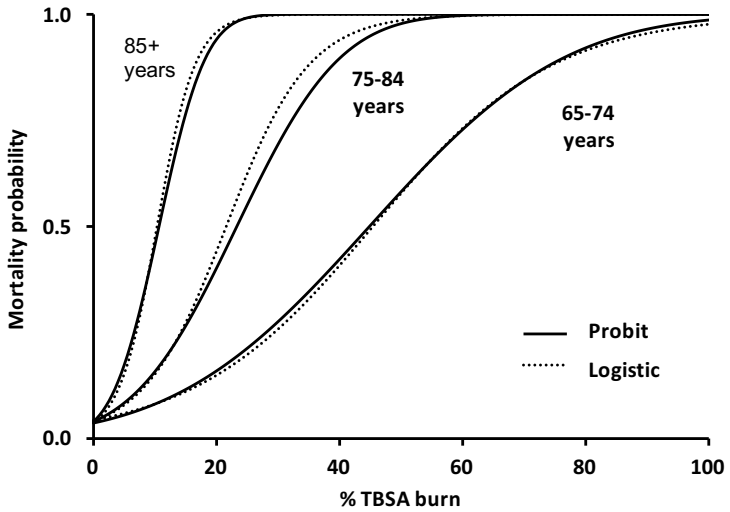

Figure 2-4. Comparison of logistic regression (dotted lines) and probit analysis (solid lines) for mortality probability in different age-groups (85+ years, 75-84 years and 65-74 years) when related to percentage total body surface area (TBSA) burn.

2.3.3 Comparison to previously published data

The admission characteristics of elderly burn injured patients between the two study periods (1999-2003 and 2004-2012) were comparable in terms of age and gender (Table 2.1). The average burn size was smaller in the more recent cohort reflected in a significant difference in revised Baux scores (p=0.021). The aetiology was similar with flame and scalds predominant in both cohorts, however an increased incidence of flash burns was seen (2 % versus 11 %; p=0.014). Burns to the head and buttocks became more common, but burns to the lower limb and perineum became less frequent. The overall observed mortality decreased from 34.9 % to 14.9 % (p=0.001). When stratified into burn size groups (minor (<5 % TBSA), small (5-10 % TBSA), medium (10-20 % TBSA) and large (≥20 % TBSA)), reductions in mortality were seen in all groups, but the difference was significant in the medium burn size group (p<0.001). Mortality reduced in surgically treated patients from 23 % to 11.5 % (p=0.135) and in non-surgically managed patients from 45.5% to 18.3% (p=0.003) the difference being statistically significant in the latter group. Comparing surgical management, there was no change in the proportions of patients managed surgically, however the median time to first excisional surgery reduced from six to five days (p=0.046). There was no significant difference in the proportions of patients treated with topical silver sulfadiazine-cerium nitrate, which includes patients who required late surgery after eschar separation.

2.3.4 Comparison with previously published studies

A literature search of the MEDLINE and EMBASE journal databases was conducted using OVID (https://ovidsp.ovid.com/) and using the keywords ‘elderly’, ‘geriatric’,

‘aged’ AND ‘burn*’ OR ‘thermal injury’ OR ‘burn injury’. Articles published in English after the year 2000 to present day were reviewed and key data extracted. Articles that did not include key demographic (lower age cut off and burn size) and mortality outcome data were excluded. A total of 16 studies were identified that met the inclusion criteria (table 2.6) and the lower age cut-off used varied across studies from 55-75 yrs. The smallest cohort reported included only 59 patients (289) and the largest was a study from the US National Burn Repository database (NBR) of 23,180 patients (6). Flame burn was the common mechanism of sustaining a burn in 69% (11/16) of the studies. Only two studies reported scald as the most common mechanism and both were from China (289,290). The average burn size reported was very variable and ranged from 7.6% TBSA in a study from Northern Ireland (291) up to 23.0% TBSA in a large study from the USA (292). Mortality rate was the only outcome that was consistently reported across all studies and ranged from 48% in a study from Chile (141) to 6.8% in at study from China (289).

Comparing our 2004-2012 cohort to other studies from other developed world burn centres, our mean burn size is one of the smallest published, but similar (7.5 vs 7.6 % TBSA) to a cohort published in 2009 by a group in Northern Ireland. Our observed mortality is also comparable to this cohort and also other developed world cohorts from the USA (6) and Australia (293).

	Author	Study Period	Origin	Age group	n	Mean age (y)	Inhalation injury (%)	TBSA (%)	Mortality (%)
(a)	**Wearn *et al*, 2014**	2004-2012	UK	≥65 y	228	78.5	13	Mean 7.5	14.9
	Albornoz *et al*, 2011 [25]	2006-2009	Chile	>65 y	66	--	28	Median 13.0	48.0
	Khadim *et al,* 2009 [26]	1996-2005	UK	≥65 y	143	76.7	7	Mean 7.6	12.5
	Lumenta *et al*, 2008 [27]	1990-2003	France	≥65 y	265	76.5	17.7	Mean 17.1	30.6
	Macrino *et al*, 2008 [28]	2003-2006	USA	≥65 y	179	75.4	23	Mean 10.6	16.0
	Rao *et al*, 2006 [20]	1999-2003	UK	≥65 y	63	80.4	14	Mean 9.9	34.9
	Chang *et al,* 2005 [29]	1998-2002	USA	>65 y	94	76.1	21.3	Mean 15.5	23.4
(b)	**Lionelli *et al,* 2005 [30]**	1972-2000	USA	≥75 y	201	81.0	27	Mean 23.0	47.0
	Mahar *et al*, 2008 [31]	2002-2006	Australia	≥70 y	80	79.5	19	Mean 15.5	18.8
(c)	**Liu *et al*, 2013 [32]**	2003-2009	China	≥60 y	103	69.5	13.6	Mean 19.7	11.7
	Yin *et al,* 2010 [33]	1996-2004	China	≥60 y	201	69.3	--	Mean 11.7	8.0
	Wong *et al*, 2007 [34]	2000-2005	China	≥60 y	59	--	--	Mean 12.0	6.8
	Mabrouk *et al*, 2003 [35]	1995-2001	Egypt	≥60 y	97	64.5	12	Mean 21.4	31.9
	Wibbenmeyer *et al*, 2001 [17]	1977-1996	USA	≥60 y	308	71.5	16	Median 13.0	30.2
	Ho *et al*, 2001 [36]	1993-1999	China	≥60 y	94	73.8	4.3	Mean 13.3	7.4
(d)	**Pham *et al,* 2009 [13]**	1991-2005	USA	≥55 y	23,180	--	11.3	Mean 9.6	17.1
	Lundgren *et al*, 2009 [37]	1999-2003	USA	≥55 y	325	68.0	11.3	Mean 14.9	18.5

Table 2-6. Summary demographic and mortality data for published studies of elderly burn injured patients since 2000, subdivided by age group cut off studied: a) ≥65 years b) ≥70 and ≥75 years c) ≥60 years and d) ≥55 years. TBSA = total body surface area.

2.4 Discussion

The Birmingham Burns Centre is a high-throughput burn centre in the UK admitting approximately 450 patients with burn injuries every year and has a long pedigree of publishing analyses of its mortality data [15,24-26]. The main finding from our study is an improvement in observed mortality compared to the previously published cohort (1999-2003). The mortality rate was reduced in all TBSA groups. This improvement follows the continued trend of improved burn survival in all age-groups over the last 65 years at our institution [15]. We believe this improvement is partly attributable to changes in injury severity of admitted patients, but also to technological advances, improved infrastructure and implementation of clinical guidelines.

Firstly, the proportion of smaller burn size admissions has increased from 30 % to 53 % in the more recent study period (p=<0.001). This increase in the proportion of minor elderly burn admissions may be due to an increased number of referrals of smaller injuries from peripheral hospitals. Following the National Burn Care Review report in 2001 [40], the British Burn Association published national referral guidelines which stated that patients >60 years of age and those with co-existent disease e.g. cardiac limitation, respiratory limitation and diabetes should be referred to a specialized burn service. It may also reflect an increasing need to admit patients with smaller injuries due to increasing demands of an ageing population on the social care system but we have no data to support this hypothesis. In order to examine this, it would be useful to obtain data on pre-injury living status versus discharge status for the two cohorts.

The results of our study show a reduction in the time from injury to first burn excision, from a median of six, down to five days. It is unclear if this modest change has had an impact on elderly burn survival as the number of deaths in our study prohibited the use of multivariate logistic regression analysis taking into account all key confounders of age, % TBSA burn and inhalation injury, to fully examine its effect. Moreover, despite early burn excision being a modern paradigm of burn care, the question as to the benefit of this approach specifically in the elderly remains unanswered with several early studies showing mortality benefit [41-42] and others since showing no benefit [43-46]. Recent advances in peri-operative medicine, anaesthesia and surgical techniques may allow elderly patients to be more safely negotiated through an early surgical approach that has been shown to be beneficial in younger age groups [47]. In addition, during the second cohort, early Geriatric medicine and specialist anaesthetic support allowed optimization for early surgical intervention. Within our anaesthetic team a number of specialists have developed a special interest in elderly burn care and this has made an impact on outcomes of surgery in this group of patients.

All patients have benefited from the implementation of clinical guidelines including thromboprophylaxis, nutrition, infection control, antibiotic prescribing, gastro-protection and treatment of inhalation injury. Patients managed in the ICU have also benefited from increased adoption of lung protective ventilation strategies [48] and the increased use of care bundles to prevent and treat complications such as sepsis and ventilator associated pneumonia [49-50]. Between the two study periods, there have been improvements in infrastructure and systems within our hospital trust.

These include the creation of a critical care outreach team, allowing smoother transition of patients stepping down from ICU level care and earlier recognition of deterioration in ward patients. Information technology has undoubtedly had an impact, with the introduction of an electronic clinical decision support system during the early part of the second study period. This comprehensive rule based system combines drug prescribing, laboratory results, radiology, operation notes and clinical observations and has revolutionized patient care at our centre [51]. The system generates real-time early warning scores (EWS) to alert the medical team to any deterioration and the critical care outreach team automatically if thresholds are met.

Pre-existing or co-morbid disease has previously been shown to have an impact on the survival of the elderly burn patient. The number of co-morbidities appears to be an important independent predictor for the development of in hospital pneumonia, which is associated with increased risk of mortality [13]. We and other groups have shown the number of co-morbidities to influence burn survival [20, 38] and a recent study of 66,611 patients from the UK IBID database has shown that ≥3 pre-existing conditions is associated with an odds of death of 2.381 [52]. The number and type of co-morbidities are clearly important variables, however, they are confounded by the varying impact on the individual patient. An important concept within geriatric medicine is frailty, which is a multi-dimensional syndrome resulting in loss of reserve in multiple organ systems that increases an individuals vulnerability [23]. Clinical frailty scoring (FS) gives us information on the biological age of patients and has been shown in elderly burn patients to be an independent predictor of burn mortality [53,54] and risk of discharge to a skilled nursing facility [54]. In this study we

retrospectively assessed clinical frailty from the patient records using the Canadian Study for Health and Ageing (CSHA) clinical frailty scale and showed that non-survivors have a significantly higher median frailty score than survivors. This adds further weight to the existing literature (140,294) demonstrating the importance of this measure in determining outcomes in the elderly burn patient and further prospective research is warranted to investigate this more rigorously.

A review of the published cohorts of elderly patients admitted with burn injury worldwide since 2000 (table 2.6) revealed interesting differences across the world in terms of definitions of elderly and injury characteristics. Flame burns were the most common mechanism of injury except in China, where several groups have shown scald injuries to be more common. This may have a bearing on the lower mortality rates observed compared to other cohorts in addition to the linked observation of lower incidences of inhalation injury, which is widely excepted to impact on mortality. Variability was seen in the average size of burn and this may be confounded by national or even regional differences in healthcare provision and burn referral and admission policies. It is possible that in some countries with a higher incidence of burn injury in the population and therefore higher demands on burn services, only patients with more severe injuries are admitted.

Due to the confounding effects of age, inhalation injury, burn size and possibly differences in frailty and co-morbid disease, it is difficult to make direct comparisons of outcomes between burn centres based only on the observed mortality rate. Moreover, there are differences between countries in approaches to palliative care

and in many of the reviewed studies, it was unclear if early non-survivors were included in the datasets. If we had included the 12 patients in whom a very early (first 24hrs) decision to treat the patient with comfort care only then the overall observed mortality rate would indeed be higher at 19.1% (46/240). As expected, these were more severely injured patients with a mean TBSA of 65% (+/-8), mean age of 79 years (+/-4) and 100% had inhalation injury. Very few of the studies attempted to calculate the LA_{50} value for their cohort, an approach developed at the Birmingham Burns Centre (13) which takes into account burn injury size of the cohort. Another group, took the concept a step further in using the Baux score (age + burn size TBSA) and calculating the $Baux_{50}$ which also takes into account the influence of age on mortality (295).

Improvements in overall mortality rate and the LA_{50} in elderly burn patients reflect a continuing trend across all age groups at our burn centre and worldwide. This improvement appears to be related to an increased proportion of smaller burn injury referrals but is also likely to have been impacted by improvements in surgical, anaesthetic and critical care and local infrastructure. There is a trend towards earlier burn excision, which may have contributed to these improved outcomes but further research is needed into the potential benefits of this approach in this age group. Although mortality improvements have been shown, it is evident from the change in the LA_{50} over time in this age group, that these gains are lagging behind those seen in children and younger adults. Research priorities must therefore include obtaining a more complete understanding of the pathophysiological responses to burn injury in the elderly and how they compare to younger age groups. One important area to be

targeted is the impact of frailty on outcomes and whether an early assessment of frailty might aid in the stratification of care approaches. Also given the importance of infections and sepsis in determining outcomes in patients with burns, further study is needed on the age-associated decline in immune function, termed immunesenesence (143), in older patients with burn injury. Further clinical research is also needed into the benefits of early burn wound excision in the elderly in the context of improvements in peri-operative and critical care.

Chapter 3: NMR Metabolomics Analysis of the early metabolic response to severe thermal injury

3. NMR Metabolomics Analysis of the early metabolic response to severe thermal injury

3.1 Introduction

Severe thermal injury involving more than 30% of the total body surface area (TBSA) is associated with significant metabolic dysfunction, termed the hypermetabolic response (HMR) (38). The HMR begins after the initial shock or *'ebb'* phase following thermal injury, typically 3-5 days after injury and is characterized by a hyperdynamic circulation (296), increased metabolic rate (297) and increased core body temperature (193). This accompanies significant derangements in glucose synthesis, uptake and utilization (298); lipid metabolism (168), increased skeletal muscle proteolysis (234) and futile substrate cycling (194).

Evidence to date points to multiple mediators in the induction and maintenance of the highly conserved HMR and is felt to be an attempt to 1) maintain normothermia in the context of massive skin loss and 2) provide adequate substrates to fuel wound healing processes. These mediators include the pro-inflammatory cytokines such as IL-6 and IL-1β acting synergistically with the elevated levels of stress hormones: noradrenaline, adrenaline, glucagon and cortisol. The increases in metabolic rate have been measured as increases in resting energy expenditure (REE) (193) and have been shown to be more pronounced following thermal injury as compared to other forms of trauma (299) and may be prolonged for up to 2 years post-injury (42).
The consequences of the HMR for the thermally injured patient, include massive calorie consumption requiring early nutritional support, loss of lean body mass (LBM) and skeletal muscle wasting (41). The dramatic metabolic disturbances and loss of

LBM result in growth impairment in children, liver dysfunction, immune dysfunction, poor wound healing and resultant increased risk of infections, sepsis and mortality (300). A wealth of studies to-date have identified key metabolic defects including increased peripheral insulin resistance, a switch to protein catabolism as a major source of fuel with inefficient oxidation of lipids in contrast to starvation states. In addition, stable isotope studies have demonstrated that during the HMR, glycolytic-gluconeogenic cycling is increased by 250% and triglyceride-fatty acid cycling is increased by 450% (194). Pharmacological therapies try to ameloriate this maladaptive response include the use of anabolic agents such as insulin, oxandralone, propranolol and growth hormone (300). These therapies, in addition to the modalities of ambient temperature control, early enteral nutrition and early burn excision and grafting have no doubt contributed to improved outcomes for patients suffering severe burns. However, complete amelioration of the response has not been possible due to an incomplete understanding of this complex response.

Recognizing the complexity of human responses to trauma and thermal injury, researchers are starting to employ an array of systems biology approaches to try to gain more biological insight and identify novel therapeutic strategies. A number of genomic studies, using DNA microarray data from the Glue grant Host Response to injury study have led the charge in this data-driven approach with a number of new insights (301). These include a shift away from the post-injury temporally separate SIRS/CARS phase paradigm, with the genomic data showing pro-inflammatory genes and anti-inflammatory gene expression changing simultaneously within hours of injury (51). Metabolomics is another systems biology approach which focuses on

analysis of all small products of metabolism in biological systems (302) and has been recently applied to study groups of critically ill patients with acute lung injury, (303,304), ARDS (305) and sepsis (278,306,307). Individual metabolites and metabolite profiles derived from this approach can predict clinical outcomes in critically ill patients with high accuracy (281,308). We hypothesized that a metabolomics approach could be used to study early metabolic dysfunction in patients with severe thermal injury and that it could generate metabolite profiles predictive of later clinical outcomes.

3.2 Aims and objectives

1. To identify the key changes in the serum metabolome in the acute phase after severe human thermal injury in adults (aged 16-64 years) with severe burns (>15% TBSA).
2. To assess the utility of metabolomics in the prediction of later clinical outcomes in burn injury (Survival, MOF, Sepsis).

3.3 Methods

3.3.1 Study group

Patients included in the study were recruited as part of a UK multi-centre observational study called the SIFTI study (*Scientific Investigation of biological pathways Following Thermal Injury*) (UKCRN ID: 13654) and were admitted to the adult Burns Centre at Queen Elizabeth Hospital Birmingham (QEHB), UK (2012-2014). The studies in this thesis include two cohorts of patients recruited to the SIFTI

study: 1) Adults aged 16-64 years presenting with ≥15% total body surface area (TBSA) burns; 2) Elderly patients aged ≥65 years with ≥1% TBSA full-thickness burns (but <15% total TBSA). The data presented in this chapter are obtained from only 'adult patients' and analysis of data from 'elderly patients' is presented in Chapter 5.

Patients initially unable to consent to the study due to lack of capacity (injury severity, unconsciousness due to intubation) were recruited through a legal consultee advice process until they regained capacity to consent themselves. As a comparison group, six healthy volunteers (aged 18-64) underwent blood sampling in the morning between the hours of 8-10am. For each volunteer, age (years), sex, height (m), weight (kg) and body mass index (BMI) (kg/m^2) was recorded.

3.3.2 Treatment of subjects

Patients received treatment according to standardized local burn care guidelines which includes fluid resuscitation with Hartmann's solution according to the Parkland Formula (4mLs/kg/% TBSA burn), invasive monitoring of arterial blood pressure (BP) and central venous pressure (CVP) and thromboprophylaxis with low-molecular weight Heparin (LMWH). Resuscitation targets were urine output 0.3-0.5 mLs/kg/hr and mean arterial pressure (MAP) of >60 mmHg. Patients with persistent oliguria or hypotension despite adequate crystalloid volumes were given 5% human albumin solution (HAS) and inotropic support with noradrenaline. All patients received early enteral nutrition according to standard formulae in addition to enteral

supplementation of glutamine and intravenous supplementation of trace elements until wound closure. Patients requiring surgery underwent burn excision within 72hrs of admission and coverage with split-thickness skin autograft. Patients with burns >40% TBSA typically required wound coverage with combinations of autograft, cadaveric allograft and skin substitutes.

3.3.3 Data Collection

Patient demographics, burn injury details and clinical outcomes were recorded prospectively using case-report forms (CRF). Key outcomes included:

- In-hospital mortality
- Sepsis - American Burn Association (ABA) 2007 consensus trigger criteria (309)
- Multiple organ failure (MOF) - Denver 2 MOF score (33)
- Hospital length of stay (LOS)
- Intensive care LOS (ICU-LOS)
- Mechanical ventilation days
- Time to organ recovery (TTR).

3.3.4 Sampling

During the study, study day 1 (D1) was defined as the calendar day of injury and day 2 (D2) the second calendar day and so forth. All patients underwent an initial blood sampling within 24hrs of their injury. A second blood sample was taken in the morning (8-10am) between 48 and 96hrs post-burn, either on D3 or D4. Patients

admitted to the intensive care unit (ICU) had 6ml blood samples collected from the indwelling arterial catheter using a Vacuette® blood collection system into Vacuette® Z-serum clot activator tubes (Greiner Bio-One Ltd, Gloucester, UK). Patients admitted to burns ward beds typically did not have insertion of arterial catheters and therefore 6 mL blood samples were collected by peripheral phlebotomy using an arm tourniquet using the same blood collection system and tubes as above. Healthy volunteers were sampled in the same way. Blood samples were kept upright and allowed to form clot at room temperature for 30mins before processing.

3.3.5 Sample processing

Blood samples were allowed to clot for 30 minutes at room temperature with the tubes placed upright and were then centrifuged at 3000 rpm for 10 minutes at 20°C in a swinging bucket rotor centrifuge (Eppendorf Centrifuge, model 5804 R, ThermoFisher Scientific). Aliquots of 400-600 µl were placed in 1.5 ml plastic cryovials and stored upright in a freezer at -80°C. When ready for batch processing, frozen serum aliquots of 400 µl were removed thawed gently on ice. Nanosep® Omega 3000 Da (Pall Lifesciences, UK) molecular weight cut-off (MWCO) filters were prepared by washing 6 times with 500 µl of deionized water at 38°C and centrifugation in a benchtop centrifuge at 3000 x g for 15 minutes at room temperature. This step was necessary to remove any glycerol from the membrane. Following the final wash, any residual water was poured off and extra care was taken to ensure all filter membranes were free from visible water droplets.

Serum samples were vortexed and 250 µl pipetted into a fresh sterile 1.5 ml centrifuge tube. Tubes were then centrifuged at 4°C, 15,000 g for 5 minutes. Finally 200 µl of the supernatant was taken from the middle of the sample (taking care to avoid the lipid rich layer at the top) and loaded centrally onto the washed Nanosep® filter. Filters were then centrifuged at 10,000 xg for 15 mins at 4°C. Finally 1.5 ml glass champagne vials were labeled and 15 µl of 4x concentrated NMR buffer added (NMR buffer: D_20/H_20 (40%) containing 2,2,3,3-tetradeuteropropionic acid [TMSP] (2mM) sodium azide (0.4% w/v) and sodium phosphate (100mM) pH 7.0). A 45 µl aliquot of each serum filtrate was then pipetted into a glass champagne vial and gently mixed by pipetting. Vials were then stored upright at -80°C until ready for spectroscopic analysis.

3.3.6 NMR Spectroscopy

Champagne vials containing prepared serum were defrosted at room temperature and the order of the samples randomized. A 35 ul aliquot of sample was loaded into 1.7 mm SampleJet glass NMR tubes (Bruker Corp., USA) using a Bruker Autosampler robot (Bruker Corp., USA). NMR tubes were cleaned with filter paper and methanol to remove dust and the 96-tube rack placed in the Bruker SampleJet sample changer at 6°C. One- dimensional (1D) ^{1}H NMR spectra were acquired at 300 K using a standard spin-echo NOESY (Nuclear Overhauser Effect SpectroscopY) pulse sequence with water suppression using pre-saturation on a Bruker AVANCE II 600 MHz NMR spectrometer (Bruker Corp., USA) equipped with a 1.7 mm cryoprobe. Spectral width was set to 12 ppm and scans were repeated 128 times.

3.3.7 Pre-processing of NMR spectra

The 1D-NMR spectral data was imported into MATLAB V2013a (MathWorks, Natick, USA) and were pre-processed using software packages called NMRLab (V3.5) (310) Metabolab (V3.5) (311). Spectra were individually inspected and any abnormal spectra were excluded e.g. spectra with significant artefact from protein content. Spectra were autophased and then calibrated by aligning TMSP peak to 0 ppm. Baseline correction was applied using a spline fit, the water region and TMSP standard peaks were removed and spectra were truncated to 0.8-10 ppm). Spectra were then aligned using a MATLAB algorithm *ic*oshift (312) and divided into 0.005 ppm (2.5 Hz) chemical shift bins. Spectral normalization was performed using Probabilistic Quotient Normalization (PQN) (313) and a g-log transformation was applied (Parsons et al., 2007). The data were then assembled into a data matrix, each row representing an individual bin.

3.3.8 Statistical analysis of metabolomics data

Data analysis was performed using PLS Toolbox software Version 7.5.2 (Eigenvector Research, INc. Manson, USA) running in MATLAB (Release 2013a, Mathworks, Natick, USA). Data bins were mean-centred and subjected to first unsupervised analysis using principle components analysis (PCA) (314) and scores plots constructed. PCA, also known as singular value decomposition (SVD) or eigenvector analysis, allows an initial overview and decomposition of the multi-variate data, identification of major sources of variation in the data, reveal possible clustering of samples and identification of outliers (315). Outliers are defined as those falling outside of the 95% confidence interval of the Hotelling's T-squared (T2) distribution.

This is seen as an ellipse on the PCA scores plot (315). Outliers were then removed from subsequent supervised multi-variate analyses as these can bias the resulting models masking true differences between classes. Loadings plots were also constructed which can be used to identify NMR spectral peaks that are responsible for clustering or separation among the sample set (254).

Data were also analysed using Partial Least Squares Discriminant analysis (PLS-DA) and orthogonal PLS-DA (OPLS-DA). Both techniques are supervised classification methods that aim to create models that explain the maximum covariance between the metabolite dataset (x) (predictor variables) and two or more classes (training variables) e.g. burn injured patients and healthy control groups. OPLS-DA is a modification to PLS-DA which separates the systematic variation in the dataset into two components: 1) *the predictive component* – summarizes variation in the dataset that is related to discrimination of classes 2) *the orthogonal component* – this summarizes variation in the dataset that is unrelated to the class response and therefore unhelpful in class discrimination. The advantages of this modification are easier interpretation of models and in highlighting unexpected systematic variability as a result of biological variation or experimental bias (316). These techniques are prone to model over-fitting of that data and therefore cross-validation was applied using 10-fold Venetian blinds cross-validation which randomly selects and excludes blocks of the data from the model to determine its accuracy in assigning class membership (317). PLS-DA and OPLS-DA outputs can be visualized graphically in the form of scores plots constructed from two or more latent variables (LVs) which are linear combinations of the original variables preserving as much co-variance between the dataset (X) and the classes (Y) as possible from the original dimensions

(318). These plots are also outputs from PCA and allow identification of patterns, clustering and outliers in 'statistical space'. The loadings vectors from PCA, PLS-DA and OPLS-DA are visualized on loadings plots which can be used for identification of the NMR spectral signals and thus metabolites responsible for separation or clustering of samples (254).

The performance of PCA, PLS-DA and OPLS-DA models was evaluated with metrics provided by the PLS-Toolbox software including the R^2 and Q^2 metrics. R^2 is the percentage of variation explained by the model, a quantitative measure of well the models are able to mathematically reproduce the data in the dataset (319). Q^2 is the predicted variation or quality of prediction and was obtained through cross-validation. A Q^2 value of >0.5 shows good predictive ability but >0.9 is outstanding; the difference between Q^2 and R^2 is also important and this should not exceed 0.2-0.3 (319). In order to evaluate the discriminatory power of the multi-variate models to predict class groups (e.g. burn patient vs. healthy control) confusion matrices were constructed and accuracy (%), sensitivity (%), specificity (%), negative predictive value (NPV) and positive predictive value (PPV) were calculated. In addition, Receiver Operator Characteristic Curves (ROC) were constructed using PLS-Toolbox and the area under the receiver operating curve (AUROC) values calculated for each model both before and after cross-validation.

In order to assess the most important contributing metabolites to multivariate models, we sought to identify the metabolite peaks with the highest contribution to each model using their variable importance in projection (VIP) scores (320,321). The metabolite peaks with the 20 highest VIP scores >1 in each model were then

identified from the 1D NMR spectra using Human Metabolome Database version 3.6 (www.hmdb.ca) and Chenomx NMR suite (Chenomx, professional version 4.0, Chenomx Inc, Canada).

3.3.9 Statistical analysis of demographic data

Demographic and injury data were compared using SPSS v23.0 statistical software (IBM, USA). Datasets were assessed for normal distribution using the Shapiro-Wilkes test. Parametric data are displayed as means with standard deviation and groups compared using the Independent Samples T-Test. Non-parametric data are displayed as medians with interquartile range (IQR) and groups compared using Mann-Whitney U-test. Categorical variables were compared using Fisher's exact test. Statistical significance was considered at a probability of p-value <0.05.

3.4 Results

3.4.1 Demographics and outcomes

A total of 37 patients were included in this cohort with a mean age of 36 (+/-12) years, a male:female ratio of 1.6:1 and mean burn size of 39.2 (+/-21.9) % TBSA. The demographics of the cohort are summarized in Table 3.1. The majority of patients sustained flame burns (78%) with the remainder of injuries being due to flash or scald mechanism (Figure 3.1). In terms of outcomes, 10 patients did not survive their admission giving a mortality rate of 27%. A total of 16 patients (43%) experienced at least one episode of multiple organ failure (MOF) and 19 patients (51%) experienced sepsis. The outcomes for the study cohort are summarized in table 3.3 and the demographics of the outcome groups are summarized in Table 3.2 (survivors vs. non-survivors), Table 3.4 (sepsis vs. no-sepsis) and Table 3.5 (MOF vs. no MOF). Demographics for the healthy volunteers are summarised in Table 3.6.

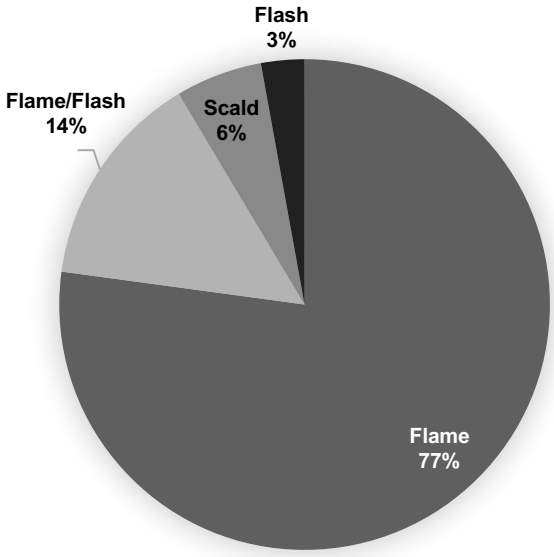

Figure 3-1. Mechanism of injury.

Admission parameters	Values
n	37
Age (years)	36.0 (+/- 12.0)
Male n (%)	23 (62)
BMI (kg/m^2)	26.2 (+/-4.6)
TBSA (%) (IQR)	38 (22-54)
TBSA-FT (%) (IQR)	17 (7-50)
Inhalation injury n (%)	17 (46)
ICU Admission n (%)	23 (62)
APACHE II first 24hrs (IQR)	26 (9-30)
SOFA first 24hrs (IQR)	7.0 (2-11)
Denver MOF first 24hrs (IQR)	2 (0-3)
R-Baux	83.0 (+/-31.1)
ABSI (IQR)	8 (6-11)
BOBI (IQR)	3 (1-5)

Table 3-1. Demographic and injury data. Abbreviations: APACHE (Acute physiology, age and chronic health evaluation score), SOFA (Sequential organ failure assessment) score, ABSI (Abbreviated burn severity of illness) score and BOBI (Belgian outcomes in burn injury) score.

Admission data	Survivors	Non-survivors	*p-value*
n	27	10	
Age (years)	32.4 (+/-11.2)	46.0 (+/-8.1)	0.001
Male n (%)	17 (63)	6 (60)	0.580
BMI (kg/m^2)	25.5 (+/-4.6)	27.9 (+/-4.8)	0.173
TBSA (%)	27.5 (17.0-45.0)	50.0 (44.5-62.8)	0.004
TBSA-FT (%)	15.0 (4.5-36.0)	50.0 (36.8-60.0)	0.001
Inhalation injury n (%)	8 (30)	9 (90)	0.002
ICU Admission n (%)	13 (48)	10 (100)	0.006
APACHE II first 24hrs	17 (7-28)	31 (30-35)	<0.001
SOFA first 24hrs	5 (1-10)	13 (9-14)	<0.001
Denver first 24hrs	0 (0-3)	3 (2-6)	0.004
R-Baux	71.5 (+/-27.1)	114.2 (+/-17.0)	<0.001
ABSI	7 (5-8)	11 (10-12)	0.003
BOBI	1 (1-4)	5 (5-6)	<0.001

Table 3-2. Comparison of admission characteristics of survivors and non-survivors. Abbreviations: APACHE (Acute physiology, age and chronic health evaluation score), SOFA (Sequential organ failure assessment) score, rBaux (Revised Baux Score), ABSI (Abbreviated burn severity of illness) score and BOBI (Belgian outcomes in burn injury) score.

Outcome variable	Value
Mortality n (%)	10 (27)
MOF (Denver 2) n (%)	16 (43)
Time to organ recovery (days)	13.5 (+/- 20.8)
Sepsis n (%)	19 (51)
Number of septic episodes/patient (n)	2 (+/-2)
ICU LOS (days)	18.2 (+/- 24.9)
Mechanical Ventilation days	14.9 (+/- 22.8)
Hospital LOS (days)	45.9 (+/- 45.4)
LOS (days/% TBSA)	1.1 (+-0.8)

Table 3-3. Clinical outcomes for cohort of adults with ≥15% TBSA burns. Abbreviations: MOF (multiple organ failure), ICU (Intensive care unit), LOS (length of stay), TBSA (total body surface area).

Admission data	Sepsis	No sepsis	*p-value*
n	26	11	
Age (years)	37.9 (+/-12.5)	31.7 (+/-10.1)	0.159
Male n (%)	15 (58)	8 (73)	0.477
BMI (kg/m^2)	25.9 (+/-4.7)	31.7 (+/-10.1)	0.669
TBSA (%)	43.5 (27.3-55.5)	17.0 (16.0-31.0)	0.005
TBSA-FT (%)	31.5 (14.1-52.6)	11.0 (0.0-25.0)	0.019
Inhalation injury n (%)	15 (58)	2 (18)	0.036
ICU Admission n (%)	20 (77)	3 (27)	0.008
APACHE II first 24hrs	29 (18-30)	7 (2-18)	0.009
SOFA first 24hrs	10 (6-12)	1 (0-2)	0.006
Denver first 24hrs	2 (1-3)	0 (0-0)	0.033
R-Baux	92.3 (+/-27.8)	61.2 (28.6)	0.004
ICU LOS (days)	25.6 (+/-26.5)	0.9 (+/-2.1)	<0.001
Hospital LOS (days)	59.8 (+/-47.7)	13 (+/-5.6)	<0.001
LOS (days/TBSA)	1.3 (+/-0.8)	0.6 (+/-0.3)	0.001
MVD (days)	20.9 (+/-24.9)	0.72 (+/-2.1)	<0.001
Mortality	8 (31)	2 (18)	0.361
MOF	14 (54)	2 (18)	0.071

Table 3-4. Comparison of admission characteristics of septic and non-septic groups. Abbreviations: APACHE (Acute physiology, age and chronic health evaluation score), SOFA (Sequential organ failure assessment) score, rBaux (Revised Baux Score), LOS (length of stay), ICU (Intensive Care Unit), TBSA (Total body surface area burned), FT (full thickness burn), MVD (mechanical ventilation days)

Admission data	MOF	No MOF	*p-value*
n	16	21	
Age (years)	43.0 (+/-9.5)	30.7 (+/-11.2)	0.001
Male n (%)	9 (56)	14 (67)	0.733
BMI (kg/m^2)	28.0 (+/-4.6)	24.7 (+/-4.4)	0.034
TBSA (%)	51.0 (43.0-65.8)	23.0 (16.5-30.5)	<0.001
TBSA-FT (%)	42.4 (29.3-55.0)	13.0 (4.0-18.3)	<0.001
Inhalation injury n (%)	13 (81)	4 (19)	<0.001
ICU Admission n (%)	16 (100)	7 (33)	<0.001
APACHE II first 24hrs	30 (29-34)	10 (6-25)	<0.001
SOFA first 24hrs	11 (10-14)	2 (0-6)	<0.001
Denver first 24hrs	3 (2-4)	0 (0-2)	<0.001
R-Baux	111.8 (+/-20.2)	61.1 (+/-16.5)	<0.001
ICU LOS (days)	37.1 (+/-27.8)	3.9 (+/-6.2)	<0.001
Hospital LOS (days)	64.7 (+/-59.2)	31.6 (+/-24.0)	0.049
LOS (days/TBSA)	1.1 (+/-0.9)	1.1 (+/-0.6)	0.964
MVD (days)	31.2 (+/-26.9)	2.5 (+/-4.5)	0.001
Mortality	10 (63)	0 (0)	<0.001
Sepsis	14 (88)	12 (57)	0.071

Table 3-5. Comparison of admission characteristics of MOF and non-MOF groups. Abbreviations: APACHE (Acute physiology, age and chronic health evaluation score), SOFA (Sequential organ failure assessment) score, rBaux (Revised Baux Score), LOS (length of stay), ICU (Intensive Care Unit), TBSA (Total body surface area burned), FT (full thickness burn), MVD (mechanical ventilation days).

Parameter	Healthy controls	Patients	p-value[$]
n	6	25	
Age (years)	36.2 (+/-4.9)	34.7 (+/-2.2)	0.762
Male n (%)	3 (43)	15 (60)	0.669
BMI (kg/m^2)	24.1 (+/-0.6)	25.3 (+/-0.8)	0.277

Table 3-6. Comparison of demographics between burn injured patients and healthy controls. Abbreviations: BMI (Body mass index). $ = Fisher's Exact test for comparison of proportions, Independent samples T-test for comparison of means.

3.4.2 Changes in the early post-burn metabolome in young adults

A total of 79 blood samples were collected from 37 patients and 6 healthy controls. Metabolomics data were analysed from 69 patient serum and 6 healthy control samples, as 4 patient samples (5%) contained residual protein which perturbed the quality of the NMR spectra. The full pre-processed dataset was first subjected to PCA to identify any general trends or unexpected clustering. A 3 principle component (PC) model was able to explain the following percentages of variation: PC1 (18.32%), PC2: (14.05%), PC3 (11.63%) (Figure 3.2) after removal of 5 outlier samples that fell outside the Hotelling's T^2 ellipse. A PLS-DA model with 4 LVs discriminated between samples from the patients and healthy controls with 100% sensitivity and 100% specificity with scores plots confirming good separation of the two classes (R^2: 0.8, Q^2 0.6) (Figure 3.3). The AUROC for this model was 1.00 after 10-fold cross-validation, confirming the model accurately predicted samples as being from burn patients or healthy controls based on the metabolite peaks.

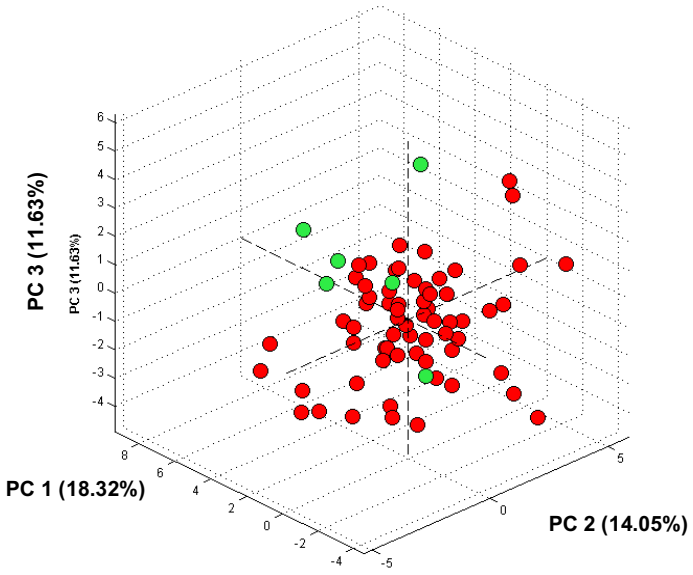

Figure 3-2. PCA 3D scores plot, 3-PCs. Adult severe burn samples and healthy control samples. Green circles = healthy controls, red circles = patient samples from adults with burn >=15% TBSA.

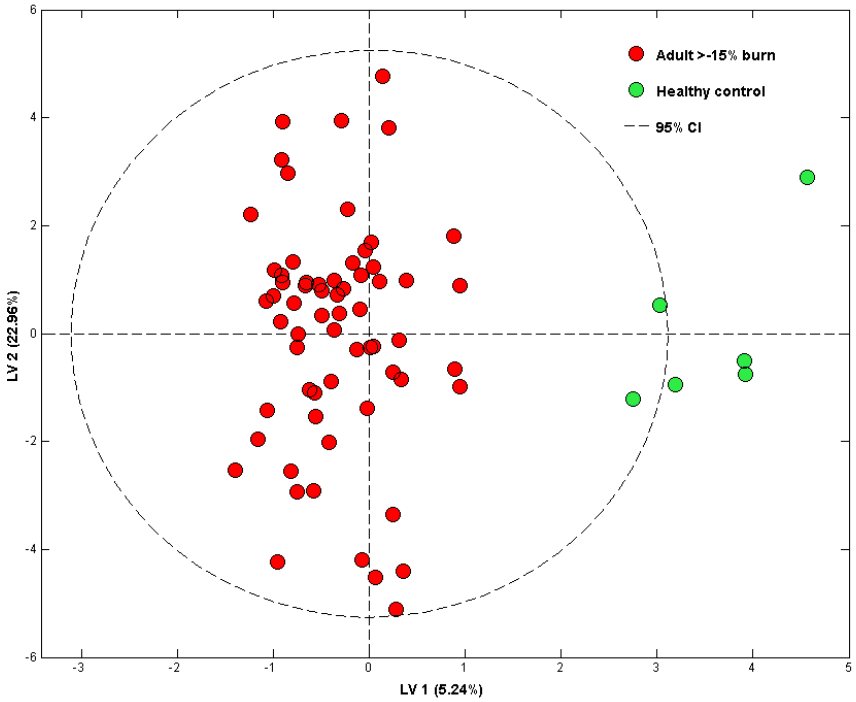

Figure 3-3. PLS-DA scores plot showing good discrimination of burn injured patient samples (red circles) and healthy control samples (green circles). Model sensitivity = 100% and specificity = 100% (R^2: 0.8, Q^2 0.6).

To study the influence of time of sampling from the time of injury, the samples were grouped as follows: 1) 0-24 hrs post-injury 2) 24-48 hrs post-injury, 3) 48-72 hrs post-injury 4) >72hrs post-injury. Using these classes PLS-DA analysis revealed a grouping of the 0-24hrs samples away from the other 3 groups which clustered together mostly separated by latent variable (LV) 1 (Figure 3.4). OPLS-DA was then performed, grouping the samples into two groups 1) 0.24 post-injury and 2) 24-84 hrs post injury and the model was able to discriminate between the two groups of samples with 97% sensitivity and 100% specificity (R2 0.8, Q2 0.5) (Figure 3.5). These results highlighted the need to use these two time-point groups separately for the clinical outcome prediction analyses.

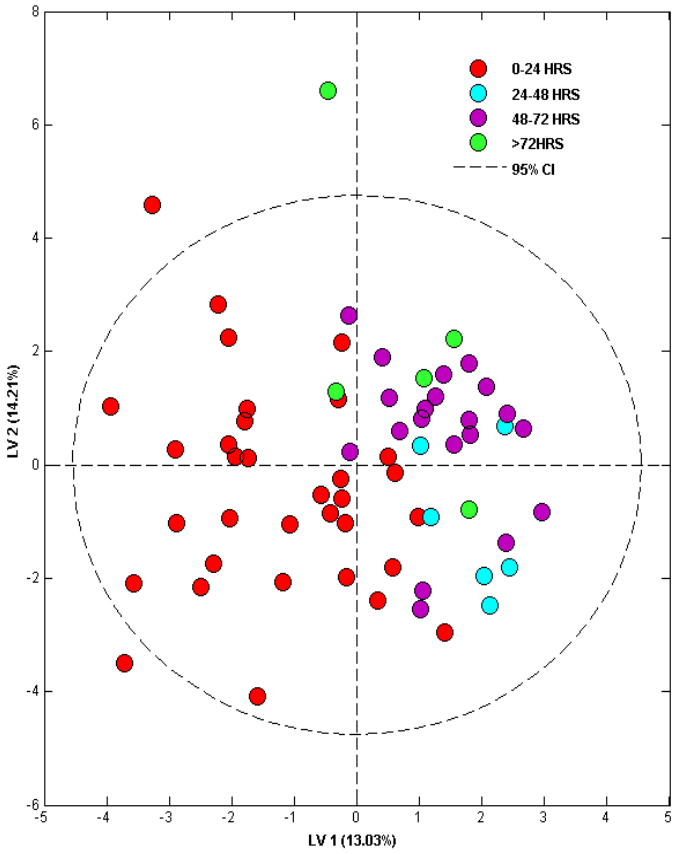

Figure 3-4. PLS-DA Scores plot with samples classified into four groups according to the time of sampling from the initial burn injury.

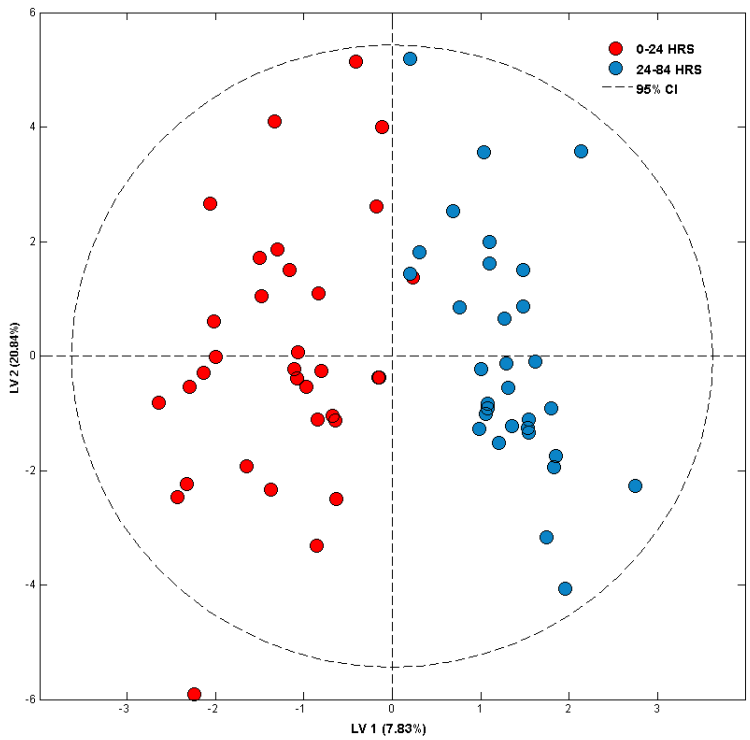

Figure 3-5. OPLS-DA Scores plot with samples grouped into 0-24hrs post-injury samples and 24-84hrs post-injury samples. The model shows good discriminatory ability to classify these time-point groups. (Sensitivity 97%, specificity 100%, AUROC 0.94, R2: 0.8, Q2: 0.5).

Given that time-dependent differences in the post-burn metabolome within the first 96hrs post-injury were demonstrated, a multi-variate analysis of the initial sample (taken ≤24hrs) metabolomics data in relation to healthy controls data was performed. OPLS-DA discriminated between the first 24hr patient samples (n=37 and matched control samples (n=7) with 100% sensitivity and specificity (5 LVs, Q2: 0.9, R2: 0.6, AUROC: 1.00, permutation test *p*=0.008). The scores plot from this model (Figure 3.6) shows good discrimination of the two groups and the VIP loadings plot (Figure 3.7) shows the key metabolite peaks contributing to the model.

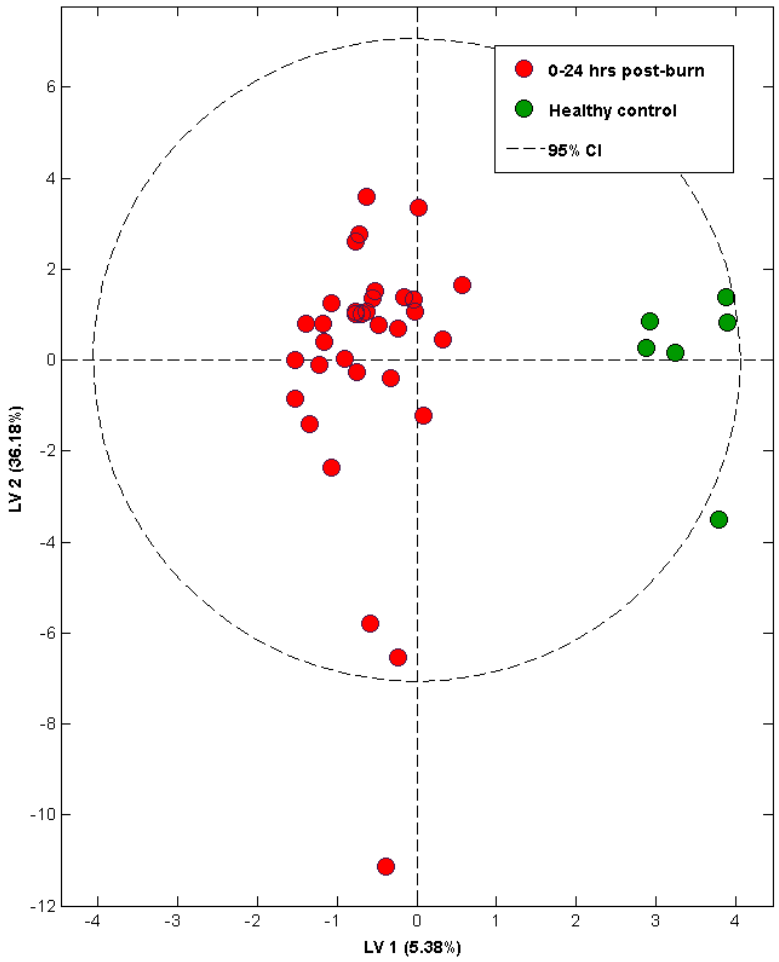

Figure 3-6. Scores plot of OPLS-DA of samples taken in the first 24hrs post-injury compared to healthy control samples showing good model discrimination (Q2: 0.9, R2: 0.6, p=0.008).

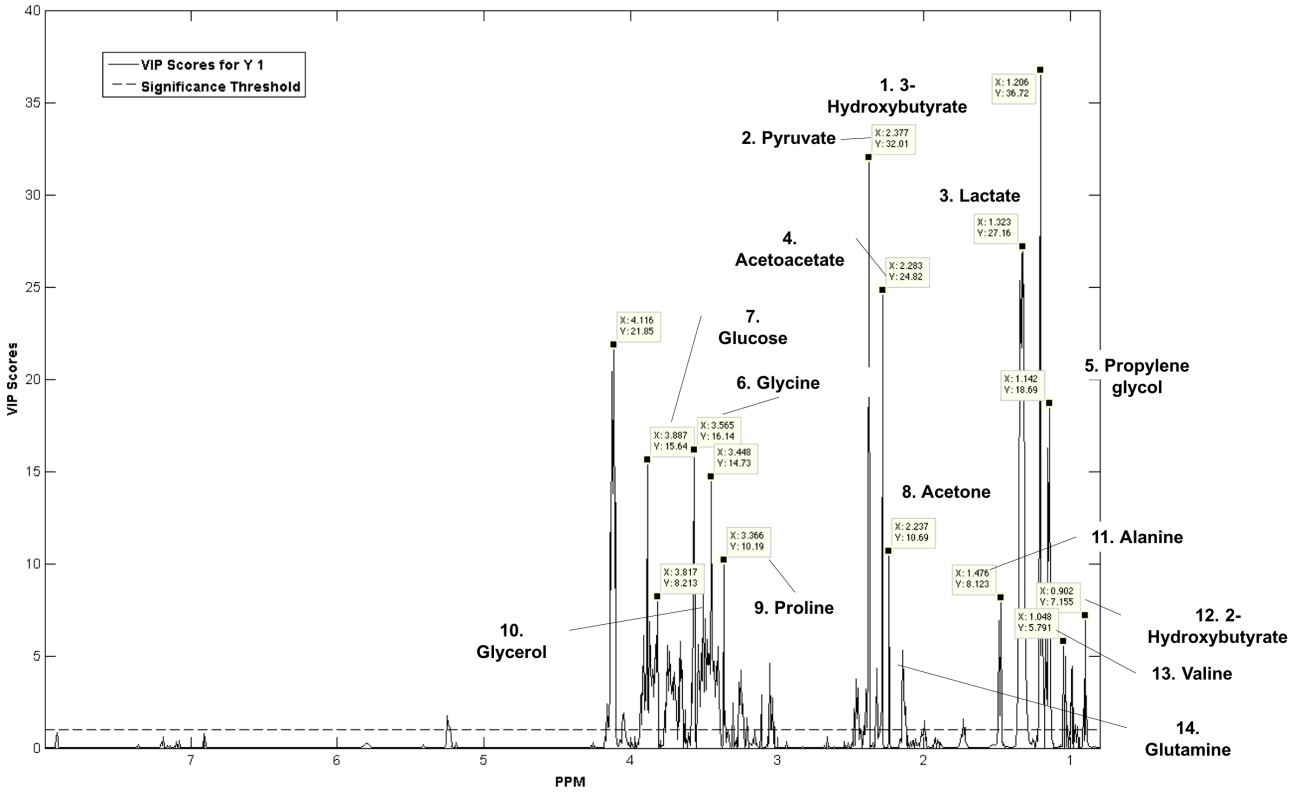

Figure 3-7. VIP (variable importance in projection) loadings plot from OPLSDA showing NMR spectral peaks contributing to the model. The height of the peaks corresponds to VIP score and therefore greatest contribution to the variance between the first 24hrs samples from burn patients and healthy controls.

Spectral fitting to identify metabolites was performed for NMR peaks falling within the top ranked 50 spectral bins according to their VIP score. A total of 14 unique serum metabolites fell within these bins and are listed in Table 3.7 and are ranked according to VIP scores. The chemical shift values (ppm) for all peaks identified for each metabolite in the top 50 spectral bins are listed. The model showed that ketone bodies (e.g. acetoacetate, 3-Hydroxybutyrate, 2-Hydroxybutyrate, acetone), lactate, glucose, pyruvate, glycerol and polyethylene glycol were higher in burn patients compared to controls. Amino-acid metabolites such as alanine, glycine, proline,

valine and glutamine were all lower in the burn patients compared to the controls.

Rank	Metabolite	Change[$]	VIP*	Chemical shift of peak bins (ppm)
1	3-Hydroxybutyrate	↑	36.72	1.17, 1.19, 1.21, 2.37
2	Pyruvate	↑	32.01	2.38
3	Lactate	↑	27.16	1.31, 1.32, 1.33, 1.34, 1.35, 4.11, 4.12, 4.13
4	Acetoacetate	↑	24.82	2.28, 3.43
5	Propylene glycol	↑	18.69	1.14, 1.15
6	Glycine	↓	16.14	3.57, 3.58
7	Glucose	↑	15.64	3.40, 3.42, 3.44, 3.45, 3.47, 3.4.8, 3.49, 3.50, 3.51, 3.52, 3.74, 3.75, 3.83, 3.86, 3.87, 3.89, 3.91
8	Acetone	↑	10.69	2.24
9	Proline	↓	10.19	3.37
10	Glycerol	↑	8.46	3.54, 3.57, 3.66, 3.67
11	Alanine	↓	8.12	1.48, 1.49
12	2-Hydroxybutyrate	↑	7.16	0.90
13	Valine	↓	5.79	0.98, 1.00, 1.04, 1.05
14	Glutamine	↓	5.32	2.14

Table 3-7. Metabolites identified within the top 50 ranked peaks in OPLS-DA model discriminating samples from burn patients within first 24hrs post injury (n=37) and from matched healthy controls (n=7). Metabolites are ranked according to highest VIP score. $ ↑ indicates metabolites that are higher in burn injured patient serum relative to healthy controls, ↓ indicates metabolites that are lower in burn injured patient serum relative to controls.* Highest VIP (Variable Importance Projection) score for any peak for each metabolite PPM: Parts per million.

To determine if the presence of these metabolites persisted PCA and OPLS-DA was then applied to the NMR data from patient sera collected in the period 24-84 hrs post-injury and the same healthy control sera. Two outlying samples were removed following the PCA and OPLS-DA with 3 LVs showed excellent discrimination between the 24-84hrs post-injury samples and the control samples as shown by the scores plot (Figure 3.8). The model showed 100% sensitivity and specificity at discriminating between patient and control samples (R2 0.84, Q2 0.66, permutation *p*=0.010) and ROC analysis yielded an AUROC of 1.00. The loadings VIP plot shows the most highly weighted peaks in the model (Figure 3.9).

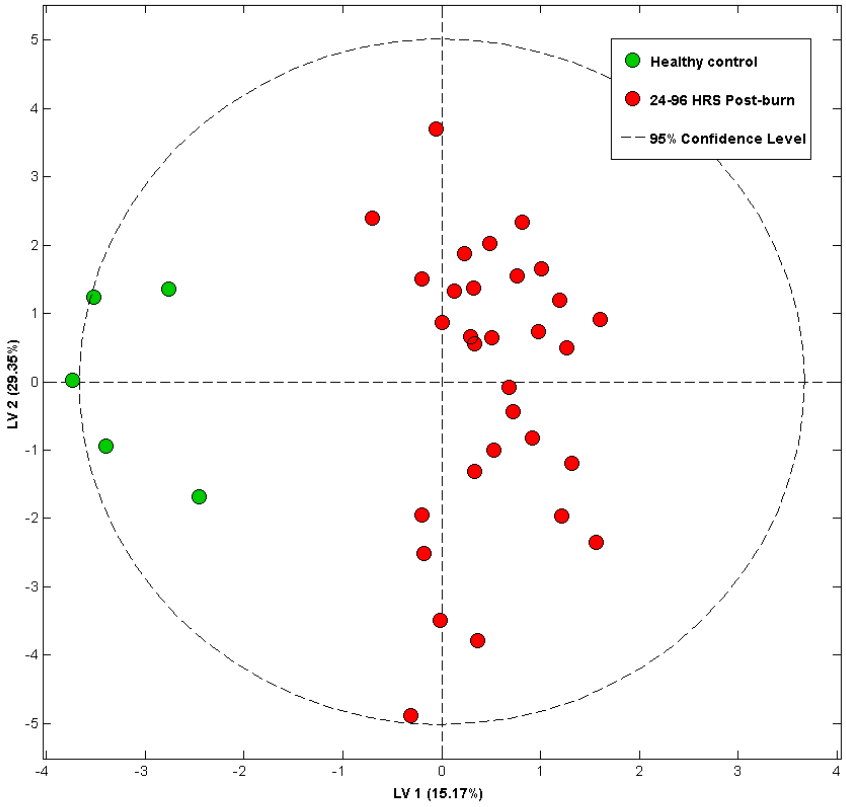

Figure 3-8. Scores plot from OPLS-DA of serum samples from two groups: 1) Burn injured patients taken >24hrs and <84hrs post-injury 2) Matched healthy volunteers (control). The 3 LV model, after 10-fold cross validation shows 100% sensitivity, 100% specificity, R2: 0.84 and Q2: 0.66, AUROC: 1.00.

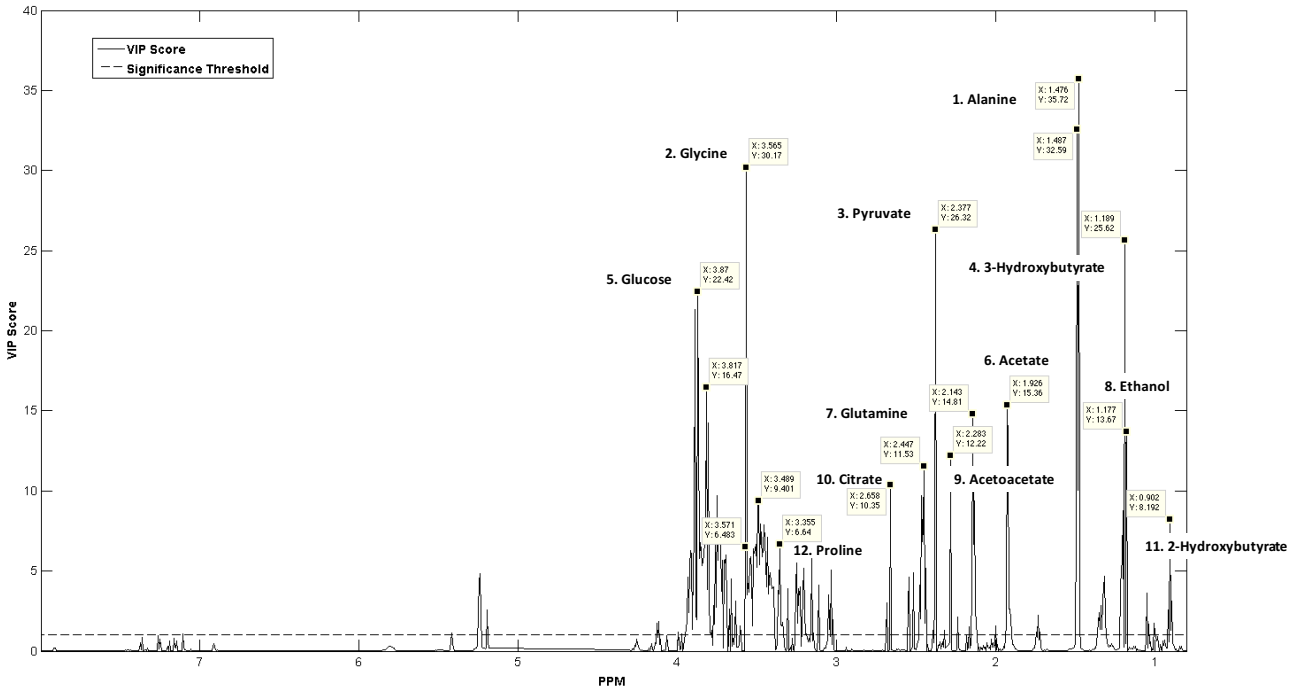

Figure 3-9. VIP loadings plot from OPLSDA showing NMR spectral peaks contributing to the model. The height of the peaks corresponds to VIP score and therefore greatest contribution to the variance between the 24-84hrs samples from burn patients and healthy controls.

As before, spectral fitting was performed for NMR peaks within the 50 highest weighted spectral bins in the OPSL-DA model. A total of 12 unique serum metabolites fell within these bins and are listed in Table 3.8 and are ranked according to VIP scores. The chemical shift values (ppm) for all peaks identified for each metabolite in the top 50 spectral bins are listed. The most highly weighted metabolites changed compared to the first 24hr samples. Reduced levels of alanine and glycine were most significantly contributing to the model but again pyruvate, glucose and ketone bodies were increased compared to controls. Lactate did not feature in the top 50 bins as in the early samples, suggesting a return towards normal levels following the resuscitation phase.

Rank	Metabolite	Change[$]	VIP*	Chemical shift of peak bins (ppm)
1	Alanine	↓	35.72	1.48, 1.49
2	Glycine	↓	30.17	3.57
3	Pyruvate	↑	26.32	2.38
4	3-Hydroxybutyrate	↓	25.62	1.19, 1.20
5	Glucose	↑	22.42	3.43, 3.45, 3.46, 3.47, 3.48, 3.49, 3.51, 3.52, 3.73, 3.75, 3.81, 3.82, 3.83, 3.85, 3.86, 3.87, 3.89, 3.92
6	Acetate	↓	15.36	1.92, 1.93
7	Glutamine	↓	14.81	2.45, 3.57
8	Ethanol	↓	13.67	1.18
9	Acetoacetate	↑	12.22	2.28, 3.45
10	Citrate	↓	10.35	2.67
11	2-Hydroxybutyrate	↑	8.19	0.90
12	Proline	↓	6.64	3.35

Table 3-8. Metabolites identified within the top 50 ranked peaks in OPLS-DA model discriminating samples from burn patients taken 24-84 hrs post injury (n=37) and from matched healthy controls (n=7). Metabolites are ranked according to highest VIP score. $ ↑ indicates metabolites that are higher in burn injured patient serum relative to healthy controls, ↓ indicates metabolites that are lower in burn injured patient serum relative to controls.* Highest VIP (Variable Importance Projection) score for any peak for each metabolite PPM: Parts per million.

\

3.4.3 Metabolomics to predict clinical outcomes

3.4.3.1 Prediction of mortality

To determine if the metabolic profile of patient's serum during the first 24hrs post burn-injury could predict clinical outcomes, NMR metabolomics data from 37 patients were subjected to PCA and OPLSDA. PCA revealed two samples lying outside the Hotelling's confidence Ellipse and were removed before generating OPLSDA models. An OPLSDA model with 3 LVs showed good discrimination between survivor and non-survivor groups with high sensitivity and specificity (Table 3.10). The score scatter plot shows the model discrimination is mainly with the first LV (Figure 3.10). Receiver Operating Characteristic Curve (ROC) analysis demonstrated excellent discriminatory ability to predict survival with a cross–validated area under the ROC curve of 0.92 (Figure 4.11).

Parameter	Value
Latent variables (n)	3
Samples	35
Accuracy % (95% CI)	89 (72-97)
Sensitivity % (95% CI)	78 (40-97)
Specificity % (95% CI)	92 (75-99)
PPV % (95% CI)	78 (46-94)
NPV % (95% CI)	92 (81-98)
AUROC	0.92
R^2	0.76
Q^2	0.47
Permutation test *p*-value	0.011

Table 3-9. Summary of statistical measures of performance of cross-validated OPLSDA model to predict mortality of patients from early serum metabolomics profiles. PPV = Positive predictive value, NPV = negative predictive value, AUROC = Area under the receiver operating characteristic curve.

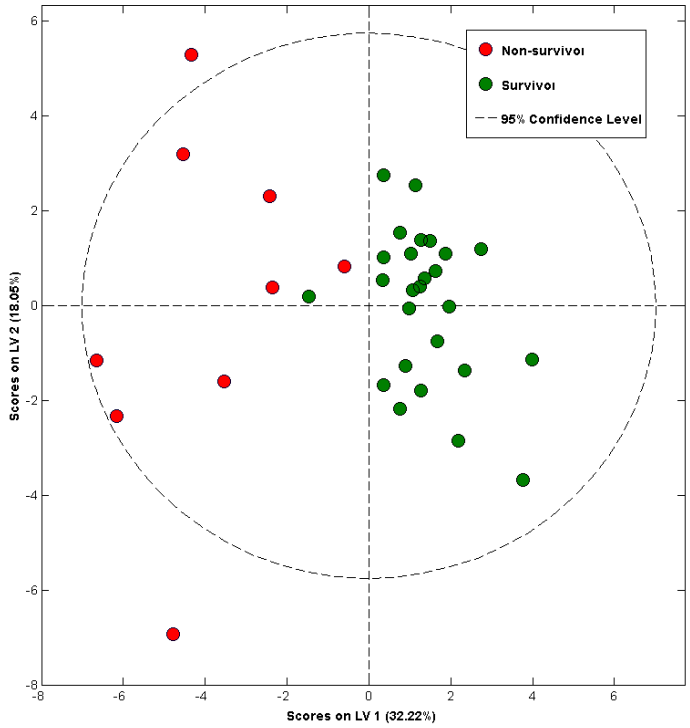

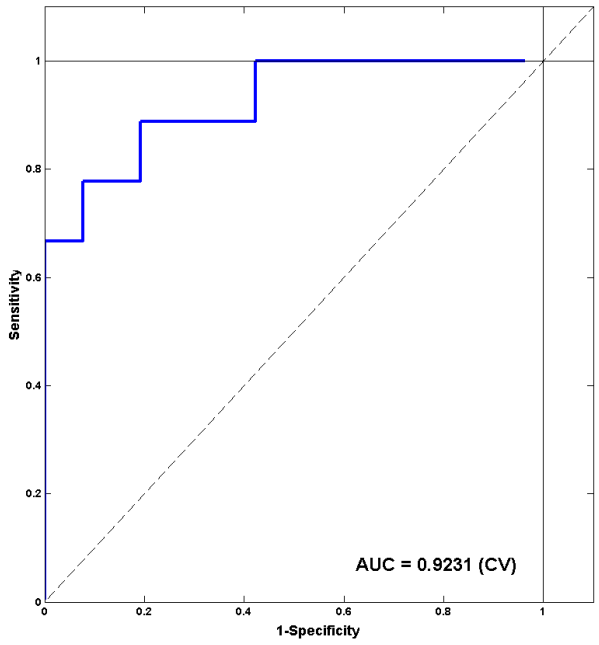

Figure 3-10. A) Scores plot from OPLSDA 3 LV model discriminating between early (0-24hr) serum samples from survivors and non-survivors. The 3 LV model, after 6-fold cross validation shows 89% accuracy, 78% sensitivity, 92% specificity, R2: 0.76 and Q2: 0.47. B) ROC curve generated from OPLSDA model showing excellent discriminatory ability to predict survival (AUROC = 0.92).

The 50 highest weighted spectral peaks in the OPSLDA survival model were identified by spectral fitting. Within that group, 12 metabolites featured with significant increases in non-survivors of 9 metabolites (75%), including 3-hydroxybutyrate, ethanol and glycerol. Relative reductions were seen in the amino acids lysine, alanine and glutamine in non-survivors.

Rank	Metabolite	Change[$]	VIP*	Chemical shift of peak bins (ppm)
1	3-Hydroxybutyrate	↑	114.03	1.18, 1.19, 1.20, 1.21
2	Ethanol	↑	85.15	1.15, 1.16, 1.17, 1.18
3	Glycerol	↑	76.27	3.64, 3.65, 3.66, 3.68
4	Kynurenine	↑	65.77	3.67, 3.68
5	Acetate	↑	45.69	1.91, 1.92, 1.93
6	Propylene glycol	↑	27.54	1.14, 1.15
7	Methylmalonate	↑	6.51	1.21, 1.22
8	Glucose	↑	2.94	3.23, 3.25, 3.35, 3.50, 3.51, 3.54, 3.55, 3.56, 3.73, 3.74, 3.92, 5.24
9	Lysine	↓	2.90	3.04
10	Lactate	↑	2.65	1.33, 1.34, 1.35, 4.12, 4.13
11	Alanine	↓	2.28	1.48, 1.49
12	Glutamine	↓	2.28	2.45, 2.46

Table 3-10. Metabolites identified within the top 50 ranked peaks in OPLS-DA model discriminating later non-survivors from survivors from serum samples taken within the first 24hrs post injury (n=37). Metabolites are ranked according to highest VIP score.

The above metabolomics workflow was used to investigate if serum metabolic profiles from the second blood samples taken after admission could predict later non-survival after burn injury. An OPSLDA model including 30 samples was created after exclusion of outliers on the PCA scores plot. A 2 LV model showed poor ability to discriminate between survivors and non-survivors with an AUROC of 0.69 (Accuracy 63% (49-80), sensitivity 76% (66-88), Specificity (33% (10-62), PPV 73% (63-84) and NPV (38% (11-69). The first 24hr serum metabolic profile therefore had better discriminatory ability to predict non-survivors than the serum profile taken 24-84 hrs post-injury.

3.4.3.2 Prediction of multiple organ failure (MOF)

The same analysis workflow was applied to examine if the metabolic profile of early serum samples taken in the first 24hrs could predict later development of multiple organ failure (MOF) as defined by a Denver MOF score of >3 for two consecutive days during admission. After exclusion of two outliers on the PCA scores plot, PCA did not show any clear clustering of the two groups (MOF vs. no MOF). A 4 LV OPLSDA model was constructed and showed discrimination of groups on the scores plot. However, after 6-fold cross-validation the model had poor discriminatory ability with AUROC to predict later MOF of 0.64 (Table 3.11).

The same workflow was then applied to serum processed from the second blood sample collected post-injury, taken 24hrs-84hrs post-injury, for the same patient group. PCA applied to this dataset showed some separation of groups mainly in the first two components. A 4 PC model was able to explain the following percentages of variation: PC1 (32.97%), PC2 (18.15%), PC3 (12.16%) and PC4 (6.75%) after removal of three outliers that were outside of the Hotelling's T^2 ellipse on the PCA

scores plot. OPLSDA was then applied to the dataset and a 4-LV model showed good discrimination of the two clinical outcome groups on the scores plot (Fig. 3.11a) and good discriminatory ability with an AUROC of 0.92 (Fig. 3.11b) (Table 3.11).

Parameter	**Values**	**Values**
Samples (time from injury)	0-24hrs	>24-84hrs
Number of samples/patients	35	29
Latent variables (n)	4	4
CV Accuracy % (95% CI)	66 (47-81)	86 (66-96)
CV Sensitivity % (95% CI)	53 (27-78)	83 (59-96)
CV Specificity % (95% CI)	75 (51-90)	88 (71-97)
PPV % (95% CI)	62 (32-85)	83 (59-96)
NPV % (95% CI)	68 (45-85)	88 (71-97)
AUROC	0.64	0.92
R^2	0.76	0.87
Q^2	0.01	0.48
Permutation test *p*-value	0.087	0.017

Table 3-11. Summary statistics for metabolomics OPLDA models discriminating serum samples from patients who either did not develop MOF or who did develop MOF. Models developed based on early samples taken in the first 24hrs post-injury and from later samples, taken 24-84hrs post-injury, are compared. CV = cross validated, CI – confidence interval, PPV = Positive predictive value, NPV = negative predictive value, AUROC = area under the receiver operating characteristic curve.

Spectral fitting was performed for NMR peaks within the 50 highest weighted spectral bins in the OPSLDA model. A total of 12 unique serum metabolites fell within these bins and are listed in Table 3.12 and are ranked according to VIP scores. Glucose peaks featured highly, occupying 23/50 (46%) of the 50 highest weighted bins. Eight of the 12 (67%) metabolites were shown to be reduced in patients who later developed MOF, these included several amino acids including alanine, proline, lysine and the branched chain amino acids (BCAA), leucine and valine.

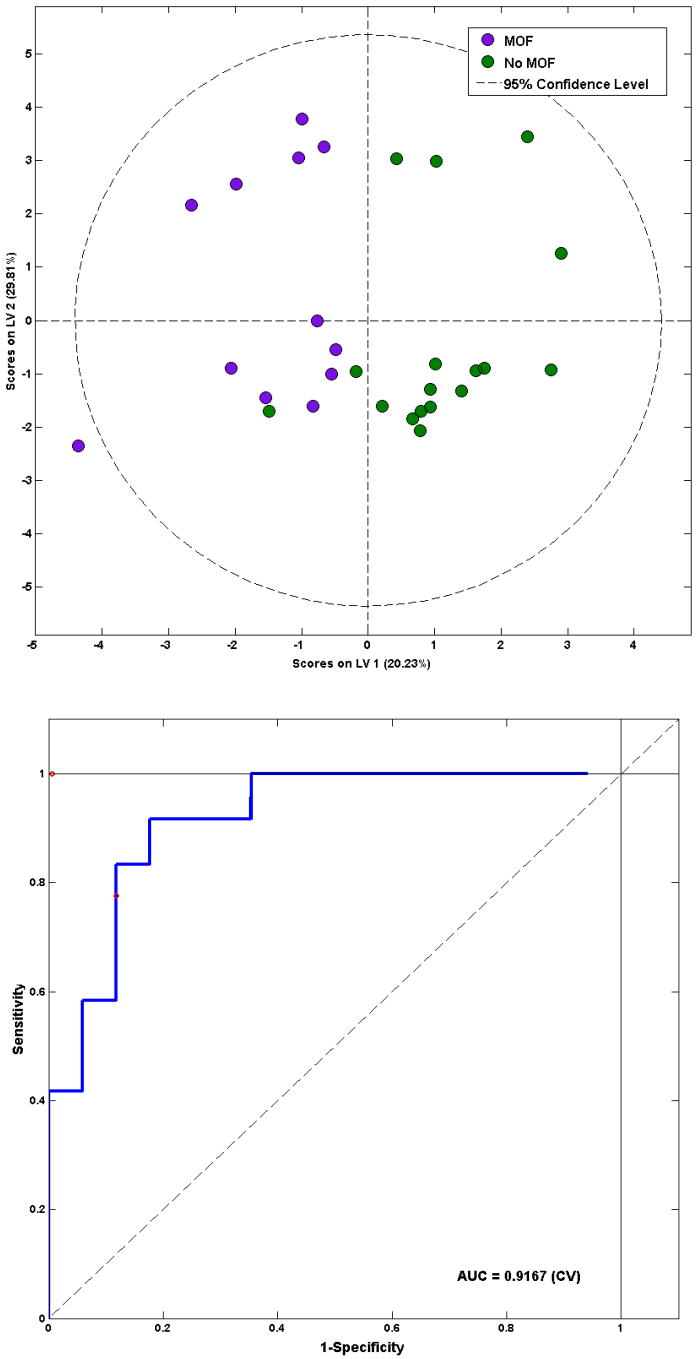

Figure 3-11. A) Scores plot from OPLSDA 4 LV model discriminating between serum samples from patients who developed MOF and those who did not. **B)** ROC curve generated from OPLSDA model showing excellent discriminatory ability to predict later MOF (AUROC = 0.92).

Rank	Metabolite	Change[$]	VIP*	Chemical shift of peak bins (ppm)
1	Glucose	↑	39.09	3.51, 3.52, 3.69, 3.71, 3.76, 3.77, 3.78, 3.79, 3.81, 3.82, 3.85, 3.86, 3.88, 3.89, 3.90, 3.92
2	Acetoacetate	↓	16.54	2.28
3	Glycerol	↑	16.10	3.58, 3.65, 3.68
4	Alanine	↓	14.75	1.48, 1.49
5	Leucine	↓	13.97	0.95, 0.96, 0.97
6	Proline	↓	13.42	3.35, 3.36
7	Lactate	↓	11.54	1.32, 1.34
8	Valine	↓	10.19	0.98. 0.99, 1.04
9	3-Hydroxybutyrate	↓	8.08	1.19, 1.21
10	Creatine	↑	7.61	3.93
11	Lysine	↓	7.44	3.04
12	Propylene glycol	↑	6.37	1.14, 1.15

Table 3-12. Metabolites identified within the top 50 ranked peaks in OPLS-DA model discriminating serum samples from patients who later developed MOF and from those who did not. Metabolites are ranked according to peaks with the highest VIP score. Arrows indicate the direction of change in patients who developed MOF relative to those who did not.

3.4.3.3 Prediction of sepsis

Two non-septic patients were excluded from the first 24hr serum samples dataset due to early non-survival within the first 7-days post-injury and therefore having an uncertain septic outcome. A final NMR dataset from 35 serum samples taken within the first 24hrs post-injury was subjected to PCA and 4 outlying samples were identified as lying outside the Hotelling's ellipse and were removed from the dataset.

The PCA was re-run and the resultant model explained the following variation in the dataset: PC1 = 22.72%, PC2 = 18.67% and PC = 12.07%. The PCA scores plot showing clustering of the septic group but not the non-septic group. Some minor separation of the groups was observed in PC1. The dataset was then subjected to OPLSDA which resulted in 2LV model explaining 29% of the variance in the data. The scores plot shows of the groups in separation in LV1 but some overlapping samples were observed. The model was able to discriminate between septic and non-septic samples with an accuracy of 74%, sensitivity of 75%, specificity of 73% and an AUROC 0.78, however the Q2 metric was poor (0.16) suggesting poor model performance (Table 3.13).

The workflow was repeated for NMR data from 31 serum samples taken from the same group of patients taken 24-84hrs post burn. One patient sample was removed due to the patient being an early non-survivor and therefore having an uncertain diagnosis of sepsis. The data was subjected to PCA and three outliers on the scores plot were identified and removed before re-running the PCA. The final PCA model with 2 PCs explained the following variation in the dataset: PC1 = 35.86% and PC2= 16.38%. The scores plot showed some clustering of septic and non-septic groups and separation was observed mainly in PC2. The filtered dataset was then subjected to OPLSDA, producing a model with 2 LVs explaining 49% of the variance in the data. The scores plot again shows good separation of groups in LV1, however, with some overlapping of samples from the two outcome groups (Figure 3.12a). The model could discriminate between the septic and non-septic groups with 79% accuracy, sensitivity of 80% and specificity of 77% and AUROC of 0.89 (Table 3.13).

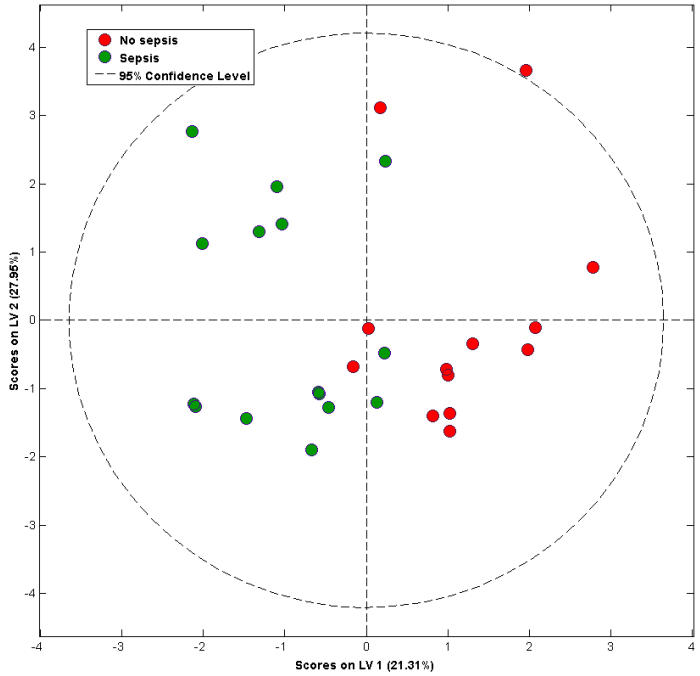

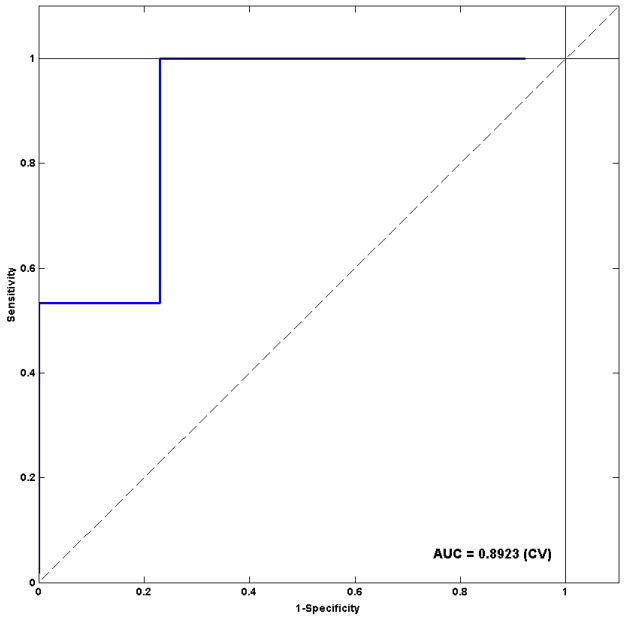

Figure 3-12 A) Scores plot from OPLSDA 2 LV model discriminating between serum samples from patients who developed sepsis and those who did not. **B)** ROC curve generated from OPLSDA model showing good discriminatory ability to predict later sepsis (AUROC = 0.89).

Parameter	Values	Values
Samples (time from injury)	0-24hrs	24-84hrs
Number of samples	31 (16 Sepsis, 15 no sepsis)	28 (15 Sepsis, 13 no-sepsis)
Latent variables (n)	2	2
CV Accuracy % (95% CI)	74 (53-89)	79 (57-92)
CV Sensitivity % (95% CI)	75 (55-89)	80 (60-93)
CV Specificity % (95% CI)	73 (52-88)	77 (53-92)
PPV % (95% CI)	75 (55-89)	80 (60-93)
NPV % (95% CI)	73 (52-88)	77 (53-92)
AUROC	0.78	0.89
R^2	0.60	0.63
Q^2	0.19	0.47
Permutation test *p*-value	0.163	0.027

Table 3-13: Summary statistics for metabolomics OPLDA models discriminating serum samples from patients who did and did not develop sepsis during their admission. Models developed based on early samples taken in the first 24hrs post-injury and from later samples, taken 24-84hrs post-injury, are compared. CV = cross validated, CI – confidence interval, PPV = Positive predictive value, NPV = negative predictive value, AUROC = area under the receiver operating characteristic curve.

Spectral fitting was performed for the top 50 NMR peak bins weighted by VIP score in the OPSLDA model (Table 3.14). This yielded 14 unique metabolites whose change in serum was highly weighted in the model discriminating patients who later developed sepsis from those who did not. The direction of change was biased towards decreases in metabolites in the septic group, with 12 of 14 metabolites (86%) being decreased relative to the non-septic group. Only glucose and propylene glycol were increased in the septic group relative to the non-septic group. In the septic group serum, relative decreases were seen in keto-acids, ethanol, methanol and amino acids including alanine, lysine, leucine and glutamine.

Rank	Metabolite	Change[$]	VIP*	Chemical shift of peaks (ppm)
1	Ethanol	↓	40.55	1.18, 1.19
2	Alanine	↓	29.71	1.48, 1.49
3	Lysine	↓	28.94	3.04
4	Acetoacetate	↓	26.71	2.28
5	3-Hydroxybutyrate	↓	18.15	1.20, 1.21
6	Lactate	↓	16.86	1.32, 1.33, 1.34, 1.35, 4.10, 4.12, 4.14
7	Glucose	↑	16.09	3.50, 3.51, 3.52, 3.69, 3.75, 3.76, 3.80, 3.81, 3.85, 3.86, 3.87, 3.88, 3.89, 3.92, 3.93
8	Methanol	↓	13.03	3.35, 3.36, 3.37
9	Leucine	↓	11.63	0.95, 0.96, 0.97
10	2-Hydroxybutyrate	↓	11.51	0.90
11	Valine	↓	8.99	0.98, 0.99
12	Glutamine	↓	8.74	2.14, 2.17, 2.46
13	Propylene glycol	↑	6.44	1.14, 1.15
14	Carnitine	↓	5.81	3.23

Table 3-14. Metabolites identified within the top 50 ranked peaks in OPLS-DA model discriminating 24-84hrs post-injury serum samples from patients who later developed sepsis and from those who did not. Metabolites are ranked according to peaks with the highest VIP score. Arrows indicate the direction of change in patients who developed sepsis relative to those who did not.

3.4.3.4 Comparison of metabolomics models with clinical prediction tool performance

Comparison was made in the discriminatory performance of the metabolomics predictive models and a number of clinical scoring and prognostic tools currently in use. Discriminatory performance was assessed by calculation of the AUROC for each model and each clinical outcome (mortality, MOF and sepsis) and the results are summarized in tables 3.15, 3.16 and 3.17. The metabolomics model performed comparably with the highest performing clinical tools with the same AUROC as for APACHE II score and the Revised Baux Score. For the outcomes sepsis and MOF, the metabolomics models also performed comparably but were outperformed by the clinical tools. The sepsis metabolomics model had the least discriminatory ability compared to the other two outcome models.

Mortality prediction (Total 35 Patients, 25 Survivors: 9 Non-survivors)	
Model	**AUROC**
Metabolomics (Serum <24hrs post injury)	**0.92**
Apache II first 24hrs	0.92
Revised Baux	0.92
Baux	0.90
BOBI	0.89
SOFA Score first 24hrs	0.86
ABSI	0.79
Denver Score first 24hrs	0.78

Table 3-15. Comparison of ability to predict mortality in young patients (aged <65 years) with >15% TBSA burn using serum metabolomics model vs. clinical prognostic tools as assessed by AUROC. Models are ordered according to AUROC value.

Multiple Organ Failure (MOF) prediction (Total 30 Patients, 16 MOF: 18 No-MOF)	
Model	**AUROC**
Revised Baux	0.99
Baux	0.97
Apache II first 24hrs	0.94
BOBI	0.94
Denver Score first 24hrs	0.94
SOFA Score first 24hrs	0.93
ABSI	0.93
Metabolomics (Serum 24-84hrs post-injury)	**0.92**

Table 3-16. Comparison of ability to predict multiple organ failure (MOF) in young patients (aged <65 years) with >15% TBSA burn using serum metabolomics model vs. clinical prognostic tools as assessed by AUROC. Models are ordered according to AUROC value.

Sepsis prediction (Total 27 Patients, 15 Sepsis: 12 No-Sepsis)	
Model	**AUROC**
Apache II first 24hrs	1.00
BOBI	1.00
SOFA Score first 24hrs	1.00
Revised Baux	0.99
Denver Score first 24hrs	0.97
Baux	0.96
ABSI	0.92
Metabolomics (Serum 24-84hrs post-injury)	**0.89**

Table 3-17. Comparison of ability to predict later sepsis in young patients (aged <65 years) with >15% TBSA burn using serum metabolomics model vs. clinical prognostic tools as assessed by AUROC. Models are ordered according to AUROC value.

3.4.4 The effect of inhalation injury on the early post-burn metabolome

The clinical data from our cohort of 37 patients shows inhalation injury has a dramatic effect on mortality with 30% of the survivor group and 90% of the non-survivor group having concomitant inhalation injury (p=0.002) (Table 3.2). Moreover, patients in the study who had inhalation injury had a higher mortality (9/17, 53%) compared to those who did not (1/20, 5%) (p=0.002). The acute changes in the serum metabolome following thermal injury were therefore further analysed considering the presence of inhalation injury on admission. The serum NMR data was analysed separately from the early (<24hrs post-injury) samples and the second serum samples (24-84hrs post-injury).

3.4.4.1 The effect of inhalation injury on changes in the early post-burn metabolome (<24 hrs post-injury)

Serum NMR metabolomics data from 37 patient samples was subjected first to unsupervised PCA analysis and then to supervised OPLSDA analysis, comparing samples from burn injured patients with and without inhalation injury. A 4 PC model could explain the following percentages of variation: PC1 (44.24%), PC2 (12.29%), PC3 (9.27%) and PC4 (8.51%). The PCA scores plot revealed no significant clustering of the two groups (Figure 3.13a). After removal of three outliers from the dataset, a 5 LV OPLSDA model showed good discrimination of clinical groups on the scores plot (Figure 3.13b). It could distinguish between samples from the inhalation injury group and the non-inhalation group with 75% accuracy, 72% sensitivity and 79% specificity. The Q^2 metric of 0.17 and non-significant permutation test suggests significant overfitting of the model (Table 3.18.). Metabolite identification was therefore not performed on the metabolite peak bins within the OPSLDA model.

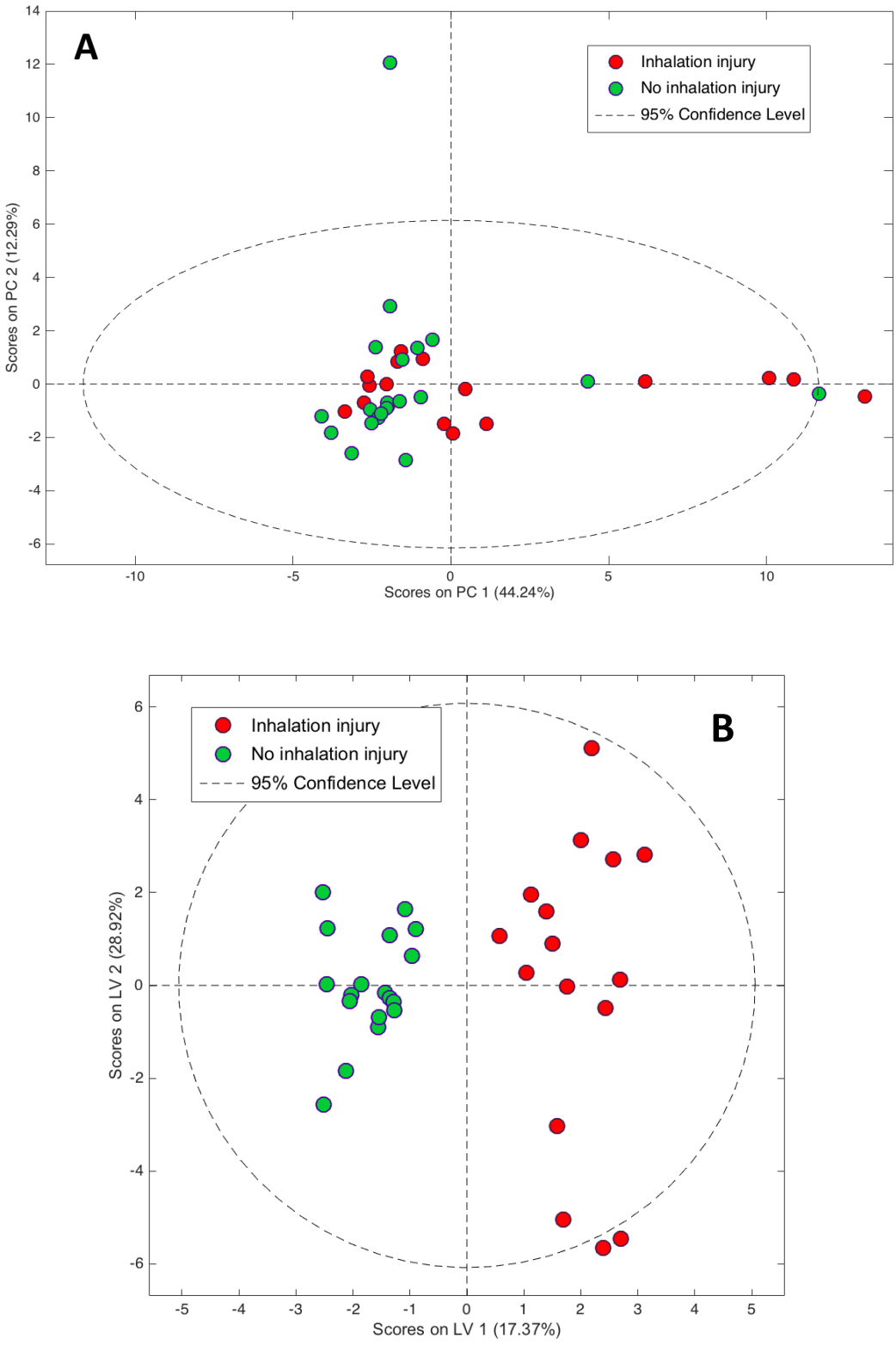

Figure 3-13. A) PCA Scores plot from serum NMR data, blood samples taken first 24hrs post burn injury. B) OPLSDA scores plot from same data set after exclusion of outliers from PCA.|

3.4.4.2 The effect of inhalation injury on changes in the post-burn metabolome (24-84 hrs post-injury)

Serum NMR data from 32 patient samples, taken between 24 and 84 hours post-injury was subjected first to unsupervised PCA analysis and then to supervised OPLSDA analysis as before. A 4 PC model could explain the following percentages of variation: PC1 35.59%), PC2 (16.79%), PC3 (10.92%) and PC4 (8.76%). The PCA scores did reveal some separation of the groups, particularly in PC1 (Figure 3.14a). Two outlier samples were removed as they fell outside the Hotelling's 95% Confidence ellipse and the data from the remaining 30 samples were subjected to OPLSDA, producing a 5 LV model with good discrimination of clinical groups on the scores plot (Figure 3.14b). The resultant metabolomics model could discriminate between inhalation injury and non-inhalation injury serum samples with 80% accuracy, 82% sensitivity and 79% specificity. The model showed acceptable R^2 (0.9) and Q^2 metrics (0.5) and a permutation test *p*-value of 0.024, demonstrating that there was not significant overfitting of the model.

As the model demonstrated good discriminatory and model fitting characteristics, spectral fitting was performed to identify the top 50 ranked spectral bins in the OPLSDA model, according to VIP score. A total of 7 metabolites were identified with the top 50 bins with glucose predominating 88% (44/50) of the peak bins (Table 3.19). Glucose was increased in the samples from patients with inhalation injury relative to those from patients with no inhalation injury. Other metabolites that were increases in the inhalation injury group included kynurenine, glycerol and allantoin, a diureide of glyoxylic acid and product of purine metabolism.

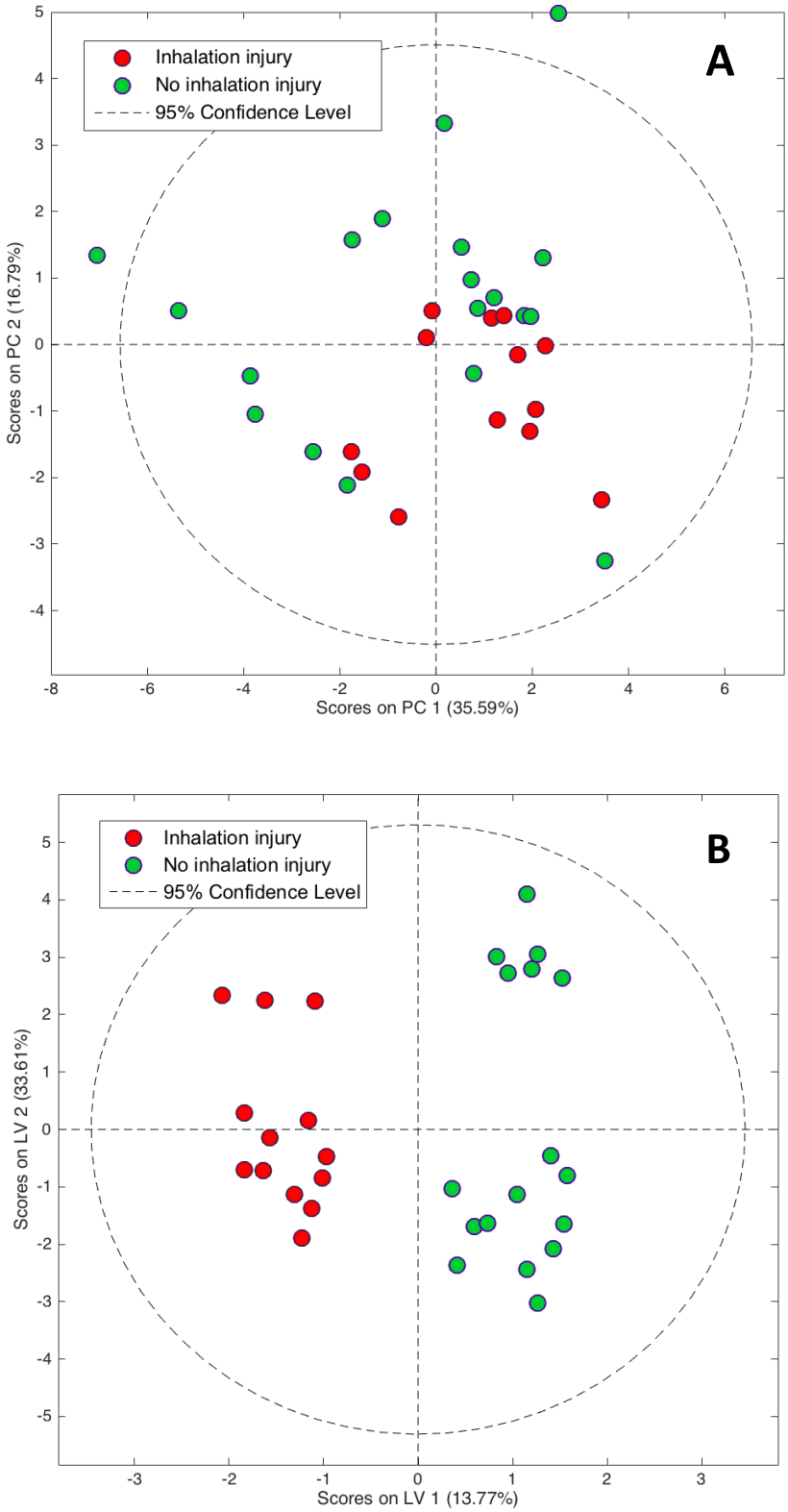

Figure 3-14. A) PCA scores plot from serum NMR data derived from blood samples taken 24-84hrs post-burn injury. B) OPLSDA scores plot of the data after removal of outliers from the PCA.

Parameter	<24hrs post-injury	24-84hrs post-injury
Samples (n)	34	30
Latent variables (n)	5	5
CV Accuracy % (95% CI)	0.75 (0.55-0.88)	0.80 (0.59-0.91)
CV Sensitivity % (95% CI)	0.72 (0.54-0.84)	0.82 (0.54-0.96)
CV Specificity % (95% CI)	0.79 (0.56-0.93)	0.79 (0.63-0.87)
PPV % (95% CI)	0.81 (0.61-0.94)	0.69 (0.46-0.82)
NPV % (95% CI)	0.69 (0.49-0.82)	0.88 (0.70-0.98)
AUROC	0.76	0.89
R^2	0.90	0.92
Q^2	0.17	0.47
Permutation test *p*-value	0.177	0.024

Table 3-18. Summary statistics for OPLSDA models generated from serum NMR metabolomics data. Comparison of discriminatory performance and fitting metrics between models generated from samples taken <24hrs post injury and samples taken 24-84hrs post-injury. CV = cross validated, CI – confidence interval, PPV = Positive predictive value, NPV = negative predictive value, AUROC = area under the receiver operating characteristic curve.

Rank	Metabolite	Change$	VIP*	Chemical shift of peak bins (ppm)
1	Glucose	↑	35.16	3.24, 3.26, 3.4, 3.41, 3.42, 3.46, 3.47, 3.48, 3.50, 3.51, 3.52, 3.69, 3.70, 3.71, 3.72, 3.75, 3.76, 3.77, 3.78, 3.79, 3.80, 3.81, 3.82, 3.83, 3.85, 3.86, 3.87, 3.88, 3.89, 3.90, 3.92, 5.24, 5.25
2	Lysine	↓	12.74	3.04
3	Kynurenine	↑	12.58	3.69
4	3-Hydroxybutyrate	↓	10.55	1.19
5	Glycerol	↑	10.27	3.67
6	Acetoacetate	↓	10.16	2.28
7	Allantoin	↑	7.65	5.42

Table 3-19. Metabolites identified within the top 50 ranked peaks in the OPLSDA model discriminating between samples from burn injured patients with inhalation injury and those without inhalation injury.

3.5 Discussion

3.5.1 Early changes in the post-burn metabolome

In this study, we applied ^{1}H-NMR metabolomics to study the acute changes in the metabolome in a cohort of patients with severe thermal injuries. ^{1}H-NMR analysis of serum samples taken during the first 96-hrs post-injury demonstrated changes in keto-acids, lactate, carbohydrates and amino acids reflective of hypoxic metabolism, increased energy production and derangements in glucose and protein metabolism. Multi-variate statistical analysis produced metabolite models that could distinguish between burn injured patients and healthy control subjects. The most highly weighted metabolites in these models were therefore reflective of the key changes in the serum metabolome after thermal injury. It was evident that metabolic changes during the first 24hrs after thermal injury were distinguishable from those during the next 24-84hrs post injury. This may represent a metabolic shift from the early 'ebb' phase towards entry into the 'flow' phase which demonstrated a different pattern of metabolites that differentiated healthy controls from patients with thermal injury.

The cohort studied was appropriate to the study of severe thermal injury, being a relative large cohort of 37 patients with an average burn size of approximately 40% TBSA. This group of patients demonstrated significant physiological derangement and organ dysfunction during the first 24hrs of hospital admission, as evidenced by high average APACHE II, SOFA and Denver MOF scores. Commensurate with a severely injured cohort, there was a high incidence of complications, including MOF (43%), sepsis (51%) and non-survival (27%). The non-survivors were significantly older, had larger TBSA injuries, greater full thickness burn area and had a higher incidence of inhalation injury and greater levels of organ dysfunction on admission.

In the OPLSDA model able to discriminate serum samples taken from patients within the first 24hrs post-injury from control samples, there were changes in metabolism reflecting alterations in glucose homeostasis, increased TCA cycle activity, increased lipolysis and increased production of pyruvate and lactate (Figure 3.16).

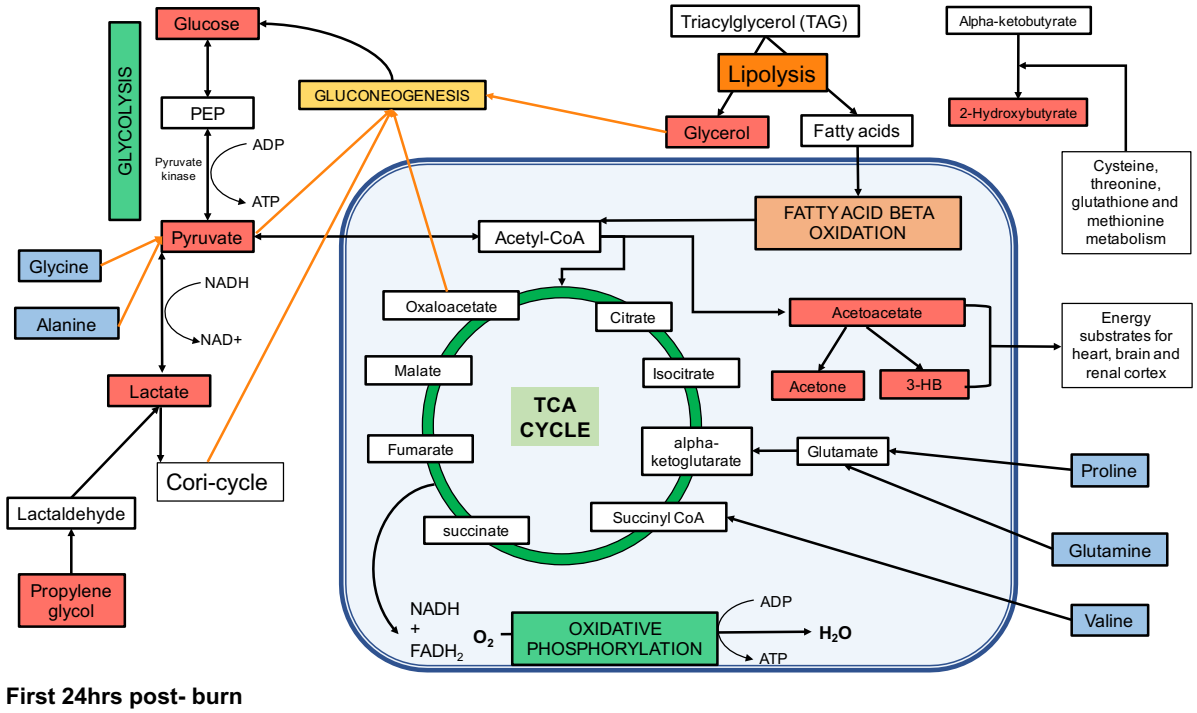

Figure 3-15. Overview of key pathways and metabolites discriminating early first 24hr serum samples taken from patients with severe thermal injuries and healthy control samples. Red metabolites were elevated relative to controls and blue metabolites were decreased relative to controls.

The most highly weighted metabolites in the model included the keto-acids ('ketone bodies') 3-Hydroxybutyrate (3-HB) and acetoacetate and lactate. In starvation states and during exercise, ketone bodies become a protein sparing energy substrate. In these scenarios, carbohydrate availability decreases, whilst peripheral lipolysis increases. There is increased uptake and beta-oxidation of fatty acids in the liver, generating acetyl CoA for entry into the tricarboxylic acid (TCA) cycle.

Simultaneously, there is upregulation of gluconeogenesis, resulting in increased utilization of oxaloacetate. This leads to an excess of acetyl CoA which is converted to acetoacetate, which can be either reduced to 3-HB in the mitochondrial matrix or slowly converted to acetone (229).

Acetoacetate and 3-HB are not simply degradation products, they are utilized by the brain, cardiac muscle and renal cortex as energy substrates (ketolysis) (322) and also have signaling activities that can influence chromatin modifications through inhibition of histone deacetylases (HDACs) (323). The OPLSDA models in this study suggest that acetoacetate remains elevated in the second phase (24-96hrs), whereas 3-HB decreases to lower levels relative to controls. This could indicate increased utilization of acetoacetate by extra-hepatic tissues as an energy substrate in preference to 3-HB. Studies of ketone bodies after severe thermal injury, trauma and sepsis have generally shown that, despite evidence of increased peripheral lipolysis and β-oxidation of fatty acids, ketone production is not increased which is hypothesized to be related to hyperinsulinaemia with increased insulin resistance (324). However, many of these studies were performed in the context of starvation and patient studies were performed before the introduction of early enteral feeding as a burn care standard(325).

A more recent study measured arterial and portal blood concentrations of ketone bodies early after polytrauma and found that at 6hrs post-injury 3-HB was elevated in the portal circulation but not systemically suggesting ketogenesis driven by the gut. At 24hrs post-injury, however, portal blood levels of 3-HB decreased whilst systemic levels increased indicating gut utilization of ketone bodies as an energy source (326).

No recent studies have been performed re-evaluating ketone body metabolism or kinetics in thermal injury. The ratio of acetoacetate and 3-HB reflect mitochondrial redox potential and one study showed that acetoacetate in arterial blood declined with time over 3-weeks post-burn and this trend was associated with the development of MOF. They also showed a decrease in the Acetoacetate:3-HB ratio over time, indicating a progressive decline in mitochondrial redox potential (327).

Pyruvate and glucose were also highly weighted in the models and show relative increases after thermal injury compared to controls. This is consistent with the known profound alterations in carbohydrate metabolism after thermal injury that are due to the combination of acute inflammation and the imbalance of catabolic stress hormones (catecholeamines, cortisol, glucagon) and the anabolic hormone, insulin. Hyperglycaemia is well documented after burn injury (328,329) and is due to increased peripheral resistance (skeletal muscle) to insulin, increased central insulin resistance (liver) and increased glucose production via glycolysis and gluconeogenesis (330). This ‘stress diabetes’ is felt to an adaptive response to injury and infection to prioritize glucose supply to non-insulin dependent vital organs unable to metabolise other substrates in the context of the stress response (331). Although the availability of glucose increases post-burn, the increase in glucose oxidation by 33% (193) is insufficient to keep up with supply (192).

The data also show increased levels of glycerol, lactate and the amino acids alanine and glycine relative to controls. Studies of the upregulated gluconeogenesis after burn injury, show that there is increased uptake of 3-carbon precursors pyruvate, lactate and amino acids, particular alanine (332). There is also increased availability

of these precursors, in addition to glycerol from increased lipolysis of triglycerides in adipose tissue (168). The elevations in lactate in the injured patients are common to all forms of critical illness and are in the initial phase due to tissue hypoxia during resuscitation. There is also a contribution from the highly specialized immune cells activated in the burn wound, that demonstrate increased lactate output even in the absence of hypoxia (201). This lactate contributes to glucose production as it is transported to the liver for gluconeogenesis and this cycle is termed the Cori-cycle (324). Another contributor to the elevations in serum lactate, could be the use of Ringer's lactate as intravenous resuscitation fluid, which is used to replace volume losses and maintain tissue perfusion during the first few days post-injury.

In addition to changes in alanine and glycine, decreases were also seen in the injured patients relative to control in other amino acids proline, valine and glutamine. The metabolic response to thermal injury when compared to non-stressed starvation bears similarities but the major difference is that in the former, the switch to lipids as the major fuel does not spare protein catabolism. After severe thermal injury, there is increased protein synthesis, but there is also increased protein catabolism and this outstrips synthesis, resulting in a net decrease in protein balance (333). This protein catabolism occurs in skeletal muscle and results in losses of lean body mass (LBM) which leads to increased rates of infection, delayed wound healing and delays in rehabilitation (330). The goal of this amino acid liberation from muscle, is to provide substrates for acute phase protein synthesis, wound healing and gluconeogenesis (228).

Glutamine is an alpha amino acid that becomes conditionally essential in critical illness states. It has been demonstrated to decrease in patients with sepsis, burns and trauma. In patients with burn injury, plasma levels decreased by 58% and remained significantly low for 3 weeks post-injury (334). Glutamine plays important roles in modulation of the immune response (334), provides a primary fuel source for enterocytes and is necessary for maintaining mucosal associated lymphoid tissue (MALT) and therefore maintenance of gut integrity (335). It also is an important precursor to the anti-oxidant glutathione, which is relevant in the context of oxidative stress that occurs after injury (336). Stable isotope studies in thermally injured patients have shown that muscle intracellular levels of glutamine are low due to increased rates of outward transport and consumption (337). Valine is a branched chain amino acid that is essential and thus must be provided in the diet. Valine can serve as a precursor to the TCA cycle intermediate succinyl CoA and therefore decreased levels after burn injury, as with glutamine and proline, may reflect increased TCA cycle flux to drive increased ATP production as part of the stress response. Valine also has an important role in the renewal of haemopoietic stem cells (338). Previous comprehensive studies of amino acid metabolism in thermally injured humans and animal models show acute decreases in valine, glycine, proline, glutamine and alanine in plasma (339). Proline and glycine are abundant amino acids in human collagen which is essential for wound healing, so wound sequestration may contribute to decreased circulating levels post-burn.

The OPLSDA metabolite model that discriminated patient serum samples taken 24-84hrs post-burn from control samples shows a different pattern to the model from earlier samples. There is increased weighting of the amino acids alanine, glycine and

glutamine suggesting increasing protein catabolism as the flow phase is entered. Citrate is lower relative to controls and this suggests that there is ongoing increased TCA cycle flux drive ATP production and therefore its consumption is increased (Figure 3.17).

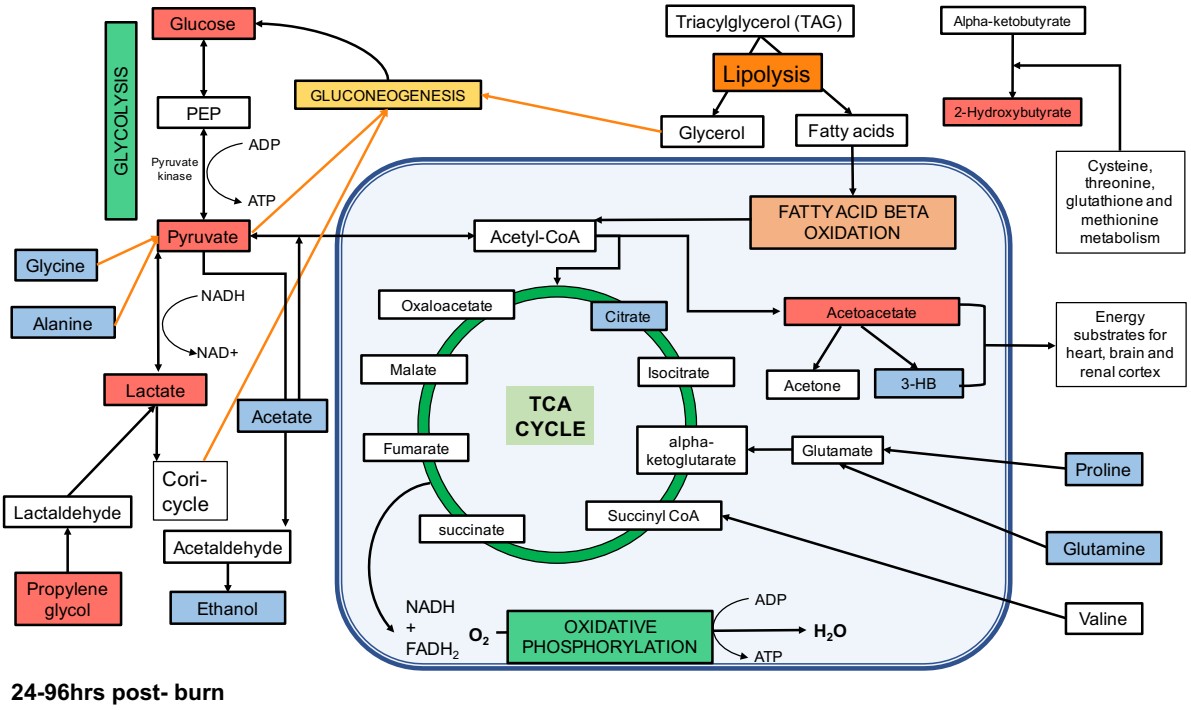

24-96hrs post- burn

Figure 3-16. Overview of key pathways and metabolites discriminating serum samples taken from patients with severe thermal injuries between 24-96hrs post-injury and healthy control samples. Red metabolites were elevated relative to controls and blue metabolites were decreased relative to controls.

3.5.2 NMR metabolomics can distinguish between burn injured patients with and without inhalation injury

Inhalation injury has long been known to be a significant determinant of outcome following thermal injury and is associated with increased mortality and length of stay (340). The clinical data from our study corroborates with previously published data, showing significantly higher mortality in the inhalation injury group. Using the early

<24hrs serum NMR data, OPLSDA could only be used to produce a model to discriminate inhalation injury samples from non-inhalation samples through overfitting of the model. As was seen with the MOF and sepsis prediction models, the data obtained from the samples taken slightly later, between 24 and 84hrs post-burn did yield useful discriminatory models for inhalation injury using OPLSDA. Possible reasons for the later data yielding better models may be that the metabolic disturbances that relate to the effects of inhalation injury may not develop until after 24hrs post-burn. Alternatively, the systemic metabolic effects specific to inhalation injury are masked in the first 24hrs post-injury by the initial systemic inflammatory and metabolic alterations secondary to the cutaneous thermal injury.

The top 50 ranked spectral bins in the 24-84hrs serum sample metabolomics model only featured 7 metabolites, owing to the predominant representation of glucose peaks in the model. Clearly, the additional inflammatory stress generated by the inhalation trauma in addition to the cutaneous burn has significant effects on glucose homeostasis. Previous studies have shown after adjusting for age and burn size, that severity of inhalation injury correlates with circulating plasma levels of cytokines IL-1RA, IL-6, IL8, G-CSF and MCP-1 (72). Other metabolites that were elevated were kynurenine, a tryptophan metabolite with immune and vasoactive effects (see section 3.5.4), glycerol and allantoin. Elevations in glycerol and decreases in lysine reflect increased fat and protein catabolism respectively. The presence of allantoin is an interesting finding, as it is a product of purine metabolism and can be generated from conversion of uric acid by reactive oxygen species (ROS). Allantoin has been described as a marker of oxidative stress in a number of inflammatory diseases

including rheumatoid arthritis (RA) and Behcet's disease (BD) (341,342). Elevations of this metabolite may reflect increased ongoing oxidative stress generated by the additional inflammatory hit of the inhalation injury and no specific studies have previously measured this metabolite in patients with thermal injury or inhalation injury.

3.5.3 NMR metabolomics reveals changes in novel serum metabolites after thermal injury

Two other unusual metabolites were observed to be elevated in the <24hr post-injury serum relative to control serum in the multi-variate model. Propylene glycol is an organic compound that is used as a food additive and as a common excipient for pharmaceuticals, the latter being a probable cause for relative elevations in the patient group. It is metabolized to either pyruvate, lactate, acetate or propionaldehyde. The organic acid 2-hydroxybutyrate (alpha-hydroxybutyrate, 2-HB) is derived from alpha-ketobutyrate produced through catabolism of threonine and methionine or as a by-product of the synthesis of glutathione (343). A recent untargeted human metabolomics study demonstrated 2-HB to be an early biomarker of insulin resistance and impaired glucose regulation. The mechanisms proposed for elevation of 2-HB include hepatic oxidative stress leading to increased demand for the anti-oxidant glutathione and elevation of the NADH/NAD+ ratio secondary to increased fatty acid oxidation (344). This metabolite has not been investigated in thermal injury, but warrants further study given its link to insulin resistance and anti-oxidant production. Severe thermal injury is documented to result in increased oxidative stress and mitochondrial dysfunction in skeletal muscle (345,346).

3.5.4 NMR metabolomics can predict poor outcomes from early serum samples after thermal injury

The second aim of this study was to evaluate if early serum metabolomics could be used to predict later poor clinical outcomes. The study has shown that ^{1}H-NMR metabolomics analysis of serum samples taken within the first 96hrs post-burn can predict poor outcomes with high accuracy including: mortality, multiple organ failure (MOF) and sepsis. The most discriminatory mortality prediction model was created from OPLSDA analysis of the serum samples taken from the first 24hrs and showed an AUROC of 0.92. The cross validated model had high specificity (92%) but only moderate sensitivity (78%). The most significantly weighted metabolites in the model included elevations in non-survivors of: 3-HB, ethanol, glycerol, kynurenine, acetate, methyl-malonate and as expected glucose and lactate. The amino acids lysine, alanine and glutamine were decreased in non-survivors, again demonstrating the relationship of protein catabolism to mortality in thermal injury, consistent with data that shows skeletal muscle catabolism correlates directly with poor outcomes (231).

Kynurenine is a major degradation product of tryptophan, with potentially toxic downstream metabolites such as quinolinic acid and 3-hydroxykynurenine which are neurotoxic and can induce free radical production. Circulating kynurenine levels have not been studied in burns, but one study showed increased urinary excretion of kynurenine in burned children (347). Kynurenine has become the subject of studies in critically ill, trauma and septic patients after observations that the enzyme indoleamine 2,3-dioxygenase (IDO) which catalyzes the breakdown of tryptophan to kynurenine has immunoregulatory effects on T-cells (348) and its expression is

responsive to cytokines Interferon-γ (349) and IL-10 (350). Moreover, IDO mediated kynurenine production in vascular endothelium contributes to vascular relaxation (351). Studies in humans, have shown that IDO expression is increased in patients with septic shock and correlated with hypotension (352). Increased IDO activity was associated with dysregulated immune responses and microvascular responsiveness in sepsis (353). Studies in trauma patients, suggest that plasma levels of kynurenine were increased on the first day post-injury in patients who later developed sepsis and increased kynurenine:tryptophan ratios predicted later MOF and death (354). Kynurenine has been investigated in the field of wound healing and has been shown to decrease scar formation in animal models of hypertrophic scar formation. This is postulated to be secondary to upregulated production of matrix metalloproteinases (MMP1 and MMP3) and suppression of the expression of type I collagen in dermal fibroblasts (355).

Methylmalonate (MMA) is a vital intermediate in lipid and protein metabolism and is a metabolite in the valine degradation pathway in addition to its roles in pyrimidine metabolism and propanoate metabolism. There are no previous studies of this metabolite in thermal injury but the metabolite accumulates in the condition methylmalonic acidaemia, caused by a defect in the enzyme methylmalonyl CoA mutase which converts methylmalonyl CoA into succinyl CoA for entry in the TCA cycle. This enzyme is vitamin B12-dependent and therefore MMA can accumulate in vitamin B12 deficiency. It can also be derived from metabolism of propionate produced by enteric bacteria and absorbed into the portal circulation, although elevations of MMA through this mechanism have only been described in methylmalonic acidaemia (356). Interestingly, MMA accumulation is also associated

with impairment of mitochondrial oxidative function, possibly through inhibitory effects on enzymes involved in mitochondrial glutamate metabolism (357). This metabolite warrant further investigation in thermal injury, given the known gut dysfunction that occurs (358) that may lead to changes in gut microflora and increased absorption of certain metabolites.

The finding of relatively increased levels of acetate in the early serum samples from non-survivors is another finding of potential interest. The two major sources of acetate in humans are endogenous production and from colonic fermentation of carbohydrates by enteric bacteria (359). Endogenous acetate is formed from acetyl CoA by acetyl CoA synthetase and acetyl CoA hydrolase and the liver is felt to be primary site of acetate metabolism (360). Acetate is known to be utilized in peripheral tissues (361) and total body oxidation may account for between 2 and 10% of energy expenditure (362). It's role in endogenous metabolism is not fully understood, but may serve to aid in the redistribution of oxidisable substrates to the myocardium and brain, particularly in situations of caloric deprivation (359).

Elevated levels acetate may be relevant to changes in metabolism in thermal injury for several reasons. Studies in diabetes mellitus have shown elevated plasma acetate concentrations, possibly due to increased availability of acetyl CoA from increased β-oxidation of fatty acids, with reduced TCA cycle activity (363). More recently, a study in rats has shown that increased acetate production by enteric bacteria, drives increased glucose stimulated insulin secretion via increased parasympathetic activity and may contribute to the development of metabolic syndrome and obesity. Within this study, they also showed that gastric provision of

acetate led to increases in insulin resistance, with increases in plasma and liver lipid and triglyceride content (364). These studies pose the question as to whether alterations in the gut function and changes in the gut microbiome after thermal injury could lead to increased enteric acetate production and absorption and could contribute to insulin resistance and alterations in lipid metabolism.

In the prediction models of MOF and sepsis, it was found that the changes in the metabolite profile of serum samples taken in the second metabolic phase (24-96hrs) showed greater discriminatory power than the early first 24hr serum profiles. The discriminatory performance of these models showed the MOF model to have an AUROC of 0.92 and the sepsis model to have an AUROC of 0.89. These models show a globally different pattern of change compared to the mortality prediction model. The predominant pattern was for metabolites to be lower in the poor outcome groups, including the ketone bodies and amino acids. This could reflect the more severe injuries seen in these poor outcome groups resulting in more dramatic fluid shifts in or more severe perturbations in metabolism. Glucose and glycerol remained higher in the poor outcome groups, reflecting the importance of hyperglycaemia and lipid metabolism in relation to later clinical outcomes.

The sepsis prediction model included some curious findings including decreases in ethanol and methanol. The detection of these metabolites from samples taken >24 is less likely to be from exogenous sources, i.e. alcohol intoxication on admission to hospital. The most likely source of these metabolites is therefore from gut bacterial metabolism, although low levels of endogenous production do occur in humans (365). Why the serum levels of these would be lower in patients who later go to

develop sepsis is not clear and confirmation of this finding would need confirmation with targeted assays. Decreases in ketone bodies in the septic group have previously been described in severe trauma, burns and sepsis. Animal models suggest this may be due to increased peripheral utilization of ketone bodies or greater impairment of hepatic ketogenesis (366).

Carnitine was also lower in the septic group and has been previously shown to be low in general for 2 weeks following thermal injury (367). Carnitine is a quaternary ammonium compound, which plays an essential role in fatty acid metabolism. It facilitates transport of long chain fatty acids across the mitochondrial membrane so they can undergo β-oxidation to generate acetyl CoA, a substrate that enter the TCA cycle to generate ATP. Circulating levels are also depleted in human sepsis (368) and animal studies have shown L-carnitine supplementation can decrease the inflammatory response to lipopolysaccharide (LPS), ameliorate lipid metabolism abnormalities and improve survival in sepsis models (369).

3.5.5 Comparison with published metabolomics studies of thermal injury

To date there has been only one other metabolomics based study of human thermal injury from a group in China. They used ^{1}H-NMR to study changes in the plasma metabolome in 21 patients with very large thermal injuries of >50% TBSA and compared the changes to 3 healthy controls (271). The mean burn size in their cohort was therefore 77% TBSA, approximately twice that of the cohort in this study. Their cohort was also slightly older and had a high proportion of male subjects. They used multi-variate analysis to construct a model, they term an ‘Eigen-metabolome’ of 12

metabolites that were significantly different between the patients and controls. In terms of similarities, their model also interestingly contained 2-HB and a metabolite in the valine synthesis/degradation pathway, alpha ketoisovaleric acid (3-methyl 2-oxobutanoate) which has been to accumulate with mitochondrial dysfunction in liver disease (370). Their model also included increased 3-methylhistidine, an amino acid formed from degradation of skeletal muscle actin and myosin. This is classically studied measured in urine as a marker of skeletal muscle catabolism (371). Interestingly, they also detected a range of hormone metabolites including aldosterone, deoxycorticosterone and 2-methyoxyestrone highlighting the importance of endocrine dysfunction after severe thermal injury. The study does suffer from some methodological issues, including utilizing sample creatinine peak to scale the metabolite data and the use of citrated blood samples which can mask the detection of other metabolites. However, the study does, complement our work in showing that metabolomics can be applied to try to understand the complex network of metabolic changes after severe thermal injury.

Metabolomics has been applied to animal models of thermal injury to study changes in muscle metabolism and develop metabolite models predict injury severity and sepsis. Righi et al used Total through Body correlation Spectroscopy (TOBSY) NMR to quantify metabolites in muscle in a mouse hind limb burn model. They showed increased levels of lipids, taurine, phosphocreatine and decreased levels of glutathione, carnosine, glucose, glutamine, glutamate and alanine in the burned limb compared to an unburned limb (269). Izamis et al measured targeted groups of blood metabolites in a 20% TBSA rat burn model and developed a neural network model that could predict the severity of the burn injury with 88% accuracy. The two

metabolites most significantly contributing to the model were very low density lipoprotein (VLDL) and acetoacetate which both inversely correlated with severity of burn. Liu et al. performed LC-MS metabolomic analysis of plasma samples in a 30% TBSA rat burn model and compared profiles of burn injury alone to burn plus caecal ligation and puncture (CLP), a recognized animal model of sepsis. They identified seven putative biomarkers of sepsis, that were significantly elevated in the burn sepsis compared to burn (372).

3.5.6 Limitations of the study

There are several limitations of the study, the first being the broad range of burn sizes included in the study which ranged from 15-95% TBSA. The potential disadvantage of this is that the less severe burns would logically have less severe metabolic derangements which could blunt observation of the changes seen in the larger injuries. Future studies should perhaps employ a lower burn size cut-off of 20 or 30% TBSA. The advantage of including a broad range of burn sizes is wider applicability of the data. Fully quantitative data on the metabolite concentrations has not been presented and calculation of these and application of traditional univariate statistics to assess if group trends hold up with give a more thorough assessment of the changes and potential biomarkers identified. From a technical point of view, pH correction was not applied to the serum samples, so there may be have been some pH variation across samples, resulting in varying shifts in metabolite peaks on the NMR spectrum for some metabolites. Generally, pH correction is more important for urine samples as human serum has a narrower pH range. Potential solutions to this would include pH correction with buffering agents, pH checking and inputting into

analysis software for automated correction or the addition of a pH reference standard such as imidazole to the samples.

3.5.7 Conclusions

Changes in the early serum metabolome after severe human thermal injury have been delineated using 1H-NMR metabolomics. The approach has allowed an assessment of the global changes in the metabolic network, with simultaneous identification of metabolites from a range of metabolite classes. Multi-variate analysis techniques have allowed the metabolomics data to be interrogated and deconvoluted to identify only the most important metabolites contributing to class differences. The changes identified in serum in the first 24hrs after thermal injury reflect increased energy production, altered glucose homeostasis, lipolysis, ketone production and increased TCA cycle activity. Many of this study's findings agree with previous targeted studies of thermal injury metabolism spanning the last 40 years, with a few exceptions that warrant further investigation. Metabolomics predicted later poor outcomes based on patient's metabolite profiles and predictive models demonstrated excellent discriminatory performance. However, the potential future utility of this approach is not to predict binary clinical outcomes which can be done equally well with currently available clinical scoring systems. Rather, this approach could be a first step on the road towards personalized healthcare, with early stratification of care pathways based on early metabolic profiles with the aim of improving outcomes in burn care. The study has also identified novel putative outcome biomarkers that could be taken forward into targeted metabolomics studies.

Future directions of this research include an analysis of urine samples from the same cohort of patients to add further weight to findings from serum and identify putative urine biomarkers of outcome. This approach could also be used to search for putative sepsis biomarkers in human thermal injury, which has not yet been studied. The focus of this study has been on the early changes in the metabolome after thermal injury and how they may relate to later clinical outcomes of the patients. The effects of thermal injury are however prolonged compared to other forms of trauma (299), with increases in resting energy expenditure (REE) persisting for up to 1 year in patients with >30% TBSA burns (REF). Metabolomics could therefore be applied to study the longitudinal changes in metabolism after thermal injury to give a global view of how the metabolic network changes across time. This may reveal changes in unstudied areas of metabolism which could be targetable with pharmacotherapeutics or nutrition to drive improvements in patient outcomes after these devastating injuries.

Chapter 4: Metabolomic study of the longitudinal metabolic response to severe thermal injury in adults

4 Metabolomic study of the longitudinal metabolic response to severe thermal injury in adults

4.1 Introduction

Severe thermal injury, defined as thermal burns affecting ≥20% of the total body surface area (TBSA), results in a profound and prolonged stress response (38). This parallels the systemic inflammatory response and is characterized by elevations in circulating stress hormones leading to a hyperdynamic circulation, hyperthermia, increased resting energy expenditure (REE), derangements in lipid and glucose metabolism and skeletal muscle proteolysis leading to dramatic reductions in lean body mass (LBM) (333). This hypermetabolic response (HMR) is a catabolic state that is seen other forms of trauma and in sepsis, but is more prolonged after thermal injury (299), in which there is evidence of ongoing metabolic derangements up to 3 years after injury (42). Although the HMR is intended to be an adaptive response to trauma, its persistence leads to delayed rehabilitation and is associated with increased morbidity and mortality (42).

Studies over the past three decades have led to an increased understanding of the biochemical and metabolic changes that occur after severe thermal injury. These have led to the introduction into clinical practice of supportive measures to try to reduce the HMR, such as early burn wound excision, improved nutritional support with adequate provision of protein, environmental warming and exercise training. Research has also led to clinical trials of pharmacotherapies including oxandralone and propranolol which have shown safety and efficacy (240,242), but no single drug has yet been shown to completely abolish the HMR. Longitudinal analysis of burn outcomes suggests modern medicine has currently reached a plateau in terms of

improvements in burn survival (284). This highlights the need for new biological information and novel therapeutic targets to drive the next step changes in burn care.

Systems biology approaches such as transcriptomics, genomics and proteomics are starting to help us recognize the complexity of the human response to thermal injury and identify new avenues of research. Metabolomics is a relatively recently developed systems biology technique that harnesses advances in analytical platforms such as Nuclear Magnetic Resonance (NMR) Spectroscopy and mass spectrometry (MS) coupled to advanced chromatographic separation techniques such as Ultra-high performance liquid chromatography (UHPLC). Metabolomics aims to quantify all low molecular weight products (<1.5kDa) of metabolism in a biological system, the spectrum of which is termed the metabolome (252). These products of metabolism, fall downstream of upstream biochemical processes such as gene transcription, protein translation, thus metabolomics can most sensitively and dynamically define the true functional state, or phenotype of an organism or system. It can also identify how the metabolome changes in response to environmental influences, diet, drugs or stimuli, for example, thermal injury.

To date, metabolomics has been applied to the study of burn injury in a limited number of studies, mainly in animal models to study metabolic changes in skeletal muscle (269,373,374) and to try to differentiate sepsis from burn related inflammation (272). The only human metabolomics study of thermal injury, utilized ^{1}H-NMR metabolomics to investigate the metabolome in a single early plasma sample taken from patients with very large burns (>50% TBSA) (271). These studies have demonstrated that metabolomics certainly has potential to yield important new

biological information regarding the complex changes in metabolism after severe thermal injury. However, the response is dynamic and changes across time, therefore a longitudinal approach may yield more useful biological data. Such longitudinal metabolomics approaches have recently been applied in study of human trauma (375) and animal models of sepsis (376).

A further exciting avenue of research is being fueled by the increasing recognition of the interplay between immune function, inflammation and metabolism. The functional coordination of immunity and metabolism is felt to be important in the development of immune responses but also in the resolution of inflammation (377). Metabolites previously considered as simple waste by-products of metabolism, are now being shown to have immunomodulatory functions. Lactate, for example, is a metabolite produced by cells under hypoxic conditions (anaerobic glycolysis) or due to high flux of glycolysis in proliferating cells. It has been recently shown to modulate pro-inflammatory migratory and effector functions of T-lymphocytes (378). The simultaneous longitudinal study of inflammation, immune cell function and the metabolome in patients with severe thermal injury may allow identification of metabolites that influence post-burn immune dysfunction.

Metabolomics therefore has the potential to provide a more global assessment of the metabolic changes that form the hypermetabolic response to severe thermal injury. This could provide new areas of therapeutic potential, to focus more targeted metabolic studies with targeted metabolomics studies and/or conventional biochemical techniques. Other potential advantages of the approach would be the first step towards developing more sophisticated metabolic monitoring of thermally

injured and other critically ill patients, thus allowing more tailored and personalized nutritional and metabolic support with the ultimate goal of improving patient outcomes.

4.2 Aims & objectives

3. To identify the longitudinal changes in the serum metabolome after severe thermal injury (≥ 15% TBSA) in adults aged 16-64 years applying a discovery-based metabolomic approach

4. To relate any metabolic changes to laboratory measures of hypermetabolism and inflammation.

4.3 Materials and Methods

4.3.1 Study group and recruitment

Samples for this study were obtained from patients recruited to a UK prospective multi-centre observational study, the SIFTI study (*Scientific Investigation of biological pathways Following Thermal Injury*, UKCRN ID: 13654). The inclusion criteria for the patients enrolled in to this study were: age ≥16 years and <65 years, thermal burns with injury size ≥15% TBSA, arrival to the burn centre and first sample obtained within the first 24hrs of injury and a complete set of 9 serum samples up to 6-months post-injury as per the study protocol (see section 4.3.4). Exclusion criteria for this study were: chemical or deep electrical injury, associated traumatic injuries with an injury severity score (ISS) of >25, early decision (first 24hrs) for comfort care only

due to severity of injury and the presence of certain co-morbid conditions (congestive cardiac failure, malignancy, patients receiving glucocorticoid therapy, multiple limb amputations). All patients included in this study were recruited and treated at the same regional burns centre at the Queen Elizabeth Hospital Birmingham (QEHB) in the UK.

Patients were recruited within the first 24 hours of sustaining injury either by direct informed consent, or, through a legal consultee if required due to the severe nature of their injuries or due to unconsciousness so that they were not able to consent themselves. This method of recruitment was agreed through an UK NHS research ethics committee (NHSREC, reference 12/EM/0432).

4.3.2 Treatment of patients

Treatment of all patients included in the study was standardized through the application of local treatment guidelines used in the QEHB burns centre. This included the use of fluid resuscitation with Ringer's lactate (Hartmann's solution) according to the Modified Parkland Formula (2-4 ml/kg/% TBSA burn) over the first 24hrs post-burn. All patients underwent invasive monitoring of central venous pressure (CVP) and arterial blood pressure and urine output and resuscitation targets were: urine output 0.5-1.0 ml/kg/hr and mean arterial pressure (MAP) of >60 mmHg. Patients with oliguria or hypotension despite adequate crystalloid resuscitation were given 250-500 ml boluses of 5% human albumin solution (HAS) and ionotropic support with noradrenaline. All patients received early enteral nutrition commenced within 24hrs of injury via a nasogastric or nasojejunal tube with energy requirements calculated using the Toronto Formula (379), with resting energy expenditure (REE) calculated using the Harris-Benedict Equation (380). Nutritional support also

included enteral supplementation of glutamine and vitamin C and intravenous supplementation of trace elements until wound closure. All patients admitted to the intensive care unit (ICU) who were expected to have prolonged ventilator support received bowel management via an indwelling bowel management system. All patients received gastro-protection with intravenous ranitidine and thromboprophylaxis with subcutaneous injections of enoxaparin. Patients requiring surgery underwent first burn excision within 72hrs of admission and coverage with split-thickness skin autograft. Patients with burns >40% TBSA typically required wound coverage with combinations of autograft, cadaveric allograft and skin substitutes.

4.3.3 Clinical data Collection

Detailed clinical data were collected for all patients in a standardized case-report form (CRF) which was later entered onto an electronic database. Data included demographics, burn injury data and clinical outcomes including length of ICU stay, total length of stay, survival, the occurrence of sepsis (ABA consensus sepsis trigger criteria) (309) and the occurrence of multiple organ failure (MOF) according to the Denver 2 MOF score (33).

4.3.4 Sample collection and preparation

Blood samples were collected between 08:00 and 10:00. A total of 9 samples for each patient were collected at the following time-points: Day 1 (D1 - first 24hrs post-injury), D3-4, D5-9, D19-24, D26-29, Month 2 (D60+/-7 days), Month 3 (D90 +/- 7 days) and Month 6 (D180 +/-14 days). Patients admitted to the ICU had 6ml blood samples collected from the indwelling arterial or central venous catheter using a Vacuette® blood collection system into Vacuette® Z-serum clot activator tubes

(Greiner Bio-One Ltd, Gloucester, UK). Patients admitted to a burns ward HDU bed who did not have an indwelling vascular catheter had blood drawn by peripheral phlebotomy using an upper arm tourniquet and using an identical blood collection system and tubes as described above. Blood samples were kept upright and allowed to form a clot at room temperature for 30mins before processing into serum aliquots. To obtain serum, blood tubes were then centrifuged at 3000 rpm for 10 minutes at 20°C in a swinging bucket rotor centrifuge (Eppendorf Centrifuge, model 5804 R, ThermoFisher Scientific). Serum aliquots of 400-600 µl were placed in 1.5 ml plastic cryovials and stored upright in a temperature monitored freezer at -80°C.

4.3.5 Sample preparation for metabolomics analysis

Serum samples were randomized from their original collection order, were assigned a new sample identifier and were batch thawed (3 batches) on ice at 4°C. Serum aliquots of 200 μl were transferred to sterile Eppendorf tubes and deproteinised by addition of 600 μl methanol, vortex mixing for 15 seconds and centrifugation for 15 minutes at 13,865 xg. After centrifugation, 370 μl aliquots of the supernatant were transferred into two sterile Eppendorf tubes and lyophilized at 45°C for 16 hours using a vacuum centrifuge (Heto-Holten VR-Maxi) attached to a refrigerated vapour trap (Thermo Scientific Savant RVT 4104, ThermoFisher Scientific, USA). A pooled Quality Control (QC) sample was also prepared by combining 50 μl aliquots of all biological samples and vortexing for one minute. 200 μl aliquots of the pooled QC sample were deproteinised and lyophilized using the same protocol as described above. The lyophilized samples were stored at 4°C until they were reconstituted in HPLC grade water/methanol in a 1:1 ratio, vortex mixed and centrifuged for 15

minutes at 15,871g. The resulting supernatants were transferred into analytical vials and placed in the UPLC autosampler and stored at 4°C during analysis.

4.3.6 Ultra-high performance liquid chromatography-mass spectrometry (UHPLC-MS)

The reconstituted serum samples were analysed by UHPLC-MS in 3 analytical batches with QC samples being analysed for the first ten injections of each batch and then after every 6 individual patient samples. All samples for one subject were analysed in the same batch and each subject was randomized across the batches. UHPLC-MS measurements were performed using and a Thermo Scientific Ultimate 3000 coupled to a Q-Exactive^{TM} Hybrid Quadropole-Orbitrap mass spectrometer (ThermoFisher Scientific, MA, USA). A Hypersil Gold C18 column was applied for metabolite separation prior to mass spectrometric detection. Samples were analysed in positive and negative ion modes separately and data were acquired in the *m/z* range 50-1000Da with a scan rate of 0.4s. The analytical method applied is available at (381).The UHPLC column was washed with 100% methanol for 60 minutes between analytical batches.

4.3.7 Pre-processing of data, quality assurance and metabolite identification

The three-dimensional (3D) raw data (*m/z* vs. retention time vs. response) was deconvoluted using the freely available XCMS software (382). The deconvolution process includes peaking picking, integration and alignment, and converts the 3D raw data into a two-dimensional (2D) matrix of samples in columns and metabolite features in rows and peak responses reported for each metabolite feature detected for each sample. A peak response is defined as the sum of intensities over a window of specified mass and time ranges.

In this study, QC samples were employed as they provide four advantages to metabolomic studies: 1) To provide instrument conditioning through initial injection of ten QC samples to provide instrument stability for important biological sample analysis; 2) To provide signal correction for instrument response drift across each batch; 3) To provide a method of quantifying analytical experiment reproducibility and 4) To permit integration of data across batches as not all samples could be run in a single batch (383). Prior to quality assurance (QA) procedures being applied to the data, metabolite features were removed that were present in <50% of the QC pooled samples. The QA process used in the study was that used for the HUSERMET project (384). Quality control-Robust Loess Signal Correction (QC-RLSC) was applied within and across the three batches to correct for technical variations in the data whilst maintaining biological variation. All features were then removed whose response had a relative standard deviation (RSD) >20% across the QC samples after QC injections 1 to 8 for each analytical batch were removed. Finally, metabolite features with >60% missing values across all the samples were removed from the dataset. The data was assessed for technical variation using Principal Component Analysis (PCA) using Metaboanalyst v3.0 (385).

Metabolite features were annotated on the QC filtered dataset using the PUTMEDID-LCMS workflows operated in the Taverna workbench (384). This putative annotation is consistent with the Metabolomics Standards Initiative (MSI) level 2 standard of reporting (386). In some cases, metabolite features were annotated with multiple metabolites due to having the same molecular formula or similar monoisotopic masses and therefore similar retention times and the same accurate *m/z*.

4.3.8 Measurement of serum cytokines

Serum cytokine measurements were performed as a 9-plex assay, measuring IL-1β, IL1-RA, IL-6, IL-8, IL-10, IL-17, TNF-α, MCP-1 and G-CSF (Performed by Dr. Peter Hampson). This was done using the Biorad Multiplex immunoassay platform and Bio-Plex 200® reader (Bio-Rad laboratories, Germany) according to the manufacturer's instructions. To calculate the concentrations of cytokines, standard curves were generated by making 4-fold serial dilutions using the standards supplied. Cytokine measurements were also conducted on serum processed from 9 healthy volunteers to serve as control values. Samples were collected and processed identically to those from the patients.

4.3.9 Measurement of urinary urea nitrogen excretion (UUN)

24 hour urine collections were conducted by regular emptying of the patient's urine catheter bag into a 5-litre sterile plastic container. Collections were started after draining all urine passed overnight from the catheter bag and collecting all urine passed between 08:00 hrs and 08:00 hrs the following day. The total volume of urine excreted was measured using a measuring a cylinder and a 5ml aliquot sent to the routine biochemistry laboratory at QEHB. Urinary urea was reported as mmol of urea in 24hrs and this was converted to urinary urea nitrogen (UUN) excretion (g/24hrs) by multiplying by 0.028.

4.3.10 Statistical analysis

Metabolomics data analysis was performed using Metaboanalyst v3.0 (385,387,388). To identify key trends in the longitudinal metabolomics data, univariate methods including one-way ANOVA with Tukey's post-hoc analysis was applied separately to the positive and negative ion mode datasets. Pre-processing of data for univariate

analysis included no imputation of missing values and normalization by sum (total peak area per sample). To select and focus on key metabolite features changing over 0-6-months post-injury, false discovery rate (FDR) corrected (Benjamini-Hochberg) p-values with a cut-off p=<0.05 were used. Multi-variate analysis methods were also used which included PCA and Partial Least Squares Discriminant Analysis (PLS-DA). For PCA and PLS-DA, pre-processing steps included KNN missing value imputation, normalization by sum and generalised-log transformation (g-log).

Patient demographic, burn injury and outcome data were analysed using univariate methods in SPSS v23.0 statistical software (IBM, USA). Datasets were assessed for normal distribution using the Shapiro-Wilkes test. Parametric data are displayed as means with standard deviation (SD) and groups compared using the Independent Samples t-test. Non-parametric data are displayed as medians with interquartile range (IQR) and groups were compared using the Mann-Whitney U-test. Categorical variables were compared using Fisher's exact test. Serum cytokine data were analysed using GraphPad PRISM v7.0 software (GraphPad Software Inc., USA). Data were assessed for normality using the Shapiro-Wilkes test and analysed using non-parametric ANOVA with Dunn's multiple comparison post-hoc test, with each data point being compared to control values measured from healthy volunteers. Statistical significance was considered at a probability of *p*-value <0.05.

4.4 Results

4.4.1 Demographics and outcomes of the study group

A total of 13 adult patients with severe burns >15% TBSA were selected from the SIFTI study for inclusion in this longitudinal study of metabolism (Table 4.1). The mean age of the study group was 36 (range 17-55) years, male:female ratio was 1.6:1 and the mean burn size was 42% (range 16-66) TBSA. Flame burn was the most common mechanism of injury (84%), with only 1 patient sustaining a scald injury and 1 patient sustaining a combined flame/flash injury. The key outcomes for the study group are summarized in Table 4.2.

Admission parameters	Values
n	13
Age (years)	36.0 (+/- 12.1)
Male n (%)	8 (62.0)
BMI (kg/m^2)	26.6 (+/-4.6)
TBSA (%) (IQR)	42.0 (19.5-61.0)
TBSA-FT (%) (IQR)	16.0 (4.0-54.8)
Inhalation injury n (%)	5 (38.5)
ICU Admission n (%)	9 (69.2)
APACHE II first 24hrs (IQR)	28.0 (9.5-29.0)
SOFA first 24hrs (IQR)	8.0 (1.0-11.0)
Denver MOF first 24hrs (IQR)	2.0 (0.0-3.5)
R-Baux	81.5 (+/- 26.8)
ABSI (IQR)	7.0 (6.0-11.0)
BOBI (IQR)	3.0 (1.0-4.5)

Table 4-1. **Demographic and injury data for adult severe burns cohort (>=15% TBSA).**
Abbreviations: APACHE (Acute physiology, age and chronic health evaluation score), SOFA (Sequential organ failure assessment) score, ABSI (Abbreviated burn severity of illness) score and BOBI (Belgian outcomes in burn injury) score.

Outcome variable	Value
Mortality n (%)	1 (7.7)
MOF (Denver > 2) n (%)	5 (38.5)
Time to organ recovery (days) (IQR)	12.0 (0.0-48.0)
Sepsis n (%)	9 (69.2)
ICU LOS (days) (IQR)	13.0 (0.0-54.5)
Mechanical Ventilation days (IQR)	10.0 (0.0-37.0)
Hospital LOS (days) (IQR)	54.0 (21.0-116.0)
Hospital LOS (days/% TBSA)	1.6 (+/- 0.7)

Table 4-2. Summary of the key clinical outcomes for the adult severe burns cohort. (MOF=multiple organ failure, ICU= intensive care unit, LOS=Length of stay, IQR=interquartile range).

4.4.2 Overview and quality assurance of data

The complete metabolomic experiment included 292 serum samples and 54 pooled QC samples (after removal of QC injections 1-8 in each analytical batch) analysed by UHPLC-MS. The raw data included 9509 metabolite features identified in positive ion mode and 8016 metabolite features identified in negative ion-mode (total of 17,525 metabolite features). QC-RLSC was applied to correct for small levels of technical variance and to integrate each analytical batch in to a single dataset for each ion mode. After quality assurance (QA) methods had been applied to the data this decreased to 4639 metabolite features in positive ion-mode (48.8%) and 3546 metabolite features (44.2%) in negative ion-mode (total 8185 metabolite features). PCA analysis was applied to assess technical variability across the 3 analytical batches after QA for the positive ion-mode (Figure 4.1a) and negative ion-mode (Figure 4.1b) datasets. The scores plots both show a good spread of the data from

across the three batches with no clear clustering of any of the 3 batches, confirming no technical problems associated with the biological data. PCA analysis comparing individual patient samples and QC pooled samples for both positive and negative ion-mode showed good tight clustering of the QC samples and a larger spread of the patient samples (Figure 4.2a and Figure 4.2b for positive and negative ion modes, separately). The data to be applied for the longitudinal study were then separated from other data.

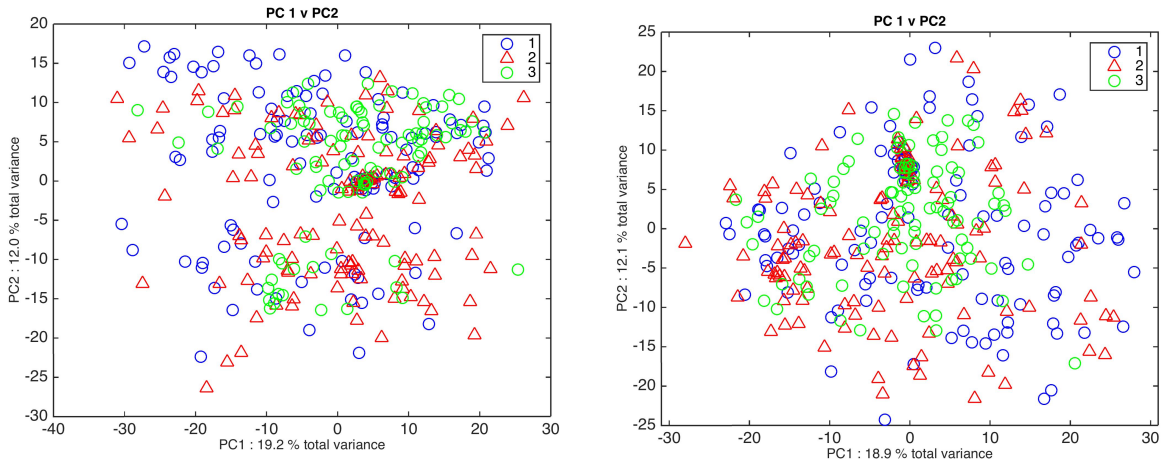

Figure 4-1 PCA scores plot of LC-MS data from serum samples in all 3 analytical batches. A: Positive ion mode data, B: Negative ion mode data.

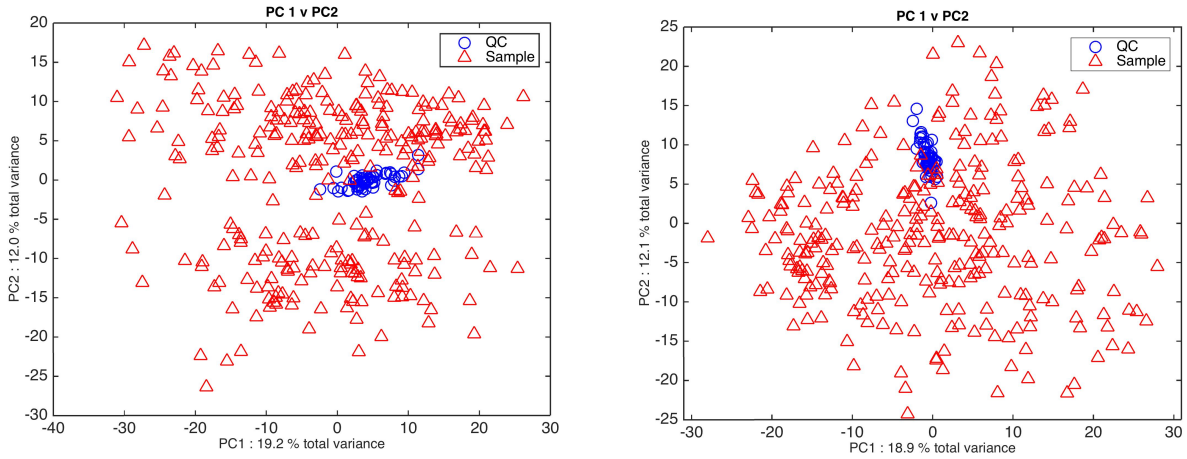

Figure 4-2. PCA scores plot of LC-MS data from individual serum samples and pooled QC samples. A: Positive ion mode data, B: Negative mode data.

4.4.3 The longitudinal changes in the serum metabolome following severe thermal injury

4.4.3.1 Overview

UHPLC-MS data from a total of 117 serum samples from 13 patients were used for analysis of the key longitudinal changes in the serum metabolome after severe thermal injury. ANOVA analysis showed a total of 459 metabolite features that were statistically significantly different ($q<0.05$ following Benjami-Hochberg method for FDR) across the study time course. The metabolite class of each metabolite feature annotation was checked using the Human Metabolome Database (HMDB) (www.hmdb.ca) and the LIPIDMAPS database (ww.lipidmaps.org). This identified 27 metabolite features with annotation from distinct metabolite classes which were removed from the final dataset, leaving 432 metabolite features from 35 classes (Table 4.3). The filtering process applied to the raw data is shown in a flow-diagram (Figure 4.3).

Further in-depth analysis focused on 348 metabolite features within eight classes in which ≥10 metabolite features were statistically significant across the time-course. These were ranked 1-8 by the number of metabolite features changing within each class (Table 4.3). Within these eight classes, changes in lipid metabolism pre-dominated with five classes represented and a total of 295 metabolite features being lipids (85%). The lipid classes were sub-classified according to the LIPIDMAPS lipid classification system to make trend analysis interpretation simpler. The longitudinal changes seen within each class are presented below, with representative trends plotted for individual metabolite features. Only metabolite features with annotations to a single metabolite sub-class were used for trend analysis.

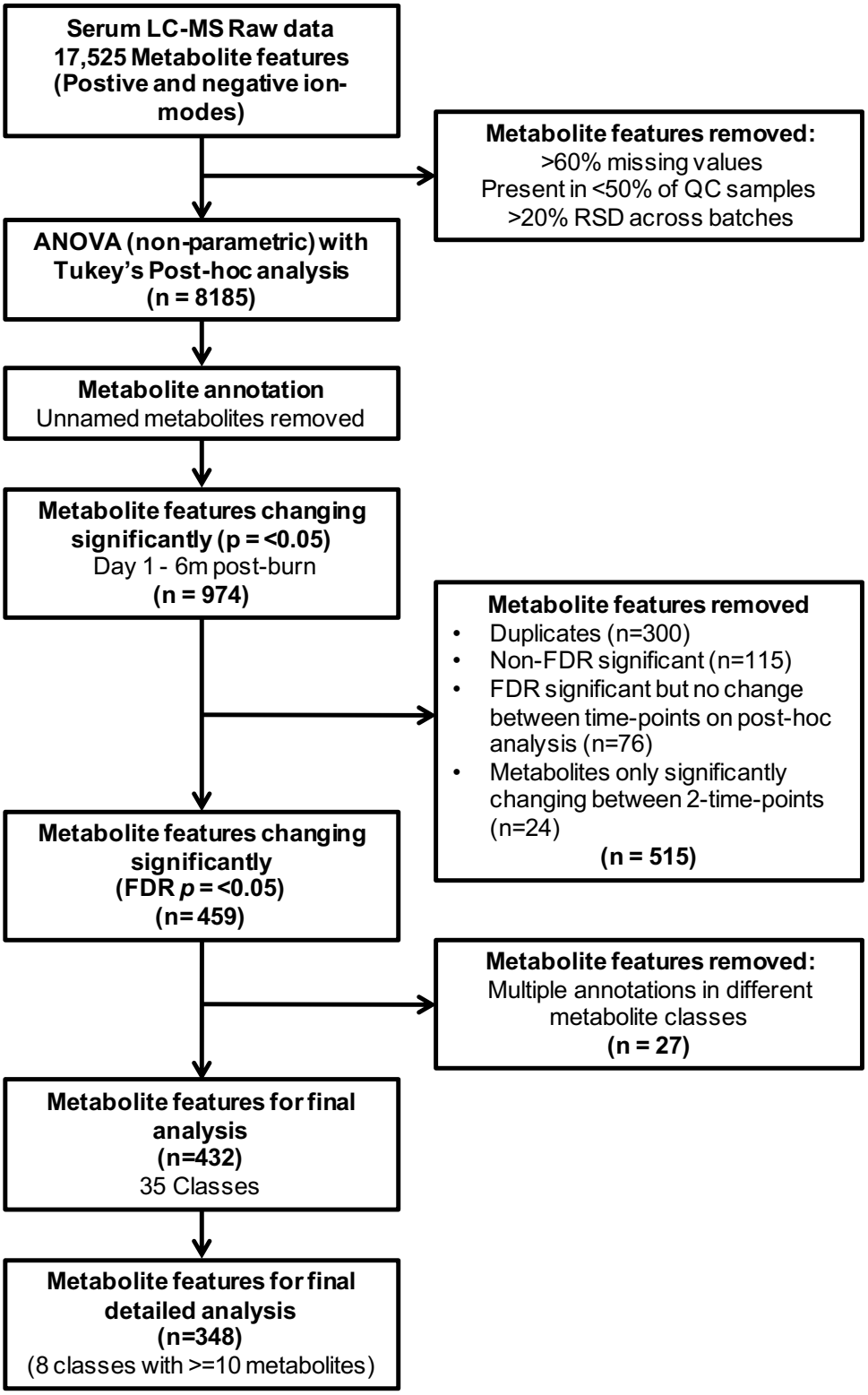

Figure 4-3. Flowchart of process of selection of metabolite features for further detailed analysis from the young severe burn LCMS data. (LC-MS = Liquid chromatography mass spectrometry, RSD = Relative standard deviation, FDR = false discovery rate)

No.	Metabolite Class	No of metabolites FDR p=<0.05
1	Fatty acyls	93
2	Glycerophospholipids	80
3	Sterol lipids	73
4	Glycerolipids	30
5	Peptides	26
6	Sphingolipids	19
7	Phenylalanine, Tyrosine and Tryptophan metabolism	16
8	Aromatic metabolites	11
9	Other mixed classes	9
10	Vitamin E metabolism	8
11	Nicotine and nicotinate metabolism	7
12	Carbohydrates	6
13	Heme metabolism	6
14	Drug metabolism	5
15	Prenol lipids	5
16	Suplhur containing metabolites	5
17	Purine and pyrimidine metabolism	4
18	Caffeine metabolism	3
19	Cysteine and methionine metabolism	3
20	Choline metabolism	2
21	Glutamate and glutamine metabolism	2
22	Histidine metabolism	2
23	Nucleotides and nucleosides	2
24	Oxidative phosphorylation metabolism	2
25	Phospholipid synthesis	2
26	Pterin metabolism	2
27	Amino sugar and nucleotide metabolism	1
28	Biotin metabolism	1
29	Folate metabolism	1
30	Lysine metabolism	1
31	Polyamines	1
32	Polysaccharides	1
33	Serotonin metabolism	1
34	TCA cycle	1
35	Vitamin B metabolism	1
	TOTAL	**432**

Table 4-3. Summary of all metabolite classes changing significantly in serum over 6 months post severe thermal injury and number of significantly changing metabolites in each class (FDR, P=<0.05).

4.4.3.2 Lipid Metabolism

Lipids make up a large proportion overall (300/432, 70%) of all the annotated metabolite features that are changing significantly over the first 6-months post thermal injury. The classes with the highest frequencies were the fatty acyls (FA) (n=92) and the glycerophospholipids (GP) (n=80). The frequencies observed in the data for all the lipid sub-classes are summarized in Table 4.4. The classes of lipids showing the greatest number of concentration changes were further subdivided per the LIPIDMAPS lipid classification system.

No.	Lipid class	No of metabolites FDR p=<0.05
1	Fatty acyls (FA)	**93**
2	Glycerophospholipids (GP)	**80**
3	Sterol lipids (ST)	**73**
4	Glycerolipids (GL)	**30**
5	Sphingoplipids (SP)	**19**
6	Prenol lipids (PR)	**5**
	Total	**300**

Table 4-4. Frequency table of lipid metabolite features significantly changing in serum across the 6 month time course after severe thermal injury.

4.4.3.3 Fatty acyl metabolism

A total of 93 fatty acyl (FA) metabolite features statistically significantly changed across the time-course in the study group (Table 4.5). Within sub-classes of FAs, the highest frequencies of significantly changing metabolites were seen in the Fatty acids and conjugates sub-class (n= 56) and Eicosanoids class (n=10).

No.	Fatty acyl sub-class	No of metabolites FDR p=<0.05
1	Fatty acids and conjugates	**56**
2	Eicosanoids	**10**
3	Fatty amides	**9**
4	Fatty alcohols	**6**
5	Fatty esters	**6**
6	Octadecanoids	**3**
7	Docosanoids	**2**
8	Fatty acyl glycoside	**1**
	Total	**93**

Table 4-5. Frequency table of fatty acyl metabolite features within each sub-class, significantly changing across the 6-month time course after burn injury.

Within the fatty acids and conjugates sub-class of fatty acyls, the commonest trend observed was a steep decline from admission normalized peak intensities to levels on D3-4 and then further decline until a nadir at 3 weeks post-injury. This was followed by a gradual increase up to M6 at which levels were close to admission levels. Examples of this trend are seen in all the sub-classes of fatty acids observed (unsaturated fatty acids, dicarboxylic acids and branched chain fatty acids) and are shown in Figure 4.4 (a-d). The next most common trend observed was an initial decline of normalized peak intensities after admission, with a nadir at D10 post-injury and then a rise with a late peak 4-8 weeks post-injury and then decline again below admission levels. Examples are shown in box and whisker plots in Figure 4.5 (a-c).

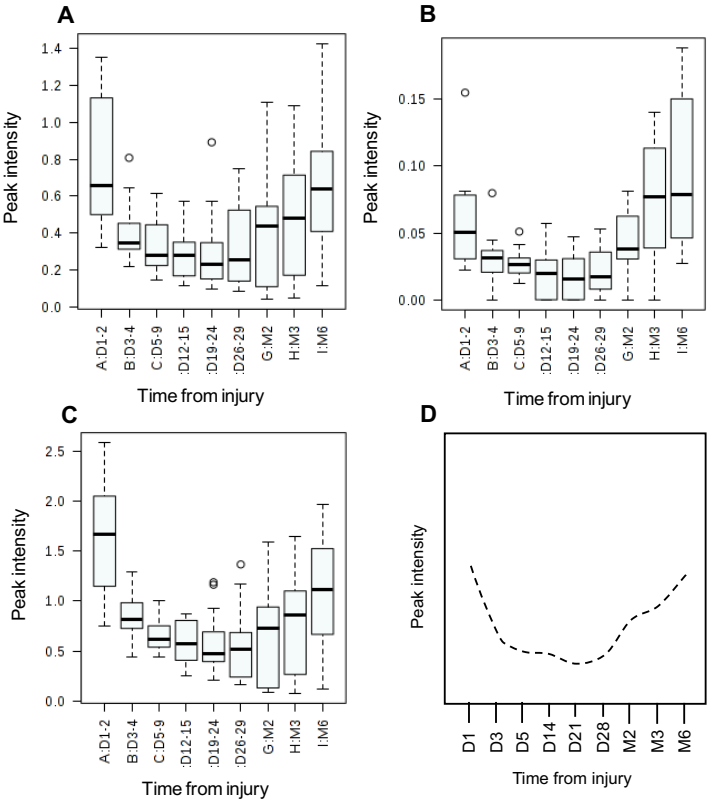

Figure 4-4 Box and whisker plots showing common longitudinal patterns of change in peak intensity seen in fatty acid metabolite features after severe burn injury. A: M3706 (methyl-hexacosadienoic acid or heptacosadienoic acid) (Branched chain FA) (p=0.0063), B: M1629, octadecatrienoic acid (Unsaturated FA) p=0.0017, C: M3386, Hexacosanedioic acid (Dicarboxylic acid) (p=0.0005) and D: Summary of trend.

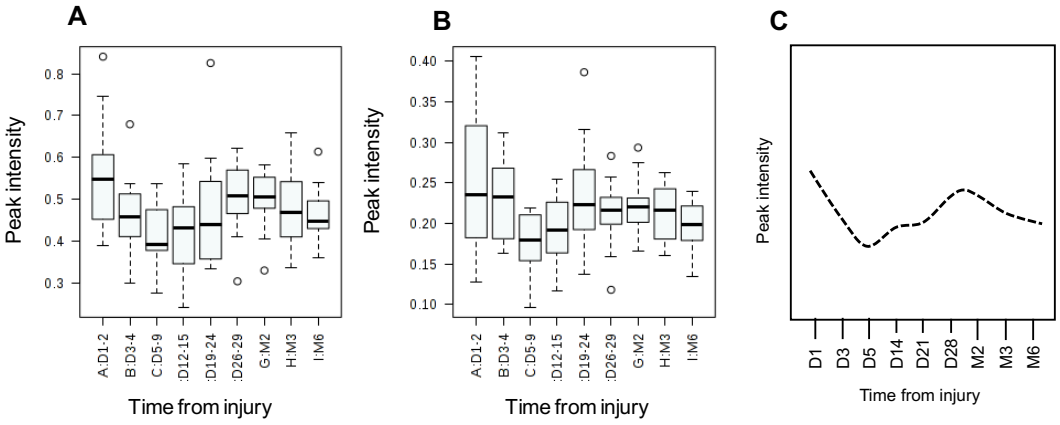

Figure 4-5. Box and whisker plots showing common longitudinal trend for fatty acid metabolite features after severe burn injury. A: M4837, tetratriacontatetraenoic acid (unsaturated FA) (p=0.0150) B: M1240, hexadecatrienoic acid (unsaturated FA) (p=0.0273) and C: Summary of trend.

Another trend seen in all sub-classes of FAs was a decline from admission levels with a plateau at low levels compared to admission and no return to peak intensity levels seen during the first 24hrs after burn injury. Examples are shown in box and whisker plots in Figure 4.6.

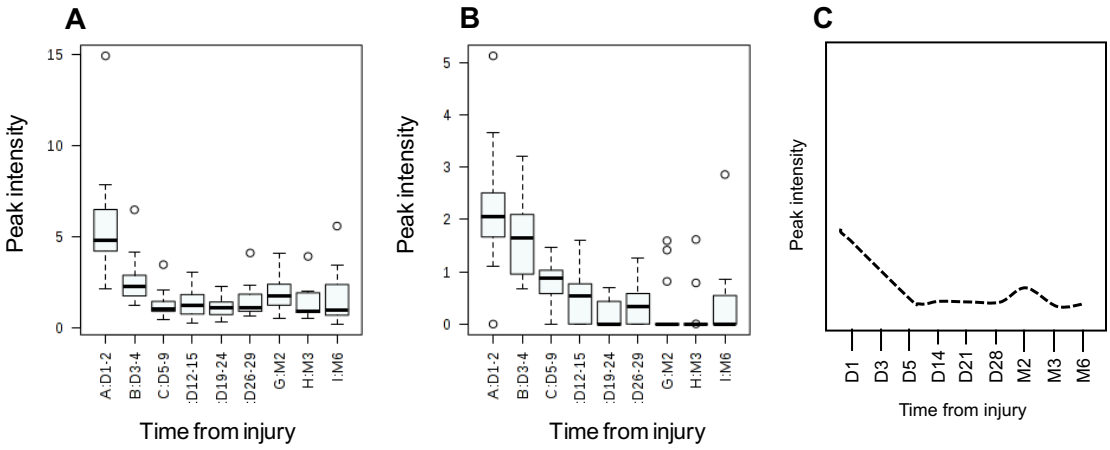

Figure 4-6. Box and whisker plots showing common longitudinal trends for fatty acid metabolite features after severe burn injury. A: M2029, Octadecenetrienoic acid (straight chain FA) (*p*=<0.0001), B: M2582, Hydroxy-tridecenoic acid and/or oxo-tridecanoic acid (Hydroxy-FA) (*p*=<0.0001) and C: Summary of trend.

4.4.3.4 Eicosanoids and Docosanoids

The eicosanoids are typically pro-inflammatory mediators primarily synthesised from arachidonic acid and in contrast the docosanoids which are derived from the fatty acids eicosapentaenoic acid (EPA) (C20:5) and docosahexaenoic acid (DHA) (C22:6) (389). Although classified in the LIPIDMAPS classification system in a separate sub-class of fatty acyls, the docosanoids are considered together in this section as they are synthesised in a similar fashion often through the same enzymes

and are biologically related in function. The docosanoids include the resolvins, protectins and maresins.

The leukotriene metabolite features showed a general trend towards increasing from the day of admission and either peaking at D5-9 or D12-15 before either continuing to decline or rising again between M2 and M6 (Figure 4.7). The three prostaglandin metabolite features showed 2 distinct patterns: 1) Increased from admission to peak at D12-15 before decline; or 2) Decreased from admission followed by fluctuating levels but generally increasing back up towards admission levels (Figure 4.8). The hydroxy/hydroperoxyeicosatrienoic acids and epoxyeicosatrienoic acids similarly showed elevated levels during the acute phase, remaining so for 2-4 weeks post-injury before declining (Figure 4.9). Two docosanoids changed significantly and each were annotated with multiple isomers including neuroprotection-D1, resolvins (D5, D6 and D7) and other DHA-related metabolites so may represent the same metabolite (Figure 4.9c).

No.	Sub-class	No of metabolites FDR p=<0.05
	Eicosanoids	**10**
1	Leukotriene	**4**
2	Prostaglandin	**3**
3	Hydroxy/hydroperoxyeicosapentaenoic acids	**2**
4	Epoxyeicosatrienoic acids	**1**
	Docosanoids	**2**
	Total	**12**

Table 4-6. Frequency table of metabolite features significantly changing in adult serum after severe burn injury in the Eicosanoid and docosanoid classes of lipids, summarized according to frequencies in each sub-class.

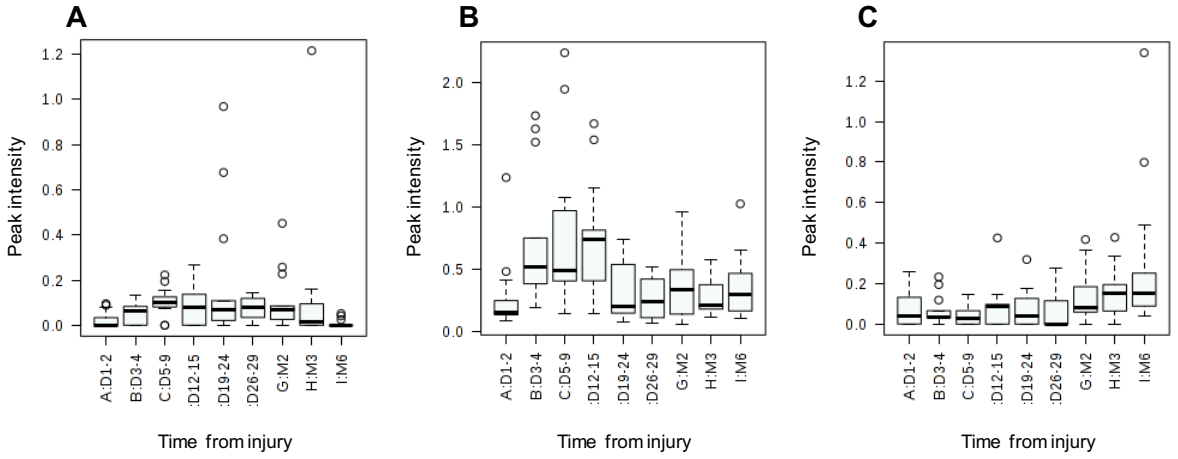

Figure 4-7. Box and whisker plots showing longitudinal trends in significantly changing leukotriene metabolite features in serum after severe burn injury. **A:** M5086, Leukotriene D5 (*p*=0.0167), **B:** 4604, N-Acetyl-leukotriene E4 (*p*=0.0002) **C:** 3457, 10,11-dihydro-20-trihydroxy-leukotriene B4 (*p*=0.0140).

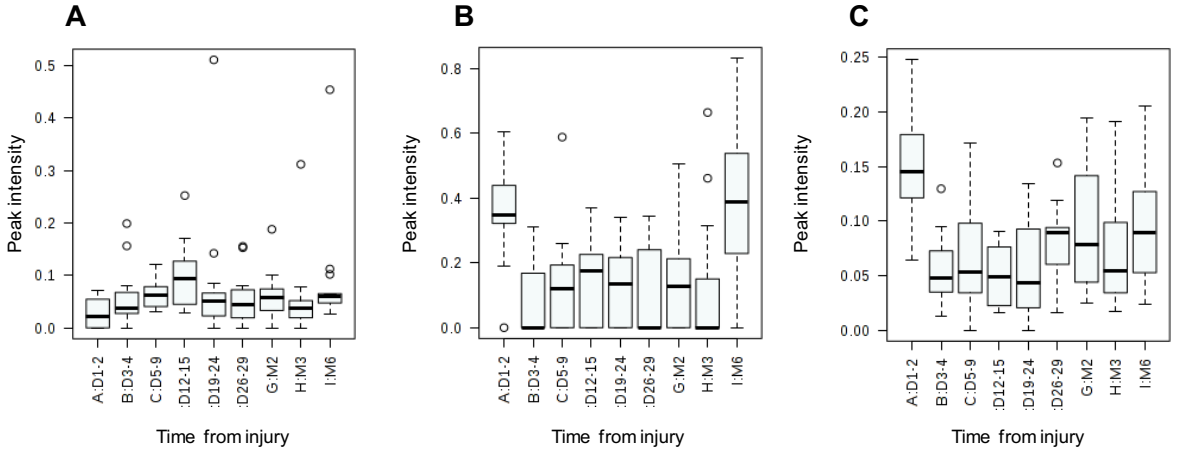

Figure 4-8. Box and whisker plots showing longitudinal trends in significantly changing Prostaglandin metabolite features in serum after severe burn injury. **A:** M4281, annotated isomers: Prostaglandin PGE2 1-glyceryl ester; 1(3)-glyceryl-PGD2;1(3)-glyceryl-PGE2;1(3)-glyceryl-PGH2; 2-glyceryl-PGD2; 2-glyceryl-PGE2; 2-glyceryl-PGH2; PGD2-1-glyceryl ester; (*P*=0.0212).**B:** M2369, annotated isomers: 11-deoxy-PGF1a;11-deoxy-PGF1b;HpEDE; PGE1 alcohol; PGF2alpha alcohol. **C:** M2502, annotated isomers: 11-deoxy-11-methylene-PGD2; 13,14-dihydroxy-11-mulinen-20-oic acid; 5a-Tetrahydrocorticosterone;9-deoxy-9-methylene-PGE2 (*P*=0.0143).

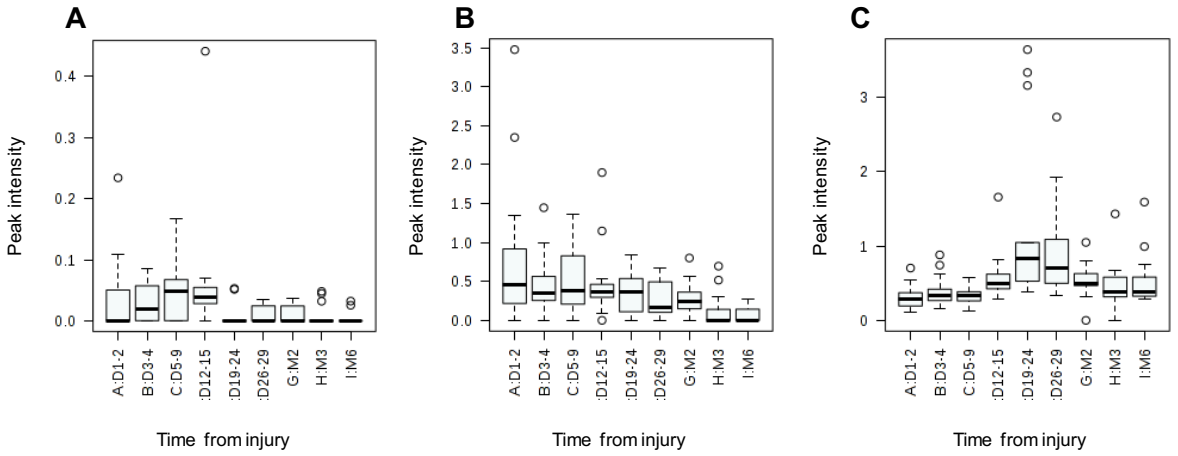

Figure 4-9. Box and whisker plots showing longitudinal change in metabolite features in: **A: Hydroxy/hydroperoxyeicosatrienoic acids:** (M1968), annotated isomers: 12S-hydroxy-5Z,8E,10E-heptadecatrienoic acid; methyl 10,11-epoxy-3,7,11-trimethyltrideca-2,6-dienoate) (p=0.0073).**B: Epoxyeicosatrienoic acids:** (M2930), annotated isomers: 5-Hydroxyeicosatetraenoic acid (5-HETE), 8-HETE; 9-HETE, 10-HETE; 11-HETE; 12-HETE; 13-HETE; 15-HETE; 16-HETE; 17-HETE; 18-HETE; 19-HETE; 20-HETE; 8,9-Epoxyeicosatrienoic acid; 11,12-Epoxyeicosatrienoic acid; 14,15-Epoxy-5,8,11-eicosatrienoic acid; 18-Hydroxyarachidonic acid; 5,6-Epoxy-8,11,14-eicosatrienoic acid (p=<0.0001). **C: Docosanoids**: (M4124), annotated isomers: 15-trans-Neuroprotectin D1; diHDHA; DiHDoHE; HpDHA; Neuroprotectin D1; Resolvin D5; Resolvin D7 (p=0.0299).

4.4.3.5 Glycerophospholipids

A total of 88 glycerophospholipid (GP) metabolite features changed significantly in adult serum after severe burn injury in the final dataset, however after removal of metabolite features that had multiple annotations within different GP classes this left 41 metabolite feature for trend analysis (Table 4.7). The highest frequency sub-classes were the glycerophosphoinositols (Phosphatidylinositols, PI) and glycerophosphocholines (Phosphatidylcholines, PC).

No.	Glycerophospholipid (GP) sub-class	No of metabolites FDR p=<0.05
1	Glycerophosphoinositols (PI)	**11**
2	Glycerophosphocholines (PC)	**9**
3	Glycerophosphoglycerols (PGP)	**6**
4	Glycerophosphoserines (PS)	**6**
5	Glycerophosphates (PA)	**5**
6	Lysoglycerophospholipid (LysoP)	**3**
7	Glycerophosphoethanolamines (PE)	**1**
	Total	**41**

Table 4-7: Frequency table of metabolite features significantly changing in adult serum after severe burn injury in the glycerophospholipid (GP) class of lipids, summarized according to frequencies in each sub-class. Metabolite features with more multiple annotations in different classes of GPs have been removed from this analysis.

Multiple individual trends were observed within each sub-class of GPs. Four trends were observed across most sub-groups: 1) The most common trend was a decline from initial values down to a nadir most commonly at 5-9 days post-injury, followed by an elevation in levels to a peak most commonly at M2 before a slight decline again (Figure 4.10); 2) The next most common trend was an initial rise in metabolite peak intensity to a peak at D5-9 before a plateau at M2 (Figure 4.11); 3) The next most common trend, was a dramatic fall from admission peak intensities over the first 3-9 days with a nadir at two-weeks, with levels rising again from M2 to reach admission day levels by M6 (Figure 4.12); 4) An unusual trend observed was an initial very low peak intensity maintained for the first 3-4 weeks post-injury and then a rise thereafter during the recovery phase with a peak at M6 or decline again from M2. (Figure 4.13).

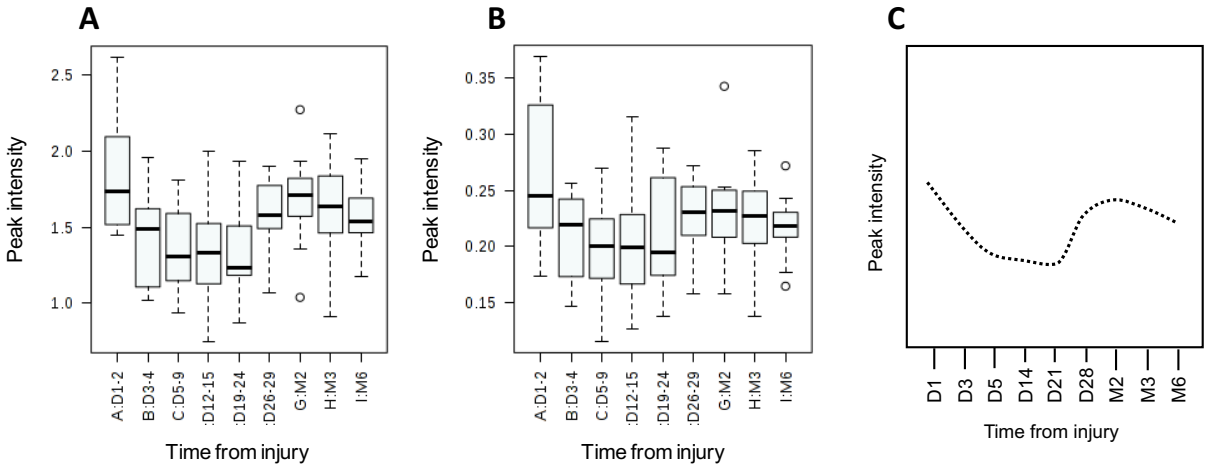

Figure 4-10. Box and whisker plots showing common longitudinal trend (1) seen within the glycerophospholipid metabolite features changing significantly in serum after severe burn injury in adults. **A:** M7672, Phosphatidylserine (PS) (39:1) (p=0.0033) **B:** M7956, Phosphatidylcholine (PC) (44:9) (p=0.0440) and **C:** Summary of trend.

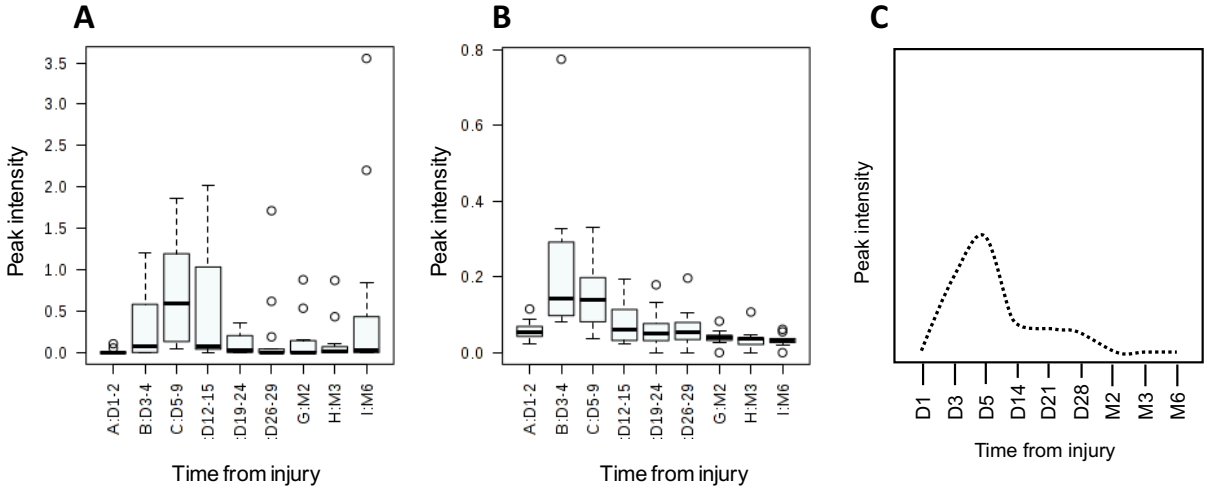

Figure 4-11. Box and whisker plots showing common longitudinal trend (2) seen within the glycerophospholipid metabolite features changing significantly in serum after severe burn injury in adults. **A:** M7910, annotated isomers: Phosphatidylinositol (PI) (43:6); PI (41:3); PI (39:0) (p=0.0012) **B:** M9316, phosphatidylglycerol (PG) (41:2) (p=0.0005) and **C:** Summary of trend.

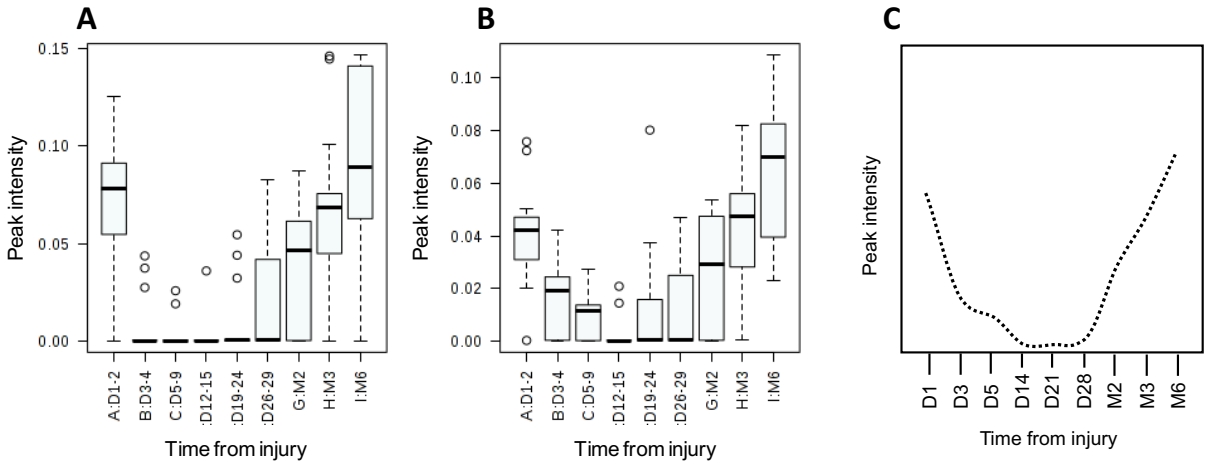

Figure 4-12. Box and whisker plots showing common longitudinal trend (3) seen within the glycerophospholipid metabolite features changing significantly in serum after severe burn injury in adults. **A:** M6589, PG (28:0) (p=<0.0001), **B:** M6703, annotated isomers PA (37:5); PA(O-16:0/15:0); PA(O-18:0/13:0) (p=<0.0001) and **C:** Summary of trend.

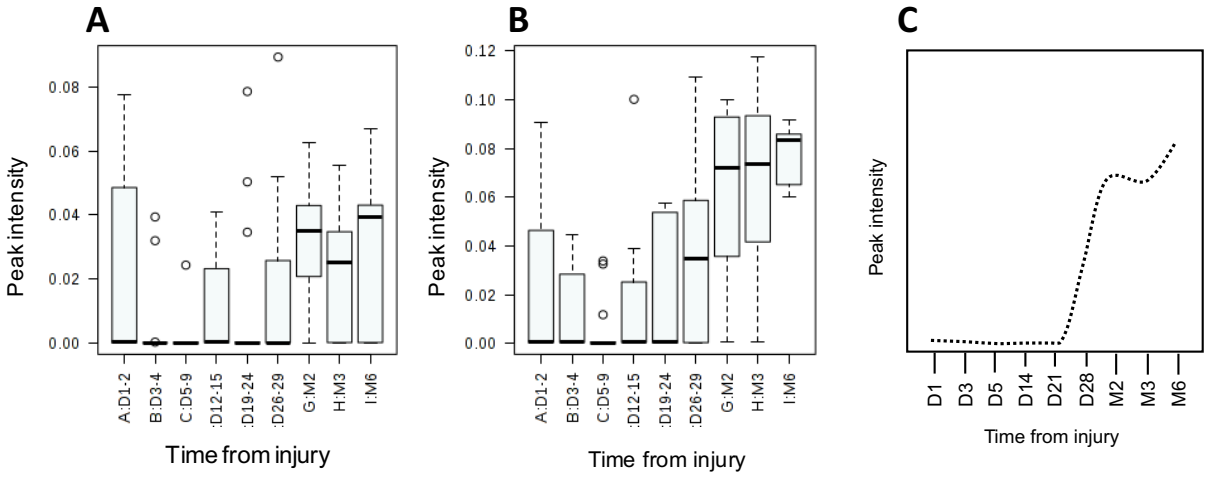

Figure 4-13. Box and whisker plots showing common longitudinal trend (4) seen within the glycerophospholipid metabolite features changing significantly in serum after severe burn injury in adults. **A:** M8123, PS (29:1), (p=0.0044) **B:** M4998, PI (14:0) (p=<0.0001) and **C:** Summary of trend.

4.4.3.6 Glycerolipids

A total of 31 glycerolipid metabolite features changed significantly across the 6-month study time course post burn injury. The sub-group with the highest frequency of statistically significant metabolite feature changes were the diradylglycerols and all 23 were further sub-classified as diacylglycerols (DG) which are glycerides consisting of two fatty acid chains covalently bonded to a glycerol molecule through ester linkages. Table 4.8 shows the frequency of significantly changing glycerolipid metabolite features.

No.	Glycerolipid sub-class	No of metabolites FDR p=<0.05
1	Diradylglycerols	**23**
2	Triradylglycerols	**4**
3	Monoradylglycerols	**4**
	Total	**31**

Table 4-8. Frequency table of glycerolipid metabolite features significantly changing longitudinally over 6-months post burn injury.

Within the four triadylglycerols, all were triacylglycerols (TG) and three of the four showed a decrease from initial levels after injury with a nadir at either D5-9 or D12-15 (Figure 4.14). The other (TG 59:0) increased over the 5-9 days post-injury before falling again to a nadir at 3 weeks and then continuing to rise again to M6. Within the DG sub-class, the predominant trend (91% of metabolite features) was a dramatic reduction from levels within the first 24hrs of injury to the second time-point, D3-4 (Figure 4.15). The peak intensities continued to decrease with a varying nadir within the first month, but most commonly at D19-24 post-injury. The levels then increased

again during the recovery phase to reach levels comparable to those observed on the day of injury by M6. A similar pattern was also seen in 50% of the monoacylglycerols (MG).

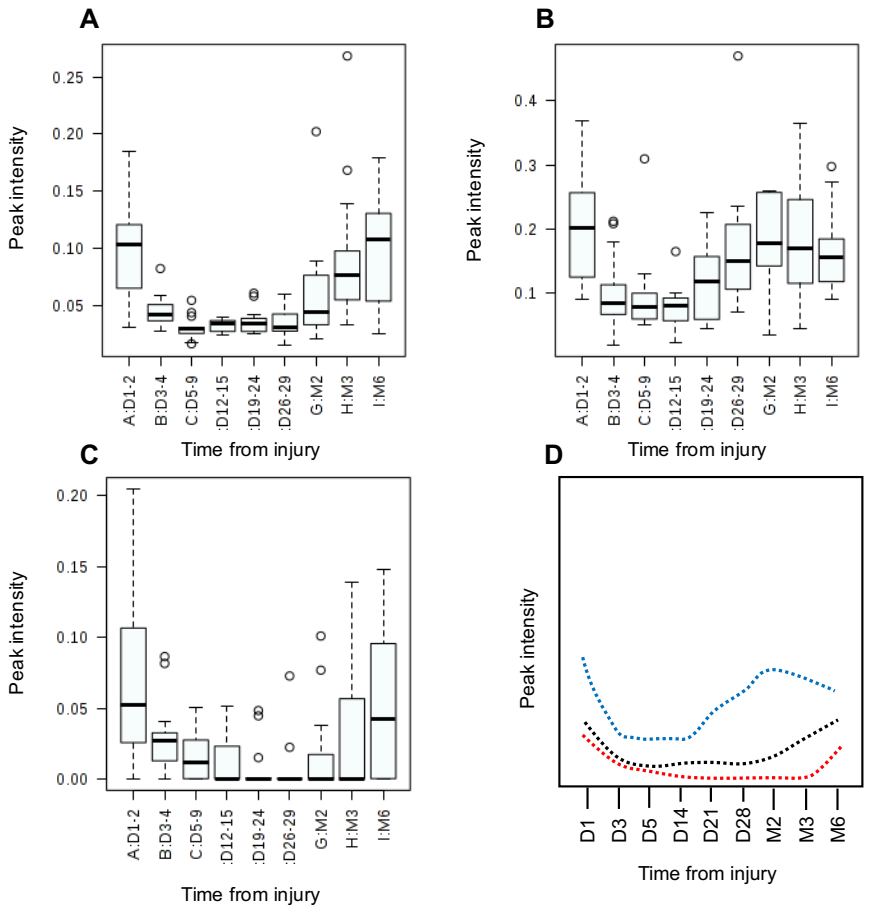

Figure 4-14: Box and whisker plots for triacylglycerol (TG) metabolite features changing significantly in serum after severe burn injury, three differing trends are observed. **A:** M6236, Triacylglycerol (33:0) (*p*=<0.0001) **B:** M7239, Triacylglycerol (50:8) <0.0001 **C:** M5635, Triacylglycerol (30:0) (*p*=0.0047) D: Summary of trends in sub-class.

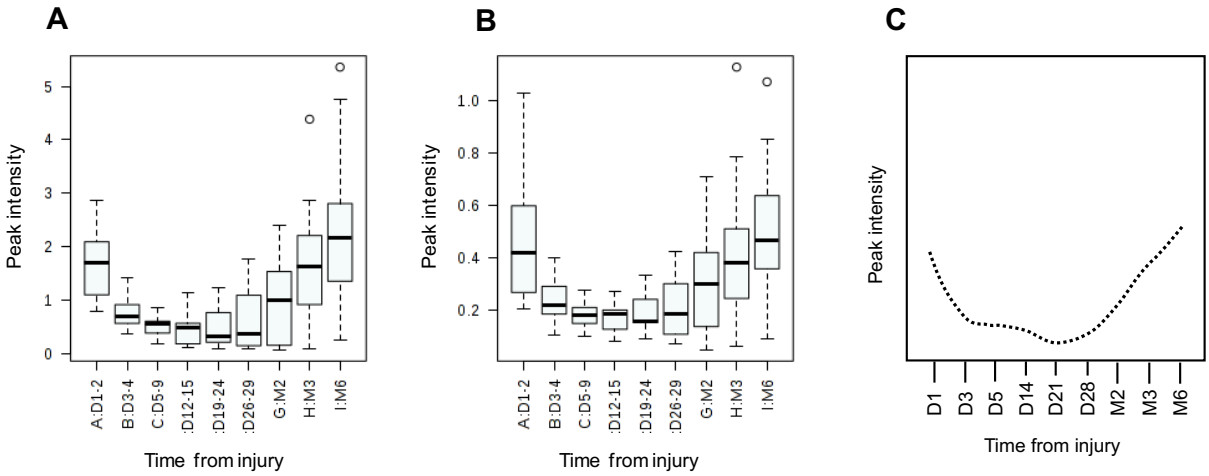

Figure 4-15. Box and whisker plots for diacylglyceride (DG) metabolite features changing significantly in serum after severe burn injury in adults. **A:** M5131, Diacylglycerol (33:4) (*p*=<0.0001); **B:** M5482, Diacylglycerol (32:3) (*p*=<0.0001) and **C:** Summary of main trend seen in the DG sub-class.

4.4.3.7 Sphingolipids

A total of 20 sphingolipid metabolite features changed significantly in serum over the 6-months post burn injury, one metabolite feature was removed from trend analysis due to annotation with multiple sub-classes. The highest frequency of significant metabolite features were in the phosphosphingolipid sub-class. There was a predominating trend pattern seen in 18/19 (95%) of the metabolite features that was previously demonstrated in the fatty acid and glycerophospholipid classes of lipids. This was an initial decline from admission levels towards a main nadir at D12-15 followed by a rise again with a late peak at M2 or M3 and a plateau or slight decline in levels at M6 (Figure 4.16). Some metabolite features displayed a small early peak at D5-9 after the initial decline and then a second decline towards the main nadir at

D12-15 (Figure 4.16a). The general pattern was displayed by metabolite features in all the sub-classes of sphingolipid.

No.	Sphingolipid sub-class	No of metabolites FDR p=<0.05
1	Phosphosphingolipid	11
2	Ceramide	4
3	Neutral glycosphingolipid	3
4	Sphingoid base	1
	Total	19

Table 4-9. Frequency table of sphingolipid metabolite features significantly changing in adult serum after severe burn injury, summarized according to frequencies in each sub-class.

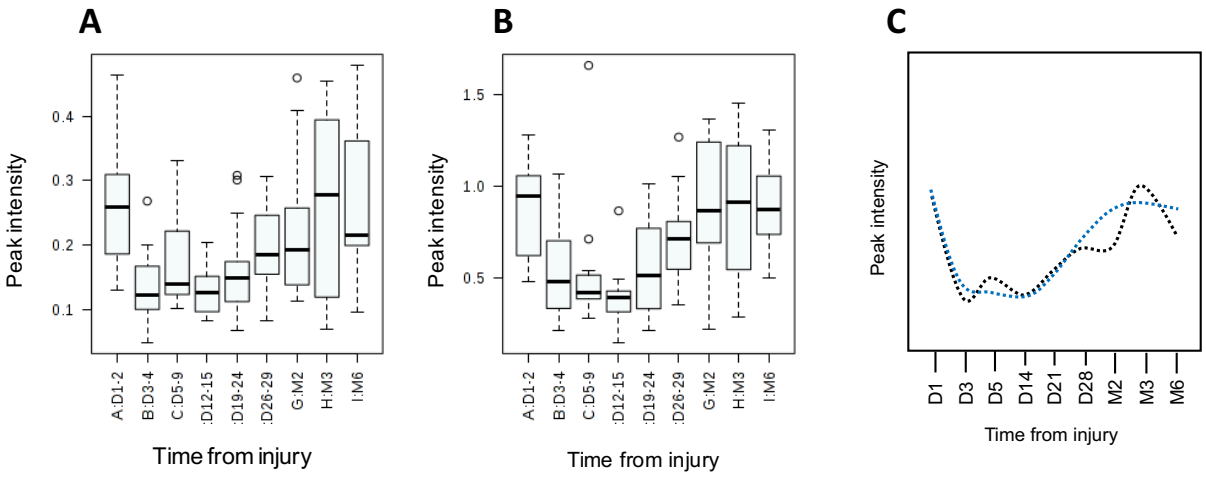

Figure 4-16. Box and whisker plots showing common longitudinal trend seen within the sphingolipid metabolite features changing significantly in serum after severe burn injury in adults.
A: M5076, Cer(d14:1/18:1); Cer(d14:2/18:0); Cer(d18:2/14:0) (Ceramide) (p=0.0005), **B:** M7303, SM(d18:1/22:1); SM(d18:2/22:0) (Phosphosphingolipid) (p=<0.0001) and **C:** Summary of trends within the class.

4.4.3.8 Sterol metabolism

A total of 68 sterol lipids changed significantly across the time-course of the study and the highest frequency seen was within the secosteroid group, which are all associated with vitamin D metabolism (n = 28) (Table 4.10). The next largest group was the steroid conjugates (n = 21) which were a mix of bile acid metabolites (n = 10) and steroid hormone metabolites (n = 10) and sterol metabolites (n = 1).

No.	Sterol lipid sub-class	No of metabolites FDR p=<0.05
1	Secosteroids (Vitamin D metabolism)	**28**
1	Steroid conjugate	**21**
2	Sterols	**9**
3	Bile acids and derivatives	**7**
4	Steroids	**2**
5	Bile alcohol	**1**
	Total	**68**

Table 4-10. Summary table of frequencies of sterol sub-class metabolite features changing significantly across study time-course after severe thermal injury.

4.4.3.9 Vitamin D metabolism

A total of 29 vitamin D metabolite features changed significantly in adult serum after severe burn injury (Table 4.12). Most of these were in the secosteroids sub-class of sterol lipids (28/29, 97%) with one being a steroid conjugate. Two main trends were observed:

1) An increase from day of admission peak intensities with a peak most commonly on D12-15, followed by a decline. Most metabolite features showing this general trend

declined back to admission levels by M2, but a few features plateaued at a slightly higher level than admission from D19-24 onwards (Figure 4.17).

2) The next most common trend seen was a decline from admission levels with a nadir on D19-24, followed by a rise back up again to within the range of admission levels by M6 (Figure 4.18).

One metabolite feature (M3837) showed an unusual trend and was annotated as 1,25-dihydroxyvitamin D_3, the active form of vitamin D in addition to other annotations including 1alpha,25-Dihydroxy-previtamin D3 (Figure 4.19). This metabolite feature showed a decline from admission levels until D12-15 where it plateaued at low peak intensities for the remainder of the study (Figure 4.19).

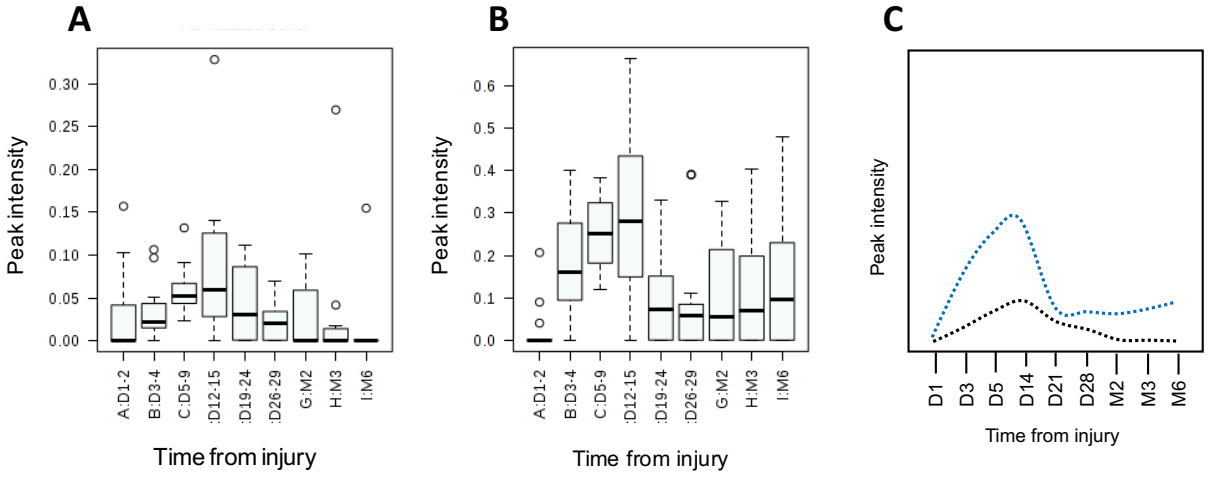

Figure 4-17. Box and whisker plots showing most common serum longitudinal trend (1) in the Vitamin D metabolite features after severe burn injury.

A: M4208, Annotated isomers: 1∝,23,25,26-tetrahydroxycholecalciferol; 6,19-epidioxy-1∝,24-dihydroxy-6,19-dihydrocholecalciferol; 6,19-epidioxy-1alpha,25-dihydroxy-6,19-dihydrocholecalciferol; 1∝,26-Tetrahydroxyvitamin D3;3∝,7∝,12alpha-trihydroxy-5∝-cholesten-26-oic acid; 3∝,7∝,12∝-Trihydroxy-5beta-cholesten-26-oic acid, (p=<0.0001).

B: M5418, 26,27-diethyl-1alpha,25-dihydroxy-20,21-methano-23-oxacholecalciferol, (p=0.0006).

C: Summary of trends.

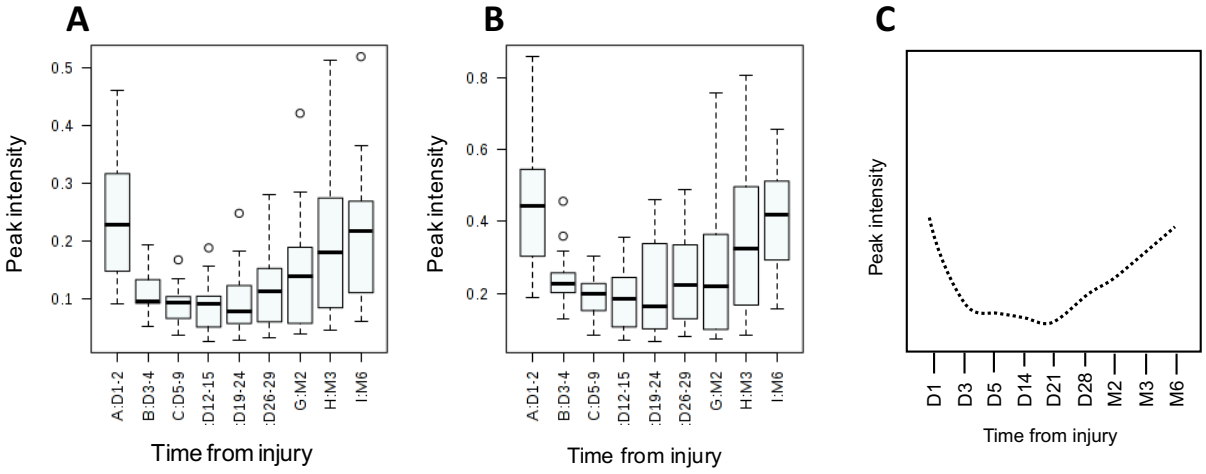

Figure 4-18. Box and whisker plots showing most common serum longitudinal trend (2) in the Vitamin D metabolite features after severe burn injury. **A:** M4285, Vitamin D3 butyrate (p=0.0002). **B:** M4018, 10-ethoxy-10,19-dihydrocholecalciferol (p=0.0005). **C:** Summary of trend.

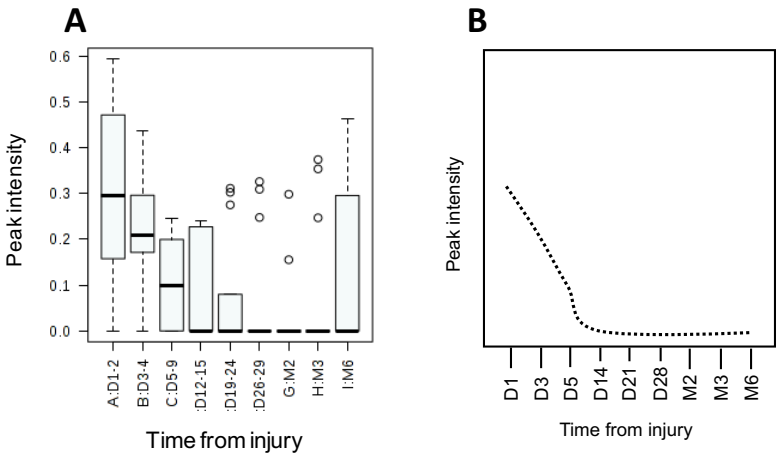

Figure 4-19. A: Box and whisker plot showing serum longitudinal trend for metabolite feature M3837 which was annotated with multiple isomers including the active form of Vitamin D (1,25-Dihydroxyvitamin D_3). Other annotated isomers: 1alpha,25-Dihydroxy-previtamin D3, 18,25-dihydroxycholecalciferol; 1alpha,18-dihydroxycholecalciferol; 1alpha,24-dihydroxycholecalciferol; 1alpha,25-dihydroxy-14-epicholecalciferol; 1alpha,25-dihydroxy-14-epiprecholecalciferol; 1alpha,25-dihydroxy-2-methylene-19-nor-20-epicholecalciferol; 1alpha,25-dihydroxy-2-methylene-19-norcholecalciferol; 1alpha,25-dihydroxy-20-epicholecalciferol; 1alpha,25-dihydroxy-3-epicholecalciferol; 1beta,25-dihydroxy-3-epicholecalciferol; 1beta,25-dihydroxycholecalciferol; 22,25-dihydroxycholecalciferol; 23,25-dihydroxycholecalciferol; 24,25-dihydroxycholecalciferol; 25,26-dihydroxycholecalciferol; 6,19-epidioxy-6,19-dihydrocholecalciferol (p=0.0090).
B: Summary of trend

4.4.3.10 Steroid conjugates

A total of 21 steroid conjugates changed significantly in serum over 6-months post-thermal injury. These could be biologically grouped into conjugates related to bile acid metabolism (n= 10), conjugates related to steroid hormone metabolism (n = 10) and those related to sterol metabolism (n = 1). The trends for all bile acid metabolite (Section 4.4.2.6) features will be presented together in one section and steroid hormone metabolite features will be discussed in another separate section (Section 4.4.2.7).

4.4.3.11 Bile acid metabolism

A total of 16 bile acid metabolite features changed significantly in serum post-burn and more than half of these were sub-classified as steroid conjugates with the remainder being bile acids and derivatives (Table 4.11). Among the steroid conjugates, there was an equal mix of taurine conjugates, glycine conjugates, glucuronides and sulfates.

No.	Bile acid sub-class	No of metabolites FDR p=<0.05
1	Steroid conjugates	**10**
2	Bile acids and derivatives	**6**
	Total	**16**

Table 4-11. Frequency table of metabolite features significantly changing in adult serum after severe burn injury in the Bile acid classes of lipids, summarized according to frequencies in each sub-class.

The predominant pattern of change across the steroid conjugates was an increase from admission levels to reach a peak most commonly at D12-15, followed by a

gradual decline towards admission levels. Some metabolite features in this sub-class displayed an earlier peak at D5-9 and some a later peak at D19-24. Within this group, a mixture of primary and secondary bile acids were observed. The primary bile acids, for example, glycocholic acid (M3866, *p*=<0.0001), generally showed a trend of elevation from admission levels with a peak at D12-15 (Figure 4.20a). Secondary bile acid conjugates, for example, Sulfoglycolithocholate (M5245, *p*=<0.0001), showed an earlier elevation either on D1 or D3-4 before decline to admission levels (Figure 4.20b). Another secondary bile acid metabolite feature, annotated as Lithocholyltaurine and Taurolithocholic acid (M4780, *p*=0.0169), showed low peak intensities for the first 10 days, then began to rise to a peak at D19-24 before returning to admission levels by M2 (Figure 4.20c).

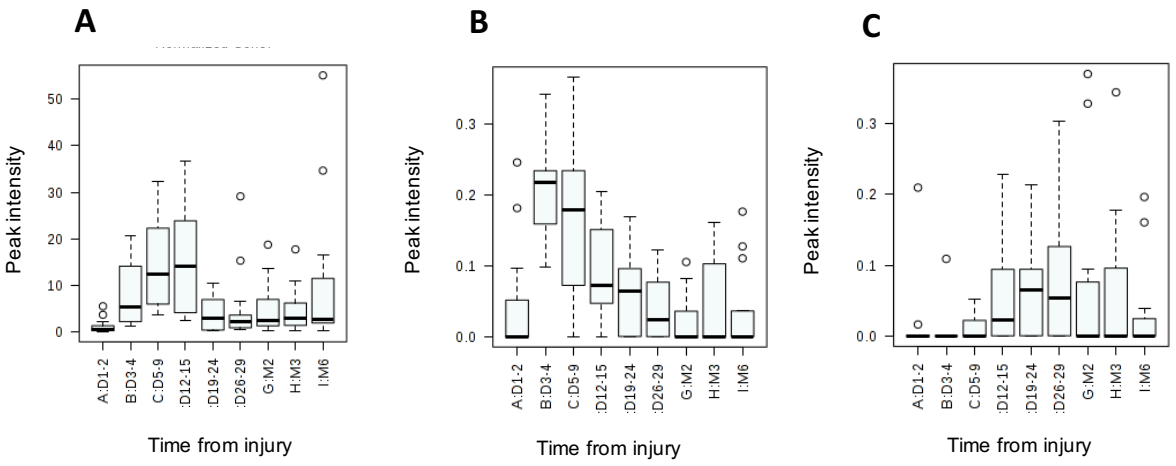

Figure 4-20. Box and whisker plots showing longitudinal trends in metabolite features from the Steroid conjugates sub-class of bile acids significantly changing in serum after severe burn injury. **A:** M3866, Glycocholic acid (primary bile acid) (*p*=<0.0001), **B:** M5245, Sulfoglycolithocholate (secondary bile acid) (*p*=<0.0001), **C:** M4780, Annotated isomers: Lithocholyltaurine; Taurolithocholic acid (secondary bile acid) (*p*=0.0169).

For the bile acids and derivatives sub-class, the predominant pattern of change seen was a decline from admission levels to a nadir at D19-24, followed by a rise again during the recovery phase back up towards admission levels. Within the bile acids and derivatives sub-class, the pattern was generally different. Except for one metabolite feature, these showed decline from admission levels with a nadir at D19-24 and then increased again to approximately reach admission levels by M6 (Figure 4.21).

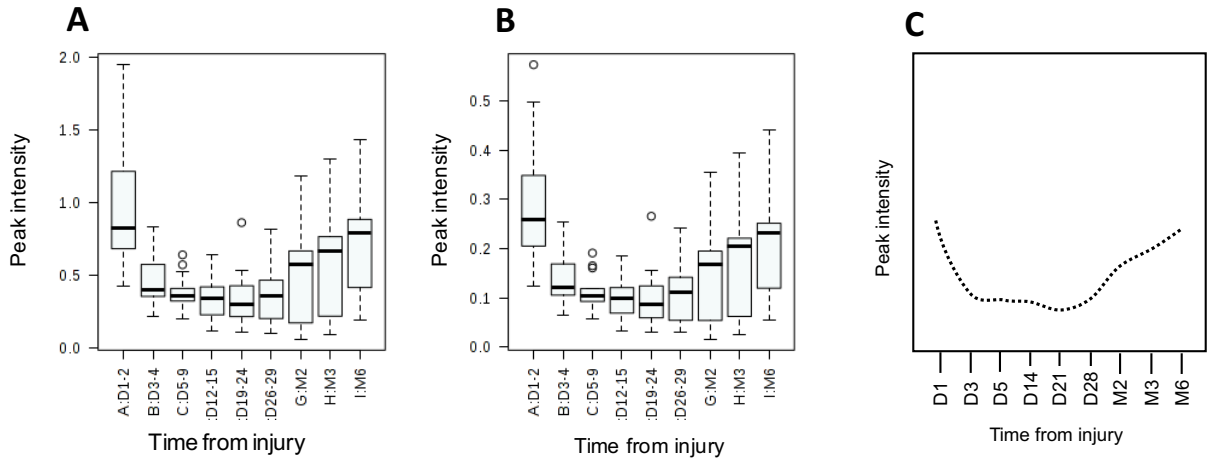

Figure 4-21: Box and whisker plots showing longitudinal trends in metabolite features from the bile acids and derivatives group of lipids significantly changing in serum after severe burn injury.
A: M3508, Annotated isomers: 5a-Cholestane-3a,7a,12a,25-tetrol; 5b-Cholestane-3a,7a,12a,23-Tetrol; 5b-Cholestane-3a,7a,12a,25-tetrol; 5beta-cholestane-3alpha, 7alpha,12alpha, 26-tetrol; Cholestane-3,7,12,25-tetrol. (p=0.0005).
B: M3519, Annotated isomers: 7-Deoxy-5b-cyprinol;"5a-Cholestane-3a,7a,12a,25-tetrol; 5b-Cholestane-3a,7a,12a,23-Tetrol; 5b-Cholestane-3a,7a,12a,25-tetrol; 5beta-cholestane-3alpha,7alpha,12alpha,26-tetrol; Cholestane-3,7,12,25-tetrol. (p=0.0006).
C: Summary of main trend seen in the sub-class.

4.4.3.12 Steroid hormone metabolism

A total of 12 metabolite features in the steroid metabolism class changed statistically significantly in serum after severe burn injury (Table 4.12).

No.	Steroid metabolism sub-class	No of metabolites FDR p=<0.05
1	Steroid conjugates *Glucuronides* *Sulfates*	**10** 8 2
2	Steroids	**2**
	Total	**12**

Table 4-12. Frequency table of steroid metabolite features significantly changing in adult serum after severe burn injury, summarized according to frequencies in each sub-class.

Within the steroid hormone metabolite group, most were steroid conjugates, mostly conjugated to glucuronic acid (defined as glucuronides). Glucuronidation occurs mainly in the liver and is the process of covalent bonding of glucuronic acid to metabolites, making them more water soluble for excretion via urine or faeces. This is used in the excretion of bile acids, drugs, steroid hormones, fatty acid derivatives and retinoids as examples. The predominant pattern in the steroid glucuronides was an initial decline from admission levels with a nadir at D12-15 and then a rise again to admission levels with a plateau at months 2-6 during the recovery phase (Figure 4.22). The sulfate conjugated steroids did not show any consistent pattern and the two steroid metabolites displayed different trend patterns (Figure 4.23).

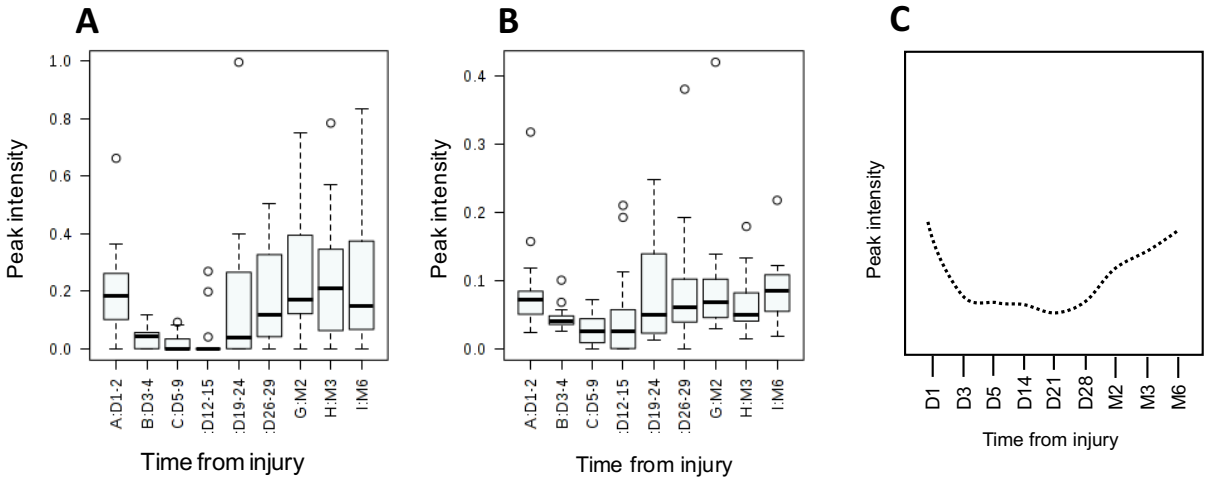

Figure 4-22.. Box and whisker plots showing serum longitudinal trends in metabolite features in the steroid hormone glucuronide conjugates after severe burn injury. **A:** M3895, Annotated isomers: Dihydrotestosterone glucuronide; Androsterone glucuronide (p=<0.0001). **B:** M3853, Annotated isomers: Dehydroepiandrosterone 3-glucuronide; Dehydroisoandrosterone 3-glucuronide; Testosterone glucuronide (p=0.0014). **C:** Summary of common trend in steroid hormone conjugates (glucuronides).

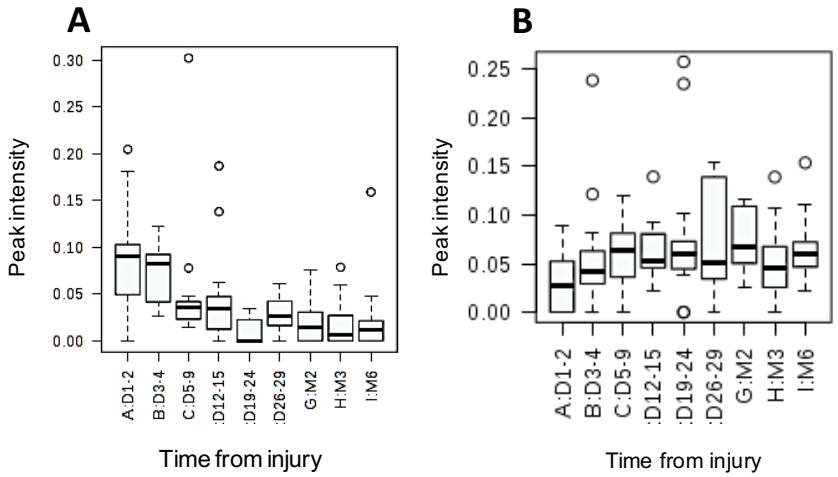

Figure 4-23. Box and whisker plots showing serum longitudinal trends in steroid metabolite features after severe burn injury. **A:** M2977, 4-Hydroxyestrone sulfate (p=0.0011). **B:** M3216, Annotated isomers: Androstenedione; Dehydrotestosterone (p=0.0254).

Within the steroid conjugates, there were six metabolites of sex steroids which all demonstrated the pattern shown in Fig 4.22. An early metabolite of early steroid hormone precursor pregnenolone was observed: pregnenolone sulfate (M3032) which demonstrated a dramatic fall in peak intensities from admission levels, with nadir D5-9 before a slow rise in levels towards M6 (Figure 4.24a). This may reflect reductions in steroid precursor pools due to increased production of stress hormones early after injury. Another metabolite feature observed, 11- Hydroxyprogesterone-11-glucuronide, is a metabolite of 11-hydroxyprogesterone, a precursor in the pathway of conversion from progesterone to the mineralocorticoids corticosterone and aldosterone (Figure 4.24b). Interestingly this showed a very similar profile to an aldosterone metabolite, Tetrahydroaldosterone-3-glucuronide (M5010) indicating significant alterations in mineralocorticoid metabolism. This was a rise from admission levels, with a peak at weeks 3-4 and then decline again (Figure 4.24c).

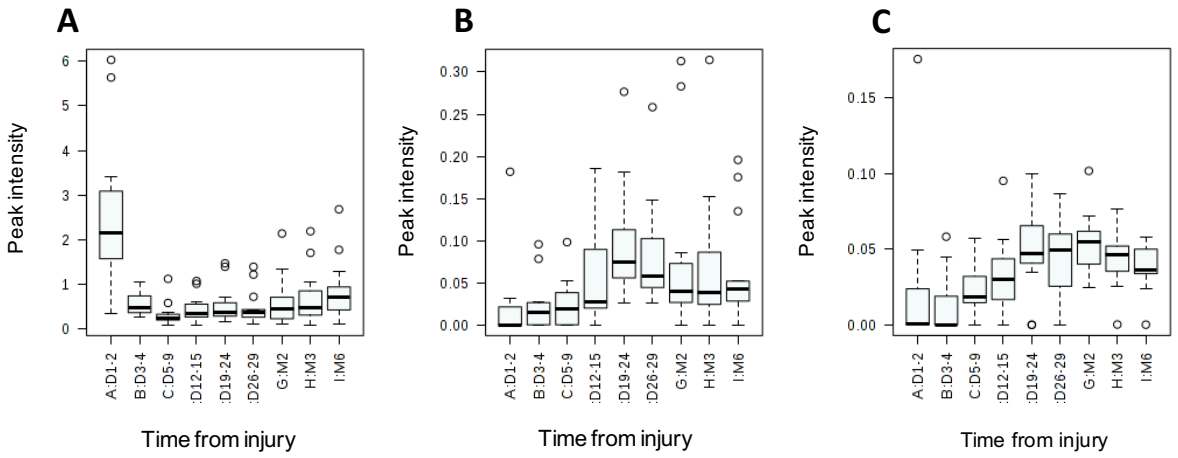

Figure 4-24. Box and whisker plots showing serum longitudinal trends in steroid hormone metabolite features after severe burn injury. **A:** M3032, Pregnenolone-sulfate (metabolite of steroid hormone precursor pregnenolone). (*p*=<0.0001) **B:** M5010, Tetrahydroaldosterone-3-glucuronide and **C:** M4810, 11-Hydroxyprogesterone 11-glucuronide. (*p*=<0.0001).

4.4.3.13 Peptide metabolism

A total of 26 metabolite features changed significantly in serum after severe burn injury were annotated as peptides and the majority (25/26, 96%) were dipeptides. The most common general trend (18/26, 69%) seen in the serum dipeptide metabolite features was an increase from peak intensities on the day of admission during the acute phase, followed by a decline during the recovery phase. The kinetics were variable across the dipeptides but the most common peak was seen at D19-24 with a decline thereafter (Figure 4.25). Four metabolites showed a slight variation, rising from admission, peaking at the same D19-24, with decline but remaining elevated at M6 compared to admission levels (Figure 4.26)

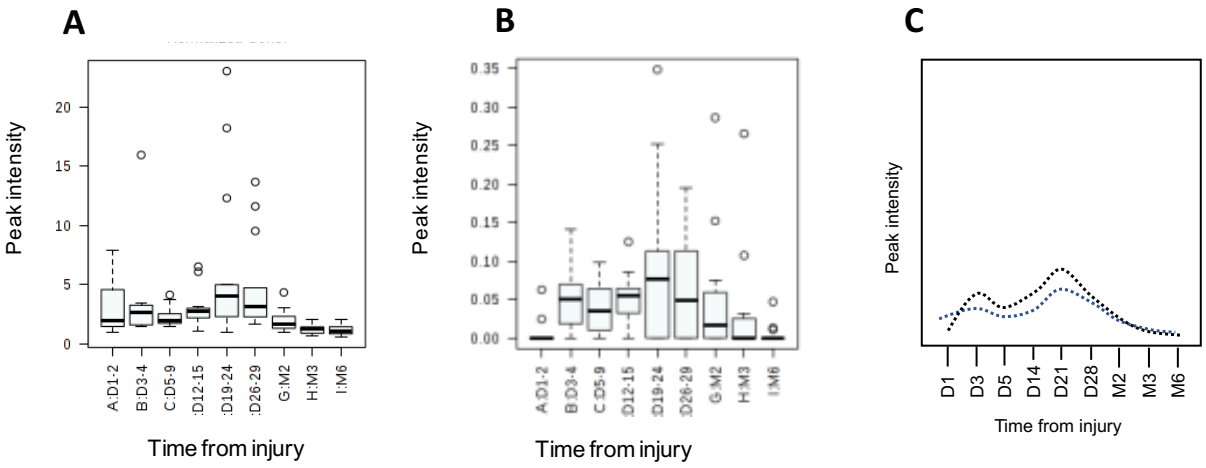

Figure 4-25. Box and whisker plots showing the most common serum longitudinal trend in peptide metabolite features after severe burn injury. **A:** M999, annotated with isomers: isoleucyl-proline and leucyl-proline (p=<0.0001) **B:** M2623, Arginyl-proline (p=0.0022) and **C:** Summary of trend.

The remainder of the peptides displayed a reduction from admission levels which continued to decline to plateau at low peak intensities relative to admission (Figure 4.27a). The single oligopeptide annotated was neuromedin N, a hexapeptide with

immunomodulatory and endocrine activities. This peptide showed a decline with nadir at 2 weeks, followed by a rise again during the recovery phase but not reaching admission levels by M6 (Figure 4.27b).

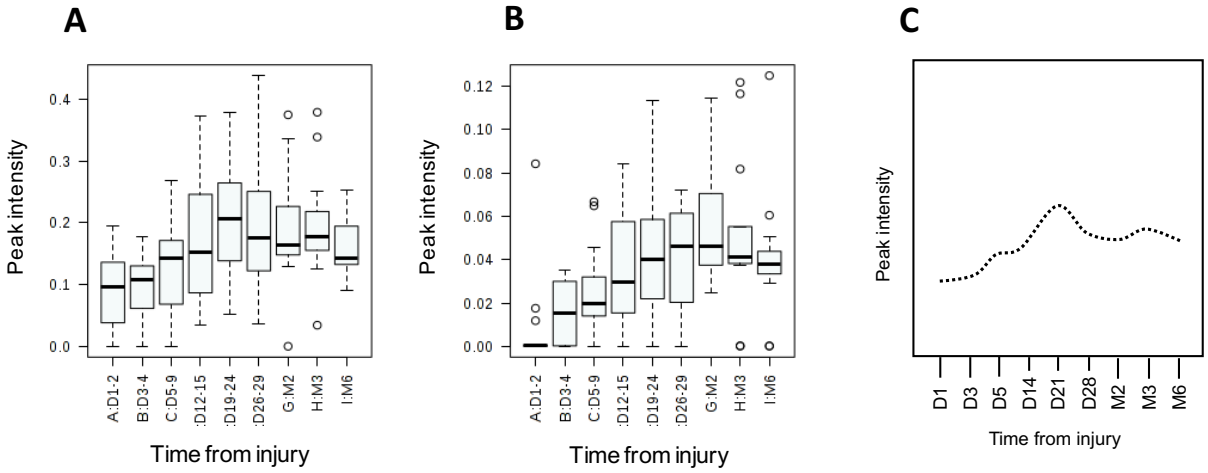

Figure 4-26. Box and whisker plots showing a variant of the common trend seen in the serum peptide metabolite features after severe burn injury. **A:** M2852, Phenylalanylphenylalanine (*p*=0.0340). **B:** M2461, Tyrosyl-Valine (*p*=<0.0001) and **C:** Summary of trend.

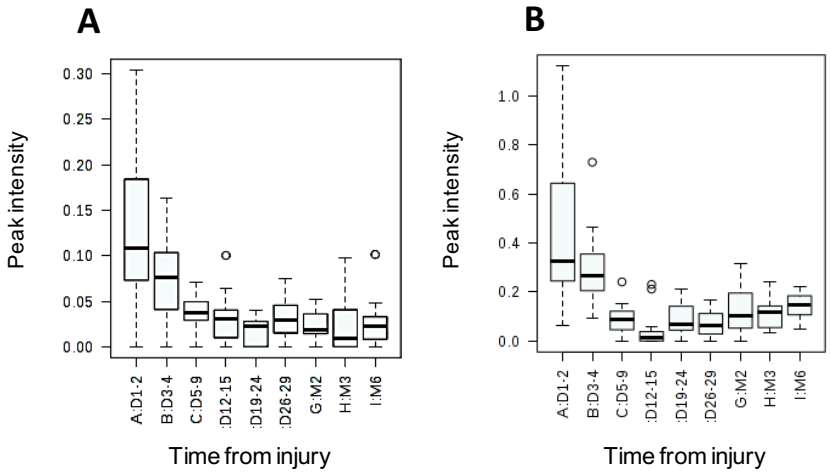

Figure 4-27. Box and whisker plots showing a peptide metabolite features changing significantly in serum post- severe burn injury that show a less common trend of reduction from initial higher peak intensity levels. **A:** M2834, Arginyl-glutamine (*p*=0.0090) and **B:** M4603, Neuromedin-N (1-4) (*p*=<0.0001).

4.4.3.14 Phenylalanine, tyrosine and tryptophan metabolism

A total of 15 metabolite features related to the metabolism of the aromatic amino acids Phenylalanine, tyrosine and tryptophan changed significantly in serum after severe thermal injury (Table 4.13). Grouping the metabolite features by the main amino acid metabolic pathways they are involved in, those involved in tryptophan metabolism were most commonly seen (9/15, 60%).

No.	Phenylalanine, tyrosine and tryptophan metabolism sub-class	No of metabolites FDR p=<0.05
1	Tryptophan metabolism	**9**
2	Tyrosine metabolism	**5**
3	Phenylalanine, tyrosine and tryptophan metabolism	**1**
	Total	**15**

Table 4-13. Frequency table of the aromatic amino acid metabolite features significantly changing in adult serum after severe burn injury, summarized by the frequencies in each sub-class.

Amongst the tryptophan metabolite features, three main trends were observed: 1) Elevation from admission peak intensities, followed by a decline after a variable peak of between 2-3 weeks post-injury as demonstrated by serotonin (M1949, p=0.0009) (Figure 4.28a), 2) Dramatic elevation from admission levels to D3-4 and then gradual decline to plateau during the recovery phase from M2 onwards as shown by tryptophanol (M1085, p=<0.0001) (Figure 4.28b) and 3) Minor decline from admission levels to nadir on D5-9, followed by elevation in peak intensities until the end of the time-course, as shown by tryptophan (M761, p=0.0003) (Figure 4.28c). Trends (1) and (2) were also observed in the tyrosine metabolite features. Interestingly four of the metabolite features are not endogenously produced

metabolites in human and are most likely bacterial metabolites including indole, indoxyl, 3-dehydroquinate and 3-maleylpyruvic acid. Indole and indoxyl, tryptophan metabolites, were elevated early after injury with an early peak the first few weeks before decline. 3-dehydroquinate displayed a much later rise with elevation between two and 4 weeks post injury and 3-maleylpyruvic acid showed an even later rise from 4 weeks with a peak at M3 before declining to M6. Another metabolite feature of interest in this group was epinephrine glucuronide, a conjugate of the sympathetomimetic neurotransmitter epinephrine, which was elevated at the admission time point and then declined over the first 4 weeks to plateau at low peak intensities thereafter.

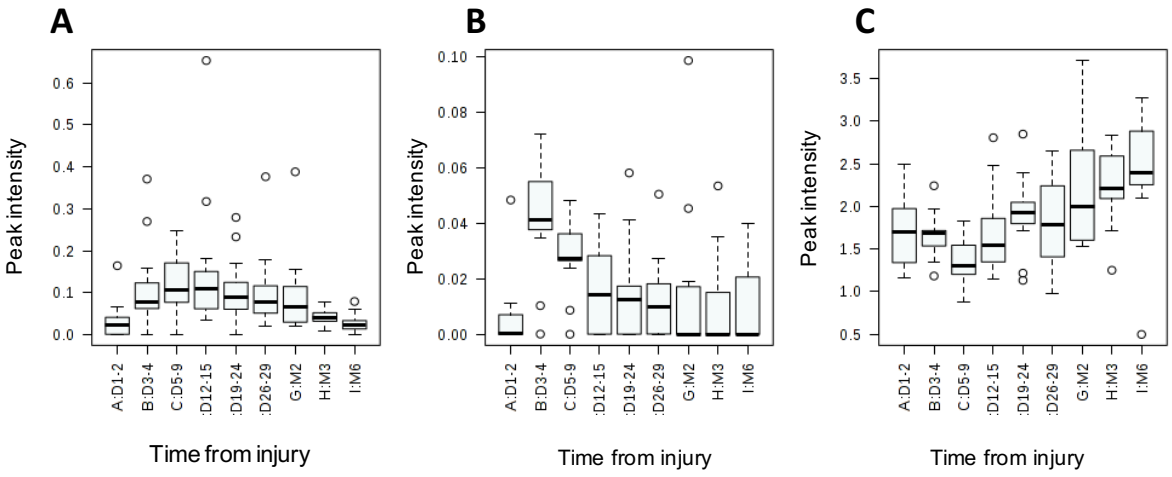

Figure 4-28. Box and whisker plots showing longitudinal trends for tryptophan metabolite features changing significantly in serum post- severe burn injury **A:** M1949, serotonin (p=0.0009). **B:** M1085, tryptophanol (p=<0.0001) and **C**: M761, tryptophan (p=<0.0001).

4.4.3.15 Aromatic metabolites

This group of 11 aromatic metabolites, are chemically heterogenous and the most common three trends observed are the same as in the aromatic amino acid metabolite features (Section 4.4.2.9). Several metabolite features may be metabolites produced by enteric bacteria including 2-benzylsuccinate, phenylethylamine, hydrophenyllactic acid and 3-(3-Hydroxyphenyl)-3-hydroxypropanoic acid (3-HPPA).

4.4.3.16 Carnitine and Acyl carnitines

Carnitine and acyl carnitines are essential for fatty acid metabolism (β-oxidation), which is the oxidation of long-chain fatty acids in the mitochondrial matrix to yield energy in the form of ATP. Fatty acids are activated by conversion to their acyl Coenzyme A (CoA) thioesters, however long chain fatty acyl CoAs cannot cross the inner mitochondrial membrane without conjugation to the highly polar carnitine molecule to form acyl carnitines. Significant changes were seen in serum carnitine and four acyl carnitines following thermal injury. (Figure 4.29).

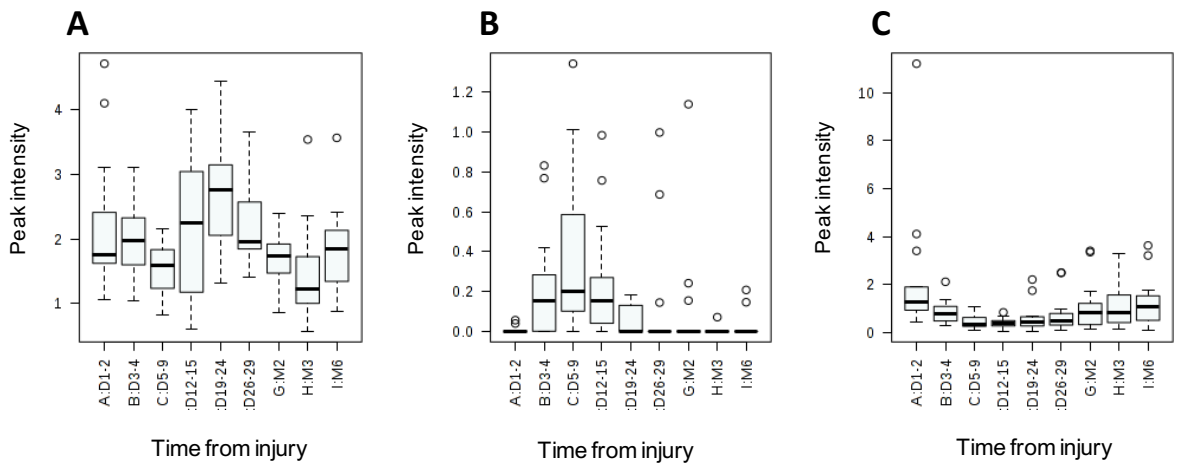

Figure 4-29. Box and whisker plots showing longitudinal trends for carnitine and acyl carnitine metabolite features changing significantly in serum post- severe burn injury **A:** M375, carnitine (*p*=0.0122) **B:** M4864, 3-Hydroxyhexadecadienoylcarnitine (*p*=<0.0001) **C**: M3072, Dodecenoylcarnitine (*p*=0.0020).

4.4.3.17 Heme metabolism

Six metabolite features related to heme metabolism changed significantly in serum post thermal injury. Bilirubin and urobilinogens showed a similar pattern with decline from admission levels and then remaining at a constant low level relative to admission (Figure 4.30a). Urobilin was also detected, which showed a rise from admission with a peak on D5-9 before declining again (Figure 4.30b). A bacterial Heme metabolite, Heme O, was also detected which showed rose from admission with peak on D3-4 before gradually declining to low peak intensities at M3-M6 (Figure 4.30c).

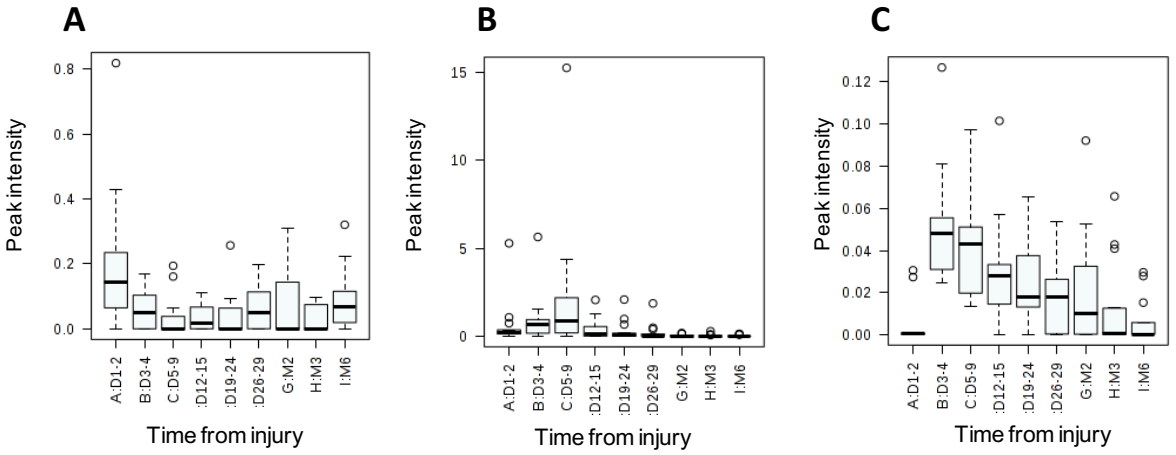

Figure 4-30. Box and whisker plots showing longitudinal trends for heme metabolite features changing significantly in serum post- severe burn injury **A:** M5250, bilirubin (*p*=0.0264) **B:** M5353, Urobilin (*p*=<0.0001) and **C**: M7455, Heme O (*p*=<0.0001).

4.4.4 The cytokine response to thermal injury and its relationship to changes in the metabolome

The pro-inflammatory cytokine IL-6 showed significant elevations compared to control values from healthy volunteers for one month post-injury (Figure 4.31a). The other classical pro-inflammatory cytokine TNF-α did not show significant increases compared to control across the whole time-course. The chemokine IL-8 showed significant increases from D3-4 until 1 month post-injury (Figure 4.31b), whilst the chemokine MCP-1 showed significant elevations on D1-2 and D3-4 (Figure 4.32a) only before levels declined. G-CSF demonstrated a similar pattern to MCP-1, and was significantly increased also until D3-4 before declining (Figure 4.32b). The anti-inflammatory cytokines, IL-10 and IL1-RA showed a significant early peak on D1-2 and then levels reduced (Figure 4.33). The cytokines IL-17 and IL-1β did not show any significant differences in patient serum concentrations across the time course compared to controls.

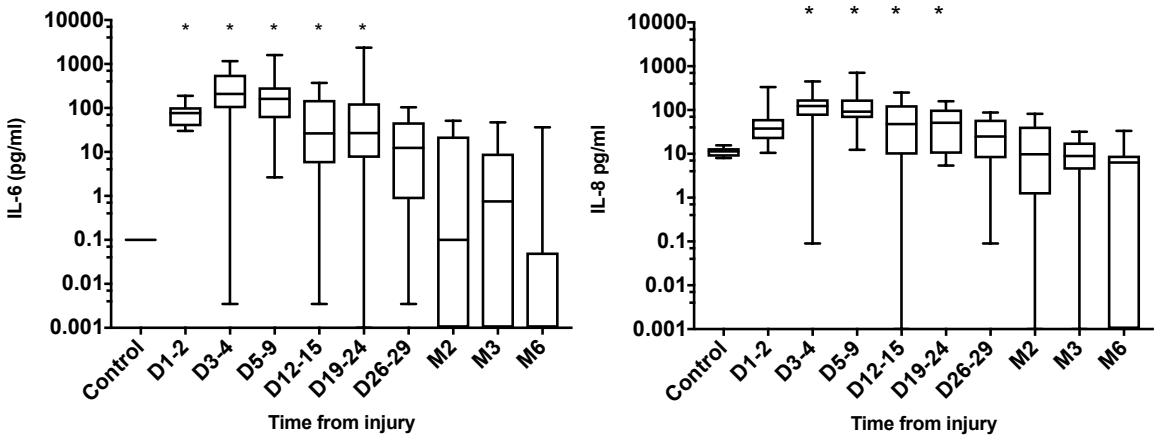

Figure 4-31. Box and whisker plots showing longitudinal changes in serum pro-inflammatory cytokines compared to control values. (*p=<0.05). **A:** Cytokine IL-6 and **B:** Chemokine IL-8.

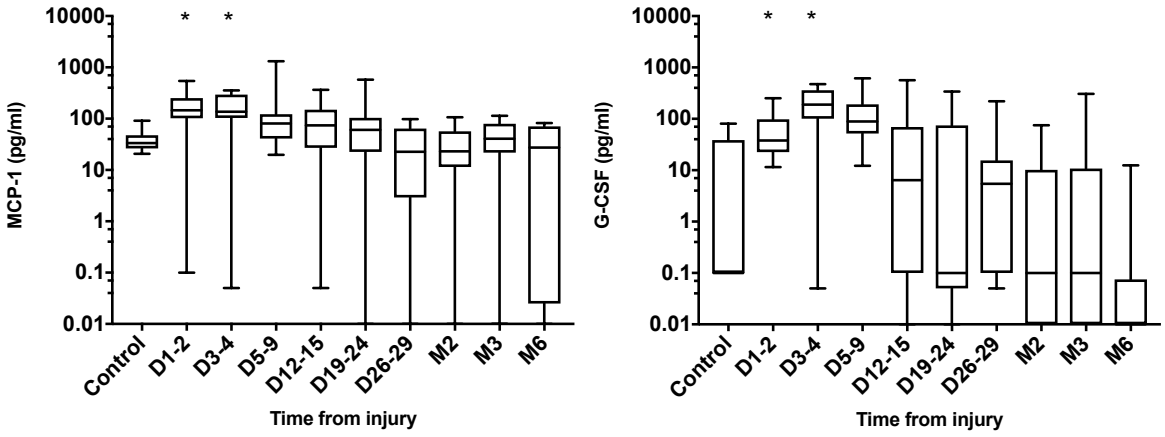

Figure 4-32. Box and whisker plots showing longitudinal changes in serum cytokines compared to control values. (*p=<0.05). **A:** Chemokine MCP-1 and **B:** Cytokine G-CSF

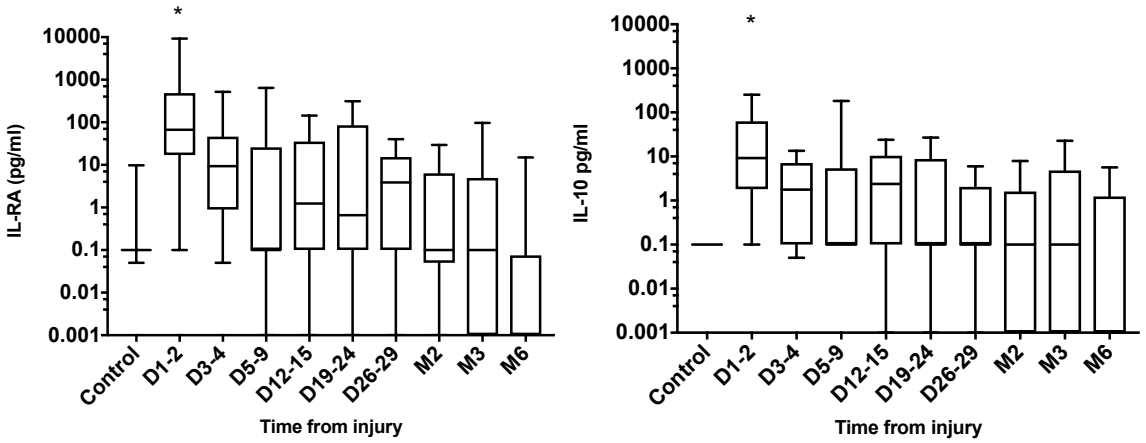

Figure 4-33. Box and whisker plots showing longitudinal changes in serum anti-inflammatory cytokines compared to control values. *p=<0.05. **A:** Cytokine IL-1RA and **B:** Cytokine IL-10

To further investigate the relationship between these changes in serum cytokines after severe thermal injury, a Spearman correlation analysis was performed between IL-6, IL-8, IL-10 and IL-RA and each of the metabolite features that changed most significantly in each metabolite class. The most significant correlations for each cytokine are presented in tables 4.14 – 4.17. IL-6 serum concentrations correlated negatively with metabolite features in 11 classes including: glycerophospholipids, sphingolipids, fatty acids, glycerolipids, peptides and bile acids. A weak positive correlation was seen with a leukotriene (N-acetyl-leukotriene E4) (r=0.2134, p=0.0233) and a lysoglycerophospholipid (LysoPC[22:6]) metabolite feature (r= 0.2540, p=0.0169). IL-8 demonstrated a greater number significantly correlated metabolite features, but showed a similar pattern to IL-6 with again a moderately strong negative correlation with a glycerophosphocholine metabolite feature (PC[O-16:0/0:0]; PC[O-8:0/O-8:0]) (r=-0.6914, p=<0.0001).

No.	Metabolite class	Metabolite features	FDR *P*-value	*r*	95% confidence interval	*P*-value
1	Glycerophosphocholines	PC(O-16:0/0:0);PC(O-8:0/O-8:0)	1.26E-07	-0.6774	-0.7685 to -0.5593	<0.0001
2	Glycerophoshoserines	PS[42:0]PS[41:1]	0.0013101	-0.5648	-0.6872 to -0.4112	<0.0001
3	Sphingolipids	SM(d18:1/22:1);SM(d18:2/22:0)	3.85E-06	-0.4791	-0.6133 to -0.318	<0.0001
4	Glycerophosphates	PA[37:5]PA(O-16:0/15:0);PA(O-18:0/13:0)	8.67E-07	-0.4451	-0.6212 to -0.2262	0.0001
5	Glycerophoshoglycerols	PG[28:0]	6.38E-09	-0.4224	-0.6285 to -0.1609	0.0018
6	Dicarboxylic acids (Fatty acids)	Tetracosanedioic acid	5.71E-05	-0.4143	-0.5602 to -0.2434	<0.0001
7	Diglycerides	DG[35:6];DG[33:3];DG[31:0]	8.88E-08	-0.3981	-0.5468 to -0.2251	<0.0001
8	Peptides	Aspartyl-Phenylalanine	2.96E-08	-0.3783	-0.5302 to -0.2028	<0.0001
9	Triglycerides	TG[33:0]	3.53E-09	-0.2898	-0.4548 to -0.1056	0.0018
10	Unsaturated fatty acids	Heneicosadienoic acid	4.78E-07	-0.2673	-0.4353 to -0.08139	0.0042
11	Bile acid (Bile acid and derivatives)	5a-Cholestane-3a,7a,12a,25-tetrol; 5b-Cholestane-3a,7a,12a,23-Tetrol; 5b-Cholestane-3a,7a,12a,25-tetrol; 5beta-cholestane-3alpha,7alpha,12alpha,26-tetrol; Cholestane-3,7,12,25-tetrol	8.78E-05	-0.2614	-0.4301 to -0.07505	0.0052
12	Leukotrienes	N-Acetyl-leukotriene E4	0.00015544	0.2134	0.0243 to 0.3877	0.0233
13	Lysoglycerophospholipids	LysoPC[22:6]	0.00063463	0.254	0.04082 to 0.4451	0.0169

Table 4-14. Summary of the significant correlations between FDR significant metabolites from ANOVA analysis (highest ranked in class) and IL-6 cytokine measurements in serum post-burn across the 6-month time course. FDR = false discovery rate, *r*=Spearman's rank correlation coefficient.

No	Metabolite class	Metabolite feature	FDR P-value	r	95% confidence interval	P-value
1	Glycerophosphocholines	PC(O-16:0/0:0);PC(O-8:0/O-8:0)	1.26E-07	-0.6914	-0.7791 to -0.5772	<0.0001
2	Glycerophoshoserines	PS[42:0]PS[41:1]	0.0013101	-0.5571	-0.6812 to -0.4018	<0.0001
3	Diglycerides	DG[35:6];DG[33:3];DG[31:0]	8.88E-08	-0.4603	-0.5981 to -0.2962	<0.0001
4	Sphingolipids	SM(d18:1/22:1);SM(d18:2/22:0)	3.85E-06	-0.4541	-0.5929 to -0.2889	<0.0001
5	Dicarboxylic acid (fatty acids)	Tetracosanedioic acid	5.71E-05	-0.4312	-0.5742 to -0.2626	<0.0001
6	Lysoglycerophospholipids	LysoPC[22:6]	0.00063463	0.4199	0.2248 to 0.5826	<0.0001
7	Leukotrienes	N-Acetyl-leukotriene E4	0.00015544	0.3413	0.1618 to 0.499	0.0002
8	Peptides	Aspartyl-Phenylalanine	2.96E-08	-0.3404	-0.4982 to -0.1607	0.0002
9	Bile acids	Taurochenodesoxycholic acid;Taurodeoxycholic acid;Tauroursodeoxycholic acid	1.30E-06	-0.3394	-0.5768 to -0.04913	0.0196
10	Glycerophosphates	PA[37:5]PA(O-16:0/15:0);PA(O-18:0/13:0)	8.67E-07	-0.3329	-0.5331 to -0.09739	0.0052
11	Triglycerides	TG[33:0]	3.53E-09	-0.3325	-0.4915 to -0.152	0.0003
12	Unsaturated fatty acids	heneicosadienoic acid	4.78E-07	-0.3281	-0.4878 to -0.1472	0.0004
13	Glycerophoshoglycerols	PG[28:0]	6.38E-09	-0.3143	-0.5467 to -0.03707	0.0232
14	Bile acid (Bile acid and derivatives)	5a-Cholestane-3a,7a,12a,25-tetrol; 5b-Cholestane-3a,7a,12a,23-Tetrol; 5b-Cholestane-3a,7a,12a,25-tetrol; 5beta-cholestane-3alpha,7alpha,12alpha,26-tetrol; Cholestane-3,7,12,25-tetrol	8.78E-05	-0.3086	-0.471 to -0.1259	0.0009
15	Steroid hormone metabolites	24-methylene-cholesterol sulfate	1.23E-09	0.2087	0.0002762 to 0.3997	0.0435

Table 4-15. Summary of the significant correlations between FDR significant metabolites from ANOVA analysis (highest ranked in class) and IL-8 cytokine measurements in serum post-burn across the 6-month time course. FDR = false discovery rate, *r*=Spearman's rank correlation coefficient.

The anti-inflammatory cytokines IL-10 and IL-1RA demonstrated generally weaker correlations to the metabolite features tested. IL-10 showed only six significant correlations with the metabolite features, with negative correlations with glycerophospholipids, sphingolipids, diglycerides, unsaturated fatty acids. A positive correlation was observed with carnitine (r=0.2039, p=0.0303). IL-1RA demonstrated a greater number of significant correlations (n=12) with the metabolite features. Negative correlations were again seen with glycerophospholipids. Weak positive correlations were observed with the steroid, 4-hydroxyestrone sulfate (r=0.3397,

p=0.0022) in addition to fatty acids, peptides, lysoglycerophospholipids and aromatics.

No.	Metabolite class	Metabolite feature	FDR *P*-value	*r*	95% confidence interval	*P*-value
1	Glycerophosphocholines	PC(O-16:0/0:0);PC(O-8:0/O-8:0)	1.26E-07	-0.4131	-0.5593 to -0.2421	<0.0001
2	Glycerophoshoserines	PS[42:0]PS[41:1]	0.0013101	-0.3092	-0.4796 to -0.1163	0.0016
3	Sphingolipids	SM(d18:1/22:1);SM(d18:2/22:0)	3.85E-06	-0.2597	-0.4286 to -0.07331	0.0055
4	Diglycerides	DG[35:6];DG[33:3];DG[31:0]	8.88E-08	-0.2352	-0.4071 to -0.04725	0.0122
5	Unsaturated fatty acids	heneicosadienoic acid	4.78E-07	-0.2323	-0.4045 to -0.04423	0.0133
6	Acyl carnitines	Carnitine	0.012249	0.2039	0.01443 to 0.3793	0.0303

Table 4-16. Summary of the significant correlations between FDR significant metabolites from ANOVA analysis (highest ranked in class) and IL-10 cytokine measurements in serum post-burn across the 6-month time course. FDR = false discovery rate, *r*=Spearman's rank correlation coefficient.

No.	Metabolite class	Metabolite feature	FDR *p*-value	*r*	95% confidence interval	*P*-value
1	Glycerophosphocholines	PC(O-16:0/0:0);PC(O-8:0/O-8:0)	1.26E-07	-0.3771	-0.5292 to -0.2014	<0.0001
2	Steroids	4-Hydroxyestrone sulfate	0.0011315	0.3397	0.1217 to 0.5265	0.0022
3	Glycerophoshoserines	PS[42:0]PS[41:1]	0.0013101	-0.3298	-0.497 to -0.1389	0.0007
4	Glycerophosphoethanolamines	PE[37:7]	2.10E-05	-0.2989	-0.5028 to -0.06355	0.0113
5	Fatty acids	Octadecenetriynoic acid	8.35E-08	0.2754	0.09006 to 0.4423	0.0032
6	Peptides	Neuromedin-N	2.54E-06	0.2602	0.05922 to 0.4409	0.0097
7	Peptides	Aspartyl-Phenylalanine	2.96E-08	-0.2371	-0.4087 to -0.04926	0.0115
8	Lysoglycerophospholipids	LysoPC[22:6]	0.00063463	0.2369	0.02257 to 0.4303	0.0263
9	Sphingolipids	SM(d18:1/22:1);SM(d18:2/22:0)	3.85E-06	-0.2303	-0.4028 to -0.04212	0.0141
10	Diglycerides	DG[35:6];DG[33:3];DG[31:0]	8.88E-08	-0.2217	-0.3951 to -0.03307	0.0183
11	Aromatics	2-Phenylglycine	1.44E-06	0.1941	-0.001268 to 0.3752	0.0451
12	Branched chain fatty acids	Corchorifatty acid A;trimethyl-tetradecatetraenoic acid	0.0019748	0.1934	0.001696 to 0.3714	0.042

Table 4-17. Summary of the significant correlations between FDR significant metabolites from ANOVA analysis (highest ranked in class) and IL-1RA cytokine measurements in serum post-burn across the 6-month time course. FDR = false discovery rate, *r*=Spearman's rank correlation coefficient.

4.4.5 Urinary urea nitrogen excretion (UUN) and its relationship to changes in the post-burn metabolome

Urinary urea nitrogen (UUN) excretion data was collected for all patients up to 3-months post-injury as thereafter, it became increasingly impractical due patients either being discharged home or having no urinary catheter. The UUN data showed a rise from admission levels to a peak at D5-9 and declining thereafter but remaining elevated above admission levels at D12-15 (Figure 4.34).

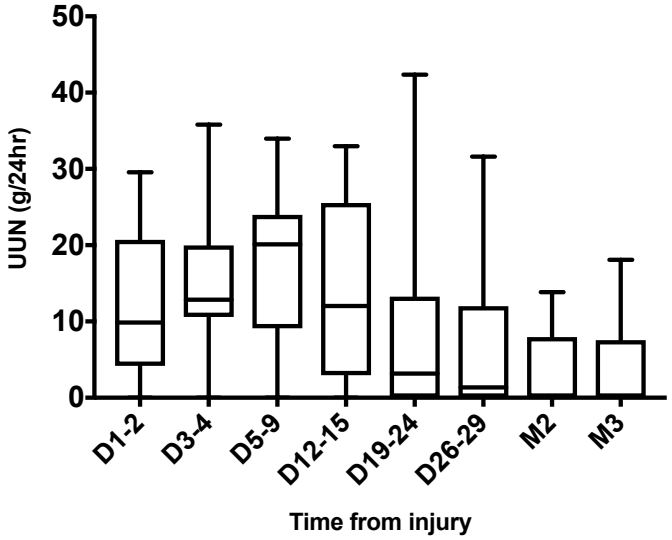

Figure 4-34. Box and whisker plots (median and IQR) showing the longitudinal trend in urinary urea nitrogen excretion (UUN) over 3-months after severe thermal injury.

The same methods were then used to correlate the UUN data with the most significantly changing metabolite features in each class from the ANOVA analysis. This showed, as with the cytokine analysis, that the strongest correlations were negatively with the glycerophosphocholine, (PC[O-16:0/0:0]; PC[O-8:0/O-8:0]) (r=-0.445, p=<0.0001). Positive correlations were observed with the steroid hormone, lysoglycerophospholipid and leukotriene metabolite features (Table 4.18).

No	Metabolite class	Metabolite feature	FDR *P*-value	*r*	95% confidence interval	*P*-value
1	Glycerophosphocholines	PC(O-16:0/0:0);PC(O-8:0/O-8:0)	1.26E-07	-0.4445	-0.5999 to -0.2569	<0.0001
2	Glycerophosphates	PA[37:5]PA(O-16:0/15:0);PA(O-18:0/13:0)	8.67E-07	-0.3343	-0.5684 to -0.05014	0.0189
3	Diglycerides	DG[35:6];DG[33:3];DG[31:0]	8.88E-08	-0.3201	-0.4982 to -0.1161	0.002
4	Glycerophoshoserines	PS[42:0]PS[41:1]	0.0013101	-0.265	-0.4644 to -0.03994	0.0183
5	Steroid hormone metabolites	24-methylene-cholesterol sulfate	1.23E-09	0.2474	0.01142 to 0.4572	0.0349
6	Lysoglycerophospholipids	LysoPC[22:6]	0.00063463	0.2424	0.007857 to 0.4517	0.0374
7	Dicarboxylic acid (fatty acids)	Tetracosanedioic acid	5.71E-05	-0.2412	-0.431 to -0.03092	0.0213
8	Sphingolipids	SM(d18:1/22:1);SM(d18:2/22:0)	3.85E-06	-0.2261	-0.4179 to -0.01498	0.0311
9	Leukotrienes	N-Acetyl-leukotriene E4	0.00015544	0.2228	0.01151 to 0.4151	0.0338
10	Triglycerides	TG[33:0]	3.53E-09	-0.2105	-0.4043 to 0.001439	0.0452

Table 4-18. Summary of the significant correlations between FDR significant metabolites from ANOVA analysis (highest ranked in class) and urinary urea nitrogen (UUN) measurements in serum post-burn across the 6-month time course. FDR = false discovery rate, r=Spearman's rank correlation coefficient.

4.5 Discussion

In this study, untargeted LC-MS metabolomics has been used to explore the global patterns of change in metabolism that occur longitudinally after severe thermal injury. There were significant changes in the serum metabolome across 35 distinct metabolite classes and several common trend patterns that were repeated across classes. The main findings are a profound early catabolic response phase lasting but declining over the first 3 weeks, before a metabolic shift occurs most likely representing a metabolic recovery phase. There were also profound shifts in the lipid metabolome, with 70% of significant changes seen in lipid classes. In addition, this untargeted approach has revealed changes in previously unstudied areas of metabolism in thermal injury which warrant further examination through targeted hypothesis testing studies. Analysis of the metabolomic data in relation to targeted

cytokine data revealed significant correlations between pro and anti-inflammatory mediators and changes in the metabolome.

4.5.1 Early post-injury catabolic phase with increased energy production

Univariate analysis revealed significant changes in large numbers of lipid metabolites, which predominated overall in the serum metabolome shifts after thermal injury. The most common trend pattern seen in the fatty acids (FAs) and triacylglycerides (TGs) was a decline from admission levels, before then increasing again after a nadir at 3-weeks post-injury. In the absence of normal control data or internal standards in our study, we cannot clearly define whether there was a decline in levels from a starting point in the normal concentration range vs. a decline from elevated levels. However, much of the evidence in the literature points to an early elevation in FAs and TGs after thermal injury.

Early studies of lipid metabolism after thermal injury showed early increases in circulating levels of free FAs (FFAs) and TGs, and this has since been shown to be due to increased lipolysis in adipose tissues (163,219,367). This is mostly in response to elevations in catecholeamines and glucagon (stress response) in the face of reduced peripherial insulin sensitivity which is seen in non-burn trauma (163). Another source of FFAs is the hydrolysis of TGs contained within chylomicrons and very low density lipoproteins (VLDL) when delivering their lipids to target cells (390). It is clear that thermally injured patients have increased rates of beta oxidation, the metabolism of FAs in mitochondria to generate ATP (168,169) and this is required to meet the vast demands for wound healing and thermoregulation. Interestingly, thermally injured patients are only able to utilize 30% of available FFAs for energy

generation, a large proportion undergo ‘futile’ cycling between hydrolysis of TGs and esterification back to TGs in the liver (194).

There are some conflicting studies in the literature suggesting that FFAs actually decrease after thermal injury (391,392) and others showing a variable response between patients (219). A number of reasons have been postulated for the conflicting data, including variations in resuscitation leading to differences in perfusion of adipose tissue and also the amount of adipose tissue present on admission and after excision of burn tissue (154). A recent targeted lipidomics study of 46 adults with burns >20%, studied the longitudinal change in 14 classes of fatty acids from the time of injury to 28 days. Their data shows initial elevated levels of both saturated and unsaturated FFAs on the day of injury before declining over the first month. They also highlighted that persistently elevated saturated FAs were associated with poor clinical outcomes and a suppressed pro-inflammatory profile and elevated levels of monounsaturated FAs (MUFA) correlate with mortality (393). If we infer from this study that our data shows initial elevations in FAs and TGs and then decline, this may be due to increased utilization and gradual reductions in peripheral lipolysis as the stress response dissipates. The later elevation after 3 weeks is unexplained and has not been described previously in the literature. This could be due to ongoing peripheral lipolysis and FA-TG substrate cycling with reduced rates of utilization through β-oxidation in the liver and in skeletal muscle due to loss of lean body mass (LBM). Another contributing factor is the hypoalbuminaemia associated with severe thermal injury which may impact FFA levels (367). Since FAs released from adipocytes are transported bound to albumin, low serum albumin during the acute phase may contribute to declining serum FFAs. Then as albumin levels increase in

the recovery phase, this may allow increased release of FAs and TG from adipocytes contributing to rising levels. Since we have shown multiple longitudinal trajectories within the FA and glycerolipid classes, changes in lipid metabolism are clearly complex and suggest varying functions and degree of utilization at different stages after injury.

A related observation that corroborates with increased lipolysis and increased β-oxidation of FAs, is that significant changes were seen in carnitine and four acyl carnitines. Carnitine decreased from admission levels before a second peak and fall at 3 weeks (Figure 4.29a). Previous studies have shown acutely decreased levels of carnitine for up to 2 weeks in plasma following burn injury. This may be due to urinary and wound losses and increased uptake and utilization by the liver and skeletal muscle (367). The second decline observed in carnitine between 3-weeks and two-months post-injury is more difficult to explain, but may be due to increased utilization again during rehabilitation as the patients start to mobilise. Late infections and sepsis may also contribute as carnitine levels are known to be depleted in sepsis (368).

Significant changes in peptide metabolism were observed, with large numbers of dipeptides increasing from admission to a peak at 3-weeks post-burn before declining. This most likely represents the increased skeletal muscle protein catabolism that is well described following thermal injury. Studies have shown that although there is concurrent increase in protein synthesis and degradation in skeletal muscle, the balance leans towards catabolism, resulting in net protein loss and wasting of skeletal muscle and therefore LBM (333). Radio-isotope studies have shown increased uptake of amino-acids in the burn wound paralleling the increased

efflux from skeletal muscle, leading to the conclusion that this response is to support wound healing (236). The protein catabolism is also felt to provide substrates for gluconeogenesis and to support the liver in the production of acute phase proteins (228). Urinary urea nitrogen (UUN) excretion is one crude measure of protein catabolism and in this cohort of patients the peak UUN occurred at D5-9, whilst the peptide peak occurred later at 3-weeks post-injury. It is accepted in the literature that whilst UUN is a significant predictor of protein balance, although it lacks the quantitative accuracy of isotope based methods in studying protein kinetics (394).

4.5.2 Endocrine changes in the metabolome

Severe thermal injury results in a profound stress response with activation of the sympathetic nervous system, with increases in the circulating catecholamines, noradrenaline and adrenaline (163). This together with activation of the hypothalamo-pituitary adrenal (HPA) axis and increased secretion of cortisol from the adrenal cortex, drives the catabolic response, increased resting energy expenditure (REE) and changes in glucose metabolism. There are significant changes in 12 steroid hormone metabolites, eight of which were metabolites involved in sex hormone pathways, typically terminal metabolites of testosterone, estrone and estriol. These generally showed a trend to decline from admission before increasing during the recovery phase. Dehydroepiandrosterone 3-glucuronide, a conjugate of Dehydroepiandrosterone (DHEA) decreased from admission with a nadir at 2-weeks before gradually increasing again. DHEA is an adrenally synthesised C19 steroid and an intermediate in the testosterone and oestrogen synthesis pathway. This and its active sulfated form (DHEAS) have been previously shown to be low for 4 weeks after burn injury (395). DHEAS is also an immune enhancer able to stimulate

neutrophil function (396). The reduction in DHEA and DHEAS may thus contribute to immuneparesis and catabolism seen in burn injury. Furthermore, in murine models of thermal injury, DHEA supplementation has demonstrated beneficial effects including normalizing hepatic cellular metabolism, minimizing immunosuppression, improving resistance to infection and preventing burn wound progression (397-400). To date there are no clinical trials of DHEA supplementation in burn injury patients, though our data suggest this may be well worthwhile pursuing.

As expected corticosteroid and mineralocorticoid pathway metabolites also changed significantly and interestingly pregnenolone, a very early steroid hormone precursor, decreased dramatically from admission levels and remained at that constant lower level for the remainder of the study. This may due to increased utilization in the synthesis of corticosteroids as part of the stress response, but has not previously been studied in thermal injury. The steroid hormone findings need to be interpreted with a hint of caution given that eight patients (62%) received anabolic steroid treatment from day 4-5 of admission in the form of oral Oxandrolone. It would be interesting with a larger cohort to examine the differences in steroid hormone metabolites between those treated with and without anabolic steroids, however burn size may confound this.

4.5.3 Inflammation and immunomodulatory metabolites

Significant changes were observed in Eicosanoid metabolite features, with leukotrienes and prostaglandins increasing acutely over the first 2-weeks post-injury. Eicosanoids are biologically active lipid mediators derived from arachidonic acid and related C20 polyunsaturated fatty acids (PUFA) and include the prostaglandins (PG), leukotrienes (LT), thomboxanes (TX), lipoxins (LX) and other derivatives. They are

known to regulate inflammatory processes, have diverse homeostatic roles and are implicated in many diseases. Eicosanoids are synthesized through oxidation of arachidonic acid or its related PUFAs by the enzymes cyclooxygenase (COX), lipoxygenase (LOX) and cytochrome P450 and via free radical mechanisms (401). Metabolites of LTD5 and of LTA4, LTE4 and LTB4 changed significantly. The latter is known to effect neutrophil recruitment and chemotaxis, vascular permeability and enhanced epithelial barrier function. There are limited studies of leukotrienes in thermal injury, however human neutrophils produce less LTB4 post-burn and an increase in biologically less active, omega oxidized metabolites. This correlated with increased bacterial growth in the burn wound (402) and a shift to higher proportions of circulating immature neutrophils (403). Later studies showed an association between decreased neutrophil adhesion to vascular endothelium and attenuated LTB4 production (404). Interestingly other studies on the SIFTI cohort have identified increased levels of immature granulocytes (IGs) and found that a combination of IG frequency, cell free DNA and rBaux score were powerful prognostic indicators for development of sepsis (405). Whether the metabolites identified here might also be of prognostic utility is worth investigating.

Prostaglandin metabolite features changing significantly after thermal injury, included annotations of metabolites of PGD2, PGF1, PGE1, PGH2 and multiple PGE-2 metabolites. PGE2 is felt to play a pivotal role in post-burn inflammation and is significantly elevated in plasma of thermally injured patients with monocytes (406,407); higher levels of PGE2 also correlated with poor outcomes (408).

The docosanoids are biologically related to eicosanoids and are synthesized from omega-3 fatty acids such as docosahexanoic acid (DHA). They include the resolvins, protectins and maresins and their roles as specialised pro-resolving mediators (SPMs) in inflammation are just being understood (409). Several docosanoid metabolite features, included annotations with neuroprotectins and resolvins were identified and showed a gradual rise from admission, peaking at 3 weeks before declining. These SPMs may have an important role in the resolution of inflammation after severe thermal injury. Furthermore, Resolvins have therapeutic potential as they have been shown in animal burn models to restore neutrophil migration defects in vivo (101), prevent dermal necrosis and neutrophil mediated damage to the burn wound (410) and ameliorate burn induced renal and hepatic tissue injury (411).

Multiplex analysis of the serum cytokines in this study, showed evidence of an ongoing inflammatory response for 4-weeks post-injury, as evidenced by significant elevations, relative to controls, in IL-6 and IL-8 for this duration. These profiles were consistent trends with previously published data (57,60,82) and the duration of inflammation comparable to a recent lipidomics study with similar injury severity (393). The cytokines MCP-1 and G-CSF were only significantly elevated for a shorter period, until D3-4 and the anti-inflammatory cytokines, IL-10 and IL1-RA were only significantly elevated during the first 24-48 hrs post injury. This very early anti-inflammatory signaling response is consistent with previous studies (412) and with the currently held theory, supported by genomic data, of early simultaneous anti-inflammatory processes driving immunosuppression early after injury (51).

The interplay between metabolism and inflammation is increasingly being studied and correlation analysis of cytokine data with the most significantly changing metabolites in serum after severe thermal injury reveals moderately significant correlations in longitudinal trends. The inflammatory cytokines correlate negatively with lipid class metabolite features including, phospholipids, sphinoglipids, fatty acids, triglycerides and diglycerides. Positive correlations were seen with a leukotriene and lysoglycerophospholipid. The anti-inflammatory cytokine trends correlated negatively with a range of lipid classes and positively with an estrogen metabolite, fatty acids, aromatics, lysoglycerophospholipids and carnitine. There was correlation between Neuromedin-N, a hexapeptide related to neurotensin and IL1-RA. Neuromedin-N has been shown in mice to have immunomodulatory properties, including stimulation of macrophage phagocytic function (413) and adherence and chemotaxis of lymphocytes (414). It has also been demonstrated to modulate the function of the hypothalamo-pituitary axis (HPA) (415). Whether the associations we have seen play a causal role in influencing the SIRS/CARS response or immuneparesis now needs further investigation.

4.5.4 Oxidative stress and mitochondrial dysfunction

Major thermal injury is known to be associated with oxidative stress, which is defined as a disruption of the balance between the production of reactive oxygen species (ROS or oxygen free radicals) and the anti-oxidant mechanisms designed to prevent them from damaging cells (416). The sources of ROS, such as superoxide anion ($0_2^{-\bullet}$), hydrogen peroxide (H_20_2) and hydroxyl radical ($^{\bullet}OH$)· are multi-factorial in burn injury. Thermal energy from the initial insult causes homolytic bond fission to generate ROS (417) and subsequent activation of inflammatory pathways activate

and stimulate neutrophils to produce ROS via their NADPH oxidase (superoxide burst) (418). Complement mediated increases in histamine activity, combined with toxic metabolites from ischaemia reperfusion injury lead to increased xanthine oxidase activity produces ROS (419). One of a cells most significant source of ROS is the mitochondrial electron transport chain (ETC) due to single electron reduction of O_2 generating the $0_2^{-\bullet}$ radical which is converted to H_20_2 (420). The other contributing sources are peroxisomal beta oxidation of fatty acids, which generates H_20_2 as byproduct and lipid peroxidation, which is the oxidative degradation of cell membrane lipids, especially PUFAs which results in the production of lipid radicals, reactive aldehydes (e.g. malondialdehyde) and other ROS (421). Smoke inhalation injury which often coexists in patients with major flame burns also results in the increases in tissue lipid peroxidation (422).

Significant changes in certain classes within the metabolome, including heme metabolism, oxidized fatty acids (OFA) and lysoglycerophospholipids are compatible with increased oxidative stress post-burn. Intravascular haemolysis after thermal injury is well documented (423,424) and one of the main mechanisms is felt to be erythrocyte damage from ROS produced by complement mediated activation of neutrophils (425). This erythrocyte destruction leads to the presence of free haemoglobin and heme in plasma (426), which is then able to cause oxidative damage in the vasculature and exposed tissues (427). In humans, the main heme degradation pathway is conversion to biliverdin by the enzyme heme-oxygenase-1 (HO-1) and subsequently to bilirubin by biliverdin reductase. HO-1 is a rate-limiting enzyme in the catabolism of heme and is inducible by many factors including oxidative stress, cytokines, hypoxia, nitric oxide and oxidized lipids (428). The

metabolomics data shows early elevations in bilirubin and downstream degradation products urobilinogen over the first 24hrs post-injury followed by decline. This is consistent with early increases in free heme from haemolysis and is consistent with animal and human published data (423-425).

Interestingly, significant changes were seen in Vitamin E metabolites, with early decline from admission levels with nadir at 3-4 weeks before a rise again during the recovery period. Vitamin E is an important anti-oxidant and has been shown to be decreased, along with other anti-oxidants, due to increased consumption in the face of increased ROS activity post-burn (429). Since the Vitamin-E metabolites continued to decline over the first 3 weeks despite supplementation, this would suggest that its initial utilization is very high or that there is ongoing utilization due to prolonged oxidative stress. Indeed, adipose tissue stores of Vitamin E have been shown to remain low for 3-weeks post-injury in severely burned children (430).

4.5.5 Changes in bile acids reflect intrahepatic cholestasis

Primary bile acids are synthesized and conjugated with glycine or taurine in the liver and represent the major excretory pathway for cholesterol in humans. The major bile acids that are synthesized in the liver are cholic acid and chenodeoxycholic acid which are conjugated with taurine or glycine before secretion into bile. Since bile acids are amphipathic they readily form micelles and are highly effective detergents, which enables them to facilitate digestion and absorption of dietary lipids. Most bile acids (95%) that are secreted in bile are reabsorbed in the terminal ileum of the small intestine and return to the liver via the enterohepatic circulation (hepatic portal vein). Small amounts of bile acids undergo faecal excretion (5%) and a very small amount reach the systemic circulation and are absorbed by the kidneys (431,432). The 200-

800mg of bile acids that escape reabsorption undergo metabolism by anaerobic bacteria in the colon, resulting in over 20 different secondary bile acids in adult faeces. The types of chemical conversions include deconjugation, oxidation, epimerization of hydroxyl groups, esterification, desulfation and 7-dehydroxylation (433).

Significant changes were seen in 16 bile acid metabolites, with primary bile acids such as glycocolic acid and glycochenodeoxycholic acid increasing from admission and peaking at 2-weeks post injury before declining. Bile acid derivatives showed a similar pattern to the fatty acids and glycerolipids with a decline from admission before increasing again after 3 weeks. These changes are consistent with alterations in bile acid synthesis and or secretion. Severe thermal injury is associated with liver dysfunction, with deranged liver function tests (LFTs), fatty infiltration of the liver with hepatomegaly and increases hepatic apoptosis (434). Autopsy studies have demonstrated the presence of intrahepatic cholestasis in 26% of cases of severe thermal injury and in all cases the patients had developed sepsis (435). No detailed studies have been undertaken in burn to identify the underlying mechanisms for cholestasis, but in studies of sepsis, intrahepatic cholestasis is associated with impaired transport of bile acids in hepatocytes (436). More recent studies are starting to unpick the mechanisms of cholestasis in critically ill patients, with evidence of down regulation of the apical bile salt export pump (BSEP) and upregulation of expression of the basolateral multidrug resistance associated protein (MRP) 3, leading to reversal of bile acid transport and reflux of bile acids back into the circulation (437). The changes in the bile acid metabolites may also be compounded

by increased cholesterol import and conversion to bile acids, demonstrated by expression profiling in animal burn models (438).

4.5.6 Changes in the post-burn metabolome suggest gut dysfunction and bacterial translocation

The human intestinal lumen contains vast concentrations of bacteria in addition to bacterial endotoxins, which are prevented in normal health from crossing the intestinal mucosa through several complex defense mechanisms. Animal studies of gut dysfunction after burns and major trauma suggested bacterial translocation across the gut barrier was a cause of systemic inflammation and multiple organ dysfunction syndrome (MODS) after injury (439-441). This translocation was theorized to occur due to the combination of physical disruption of the barrier, overgrowth of normal gut flora and impaired immunity. There are a number of contributing factors to this altered gut barrier function including, hypoperfusion during burn shock and with the use of vasoactive drugs, intestinal oedema due to systemic capillary leak and impaired peristalsis leading to bacterial overgrowth (358). The *gut origin hypothesis* of post-injury MOF, has evolved through more recent studies to the *gut-lymph hypothesis*, which proposes that gut derived inflammatory mediators in response to barrier dysfunction and gut ischaemia travel in mesenteric lymph to drive systemic inflammation and distant organ dysfunction (442). This transbiosis represents a possible novel target in burns patients as it may well contribute to the SIRS response and this is an active area of research.

Within the final dataset of metabolite features that changed significantly over 6 months post-burn, there are multiple annotations that are bacterially derived metabolites, which could be absorbed from enteric bacteria due to barrier

dysfunction. There were moderate numbers of significantly changing tryptophan metabolites which are not produced via human pathways, including: indole, indoxyl, 3-methylindole, indolelactic acid. Enteric and other bacteria metabolise tryptophan to form indole, pyruvate and ammonia using the enzyme tryptophanase and can act as an intercellular signal between bacteria and controls diverse aspects of bacterial physiology (443). These metabolites demonstrated early elevations in a similar pattern to the pro-inflammatory cytokines IL-6 and IL-8. The tyrosine precursor, 3-dehydroquinate, increased between weeks 2 and 4 post-injury. It is an intermediate in the Shikimate pathway in bacteria and plants, used in the synthesis of aromatic amino acids (444). Secondary bile acids, which are produced from bacterial degradation of primary bile acids, were also elevated early after thermal injury, with peaks either on admission or D3-4 before decline. Heme O, is an interesting metabolite, that also decreases from elevated levels on D3-4. It is a bacterially derived heme that is essential for aerobic respiration is closely related to human heme A (445). The pattern of early elevations of bacterial metabolites in serum also parallels the early increases in pro-inflammatory cytokines IL-6, IL-8, G-CSF and MCP-1.

4.5.7 Vitamin-D metabolism

There are two major forms of Vitamin D, Vitamin D_3 (cholecalciferol) and Vitamin D_2 (Ergocalciferol) and both are fat-soluble secosteroid vitamins. Both may be obtained from the diet but Vitamin D_3 is synthesised in the skin from 7-dehydrocholesterol in response to ultraviolet light (UVB). It is transported to the liver by vitamin-D binding protein (DBP) where it is converted to an inactive form through hydroxylation to 25-hydroxyvitamin D_3 (25-D_3), the major circulating form of Vitamin D. Subsequently, it is

further hydroxylated to its active form, 1,25-dihydroxyvitamin D_3 (1,25-D_3) in the kidneys. Vitamin D plays important roles in bone metabolism and calcium and phosphate homeostasis in addition to anti-inflammatory and immune-regulatory properties. Vitamin D deficiency in the general population is associated with infectious diseases, muscle weakness and increased risk of mortality (446).

A total of 29 Vitamin D metabolites changed significantly over 6-months post-burn and the predominant pattern was gradual increases in the levels of these metabolite features to a peak at 2 weeks before declining again. A smaller group of the metabolite features declined from admission and remained low for one month before increasing again. It was difficult to stratify groups of metabolite features and many had multiple annotations which makes trend interpretations difficult. One metabolite feature that was annotated with 25-D_3 and the active form, 1,25-D_3, showed a decline from admission levels over the first 2 weeks and remained almost undetectable for the rest of the study.

Previous studies in severely burned children and adults show that there is a high prevalence of Vitamin D deficiency during their admission. In children with burns of >25% TBSA, 62.3% of patients were Vitamin D deficient during admission (447). A recent large study in burned adults showed that Vitamin D levels on admission were deficient in 14.5% of patients, insufficient in 65%, and normal in 20.4%. Low levels of Vitamin D were associated with prolonged ICU and hospital LOS and increased incidence of infectious complications, sepsis and graft loss (448). No longitudinal profiling studies of Vitamin D have yet been conducted in thermally injured patients. Since severe thermal injury is associated with immunoparesis, muscle catabolism

and defects in bone metabolism and that low vitamin D levels are associated with poor outcomes, further detailed exploration of the change in vitamin D metabolites is warranted.

4.5.8 Limitations of the study

The main limitations of this study are the relatively small sample size of 13 patients. A larger sample size would increase the generalizability of the data and allow meaningful subgroup analyses such as comparison of the metabolome response to thermal injury stratified by age, burn size and outcomes such as mortality, sepsis and MOF/MODS. It would also reduce the inevitable biasing of the metabolome signals from the more severely injured patients; it is assumed that these patients show more significant changes. The dataset did include a broad range of age groups and burn sizes but the less severely injured patients were treated on the burns ward, whilst the patients with larger burns required ICU level care. There would therefore be treatment differences between these groups over time, including duration of nutritional support, use and duration of anti-catabolic drugs, use of vasopressor drugs, mechanical ventilation and renal support. The ideal cohort to study would be a larger sample size of patients with larger burns (e.g. >30%) that were all treated in the ICU, giving a more homogenous study group.

Controls were not used in this discovery phase study, with the reason that acquiring representative control metabolomics data would require a large control sample size with implications on the cost of the study. The lack of control data meant some of the interpretation of trends was more challenging but was aided by reference to previously published data. Finally, the UHPLC columns used in this study could have

caused potential bias towards resolution of lipids, contributing to the high proportion of lipid species that changed significantly across the time-course.

4.5.9 Future research and implication of the study

This study was a longitudinal discovery phase untargeted study in a small cohort of severely burn injured adults from a single bio-fluid. This has identified at least 10 target groups of metabolites to focus on and has formed some testable hypotheses. The next steps would be to scale up the study to look at a larger cohort and start to relate the important changes in the metabolome to differences in injury characteristics, age, treatment and outcomes. This larger follow-up study could be a more targeted study, allowing the use of LC-MS platforms developed for the acquisition of more quantitative data, possibly with the use of internal standards, where available. The study has shown huge changes in lipid metabolism after severe thermal injury, so lipidomics based strategies may allow more detailed investigation of these. The parent study, the UK SIFTI study has now completed its recruitment of 150 severely thermally injured patients, and therefore has generated a bio-repository of serum, plasma and urine samples that could form the basis of future metabolomics studies.

In terms of longer term utility of the metabolomics approach to the study of human thermal injury, apart from identifying new potential avenues of research, it paves the way for the development of personalized healthcare approaches in burn care. A baseline metabolic map of the expected changes after thermal injury could allow early identification of metabolic poor responders (‘outliers’) and stratification of care pathways for these patients in terms of resuscitation, organ support and nutritional support. At present, much of burn care is protocolled and nutritional support,

although adjusted according to protein and nitrogen balance, is not really tailored to an individual based on their own specific metabolic response. Another avenue for metabolomics based research is in biomarker identification for diagnostics, for example in the early recognition of sepsis, a significant challenge in the thermally injured patient. An increased number of studies are exploiting this approach in critically ill and trauma patients (280,281,372,449-452) but it has not yet been applied to human thermal injury.

4.5.10 Conclusions

Untargeted LC-MS metabolomics has been applied to serum taken from a cohort of patients with severe thermal injury and longitudinal analysis of changes in the metabolome has demonstrated a massive shift in the lipid metabolome from the time of injury, a 'lipid storm'. This is characterized by changes large numbers of fatty acids, reflecting increases in lipid catabolism and beta-oxidation. Other lipid classes with large numbers of metabolites that shift dramatically, include the glycerophosholipids and sphingolipids. There appears to be a biphasic shift in the metabolome from a catabolic state (acute phase) towards an anabolic state (recovery phase) from 3-weeks post injury onwards. In some cases, a triphasic signal is seen and this may represent late responses occurring due to later episodes of sepsis. Significant changes were seen in previously unexplored areas of the metabolome and warrant further investigation through larger targeted studies. This would facilitate a better understanding of the complex metabolic derangements that occur in patients with severe thermal injury and ultimate improve patient outcome.

Chapter 5: Metabolomics analysis of the response to thermal injury in the elderly

5 Metabolomic analysis of the response to thermal injury in the elderly

5.1 Introduction

Thermal injury in the elderly is associated with poorer outcomes for a given burn size and improvements seen in burn care have benefited this patient group the least, with the least improvement in survival in this group compared to younger adults and children (14). A retrospective study looking at 228 elderly burn patients admissions between 2004 and 2012 at the Birmingham Burns centre in the UK shows improved survival overall compared to a previous cohort (see chapter 2) (453). Age is a significant risk factor for poor outcomes after thermal injury and probit analysis shows that in the 65-74 years age group, the LA50 is approximately 40% TBSA, compared to the over 85 years age a 10% TBSA burn carries a 50% mortality (453).

The reasons postulated for poorer outcomes with advancing age include increased prevalence of comorbid disease (454), reduced physiological reserve to cope with the stress response, relatively deeper injuries to skin thinning and inability to escape the burning source (141), frailty (140,294) and delays in wound healing(455). Normal physiological ageing is also associated with alterations in immune function affecting both the innate and adaptive arms of the immune system, termed immunesenesence. This term also encompasses the increased chronic low-grade systemic inflammation with alteration of the balance of circulating cytokines (143). This is termed inflammaging and is characterized by increased pro-inflammatory cytokines IL-6 and TNF-α, whilst IL-10 levels are reduced (456). Studies in animal models of thermal injury also demonstrated increasing mortality with ageing

concomitant with increased immune suppression. Aged mice display reduced delayed type hypersensitivity (DTH) responses, decreased immune cell proliferation and a greater T_H1 to T_H2 shift in the cytokine profile relative to younger mice (457). Age related defects in innate immunity have been studied in hip fracture patients, demonstrating that neutrophil reactive oxygen species (ROS) production is reduced on admission and the defect persists for 5-weeks post-injury. The reduction was more significantly reduced in hip fracture patients who developed infectious complications (190,458). Recent genomic data from the Host Response to Injury (Glue grant) study in the US, is adding weight to the hypothesis that ageing related immunesenescence and injury related immune dysfunction become additive in the severely injured elderly patient(459). Vanzant et al. studied gene expression in circulating neutrophils in shocked trauma patients with prolonged ICU admission and compared expression profiles between groups aged <55yrs and those aged >65yrs. Interestingly, they found age-related differences in the genomic response, with elderly patients exhibiting an initial decreased perturbation of gene expression compared to the younger patients. At 4 days post injury, as genomic changes were recovering in younger patients, the elderly patients neutrophils exhibited ongoing alteration in genes related to decreased chemotaxis, increased inflammation and decreased adaptive and innate immune function (460).

Severe thermal injury is associated with a profound and prolonged inflammatory and hypermetabolic response characterized by increased resting energy expenditure (REE), hyperthermia, a hyperdynamic circulation and a multitude of metabolic defects in carbohydrate, fat and protein metabolism (333). Activation of the sympathetic nervous system and hypothalamo-pituitary adrenal (HPA) axis as well as

systemic elevations in circulating pro-inflammatory cytokines provide a milieu that promotes hyperglycaemia, central and peripheral insulin resistance, increased peripheral lipolysis and profound catabolism of skeletal muscle (300). The vast majority of thermal injury metabolism research has been focused on children and younger adults with thermal injuries >20-30% TBSA, very little is known regarding the metabolic changes in the thermally injured older patient. Physiological ageing is associated with increases in insulin resistance, changes in body composition with increased central adiposity, sarcopenia and progressive loss in mitochondrial function (461). The aim of this study was therefore to utilize metabolomics to study global patterns of change in the metabolism in thermally injured elderly patients early after injury and progressively over time during their recovery.

5.2 Aims & objectives

5. To identify the key changes in the serum metabolome in the acute phase after thermal injury in the elderly (age ≥65 years).
6. To identify the longitudinal changes in the serum metabolome after thermal injury in elderly patients (age ≥65 years).

5.3 Methods

5.3.1 Study group

This study included a cohort of elderly patients aged ≥65 years with ≥1% TBSA full-thickness burns (but <15% total TBSA) that were recruited into a UK multi-centric observational study called the SIFTI study (*Scientific Investigation of biological pathways Following Thermal Injury*) (UKCRN ID: 13654) and were admitted to the adult Burns Centre at Queen Elizabeth Hospital Birmingham (QEHB), UK (2012-2014). Any patients that were initially unable to consent to the study due to lack of capacity (injury severity, unconsciousness, confusion) were recruited through a legal consultee advice process until they regained capacity to consent themselves. As a comparison group, 5 healthy elderly volunteers (>65 years), matched to the study group by age, sex and body mass index (BMI), underwent blood sampling. Samples were taken in the morning between the hours of 8-10am. For each volunteer, age (years), sex, height (m), weight (kg) and body mass index (BMI) (kg/m^2) was recorded.

5.3.2 Treatment of subjects

All patients received treatment according to standardized local burn care guidelines which includes admission to high dependency unit (HDU) level rooms warmed to thermal neutrality. All patients received thromboprophylaxis unless contraindicated and analgesia according to standard protocols. Some patients in this group received supplemental nasogastric feeding if required following nutritional assessment by a specialist burns dietician. In patients sustaining deep burns excisional surgery was performed if appropriate in this group after medical optimization and anaesthetic assessment. Patients with deep burns that were initially deemed unsuitable for

excisional surgery and skin grafting were treated with daily topical application of Flammacerium® cream. These patients underwent eschar excision and skin grafting as necessary when their medical condition had been optimised.

5.3.3 Data Collection

Patient demographics, burn injury details and clinical outcomes were recorded prospectively using case-report forms (CRF). Key outcomes included:

- In-hospital mortality
- Pneumonia (CDC criteria, www.cdc.gov)
- Sepsis - American Burn Association (ABA) 2007 consensus trigger criteria (309)
- Multiple organ failure (MOF) - Denver 2 MOF score (33)
- Hospital length of stay (LOS)
- Intensive care LOS (ICU-LOS)
- Mechanical ventilation days

5.3.4 Sampling

During the study, study day 1 (D1) was defined as the calendar day of injury and day 2 (D2) the second calendar day and so forth. All patients underwent an initial blood sampling within 24hrs of their injury. A second blood sample was taken in the morning (8-10am) between 48 and 96hrs post-burn, either on D3 or D4. These two samples were utilised for the NMR metabolomics study. For the LCMS longitudinal metabolomics study, further samples were taken at the following timepoints: D5-9, D19-24, D26-29, Month 2 (D60+/-7 days), Month 3 (D90 +/- 7 days) and Month 6 (D180 +/-14 days). 6mL blood samples were collected either via peripheral

venepuncture using an arm tourniquet or via a central venous catheter (CVC) or arterial line if present. Blood was collected using a Vacuette® blood collection system into Vacuette® Z-serum clot activator tubes (Greiner Bio-One Ltd, Gloucester, UK). The same blood tubes were used throughout the study. The same peripheral phlebotomy technique and equipments was used for the healthy volunteers. Blood samples were kept upright and allowed to form clot at room temperature for 30mins before processing into serum.

5.3.5 Processing of serum

Blood samples were clotted for 30 minutes at room temperature with the tubes placed upright and were then centrifuged at 3000 rpm for 10 minutes at 20°C in a swinging bucket rotor centrifuge (Eppendorf Centrifuge, model 5804 R, ThermoFisher Scientific). Aliquots of 400-600 µL were placed in 1.5 mL plastic cryovials and stored upright in a freezer at -80°C.

5.3.6 Serum sample preparation

Serum samples were prepared for NMR analysis identically to that described in Chapter 3, see section 3.3.4. Serum samples for LCMS analysis were thawed, prepared and deproteinised using the same techniques described in Chapter 4, see section 4.3.4.

5.3.7 NMR Spectroscopy

Prepared serum samples were analysed on a Bruker AVANCE II 600 MHz NMR spectrometer (Bruker Corp., USA) equipped with a 1.7 mm cryoprobe using the methods described previously in Chapter 3, see section 3.3.6. The 1D-NMR spectral

data was imported into MATLAB V2013a (MathWorks, Natick, USA) and were pre-processed using NMRLab (V3.5) (310) Metabolab (V3.5) (311). Pre-processing was performed as described previously in Chapter 3, see section 3.3.7.

5.3.8 Ultra-high performance liquid chromatography-mass spectrometry (UHPLC-MS)

Reconstituted serum samples were analysed together with QC samples for quality assurance using a Thermo Scientific Ultimate 3000 coupled to a Q-Exactive^{TM} Hybrid Quadropole-Orbitrap mass spectrometer (ThermoFisher Scientific, MA, USA) as described previously in Chapter 4, see section 4.3.6.

5.3.9 Statistical analysis of NMR metabolomics data

Data analysis was performed using PLS Toolbox software Version 7.5.2 (Eigenvector Research, INc. Manson, USA) running in MATLAB (Release 2013a, Mathworks, Natick, USA). Data analysis approaches were as described in Chapter 3, section 3.38 and included principle components analysis (PCA) and orthogonal partial least squares discriminant analysis (OPLSDA). The metabolite peaks highly weighted in the multi-variate models according to VIP scores were identified from the 1D NMR spectra using Human Metabolome Database version 3.6 (www.hmdb.ca) and Chenomx NMR suite (Chenomx, professional version 4.0, Chenomx Inc, Canada).

5.3.10 Data pre-processing, quality assurance metabolite identification for LCMS study

The pre-processing, quality assurance (QA) and metabolite identification methods were identical to those previously described in Chapter 4, section 4.3.7.

5.3.11 Statistical analysis of LCMS data

Metabolomics data analysis was performed using Metaboanalyst v3.0 (385,387,388). Univariate analysis was applied to the dataset using one-way ANOVA with Tukey's post-hoc analysis this was applied separately to the positive and negative ion mode datasets. Pre-processing of data for univariate analysis included missing value imputation and data was normalized by sum (total peak area per sample). Statistically significant metabolites were selected using p-value <0.05.

5.3.12 Statistical analysis of demographic data

Demographic and injury data were compared using SPSS v23.0 statistical software (IBM, USA). Datasets were assessed for normal distribution using the Shapiro-Wilkes test. Parametric data are displayed as means with standard deviation and groups compared using the Independent Samples T-Test. Non-parametric data are displayed as medians with interquartile range (IQR) and groups compared using Mann-Whitney U-test. Categorical variables were compared using Fisher's exact test. Statistical significance was considered at a probability of *p*-value <0.05.

5.4 Results

5.4.1 1H-NMR Metabolomics analysis of the early metabolic response to thermal injury in the elderly

5.4.1.1 Demographics and outcomes

A total of 15 patients were included in the NMR study with a mean age of 78.2 (+/-10.7) years, a male-to-female ratio of 1:3 and median burn size 6 % TBSA (IQR:3-13). The demographics of the cohort are highlighted in table 5.1. The commonest injury mechanisms were flame (40%) and contact (40%) burn and scald (20%) (Figure 5.1). No patients sustained an inhalation injury but two patients required admission to the ICU during their hospital stay for treatment of sepsis.

Admission data	Cohort B
n	15
Age (years)	78.2 (+/-10.7)
Male n (%)	5 (33)
BMI (kg/m^2)	25.1 (+/-4.8)
TBSA (%) (IQR)	6 (3-13)
TBSA-FT (%) (IQR)	3 (2-6)
Inhalation injury n (%)	0.0 (0)
Co-morbid disease	14 (93)
ICU Admission n (%)	2 (13)
APACHE II first 24hrs (IQR)	13 (10-18)
SOFA first 24hrs (IQR)	1.0 (0-4)
Denver MOF first 24hrs (IQR)	0 (0-2)
R-Baux	85.1 (+/-11.2)
ABSI (IQR)	7 (7-8)
BOBI (IQR)	2 (2-3)

Table 5-1. Demographic and injury data for elderly patients in NMR study. Abbreviations: TBSA (Total body surface area), BSA-FT (full thickness) APACHE (Acute physiology, age and chronic health evaluation score), SOFA (Sequential organ failure assessment) score, ABSI (Abbreviated burn severity of illness) score and BOBI (Belgian outcomes in burn injury) score.

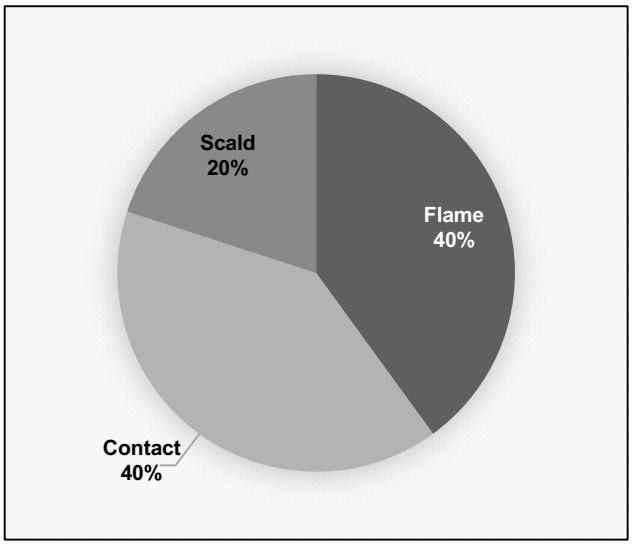

Figure 5-1. Mechanism of injury for elderly patients in NMR study.

Within the study cohort 3 patients did not survive giving an observed in-hospital mortality rate of 20%. Two patients developed at least one episode of MOF (13%) and 5 patients developed pneumonia (33%) and 5 patients developed at least one episode of sepsis (33%). The outcomes for the cohort are summarized in table 5.2.

Outcome variable	**Value**
In-hospital mortality n (%)	3 (20)
MOF (Denver 2) n (%)	2 (13)
Sepsis n (%)	5 (33)
Number of septic episodes/patient (n)	1 (+/-1)
Pneumonia	5 (33)
ICU LOS (days)	0.3 (+/- 0.8)
Mechanical Ventilation days	0.1 (+/- 0.4)
Hospital LOS (days)	24.0 (+/- 22.8)
LOS (days/% TBSA)	6.5 (+/-11.3)

Table 5-2. Clinical outcomes for elderly patients in NMR study. Abbreviations: MOF (multiple organ failure), ICU (Intensive care unit), LOS (length of stay), TBSA (total body surface area).

To assess the change in the metabolome early after burn injury in the elderly patient group, six control subjects underwent blood sampling. The demographics of the control group were not statistically different to the patient group (Table 5.3).

Parameter	Healthy Elderly controls	Patients (Cohort B)	*p*-value[$]
n	5	15	
Age (years)	71 (70-77)	77 (67-89)	0.735
Male n (%)	3 (60)	5 (33)	0.347
BMI (kg/m^2)	25.3 (21.5-29.0)	25.5 (20.3-29.1)	1.000

Table 5-3. Comparison of demographics between burn injured patients and healthy elderly controls. Abbreviations: BMI (Body mass index). $ = Fisher's Exact test for comparison of proportions, Mann-whitney U-test for comparison of medians between groups.

5.4.1.2 Changes in the metabolome after burn injury in the elderly patient

A total of 35 blood samples were collected, 30 from 15 elderly burn injured patients and 1 from each of 5 healthy elderly controls. NMR spectral data was obtained from 26 patient serum samples and 5 healthy control samples, as 4 samples (11%) had protein contamination interfering with spectral quality. The NMR data from the first 24hrs post-injury samples and control samples was first subjected to unsupervised PCA to look for any general trends or unexpected clustering. A 3-principle component (PC) model could explain the following percentages of variation: PC1 (31.12%), PC2: (19.39%), PC3 (12.55%) after removal of 1 outlier sample that fell outside the Hotelling's T^2 confidence ellipse. The PCA scores plot showed some clustering of the control and patient samples, particularly in the first two PCs.The dataset (with 2 PCA outliers removed) was then subjected to OPLS-DA analysis. A model with 3 LVs could discriminate between the elderly burn patient samples and elderly control samples with 100% Sensitivity and 89% specificity after 5-fold cross-

validation. The scores plots show good separation of the two classes (Figure 5.2) (R^2: 0.9, Q^2 0.7) and the AUROC for this model was 0.98 after cross-validation, confirming the model discriminated first 24hr post-injury patient samples from control samples based on NMR spectral profiles. The VIP loadings plot (Figure 5.3) shows the key metabolite peaks contributing to the model.

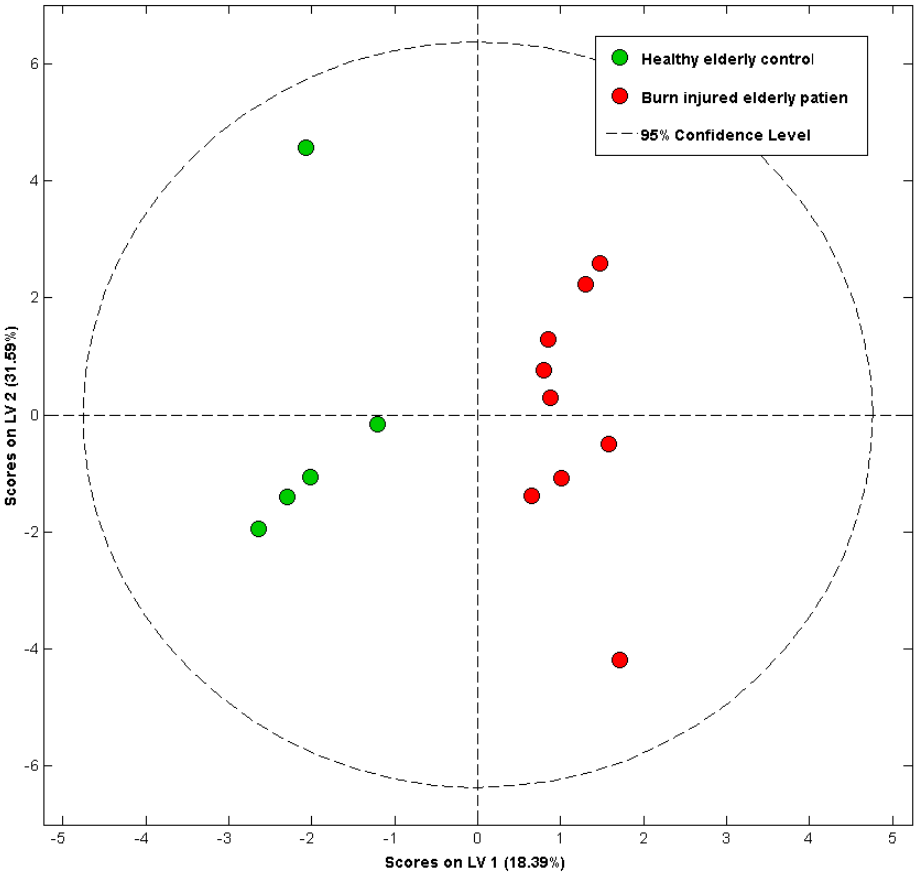

Figure 5-2. OPLS-DA Scores plot of serum samples taken in the first 24hrs post-burn vs. matched healthy controls. Burn injured elderly patients (red) separate away from healthy controls (green).

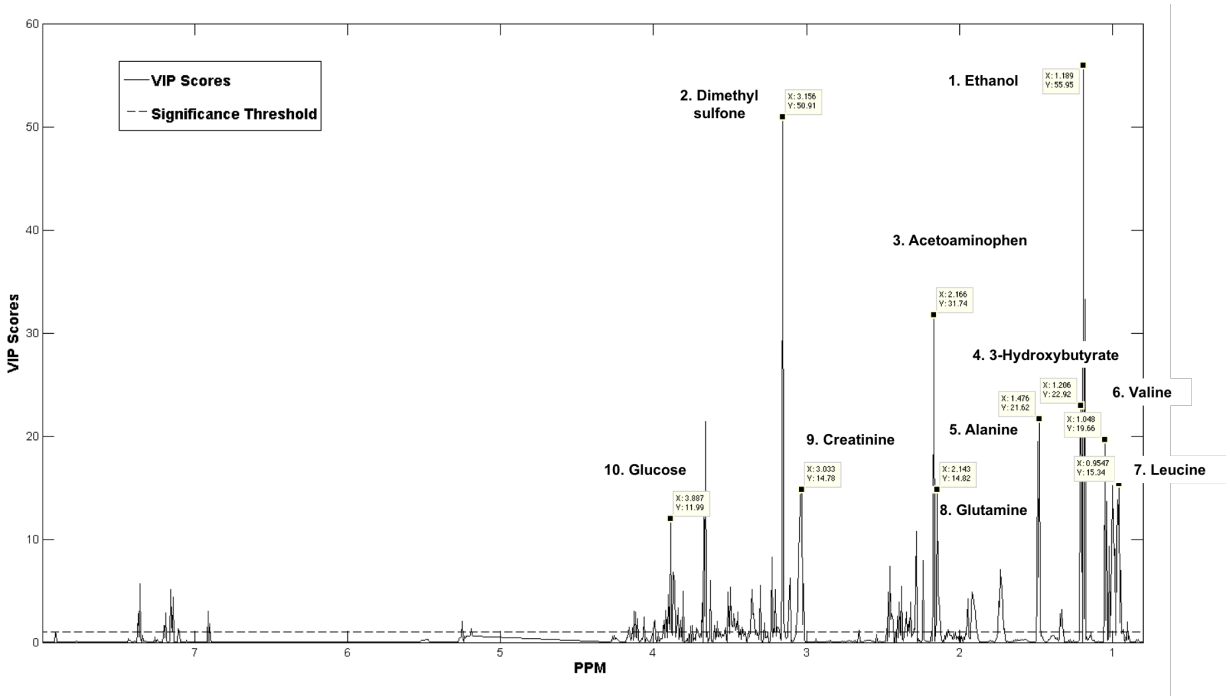

Figure 5-3. VIP loadings plot from OPLSDA discriminating elderly patient samples taken in first 24hrs post-burn and elderly healthy controls. NMR spectral peaks contributing to the model are labelled. The height of the peaks corresponds to VIP score and therefore greatest contribution to the variance between the first 24hrs samples from elderly burn patients and healthy elderly controls.

NMR spectral peak assignment was performed for the top 50 peak bins weighted in the OPLSDA model according to the VIP score. A total of 21 metabolites were identified through spectral fitting of the 1D NMR peaks and these are listed in table 5.4. 2 metabolite peaks were not identifiable using the Chenomyx spectral library and require further investigation to assign metabolites. The PPM values for these peak bins were 7.1595 and 7.3585 and were ranked 43rd and 49th according to VIP scores. A total of 14 metabolites were decreased in patients relative to controls and 7 metabolites were increased in patients relative to controls. Decreases were seen in the patients relative to controls of ethanol, dimethyl sulfone, creatinine, creatine, 7 amino acids, betaine and methanol. Increases were seen in acetaminophen

(paracetamol), glucose, ketone bodies (3-hydroxbutyrate, acetoacetate and acetone), myo-inositol and pyruvate.

Rank	Metabolite	Change[$]	VIP*	Chemical shift of peaks (ppm)
1	Ethanol	↓	55.95	1.18, 1.19, 1.20, 3.66. 3.67
2	Dimethyl sulfone	↓	50.91	3.16
3	Acetaminophen	↑	31.74	2.17
4	3-Hydroxybutyrate	↑	22.92	1.21
5	Alanine	↓	21.62	1.48, 1.49
6	Valine	↓	19.66	0.99, 1.00, 1.01, 1.04, 1.05
7	Leucine	↓	15.34	0.94, 0.96, 0.97,
8	Glutamine	↓	14.82	2.14, 2.45
9	Creatinine	↓	14.78	3.03, 3.04
10	Glucose	↑	11.99	3.50, 3.86, 3.87, 3.89
11	Acetoacetate	↑	10.73	2.28
12	Creatine	↓	10.23	3.04, 3.05
13	Isoleucine	↓	9.34	1.02
14	Carnitine	↓	8.28	3.23
15	Acetone	↑	7.96	2.24
16	Lysine	↓	7.03	1.73
17	Phenylalanine	↓	6.21	3.11
18	Myo-inositol	↑	6.05	3.63
19	Betaine	↓	5.51	3.30
20	Pyruvate	↑	5.47	2.38
21	Methanol	↓	5.15	3.35

Table 5-4. Metabolites identified within the top 50 ranked peaks in OPLS-DA model discriminating early first 24hrs serum samples from Elderly patients and elderly control subjects. Metabolites are ranked according to peaks with the highest VIP score. Arrows indicate the direction of change in patient samples compared to controls. (VIP – Variable Importance of Projection, PPM – parts per million).

The same workflow was utilised to study the changes in the serum metabolome in elderly patients after the first 24hrs post burn-injury but within the first 3-days post-burn (up to 96hrs). NMR spectral data obtained from serum samples taken >24-96 hrs post-burn from 14 patients and 5 elderly control subjects was subjected to PCA. This identified two outliers (1 control, 1 patient) which were removed, resulting in a PCA that explained the following percentage of variation in the model: PC1 = 39.87%, PC2 = 16.96% and PC3 = 14.68%. Some clustering and separation of control and patient samples was seen on the 3D scores plot of all 3 components. The filtered dataset was then subjected to OPLSDA. A 2-LV model (Figure 5.4) discriminated between elderly control serum samples and patient samples taken 24-74 hrs post-burn with 100% accuracy, sensitivity and specificity. The metrics form the confusion matrix showed better overall performance of this model than the model employing earlier samples, however the Q2 metric was lower (Table 5.5).

Parameter	**First 24hrs**	**24-74 hrs**
Latent variables (n)	3	2
Samples	14 (9 Patient, 5 control)	16 (12 Patient, 4 control)
Accuracy % (95% CI)	93 (61-93)	100 (83-100)
Sensitivity % (95% CI)	89 (64-89)	100 (83-100)
Specificity % (95% CI)	100 (56-100)	100 (49-100)
PPV % (95% CI)	100 (72-100)	100 (83-100)
NPV % (95% CI)	83 (46-83)	100 (49-100)
AUROC	0.98	1.00
R^2	0.93	0.76
Q^2	0.72	0.56

Table 5-5. Summary of statistical measures of performance of cross-validated OPLSDA model to discriminate between Elderly patient samples taken 24-74 hrs post-burn and healthy elderly control samples. PPV = Positive predictive value, NPV = negative predictive value, AUROC = Area under the receiver operating characteristic curve.

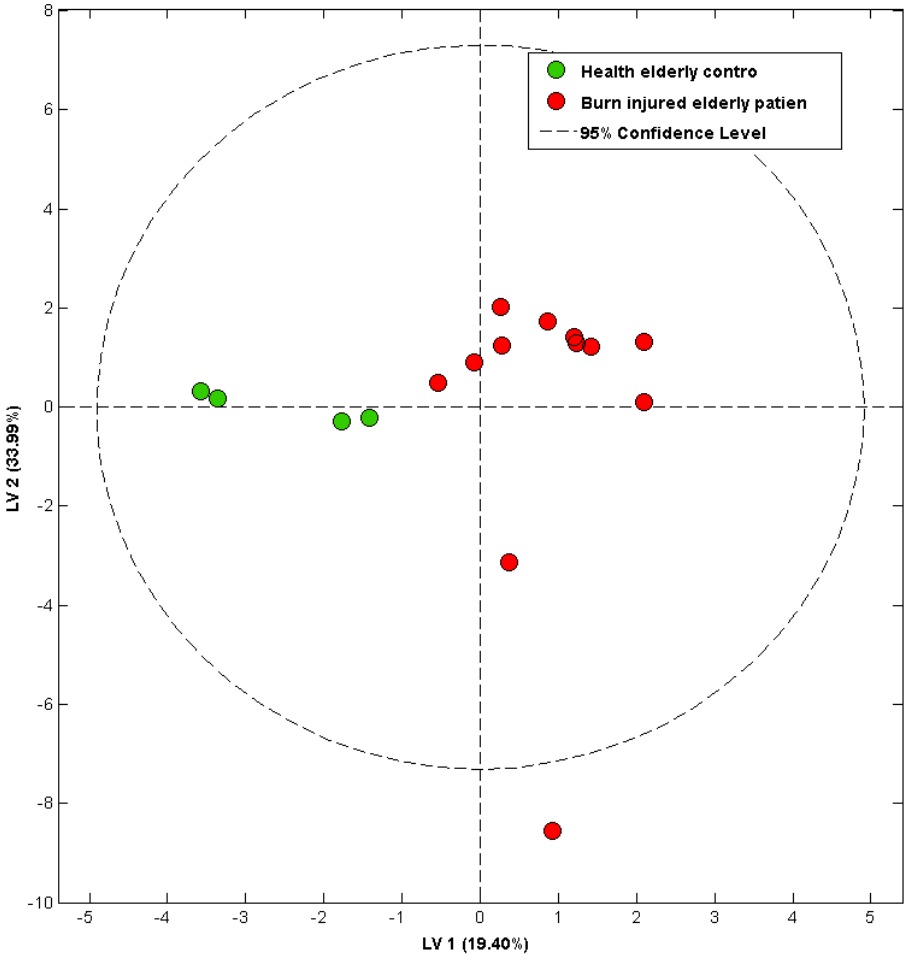

Figure 5-4. OPLS-DA Scores plot of serum samples taken 24-96hrs post-burn vs. matched healthy controls. Burn injured elderly patients (red) separate away from healthy controls (green).

The peak bins within the model were arranged by VIP score and the top 50 peaks identified and annotated with metabolites from a representative patient sample NMR spectrum using spectral peak fitting as before. The metabolites identified are shown in table 4.16. A total of 19 distinct metabolites were identified by spectral fitting from the top 50 ranked peak bins in the OPLSDA model discriminating between 24-74 post-burn elderly patient samples and elderly control samples. Two metabolite peaks were not identifiable using the spectral library and require further investigation to assign metabolites. The PPM values for these peak bins were 1.1537 and 3.6766

and were ranked 33rd and 48th according to VIP scores. Within the 17 identified metabolites, 10 were increased and 7 decreased in patient samples relative to control samples. As with the earlier serum samples, there were decreases in dimethyl sulfone, ethanol and 5 amino acids. Relative increases were seen in glycerol, ketone bodies, glucose, 3-methyl-2-oxovalerate, myo-inositol and succinate.

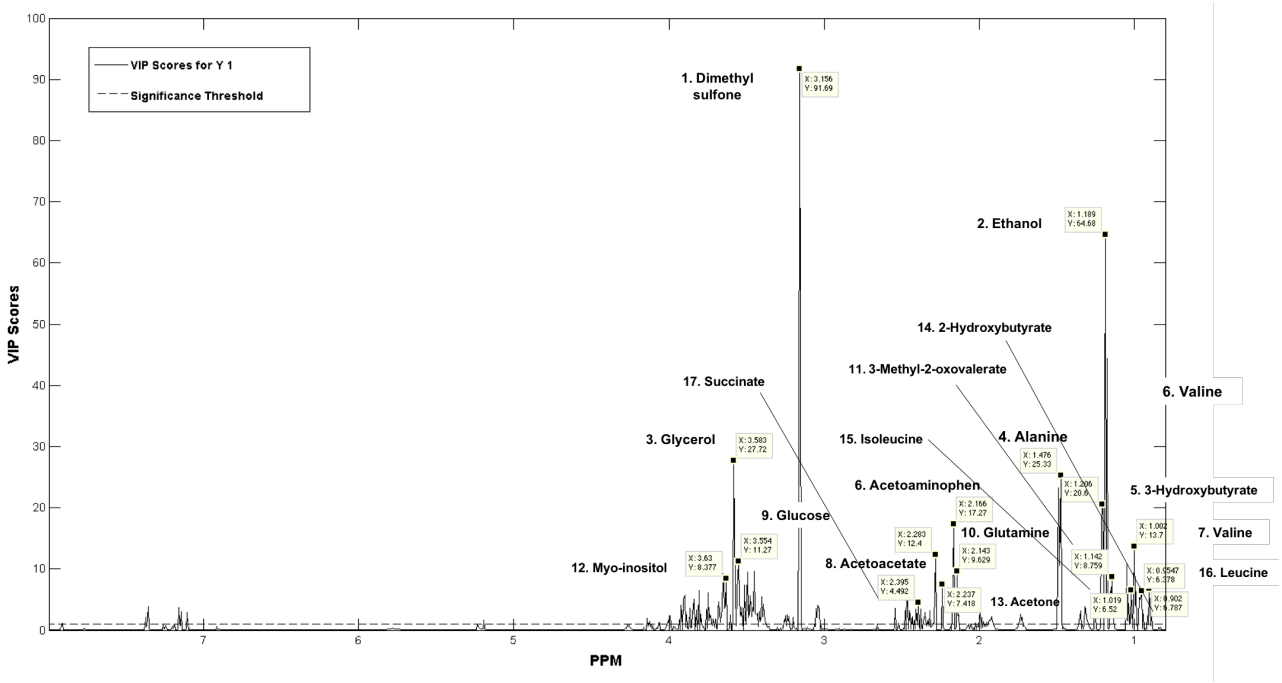

Figure 5-5: VIP loadings plot from OPLSDA discriminating elderly patient samples taken 24-96hrs post-burn and elderly healthy controls. NMR spectral peaks contributing to the model are labelled. The height of the peaks corresponds to VIP score and therefore greatest contribution to the variance between the first 24hrs samples from elderly burn patients and healthy elderly controls.

Rank	Metabolite	Change[$]	VIP*	Chemical shift of peaks (ppm)
1	Dimethyl sulfone	↓	91.69	3.16
2	Ethanol	↓	64.68	1.18, 1.19, 1.20
3	Glycerol	↑	27.72	3.58, 3.65
4	Alanine	↓	25.33	1.48, 1.49
5	3-Hydroxybutyrate	↑	20.60	1.21
6	Acetaminophen	↑	17.27	2.17
7	Valine	↓	13.70	0.99, 1.00, 1.01, 1.05
8	Acetoacetate	↑	12.40	2.28
9	Glucose	↑	11.27	3.40, 3.45, 3.48, 3.50, 3.51, 3.55, 3.56, 3.57, 3.75, 3.81, 3.84, 3.90
10	Glutamine	↓	9.63	2.14, 2.46
11	3-Methyl-2-oxovalerate	↑	8.76	1.14, 1.15
12	Myo-inositol	↑	8.38	3.63
13	Acetone	↑	7.42	2.24
14	2-Hydroxybutyrate	↑	6.79	0.90
15	Isoleucine	↓	6.52	1.02
16	Leucine	↓	6.38	0.95. 0.96, 0.97
17	Succinate	↑	4.49	2.39

Table 5-6: Metabolites identified within the top 50 ranked peaks in OPLS-DA model discriminating serum samples taken 24-96hrs post-burn from Elderly patients and elderly control subjects. Metabolites are ranked according to peaks with the highest VIP score. Arrows indicate the direction of change in patient samples compared to controls. (VIP – Variable Importance of Projection, PPM – parts per million).

5.4.2 Longitudinal LCMS metabolomics analysis of the elderly response to thermal injury

5.4.2.1 Demographics of the study group

A total of 6 patients were included in the longitudinal metabolomics analysis. The mean age for the cohort was 74.6 (+/-11.1) years and the median burn size was 4.5 (3.0-13.1) %TBSA (Table 5.7). This was comparable with data from the retrospective analysis performed of 2004-2012 elderly burn admission (Chapter 2), suggesting that they were a representative sample to study. In terms of outcomes no patients died during their hospital stay but 1 developed MOF (17%) and 2 developed infectious complications and were diagnosed with sepsis (33%).

Admission parameters	Values
n	6
Age (years)	74.6 (+/-11.1)
Male n (%)	2 (33)
BMI (kg/m^2)	23.3 (+/-6.0)
Co-morbidities	5 (83)
TBSA (%) (IQR)	4.5 (3.0-13.1)
TBSA-FT (%) (IQR)	2.7 (2-5.6)
Inhalation injury n (%)	0 (0)
ICU Admission n (%)	1 (17)
APACHE II first 24hrs (IQR)	14.5 (4.5-18.0)
SOFA first 24hrs (IQR)	1 (0-5)
Denver MOF first 24hrs (IQR)	1 (0-2)
R-Baux	81.4 (+/-9.1)
ABSI (IQR)	7 (7-8)
BOBI (IQR)	2 (2-2)

Table 5-7. Demographics and injury data for the elderly patients included in the longitudinal LCMS study. Abbreviations: APACHE (Acute physiology, age and chronic health evaluation score), SOFA (Sequential organ failure assessment) score, ABSI (Abbreviated burn severity of illness) score and BOBI (Belgian outcomes in burn injury) score, R-Baux (Revised Baux Score).

Outcome variable	Value
In hospital mortality n (%)	0 (0)
Mortality at 1 year	1 (17)
MOF (Denver > 2) n (%)	1 (17)
Sepsis n (%)	2 (33)
Pneumonia	2 (33)
Wound infection	1 (17)
ICU LOS (days) (IQR)	0.0 (0.0-0.8)
Mechanical Ventilation days (IQR)	0.0 (0.0-0.3)
Hospital LOS (days) (IQR)	24.5 (16.5-45.8)
Hospital LOS (days/% TBSA)	5.8 (+/-4.9)

Table 5-8. Summary of outcomes data for the elderly patients included in the LCMS longitudinal study. (MOF=multiple organ failure, ICU= intensive care unit, LOS=Length of stay, IQR=interquartile range).

5.4.2.2 Overview of metabolomics data

A total of 42 serum samples were analysed from the 6 thermally injured elderly patients in the study. The samples were run within the same batches as the young adult severe burn cohort presented in Chapter 4 with the use of pooled QC samples. The quality assurance of the overall dataset was checked with PCA and is presented in Chapter 4, section 4.4.1.1. After removal of metabolite features with >60% missing values, those with <50% of the features present in the QC samples and those with >20% relative standard deviation (RSD) across batches, 8185 metabolite features remained for the ANOVA analysis. ANOVA applied to the positive and negative ion mode datasets separately identified 379 metabolite features changing significantly (p=<0.05) from the time of injury to 6-months follow-up. No metabolite features were identified with an FDR corrected p-value<0.05 and therefore the uncorrected p-values were utilised for feature selection. From this dataset, 312 metabolite features

were filtered according to the criteria used in the young adult burn study, leaving a total of 67 metabolite features for final analysis. Trend analysis then focused on a final 50 metabolite features in 13 classes after removal of mixed class annotations (Figure 5.6).

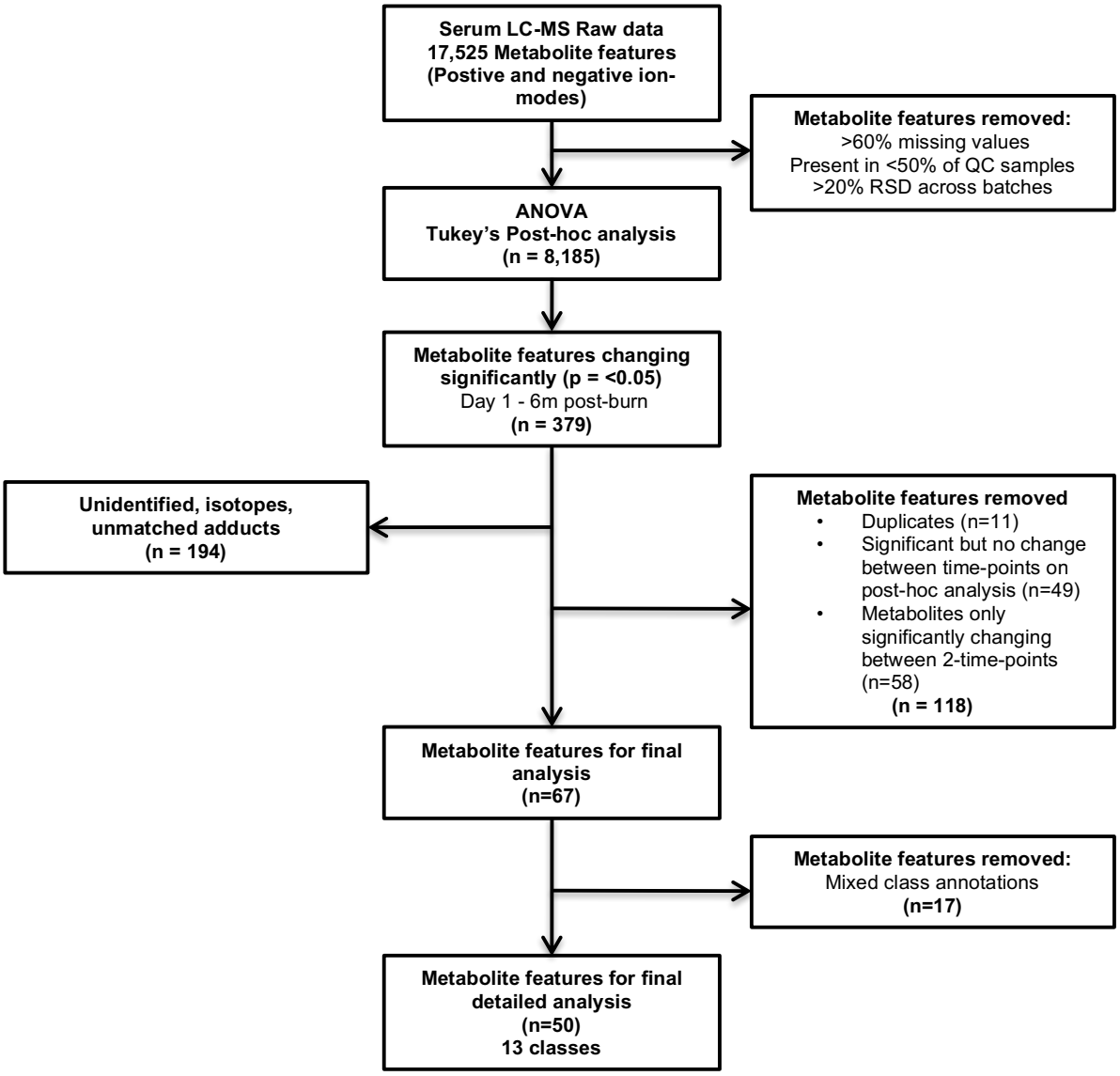

Figure 5-6. Flowchart of process of selection of metabolite features for further detailed analysis from elderly burn LCMS serum data. (LC-MS = Liquid chromatography mass spectrometry, RSD = Relative standard deviation).

Within the final 67 metabolite features dataset the class with the highest frequency of significantly changing metabolite features was the glycerolipids (acyl glycerides), followed by mixed classes and then polyketides, fatty acyls and steroid hormone metabolites (Table 5.9).

No.	Metabolite Class	No of metabolites p=<0.05
1	Glycerolipids	9
2	Mixed classes	8
3	Sterols	8
4	Polyketides	7
5	Fatty acyls	6
6	Mixed lipid classes	6
7	Aromatics	5
8	Bile acid metabolism	5
9	Carbohydrate metabolism	2
10	Prenol lipids	2
11	Peptides	2
12	Eicosanoids	1
13	Glycerophospholipids	1
14	TCA cycle intermediate	1
15	Sulfoxides	1
	Total	**67**

Table 5-9. **Summary of all metabolite classes changing significantly in serum over 6 months post thermal injury in thermally injured elderly patients** and number of significantly changing metabolites in each class (*p*=<0.05).

5.4.2.3 Lipid metabolism

In the overall dataset 36 metabolite features (54%) were lipids showing significant disturbances in lipid metabolism as seen in the young adults with more severe

thermal injuries. Among the lipid classes, 9 glycerolipids and 6 fatty acyls changed significantly. All of the glycerolipids were annotated as diacylglycerides (DG). All of these DGs displayed a pattern of decline from admission levels to a nadir at M2, followed by elevation from M2 to M6. Representative metabolite features are shown in Figure 5.7.

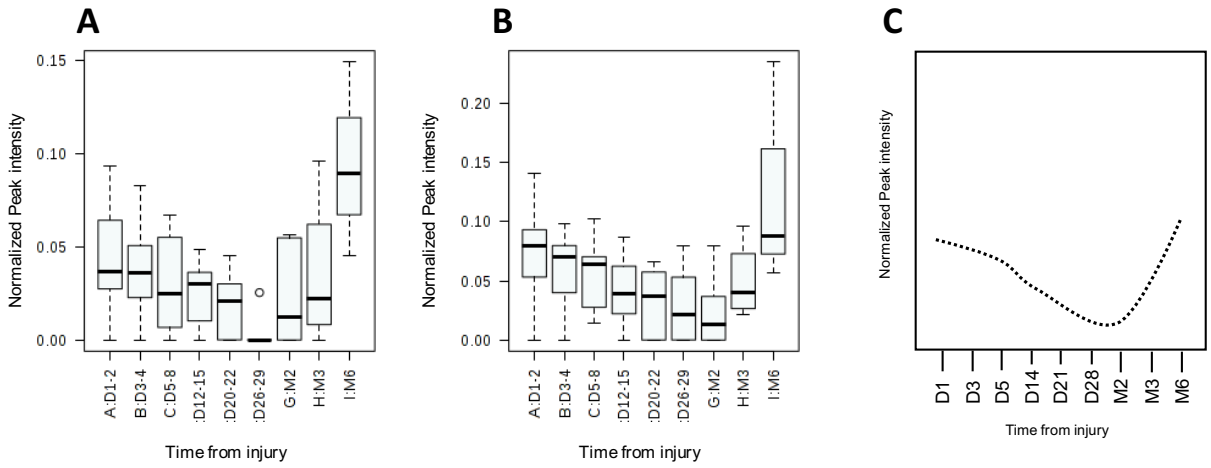

Figure 5-7. Box and whisker plots showing common longitudinal trend for diacylglycerols after thermal injury in the elderly. A: M5764, DG(34:3) (p=<0.001) B: M4964, DG(28:1) (p=0.016) and C: Summary of trend.

Within the 6 fatty acyl metabolites identified, there was a mixture of unsaturated fatty acids, fatty esters, fatty amides and octadecanoids. The predominant trend was very similar to that seen in the DGs with a decline from admission to a nadir at M2 before increasing again to M6 (Figure 5.8a and b). One metabolite feature, annotated as N-ethyl arachidonoyl amine and N,N-dimethyl arachidonoyl amine, a fatty amide, showed a different pattern with a rise from admission to a peak at 2 weeks before declining again to low or undetectable levels during the later recovery phase (Figure 5.8c).

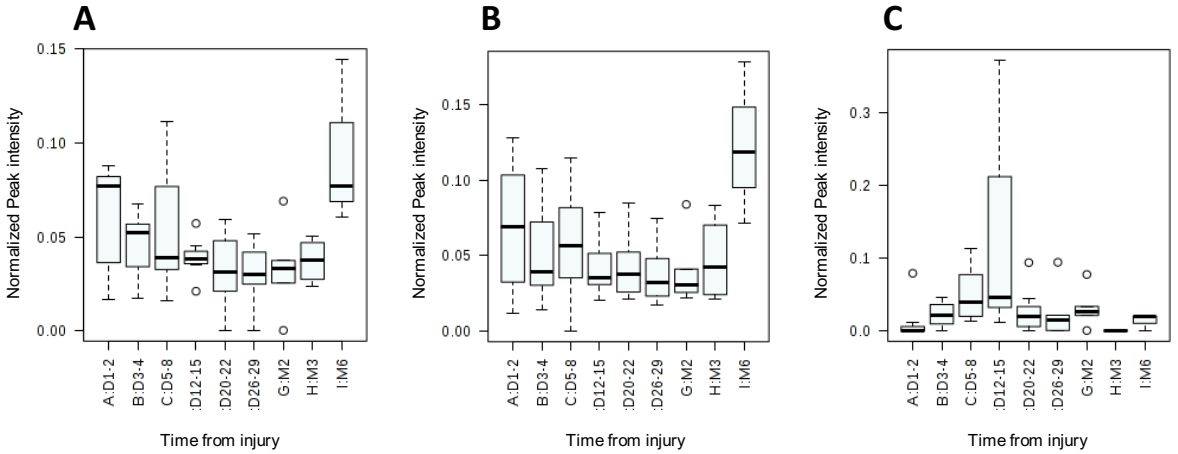

Figure 5-8. Box and whisker plots showing common longitudinal trend for fatty acyls after thermal injury in the elderly.

A: M960, annotations: :5,8-Tetradecadienoic acid; 6,9-tetradecadienoic acid; Alepric acid; Allyl undecylenate; alpha-Terpineol butanoate; Bornyl butyrate; Ethyl -dodecadienoate; Geranyl 2-methylpropanoate;Goshuyic acid;Isobornyl isobutyrate; Linalyl butyrate; Linalyl isobutyrate;Neryl butyrate; R-cucujolide III;S-cucujolide III. (p=<0.009)

B: M4802, annotations: Mayolene-16; hentriacontane-14,16-dione; Pentadecyl palmitoleate; (p=0.022)

C: M3135, N-ethyl arachidonoyl amine and N,N-dimethyl arachidonoyl amine (p=0.017)

5.4.2.4 Steroid hormone metabolism

Within the group of 8 sterol lipids changing significantly, 4 metabolite features were related to steroid hormone metabolism. Ptilosteroid A is a a saturated derivative of the C21 steroid, pregnane. Tetrahydroaldosterone-glucoronide and cortolone-glucoronides are mineralocorticoid and glucocorticoid steroid conjugates allowing excretion of these in bile. Ptilosteroid A (p=0.001) showed a trend of decline from admission to nadir at M2 and levels increased at M6 (Figure 5.9a). The other steroids showed a common pattern of decline from admission levels to a plateau between D5-8 and M2 before increasing again at from M3-M6 (Figure 5.9b and c).

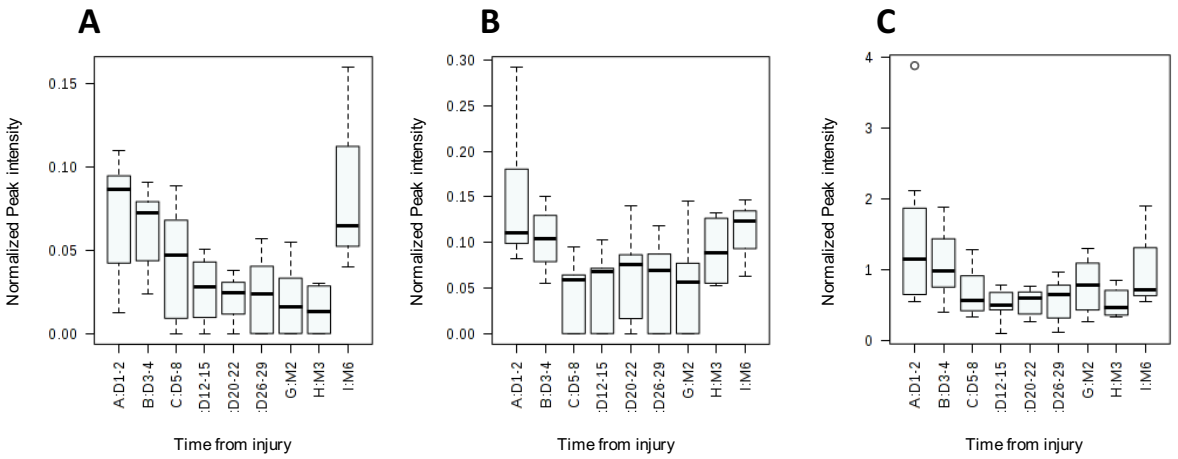

Figure 5-9. Box and whisker plots showing common longitudinal trend for steroid hormone metabolites after thermal injury in the elderly. A: M3639, Ptilosteroid A (p=0.001) B: M5488, tetrahydroaldosterone-glucuronide (p=0.007) and C: M4798, cortolone-glucuronide (p=0.024).

5.4.2.5 Bile acid and heme metabolism

Within the dataset, 4 bile acid metabolites changed significantly over the course of the study and showed a trend of elevation from the time of injury to a peak at either D5-8 or D12-15 (Figure 5.10b and c). Two of the bile acids metabolites also showed a late peak at M3, but the interquartile range is very large for that timepoint. One metabolite feature was annotated with urobilin and urobilinogen, heme degradation pathway metabolites and they showed a trend of early elevation after injury for at least 4 days. Levels were then low or undetectable from D5-8 until M3 before increasing again at M6 (Figure 5.10a).

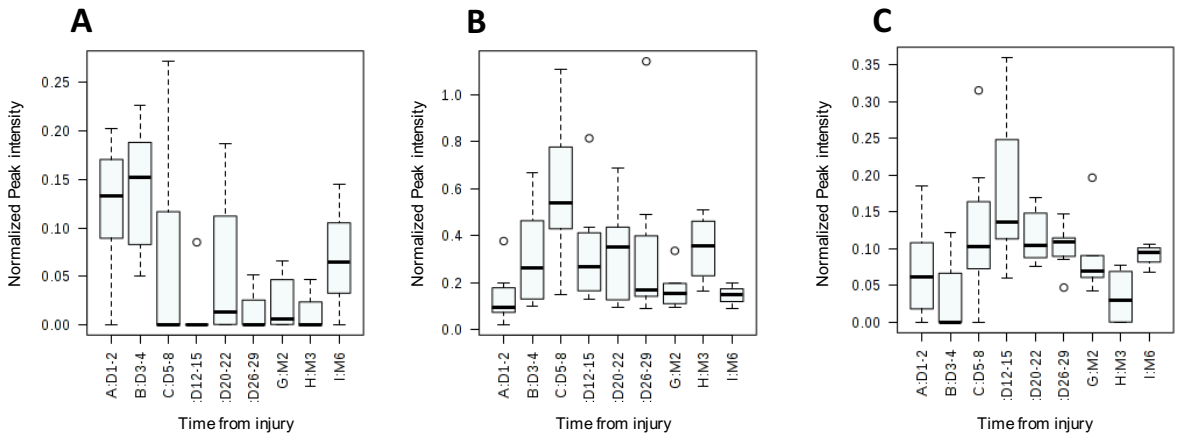

Figure 5-10. Box and whisker plots showing common longitudinal trend for Heme and bile acid metabolites after thermal injury in the elderly.

A: M5543, d-urobilinogen, urobilin (*p*=0.003)

B: M5407, 3a,12b-Dihydroxy-5b-cholanoic acid; 3a,7a-Dihydroxycholanoic acid; 3alpha,15alpha-dihydroxy-5beta-cholan-24-oic acid; 3b,12a-Dihydroxy-5a-cholanoic acid; 3b,12a-Dihydroxy-5b-cholanoic acid; 3b,12b-Dihydroxy-5b-cholanoic acid; 3b,7a-Dihydroxy-5b-cholanoic acid; 7a,12b-dihydroxy-5b-Cholan-24-oic acid; 7b,12a-Dihydroxycholanoic acid; Allochenodeoxycholic acid; Allodeoxycholic acid; Avideoxycholic acid;Chenodeoxycholic acid; Deoxycholic acid; Hyodeoxycholic acid; Isodeoxycholic acid; Isohyodeoxycholic acid; Isoursodeoxycholic acid; Murocholic acid; Ursodeoxycholic acid; 3beta-(3-methyl-butanoyloxy)-villanovane-13alpha,17-diol (*p*=0.007)

C: M5470, Taurochenodeoxycholate-3-sulfate;Taurochenodeoxycholate-7-sulfate; AFN911; 10-Deoxymethymycin (*p*=0.010).

5.4.2.6 Carbohydrates and TCA cycle metabolism

Two carbohydrate metabolites were identified as changing significantly and both had multiple annotations. They showed almost opposite trends across time with M1255 declining from admission with a nadir at 3 weeks before increasing again and peaking at M3. M1787 declined slightly from admission before peaking 3 weeks and declining again to M2 before increasing again (Figure 5.11 a and b). One TCA cycle intermediate, oxoglutaric acid (*p*=0.002) changed significantly across the course of

the study and this was also identified in the young adult severe burns analysis. Interestingly it showed the same trend pattern as the carbohydrate M1255 (Figure 5.11c).

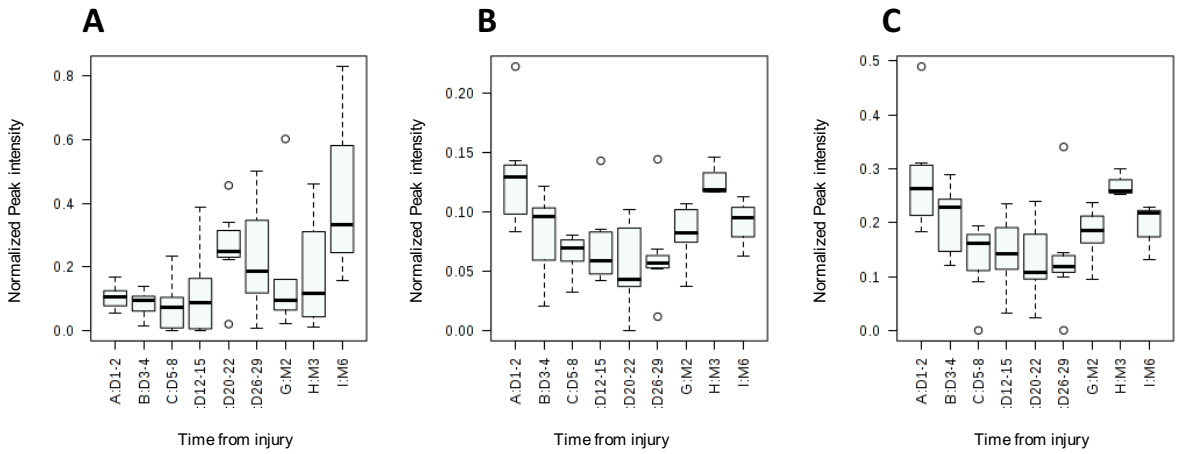

Figure 5-11. Box and whisker plots showing common longitudinal trend for carbohydrates and TCA cycle intermediates after thermal injury in the elderly.

A: M1787, 1-Deoxy-D-xylulose 5-phosphate; Deoxyribose 1-phosphate; Deoxyribose 5-phosphate; 2-Keto-3-deoxy-D-gluconic acid; 3-Keto-b-D-galactose;D-Arabino-hexos-2-ulose; Galactonolactone; Gluconolactone;L-Gulonolactone; Methylthiomethyl 2-methylbutanethiolate; Melizame; 2-Acetyl-3-methylpyrazine; N-Methylnicotinamide; A (p=0.02)
B: M1255, 3-Deoxy-D-glycero-D-galacto-2-nonulosonic acid; Allopurinol riboside; Arabinosylhypoxanthine; Inosine; Ethyl glucuronide; (p=0.002)
C: M1502, oxoglutaric acid (p=0.003).

5.4.2.7 Peptides

Two peptide metabolite features changed significantly across the course of the study including Neuromedin N(1-4) (p=<0.001) and Melanostatin (p=0.041). Neuromedin N(1-4) is a hexapeptide with known immunomodulatory and endocrine properties and showed the same trend pattern as seen in the young adult severe burn group. Melanostatin (p=0.041) is a peptide hormone produced in the hypothalamus and

inhibits the release of melanocyte-stimulating hormone. It was undetectable until M3 where it showed a slight rise and then decline again.

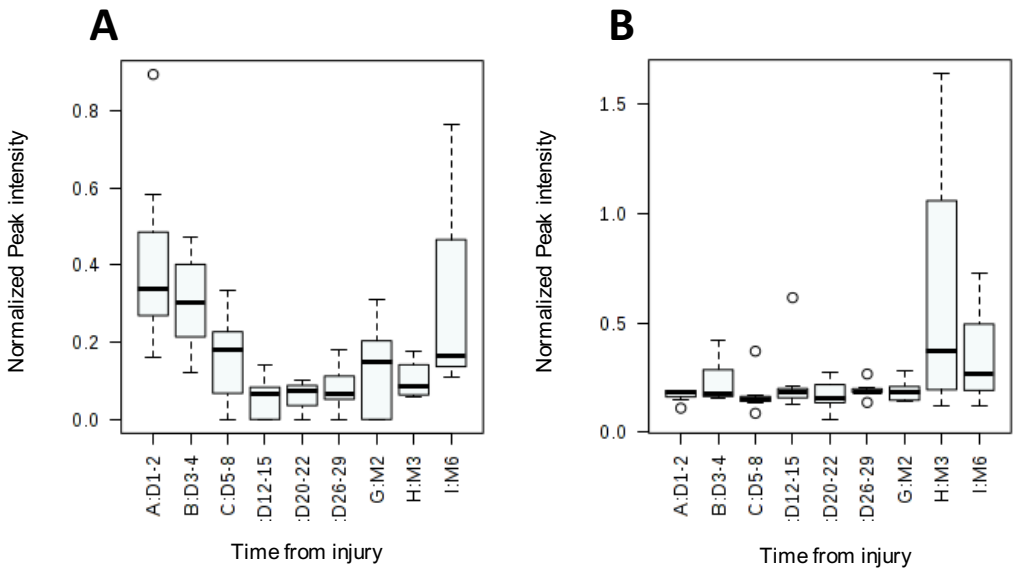

Figure 5-12. Box and whisker plots showing common longitudinal trend for steroid hormone metabolites after thermal injury in the elderly. A: M4603, Neuromedin N(1-4) (*p*=<0.001) B: M2528, Melanostatin (*p*=0.041).

5.5 Discussion

In this study ^{1}H-NMR metabolomics has been used to explore the early changes in serum after thermal injury in a cohort of 15 thermally injured elderly patients. Secondly, a preliminary study of the longitudinal changes in the metabolome after thermal injury in elderly patients has been conducted using a discovery phase LC-MS metabolomics approach.

5.5.1 NMR metabolomics analysis of the early response to thermal injury

In the first study, we have shown that serum metabolomics profiles could be utilised to discriminate between early serum samples (0-96hrs post-injury) taken from

thermally injured elderly subjects and samples from healthy elderly control subjects. Multi-variate models showed high discriminatory performance as assessed by accuracy, sensitivity and specificity and ROC analysis. The predominant pattern of change in the first 24hrs post-injury samples was of relative decreases in metabolites compared to controls with 14/21 (67%) of the top 50 weighted metabolites in the model. The pattern changed in the second samples taken between 24 and 96 hrs post-injury with a predominant pattern of increases in metabolites relative to control subjects with 10/17 (59%) of metabolites being increased. Interestingly, this was the opposite pattern to that seen in the study of younger adults with more severe injuries. The other interesting finding when comparing the results of the two different cohorts is that in the elderly cohort there were greater variation in the number of different metabolites featuring within the top 50 weighted ones in the OPLSDA models. In the younger adult models, several metabolites dominated with multiple peaks featuring in the highest weightings, including glucose, 3-hydroxybutyrate and lactate. This may represent more significant peturbations in these metabolites relative to the control subjects.

As was seen in the ^{1}H-NMR study of larger burns in younger adults, many amino acids, both essential and non-essential were shown to decrease after thermal injury, suggesting this is not an age specific response. These changes are consistent with previous findings in the burn literature (462,463). It was an unexpected finding that there would be so many changes in amino acids in the elderly group relative to controls, since the average burn size for the group was only 6% TBSA versus 38% TBSA in the young adult group. These decreases seemed to persist in the second sample with ongoing relatively lower levels of even essential amino acids valine,

isoleucine and leucine. The underlying cause of these reductions is unclear as circulating levels only tell half the story without knowing the whole-body kinetics and flux of these amino acids. This may represent acute increases in utilisation by the burn wound and liver for acute phase protein synthesis(228). If these findings do however represent acute skeletal muscle catabolism as has been shown in children and adults with much larger injuries, then this could have an impact on the delayed recover of elderly patients with thermal injury. This could be especially problematic since with increasing age it is known there is increasing loss of skeletal muscle, known as sarcopenia, due to altered muscle metabolism, contributing to increased frailty (464). Longer-term quantitative data on blood changes and whole-body kinetics of amino acids, combined with ultrasound measurement of muscle thickness and functional measurement of muscle function are a priority in the elderly burn patient.

As was seen in the younger adult cohort, the elderly patients also exhibited increases in ketones, glucose and pyruvate relative to controls. In the second sample, increases were seen in succinate, the TCA cycle intermediate. These data suggest that despite smaller injuries, there may also be a significant enough stress response in the elderly after thermal injury to increase energy demands and altered glucose homeostasis. Ageing is associated with increases in insulin resistance (IR), which may be potentially worsened by the metabolic changes in thermal injury. A recent study looking at a cohort of elderly patients with moderate sized burns (median TBSA, 15%) compared inflammatory and metabolic indices with an injury severity matched group of younger patients with burn injury. They found the elderly patients had average higher daily glucose levels and a greater insulin requirement which persisted for the whole study period of 1 month post-injury. The study also performed

oral glucose tolerance testing (OGTT) and found no differences in insulin resistance between the age groups but did find that the elderly had impaired insulin production by the pancreas (465). The consequences of more persistent hyperglycaemia are increased risk of infections, decreased wound healing and increased mortality (466).

Other observations of interest that were not seen in the younger adult cohort, include elevations in myo-inositol, a cyclic polyalcohol and source of important second messengers in cells. Studies in rat burn models have shown that D-myo-inositol-1,2,6-triphosphate (IP3), a metabolite of myo-inositol, decreased burn oedema and inflammation and inhibition of dermal ischaemia after burn (467). Elevations in this metabolite may therefore be protective in response to deeper thermal injury, preventing inflammation mediated burn wound progression. Decreases in ethanol in the patient group relative to controls could either be due to alcohol consumption by the healthy volunteers or alterations in gut metabolism. Dimethyl sulfone ($DMSO_2$) is normally found in human plasma and CSF and can be derived from food sources and endogenous conversion of methanethiol which is derived from gut bacterial metabolism (468). This decrease in $DMSO_2$ in the patients seen at both time points is curious and could be related to acute alterations in gut perfusion or gut microbial metabolism.

Decreased alterations in dimethyl sulfone and ethanol in the patients relative to controls are a curious finding and could be a spurious result owing to volunteers drinking alcohol prior to sampling. The $DMSO_2$ levels could be related to altered gut bacterial metabolism in the patients relative to controls. Alternatively, it could be due to alterations in methanthiol metabolism in blood

5.5.2 LCMS metabolomics study of the longitudinal response to thermal injury in the elderly.

In the second study, we have performed a preliminary untargeted longitudinal metabolomics analysis of a small cohort of elderly patients with thermal injury. The same analytical methods and approach were used as for the longitudinal study conducted on a cohort of younger adults with severe burns >15% TBSA (Chapter 4). The first finding that relative to the younger cohort, there were much fewer metabolite features that changed significantly across the 6-months of the study (67 vs. 432). and none that were significant according to FDR correction. There are several possible explanations for this finding. Certainly, the much smaller cohort of patients with far fewer serum samples included in the analysis will have impacted the number of metabolite features demonstrated as significant. Secondly, the severity of injury was much lower in the elderly cohort and since hypermetabolism correlates directly with burn size (71), it seems logical that there would be overall less changes in the metabolic network with a smaller injury burden. As part of the filtering process, any metabolite features that only changed significantly between two time-points were filtered out. Re-examining the raw data, there were another 28 metabolites that changed significantly between the either of the initial two samples and the other time-points in the first two weeks. Briefly looking at the annotations for these, they include heme metabolites (bilirubin, biliverdin), bile acids, steroid hormone, eicosanoids and docosanoids. These metabolites are associated with oxidative stress, stress response and inflammation and since they are only significantly changing at early time-points, this may represent a short stress response in this cohort. In order to test this hypothesis, it would useful to conduct a much larger study, with a range of burn

injury sizes included for burn size group comparisons and correlations against injury severity.

Comparison of the elderly burn LC-MS data with the younger adult burn dataset, shows that there were, despite the differences in injury size, similar classes of metabolite features that changed significantly across the time course. There were again large numbers of lipid metabolite features that changed significantly including multiple glycerolipids and fatty acids. The glycerolipid class was entirely made up of DGs which could be related to increased triglyceride breakdown in adipose tissue. This is a potentially interesting finding since increased intracellular levels of DGs, together with fatty acyl CoAs, have been linked with muscle insulin resistance through protein kinase C activation triggering signalling cascades modulating the insulin receptor substrate-1 (IRS-1) activity (469). Another similarity between the datasets is the most common trend pattern seen across classes was very similar, with a reduction from admission levels to a nadir, albeit later in the case of the elderly patients, being at 2-months post-injury. This raises the possibility of a delayed recovery in metabolic responses. There was again evidence of oxidative stress with early increases in circulating heme metabolites and evidence of biliary dysfunction with several bile acids peaking within the first 2 weeks post-injury. Neuromedin-N was found to be most highly significantly changing metabolite and displayed a similar pattern as seen in the younger adult cohort, suggesting a common response irrespective of age. It is related to the neurotensin family of neuropeptides innate and adaptive immunomodulatory properties and can modulate the HPA axis. This metabolite should be investigated further to investigate potential roles in post-injury immunosuppression and endocrine dysfunction.

5.5.3 Limitations of the study

The main limitations of this work as that given the sample size, it is essentially preliminary in nature and larger analysis of the remainder of the SIFTI cohort of patients could be analysed as a next step to confirm or refute the findings above. It would be worthwhile including larger burns in the elderly group, accepting the difficulties in following up these patients who are often repatriated to intermediate care or other hospitals once they are out of their acute phase.

5.5.4 Conclusions

In this study, we have utilised complementary analytical platforms to apply metabolomics to the study of thermal injury in an understudied subgroup of burn patients who suffer poorer outcomes relative to their injury burden. The metabolomics data has highlighted similarities and differences between metabolic changes early and across the recovery phase between older and younger thermally injured patients. Further larger studies are warranted to confirm the study's preliminary findings.

Chapter 6: General discussion

6 General discussion

6.1 Overview

The focus of this thesis has been on applying metabolomics, a systems biology approach, to the study of metabolic changes after severe thermal injury. The hypermetabolic response that ensues after severe cutaneous burns is profound, prolonged and associated with poor clinical outcomes (333). Much of the knowledge so far acquired regarding post-injury metabolic disturbances has been gleaned from targeted studies of classes of metabolites. Although these studies have led to advances in burn and trauma care, clinical outcomes are plateauing.

The Scientific Investigation of biological pathways Following Thermal Injury (SIFTI) study was an ambitious project set up at the Birmingham Scar Free Foundation Burns Research Centre in the UK with the aim of studying in parallel the immune, inflammatory, endocrine and metabolic responses to severe thermal injury. The research presented in this thesis focused on a sub-cohort of these severely injured patients, applying both ^{1}H-NMR and LC-MS metabolomics, to study global changes in metabolic networks after thermal injury. The study has shown that there are early global metabolic profiles that distinguish patients who go to develop poor outcomes from those who have an uncomplicated recovery. Applying metabolomics analysis longitudinally after thermal injury, has identified major shifts in lipid metabolism, a 'lipid storm' paralleling changes in metabolites reflective of increased energy production, oxidative stress and inflammation.

6.2 Metabolomics as an approach to study the acute response to severe thermal injury

The application of ^{1}H-NMR metabolomics of serum samples taken within the first 96hrs of thermal injury highlighted significant changes in the metabolome during the first 24hrs after injury that were different to those seen 24-96hrs post injury. This may represent transitioning from the 'ebb' into 'flow' or 'plateau' phases first described by Cuthbertson in 1942 (146). During the first 24hrs, key changes in the metabolome reflected anaerobic metabolism (↑lactate), increased glucose availability and increased energy production through glycolysis (↑pyruvate) and increased mobilization of fat stores (↑glycerol), most likely to provide fatty acids for β-oxidation. This findings do perhaps validate the metabolomics data, since they agree with published studies demonstrating post-burn hyperglycaemia (173) and increased lipolysis (367). The acute relative decreases in the non-essential amino acids (NAA) alanine, glycine, proline and glutamine and the branched chain amino acid, valine are also consistent with previous studies (462,463). The explanation for these changes is net protein catabolism, despite increases in protein synthesis to skeletal muscle with increased flux towards the burn wound and liver, providing substrates for wound healing and gluconeogenesis and acute phase protein synthesis respectively (228).

One finding that disagrees with some studies of the metabolic response to injury is the relative increases in ketone bodies seen in the early samples taken in the first 24hrs post injury. Although ketogenesis is a normal response to starvation with aim of sparing muscle protein catabolism, many studies have found that the stress response to injury and infection does not induce a ketogenic response and skeletal muscle amino acids are mobilized. Many of these studies were performed in the 1970's and early 1980's prior to the introduction of early enteral feeding. Moreover,

more recent studies in traumatic injury have shown a gut-liver interaction, with initial ketogenesis in the gut, followed by gut ketolysis and liver ketogenesis at 24hrs post injury (326). Perhaps it is time for a further reappraisal of ketogenesis following thermal injury as it may contribute a useful source of energy early of injury in some tissues.

6.3 Metabolomics to predict later clinical outcomes

The metabolite profile during the first 24hrs after thermal injury was predictive of later mortality, demonstrating the relationship of the early metabolic response to later complications. Elevations were seen in previously studied metabolites such as glycerol, glucose, ketone bodies and lactate probably reflective of increased metabolic dysfunction in related to increased severity of injury in the non-survivor group (mean TBSA: 50%, non-survivors vs. 27.5%, survivors). Several potential interesting metabolites were weighted highly in this model that could warrant further investigation in targeted studies.

Kynurenine is a product of the tryptophan degradation pathway and has been recently investigated in non-burn trauma. These studies showed early elevations predicted later sepsis, whilst increased kynurenine:tryptophan ratios predicted later MOF and non-survival (354). In addition, elevations in critical ill patients of the toxic metabolite of kynurenine, quinolinic acid, was able to predict later development of sepsis with good discriminatory power (470). The biology behind these associations is unclear, but kynerenine and the enzyme that produces it from tryptophan, indoleamine 2,3-dioxygenase (IDO), has links to vascular endothelial dysfunction (352) and immunoregulatory functions (348). There are no studies examining

kynurenine metabolism in relation outcomes in thermally injured patients, but a study in children with large burns demonstrated increased tryptophan metabolism associated with an increase in urinary excretion of kynurenic acid and kynurenine (471). A number of recent metabolomics studies have also highlighted kynurenine as an important biomarker that is associated with sepsis related mortality in a non-human primate model (278) and in humans (282,308).

Two other metabolite of interest in the mortality prediction model are methylmalonate (MMA) and acetate which could potentially be metabolite signals of early gut dysfunction during the resuscitation phase. MMA is an endogenous metabolite in the valine degradation pathway but is also produced by enteric bacteria through metabolism of propionate and can be absorbed in the portal circulation (356). Acetate could be related to endogenous acetyl CoA metabolism in the liver due to acetyl CoA excess from fatty acid oxidation and can be oxidized by the peripheral tissues, particularly in the heart and brain. Alternatively, it could also be derived from enteric bacterial metabolism and studies an animal model of obesity and metabolic syndrome has found links between gut bacterial derived acetate and abnormalities in insulin secretion and sensitivity (364).

Metabolite profiles from serum samples taken 24-96hrs post-injury were able to predict the later development of sepsis and MOF in this cohort of thermally injured patients. It is not clear why the first 24hr serum samples were more predictive of mortality but the later samples during the flow phase were more predictive of these other outcomes. Interestingly the pattern of change in these two models demonstrated a higher proportion of metabolites that were relatively decreased in the poor outcome groups. Many of these relatively decreased metabolites were amino

acids, reflecting early skeletal muscle protein catabolism in the flow phase. This is not a surprising finding given that the sepsis and MOF groups of patients had significantly larger burns than their counterparts and burn size is a predictor of the extent of protein catabolism post-burn (234). Burn size (TBSA) is also an independent predictor of the degree of hypermetabolism as measured by resting energy expenditure (REE) (71).

Currently no other studies have attempted to use early metabolomic profiles to predict later clinical outcomes in human thermal injury. The approach has been used in predict survival following severe trauma (472) and critically ill patients on admission to the ICU (308). Cohen et al. studied 32 severely injured patients and performed whole blood extraction ^{1}H-NMR metabolomics from samples taken on admission and identified 7 metabolites that discriminated later survivors from non-survivors. These metabolites included glucose, lactate, glycerol, β-hydroxybutryrate as in this study, plus glutamate and triacylglycerides and monounsaturated fatty acids (472). Rogers et al. studied ICU admission plasma samples from 90 critically ill patients and 149 adults with pneumonia presented to the emergency department. Using GCMS and LCMS and Bayesian Network analysis they identified 31 plasma metabolites that were predictive of 28-day mortality in both cohorts of patients, which included amino acid metabolites, acyl carnitines, glycerophospholipids and bile acids (308). They highlight that one third of 187 metabolites differed between the outcome groups and thus metabolomics has the advantage of being able to simulataneously quantify metabolites across a range of classes to uncover novel biological information. Only one study has utilized metabolomics as an approach to try to predict later sepsis in trauma patients. In this small study, Blaise et al. used ^{1}H-NMR

to measure metabolite profiles in plasma samples taken from 22 severely injured patients on admission to ICU. Their multi-variate model included β-hydroxybutryrate, citrate, aspartate and allantoin and predicted later sepsis in this cohort with an AUC of 0.778 (275). The model statistics suggest significant overfitting, highlighting the important of cross-validation in metabolomics.

6.4 Metabolomic analysis of longitudinal changes in metabolism after thermal injury

Untargeted LC-MS metabolomics was applied to study global changes in metabolism after severe thermal injury in young adults. This novel approach revealed widespread changes in 35 classes of metabolites across the metabolome and profound alterations in circulating lipids and lipid metabolism, possibly reflecting a 'lipid storm' after severe thermal injury. There also appeared to be several common patterns across different classes of metabolites. Many, including fatty acids (FAs), glycerolipids, glycerophospholipids and sphingolipids demonstrated a reduction from injury levels down to a nadir at 3 weeks, before levels elevated again towards admission levels during the recovery phase. The majority of peptides showed an inverse pattern to this, peaking at 3-weeks post-injury. These temporal changes may represent the catabolic phase after major thermal injury which appeared to outlast the changes in nitrogen excretion observed which peaked at 10-days post-injury.

The significant shifts in lipid metabolites after severe thermal injury is an interesting finding and changes in FAs and glycerolipids are compatible with the known stress hormone mediated increases in peripheral adipose lipolysis to generate substrates for energy production via mitochondrial β-oxidation (169). The widespread changes

in FAs corroborates the recently published targeted metabolomics study by Jeschke et al. in which they demonstrate acute increases in all major classes of FAs, followed by decline. Importantly, they also highlight a metabolite signal of poor outcomes, with non-survivors demonstrating persistently elevated plasma FAs, particularly saturated FAs (SFA), monounsaturated FAs (MUFA) and ω-6 polyunsaturated FAs (ωPUFA) (393). Fatty acid metabolism is intrinsically linked with inflammation and depending upon the sub-type, some have beneficial roles in resolving inflammation and some are pro-inflammatory. SFA have been shown to induce inflammatory gene expression via toll-like receptor 4 (TLR4) signaling in vitro and PUFA have been demonstrated to be able block inflammatory responses induced by LPS (473). The ω-6 PUFAs such as arachidonic acid are also precursors for the pro-inflammatory eicosanoids and ω-3 PUFAs such as docosahexeanoic acid (DHA) and eicosapentaenoic acid (EPA) are precursors for the synthesis of docosanoids or specialized pro-resolving mediators (SPMs) such as the resolvins, protectins and maresins (409). These have not yet been extensively studied in thermal injury but several of these SPMs were identified in the LCMS analysis as increasing from admission and peaking at around 3-weeks post-injury. A recent genomic study in polytrauma patients demonstrated that patients with uncomplicated recoveries had higher expression of resolving genes and lower expression of leukotriene genes across the 28-days post-injury (474). Fatty acid and docosanoid metabolism in thermal injury certainly required further detailed investigation to examine the links between lipid profiles and clinical outcomes.

Another interesting observation from the LCMS data was the detection of probable bacterially derived metabolites that changed significantly, with early elevations that showed the same pattern observed with the pro-inflammatory cytokine levels in the cohort. The appearance of these metabolites in the blood of severly injured patients, such as the tryptophan metabolites, indole, indoxyl and 3-dehydroquinate and Heme O could represent potential early biomarkers of gut ischaemia and inflammation. Further study of these in a targeted study with indirect measures of gut perfusion and monitoring of poor gut dysfunction related outcomes such as enteral feeding intolerance is warranted.

A final group of metabolites of interest in the study were the sex steroid hormone metabolites. Most of these demonstrated a trend of decline from admission levels to a nadir at 2-3 weeks before increasing again, including a degradation metabolite of the androgen precursor dehydroepiandrosterone (DHEA). The sulfated form of DHEA, DHEAS has already been demonstrated to decrease for up to 4 weeks post burn injury (395). Recent studies from our own institution in a large cohort of severely injured military patients have shown serum DHEA and DHEAS levels were low after injury with the latter remaining low for 6- months post-injury (MA Foster, unpublished data). DHEAS has also been shown to be low in other systemic inflammatory disease states such as sepsis. Targeting DHEA/DHEAS pathway represents a potentially beneficial strategy in severe thermal injury since DHEAS has anabolic and immune enhancing properties. This includes the stimulates of neutrophil superoxide burst generation (396). In the SIFTI cohort, including some of the patients in this study, our group has shown neutrophil superoxide burst activity and phagocytic function is

reduced after thermal injury for 28 days and decreases were greater in patients who developed sepsis (405).

6.5 Thermal injury in the elderly and changes in metabolism

The elderly are an understudied group in the context of thermal injury. Many studies have highlighted that they experience poorer outcomes for a given burn size, but few studies have attempted to understand the pathophysiological mechanisms underlying this. A retrospective study at our centre highlights some improvements in outcomes in elderly burn injured patients over the last decade (453). We hypothesize this to be due general improvement in burn care, local infrastructure, use of burn care guidelines locally and increasing involvement of geriatric physicians. The study also highlights that burn mortality in this group remains high and one of the leading causes of death are infection related complications. We sought to use metabolomics as an approach to study metabolic changes in thermally injured elderly patients to see if new pathophysiological information could be acquired to generate new hypotheses. ^{1}-H NMR metabolomics analysis revealed similar increases in glucose, ketones and similar decreases in amino acids in serum samples taken during the first 96hrs post-injury. Relative decreases in multiple essential and non-essential amino acids suggests increased utilization as energy substrates and for wound related protein synthesis. Further studies are required if these metabolic signals reflect increased skeletal muscle catabolism which could impact recovery from even small burn injuries in aged individual who may already have age related sarcopenia. Altered glucose metabolism was also observed, consistent with findings in recent

studies that elderly patients have higher average daily glucose levels and higher insulin requirements than injured size matched younger counterparts (465).

A preliminary LC-MS metabolomics study of the longitudinal response to thermal injury in a relatively small cohort of elderly patients revealed less overall significant changes compared to the younger cohort. This was probably related to the relatively small sample size but reduced metabolic response to different injury severity may have been contributory. There were however many similar areas of metabolism changing after relatively small injuries in the elderly group including changes in glycerolipids, fatty acids, steroid hormones, bile acids and heme metabolites.

6.6 Strengths and limitations

The main strengths of this research are firstly the overarching SIFTI study. The study is unique in its combination of prospective detailed collection of clinical and outcomes data whilst collecting multiple biofluids for parallel analysis of immune, inflammatory, metabolic and endocrine indices. This type of research study has not been conducted in the UK or Europe before and is a large collaborative of many research groups. The study has utilized two different analytical techniques used in metabolomics which have allowed complementary coverage of the post thermal injury metabolome. Discovery based approaches have been used rather than targeted metabolomics allowing us to both confirm the findings of previous studies and find new avenues of research and testable hypotheses.

In the NMR study, the main limitations are that the metabolite concentrations were not calculated due to problems with batch process analysis using the Chenomx software. This may be related to subtle differences in sample pH, which was not problematic for the multi-variate analysis of spectral peaks since an alignment algorithm was used. Future studies should include pH standardization or the use of a pH 'indicator' metabolite such as imidazole. The next step for completion of this work, would the calculation of metabolite concentrations and univariate statistical analysis to assess if inter-group differences observed in multi-variate analysis still hold true. The number of controls used could be increased diversity among that group and ensure a representative healthy metabolome for comparison. Other limitations of the study include the relatively small sample sizes in the elderly study, accepting the difficulties in recruiting and following up this patient group. With completion of the SIFTI study recruitment, a larger cohort of elderly patients have been recruited, provided samples for future work.

6.7 Future studies

Further studies planned include further correlation of the data with markers inflammation and immune dysfunction collected in the SIFTI study, including neutrophil phagocytic and superoxide activity, mitochondrial DNA and sex hormone analysis including DHEA/DHEAS and cortisol. ^{1}H-NMR and LC-MS data has also been acquired from urine samples collected from the same cohort of patients, allowing cross-biofluid comparisons of the data. An attractive prospect is the identification of a novel sepsis biomarker or biomarker panel to try to diagnosis sepsis earlier and with greater accuracy. This has been a particular area of focus of

metabolomics studes in critical care and trauma and several studies have identified promising candidate biomarkers (277,279,281,282,308). The main challenge with sepsis biomarker studies has been obtaining a clear clinical definition of sepsis as a 'gold standard', hence many studies have focused on more severe groups such as those with septic shock. The clinical definition of sepsis has recently been redefined (475) so applying this in future studies may increase the chances of feeding the biomarker needle in the metabolome. A number of potential novel biomarkers have been identified in this study that warrant further targeted investigation including: 1) kynurenine metabolites and Neuromedin-N as potential immunomodulatory agents contributing to post-burn immune dysunction, 2) bacterial metabolites (Heme O, acetate, methylmalonate, indole metabolites, secondary bile acids) as markers of gut dysfunction and bacterial translocation.

In addition to biomarker discovery and generation of new biological information for hypothesis testing, metabolomics analysis has other potential used in the field of burn care research. The ^{1}H-NMR study of early serum samples demonstrates that there is any early systemic metabolic signal which related to later clinical outcomes. Early metabolic profiles could be used to potentially stratify patients into those highly likely to develop complicated outcomes and those not, so that those patients who need more aggressive or intensive treatment can be prioritized. This approach could open the door to personalized healthcare approaches with tailored rescuscitation, drug therapy and nutritional support personalized to ongoing monitoring of the metabolic response. Another exciting area is pharmacometabolomics, which is the use of biofluid metabolic profiles to predict beneficial and negative effects of drugs (476). One of the major difficulties in setting up clinical trials, particularly in the field of

critical care, is identification of target groups of patients that drugs will benefit. It has been advocated in the field of sepsis, that biomarker driven studies should be used to identify at risk individuals who are most likely to benefit from a new treatment (477,478). A follow-up study to SIFTI (SIFTI-2) has recently opened at the Birmingham Scar Free Foundation Burns Research Centre, specifically geared towards identification of early biomarkers of sepsis and any biomarkers identified from the present cohort could be validated in this second study.

References

1. Peck MD. Epidemiology of burns throughout the world. Part I: Distribution and risk factors. *Burns : journal of the International Society for Burn Injuries* 2011;37(7): 1087–1100.

2. Dunn KW, National Burn Care Review Committee. *National Burn Care Review 2001*. [Online] specialisedservices.nhs.uk. Available from: http://www.specialisedservices.nhs.uk/library/23/National_Burn_Care_Review_2001.pdf [Accessed: 7 March 2013]

3. Brewster CT, Coyle B, Varma S. Trends in hospital admissions for burns in England, 1991-2010: a descriptive population-based study. *Burns : journal of the International Society for Burn Injuries* 2013;39(8): 1526–1534.

4. Rivara FP. Developmental and behavioral issues in childhood injury prevention. *Journal of developmental and behavioral pediatrics* 1995;16(5): 362–370.

5. Brusselaers N, Monstrey S, Vogelaers D, Hoste E, Blot S. Severe burn injury in europe: a systematic review of the incidence, etiology, morbidity, and mortality. *Critical Care* 2010;14(5): R188.

6. Pham TN, Kramer CB, Wang J, Rivara FP, Heimbach DM, Gibran NS, et al. Epidemiology and Outcomes of Older Adults With Burn Injury: An Analysis of the National Burn Repository. *Journal of Burn Care & Research* 2009;30(1): 30–36.

7. US National Burn Repository Report 2012. 8th ed. 2012; 1–139.

8. Redlick F, Cooke A, Gomez M, Banfield J, Cartotto RC, Fish JS. A survey of risk factors for burns in the elderly and prevention strategies. *Journal of Burn Care & Rehabilitation* 2002;23(5): 351–6.

9. Sheridan RL, Tompkins RG. What's new in burns and metabolism. *Journal of the American College of Surgeons* 2004;198(2): 243–263.

10. Herndon DN. *Total Burn Care*. 4th ed. Saunders; 2012.

11. Wolf SE, Rose JK, Desai MH, Mileski JP, Barrow RE and Herndon DN Mortality determinants in massive pediatric burns. An analysis of 103 children with > or = 80% TBSA burns (> or = 70% full-thickness). *Annals of surgery* 1997;225(5): 554.

12. Klein MB, Goverman J, Hayden DL, Fagan SP, McDonald-Smith GP, Alexander AK, et al. Benchmarking outcomes in the critically injured burn patient. *Annals of surgery* 2014;259(5): 833–841.

13. J P Bull. A Study of Mortality in a Burns Unit: Standards for the Evaluation of

Alternative Methods of Treatment. *Annals of surgery* 1949;130(2): 160.

14. Jackson PC, Hardwicke J, Bamford A, Nightingale P, Wilson Y, Papini R, et al. Revised estimates of mortality from the birmingham burn centre, 2001-2010: a continuing analysis over 65 years. *Annals of surgery* 2014;259(5): 979–984.

15. Hussain A, Dunn KW. Predicting length of stay in thermal burns: A systematic review of prognostic factors. *Burns : journal of the International Society for Burn Injuries* 2013;39(7): 1331–1340.

16. Maan ZN, Frew Q, Din AH, Unluer Z, Smailes S, Philp B, et al. Burns ITU admissions: Length of stay in specific levels of care for adult and paediatric patients. *Burns : journal of the International Society for Burn Injuries*. [Online] 2014. Available from: doi:10.1016/j.burns.2014.07.026

17. Church D, Elsayed S, Reid O, Winston B, Lindsay R. Burn wound infections. *Clinical microbiology reviews*. 2006;19(2): 403–434.

18. Ziegler TR, Smith RJ, O'Dwyer ST, Demling RH, Wilmore DW. Increased intestinal permeability associated with infection in burn patients. *Archives of Surgery*. 1988;123(11): 1313–1319.

19. Klein MB, Goverman J, Hayden DL, Fagan SP, McDonald-Smith GP, Alexander AK, Gamelli RL, Gibran NS, Finnerty CC, Jeschke MG, Arnoldo B, Wispelwey B, Mindrinos, MN, Xiao W, Honari SE, Mason PH, Schoenfeld DA, Herndon DN, Tompkins RG. Benchmarking Outcomes in the Critically Injured Burn Patient. *Annals of surgery*. 2014;259(5): 833–841.

20. Mann EA, Baun MM, Meininger JC, Wade CE. Comparison of mortality associated with sepsis in the burn, trauma, and general intensive care unit patient: a systematic review of the literature. *Shock.* 2012;37(1): 4–16.

21. Williams FN, Herndon DN, Hawkins HK, Lee JO, Cox RA, Kulp GA, et al. The leading causes of death after burn injury in a single pediatric burn center. *Critical care.* 2009;13(6): R183.

22. Krishnan P, Frew Q, Green A, Martin R, Dziewulski P. Cause of death and correlation with autopsy findings in burns patients. *Burns : journal of the International Society for Burn Injuries*. 2013;39(4): 583–588.

23. The Surviving Sepsis Campaign Guidelines Committee including The Pediatric Subgroup*, Dellinger RP, Levy MM, Rhodes A, Annane D, Gerlach H, et al. Surviving Sepsis Campaign: International Guidelines for Management of Severe Sepsis and Septic Shock, 2012. *Intensive care medicine*. 2013;39(2): 165–228.

24. Hogan BK, Wolf SE, Hospenthal DR, D'Avignon LC, Chung KK, Yun HC, et al. Correlation of American Burn Association Sepsis Criteria With the Presence of Bacteremia in Burned Patients Admitted to the Intensive Care

Unit. *Journal of Burn Care & Research*. [Online] 2012;33(3): 371–378.

25. Mann-Salinas EA, Baun MM, Meininger JC, Murray CK, Aden JK, Wolf SE, et al. Novel predictors of sepsis outperform the American Burn Association sepsis criteria in the burn intensive care unit patient. *Journal of burn care & research.* 2013;34(1): 31–43.

26. Kumar A, Roberts D, Wood KE, Light B, Parrillo JE, Sharma S, et al. Duration of hypotension before initiation of effective antimicrobial therapy is the critical determinant of survival in human septic shock. *Critical Care Medicine*. 2006;34(6): 1589–1596.

27. Faist E, Baue AE, Dittmer H, Heberer G. Multiple organ failure in polytrauma patients. *The Journal of Trauma: Injury, Infection, and Critical Care*. 1983;23(9): 775–787.

28. Fukushima R, Alexander JW, Gianotti L, Pyles T, Ogle CK. Bacterial translocation-related mortality may be associated with neutrophil-mediated organ damage. *Shock.* 1995;3(5): 323–328.

29. Shoemaker WC, Appel PL, Kram HB. Tissue oxygen debt as a determinant of lethal and nonlethal postoperative organ failure. *Critical Care Medicine*. 1988;16(11): 1117–1120.

30. Moore FA, Sauaia A, Moore EE, Haenel JB, Burch JM, Lezotte DC. Postinjury Multiple Organ Failure: A Bimodal Phenomenon. *The Journal of Trauma and Acute Care Surgery*. 1996;40(4): 501.

31. Ciesla DJ, Moore EE, Johnson JL, Burch JM, Cothren CC, Sauaia A. A 12-year prospective study of postinjury multiple organ failure: has anything changed? *Archives of Surgery*. [Online] American Medical Association; 2005;140(5): 432–440. Available from: doi:10.1001/archsurg.140.5.432

32. Marshall JC, Cook DJ, Christou NV, Bernard GR, Sprung CL, Sibbald WJ. Multiple Organ Dysfunction Score: A reliable descriptor of a complex clinical outcome. *Critical Care Medicine*. 1995;23(10): 1638.

33. Sauaia A, Moore EE, Johnson JL, Ciesla DJ, Biffl WL, Banerjee A. Validation of post-injury multiple organ failure scores. *Shock.* 2009;31(5): 438–447.

34. Vincent JL, Moreno R, Takala J, Willatts S, Mendonça A, Bruining H, et al. The SOFA (Sepsis-related Organ Failure Assessment) score to describe organ dysfunction/failure. *Intensive care medicine*.1996;22(7): 707–710.

35. Evers LH, Bhavsar D, Mailänder P. The biology of burn injury. *Experimental Dermatology*. 2010;19(9): 777–783.

36. Jackson DM. The diagnosis of the depth of burning. *British Journal of Surgery*. 1953;40(164): 588–596.

37. Hettiaratchy S, Dziewulski P. ABC of burns: pathophysiology and types of burns. *BMJ: British Medical Journal*. 2004.

38. Jeschke MG, Chinkes DL, Finnerty CC, Kulp G, Suman OE, Norbury WB, et al. Pathophysiologic response to severe burn injury. *Annals of surgery*. 2008;248(3): 387–401.

39. Reiss E, Pearson E, Artz CP. The metabolic response to burns. *Journal of Clinical Investigation*. 1956;35(1): 62–77.

40. Yu YM, Tompkins RG, Ryan CM, Young VR. The metabolic basis of the increase of the increase in energy expenditure in severely burned patients. *JPEN. Journal of parenteral and enteral nutrition*. 1999;23(3): 160–168.

41. Hart DW, Wolf SE, Mlcak R, Chinkes DL, Ramzy PI, Obeng MK, et al. Persistence of muscle catabolism after severe burn. *Surgery*. [Online] 2000;128(2): 312–319. Available from: doi:10.1067/msy.2000.108059

42. Jeschke MG, Gauglitz GG, Kulp GA, Finnerty CC, Williams FN, Kraft R, et al. Long-Term Persistance of the Pathophysiologic Response to Severe Burn Injury. Androulakis IP (ed.) *PLoS ONE*. [Online] 2011;6(7): e21245. Available from: doi:10.1371/journal.pone.0021245.t001

43. Finnerty CC, Herndon DN, Przkora R, Pereira CT, Oliveira HM, Queiroz DMM, et al. Cytokine Expression Profile Over Time In Severely Burned Pediatric Patients. *Shock.* 2006;26(1): 13–19.

44. Bone RC, Balk RA, Cerra FB, Dellinger RP, Fein AM, Knaus WA, et al. Definitions for sepsis and organ failure and guidelines for the use of innovative therapies in sepsis. The ACCP/SCCM Consensus Conference Committee. American College of Chest Physicians/Society of Critical Care Medicine. *CHEST Journal*. 1992;101(6): 1644–1655.

45. Bone RC, Sibbald WJ. The ACCP-SCCM consensus conference on sepsis and organ failure. *CHEST Journal*. 1992.

46. Matzinger P. Tolerance, danger, and the extended family. *Annual review of immunology*. 1994;12: 991–1045.

47. Zhang Q, Raoof M, Chen Y, Sumi Y, Sursal T, Junger W, et al. Circulating mitochondrial DAMPs cause inflammatory responses to injury. *Nature*. 2010;464(7285): 104–107.

48. MacLean LD, Meakins JL, Taguchi K, Duignan JP, Dhillon KS, Gordon J. Host resistance in sepsis and trauma. *Annals of surgery*. 1975;182(3): 207–217.

49. Bone RC. Sir Isaac Newton, sepsis, SIRS, and CARS. *Critical Care Medicine*. 1996;24(7): 1125–1128.

50. Osuchowski MF, Craciun F, Weixelbaumer KM, Duffy ER, Remick DG. Sepsis chronically in MARS: systemic cytokine responses are always mixed regardless of the outcome, magnitude, or phase of sepsis. *Journal of immunology.* 2012;189(9): 4648–4656.

51. Xiao W, Mindrinos MN, Seok J, Cuschieri J, Cuenca AG, Gao H, et al. A genomic storm in critically injured humans. *The Journal of experimental medicine*. Rockefeller Univ Press; 2011;208(13): 2581–2590.

52. Gentile LF, Cuenca AG, Efron PA, Ang D, Bihorac A, McKinley BA, et al. Persistent inflammation and immunosuppression: a common syndrome and new horizon for surgical intensive care. *The Journal of Trauma and Acute Care Surgery*. 2012;72(6): 1491–1501.

53. Vanzant EL, López CM, Ozrazgat-Baslanti T, Ungaro R, Davis R, Cuenca AG, et al. Persistent inflammation, immunosuppression, and catabolism syndrome after severe blunt trauma. *The Journal of Trauma and Acute Care Surgery*. 2014;76(1): 21–30

54. Eremin O, Sewell H. *Essential Immunology for Surgeons*. Oxford University Press; 2011. 1 p.

55. Cannon JG, Friedberg JS, Gelfand JA, Tompkins RG, Burke JF, Dinarello CA. Circulating interleukin-1 beta and tumor necrosis factor-alpha concentrations after burn injury in humans. *Critical Care Medicine*. 1992;20(10): 1414–1419.

56. Drost AC, Burleson DG, Cioffi WG Jr, Jordan BS, Mason AD Jr, Pruitt BA Jr. Plasma cytokines following thermal injury and their relationship with patient mortality, burn size, and time postburn. *J Trauma*. 1993 Sep;35(3):335-9

57. Vindenes HA, Ulvestad E, Bjerknes R. Concentrations of cytokines in plasma of patients with large burns: their relation to time after injury, burn size, inflammatory variables, infection, and outcome. *The European journal of surgery = Acta chirurgica*. 1998;164(9): 647–656.

58. Teodorczyk-Injeyan JA, Sparkes BG, Lalani S, Peters WJ, Mills GB. IL-2 regulation of soluble IL-2 receptor levels following thermal injury. *Clinical & Experimental Immunology*. 2008;90(1): 36–42.

59. Schlüter B, König B, Bergmann U, Müller FE, König W. Interleukin 6--a potential mediator of lethal sepsis after major thermal trauma: evidence for increased IL-6 production by peripheral blood mononuclear cells. *The Journal of Trauma: Injury, Infection, and Critical Care*. 1991;31(12): 1663–1670.

60. Guo Y, Dickerson C, Chrest FJ, Adler WH, Munster AM, Winchurch RA. Increased levels of circulating interleukin 6 in burn patients. *Clin Immunol Immunopathol.*1990 Mar;54(3):361-71.

61. Ueyama M, Maruyama I, Osame M, Sawada Y. Marked increase in plasma

interleukin-6 in burn patients. *The Journal of laboratory and clinical medicine*. 1992;120(5): 693–698.

62. Vindenes H, Ulvestad E, Bjerknes R. Increased Levels of Circulating Interleukin-8 in Patients with Large Burns: Relation to Burn Size and Sepsis. *Journal of Trauma- Injury, Infection, and Critical Care*. 1995;39(4): 635.

63. Gosain A, Gamelli RL. A primer in cytokines. *Journal of Burn Care & Rehabilitation*. 2005;26(1): 7–12.

64. Martin C, Boisson C, Haccoun M, Thomachot L, Mege JL. Patterns of cytokine evolution (tumor necrosis factor-alpha and interleukin-6) after septic shock, hemorrhagic shock, and severe trauma. *Critical Care Medicine*. 1997;25(11): 1813–1819.

65. Marano MA, Fong Y, Moldawer LL, Wei H, Calvano SE, Tracey KJ, et al. Serum cachectin/tumor necrosis factor in critically ill patients with burns correlates with infection and mortality. *Surgery, gynecology & obstetrics*. 1990;170(1): 32–38.

66. Zhang B, Huang YH, Chen Y, Yang Y, Hao ZL, Xie SL. Plasma tumor necrosis factor-alpha, its soluble receptors and interleukin-1beta levels in critically burned patients. *Burns : journal of the International Society for Burn Injuries*. 1998;24(7): 599–603.

67. Dinarello CA. Overview of the interleukin-1 family of ligands and receptors. *Seminars in immunology*. 2013;25(6): 389–393.

68. Biffl WL, Moore EE, Moore FA, Peterson VM. Interleukin-6 in the injured patient. Marker of injury or mediator of inflammation? *Annals of surgery*. 1996.

69. Akira S, Taga T, Kishimoto T. Interleukin-6 in biology and medicine. *Advances in immunology*. 1993;54: 1–78.

70. Steinke JW, Borish L. 3. Cytokines and chemokines. *The Journal of allergy and clinical immunology*. 2006;117:S441–S445.

71. Jeschke MG, Mlcak RP, Finnerty CC, Norbury WB, Gauglitz GG, Kulp GA, et al. Burn size determines the inflammatory and hypermetabolic response. *Critical care.* 2007;11(4): R90.

72. Davis CS, Janus SE, Mosier MJ, Carter SR, Gibbs JT, Ramirez L, et al. Inhalation Injury Severity and Systemic Immune Perturbations in Burned Adults. *Annals of surgery*. 2012;257(6): 1137–1146.

73. Drost AC, Burleson DG, Cioffi WG Jr, Mason AD Jr, Pruitt BA Jr. Plasma cytokines after thermal injury and their relationship to infection. Ann Surg. 1993 Jul;218(1):74-8

74. Jeschke MG, Gauglitz GG, Finnerty CC, Kraft R, Mlcak RP, Herndon DN. Survivors Versus Nonsurvivors Postburn. *Annals of surgery*. 2014;259(4): 814–823.

75. Dehne MG, Sablotzki A, Hoffmann A, Mühling J, Dietrich FE, Hempelmann G. Alterations of acute phase reaction and cytokine production in patients following severe burn injury. *Burns : journal of the International Society for Burn Injuries*. 2002;28(6): 535–542.

76. Deshmane SL, Kremlev S, Amini S, Sawaya BE. Monocyte Chemoattractant Protein-1 (MCP-1): An Overview. *Journal of Interferon & Cytokine Research*. [Online] 2009;29(6): 313–326. Available from: doi:10.1089/jir.2008.0027

77. Moore KW, O'Garra A, de Waal Malefyt R, Vieira P, Mosmann TR. Interleukin-10. *Annu Rev Immunol.* 1993;11:165-90

78. Sherry RM, Cue JI, Goddard JK, Parramore JB, DiPiro JT. Interleukin-10 is associated with the development of sepsis in trauma patients. *The Journal of Trauma: Injury, Infection, and Critical Care*. 1996;40(4): 613–6–discussion616–7.

79. Csontos C, Foldi V, Pálinkas L, Bogar L, Röth E, Weber G, Lantos J. Timecourse of pro- and anti-inflammatory cytokine levels in patients with burns - prognostic value of interleukin-10. Burns. 2010 Jun;36(4):483-94.

80. Ozbalkan Z, Aslar AK, Yildiz Y, Aksaray S. Investigation of the course of proinflammatory and anti-inflammatory cytokines after burn sepsis. *International journal of clinical practice*. 2004;58(2): 125–129.

81. Endo S, Inada K, Yamada Y, Kasai T, Takakuwa T, Nakae H, et al. Plasma levels of interleukin-1 receptor antagonist (IL-1ra) and severity of illness in patients with burns. *Journal of medicine*. 1996;27(1-2): 57–71.

82. Finnerty CC, Jeschke MG, Herndon DN, Gamelli R, Gibran N, Klein M, et al. Temporal cytokine profiles in severely burned patients: a comparison of adults and children. *Molecular Medicine*. 2008;14(9-10): 553–560.

83. Schröder O, Laun RA, Held B, Ekkernkamp A, Schulte K-M. Association of interleukin-10 promoter polymorphism with the incidence of multiple organ dysfunction following major trauma: results of a prospective pilot study. *Shock.* 2004;21(4): 306–310.

84. Barber RC, Aragaki CC, Rivera-Chavez FA, Purdue GF, Hunt JL, Horton JW. TLR4 and TNF-alpha polymorphisms are associated with an increased risk for severe sepsis following burn injury. *Journal of Medical Genetics*. 2004;41(11): 808–813.

85. Lord JM, Midwinter MJ, Chen Y-F, Belli A, Brohi K, Kovacs EJ, et al. The systemic immune response to trauma: an overview of pathophysiology and treatment. *Lancet*. 2014;384(9952): 1455–1465.

86. Schaefer L. Complexity of danger: the diverse nature of damage-associated molecular patterns. *The Journal of biological chemistry*. 2014;289(51): 35237–35245.

87. Vénéreau E, Ceriotti C, Bianchi ME. DAMPs from Cell Death to New Life. *Front Immunol.* 2015 Aug 18;6:422

88. Scaffidi P, Mistell T, Bianchi ME. Release of chromatin protein HMGB1 by necrotic cells triggers inflammation. *Nature*. 2002.

89. Peltz ED, Moore EE, Eckels PC, Damle SS, Tsuruta Y, Johnson JL, et al. HMGB1 is markedly elevated within 6 hours of mechanical trauma in humans. *Shock.* 2009;32(1): 17–22.

90. Cohen MJ, Brohi K, Calfee CS, Rahn P, Chesebro BB, Christiaans SC, et al. Early release of high mobility group box nuclear protein 1 after severe trauma in humans: role of injury severity and tissue hypoperfusion. *Critical care*. 2009;13(6): R174.

91. Taanman JW. The mitochondrial genome: structure, transcription, translation and replication. *Biochimica et biophysica acta*. 1999;1410(2): 103–123.

92. Raoof M, Zhang Q, Itagaki K, Hauser CJ. Mitochondrial peptides are potent immune activators that activate human neutrophils via FPR-1. *Journal of Trauma*. 2010;68(6): 1328–32–discussion1332–4.

93. Schwacha MG, Rani M, Zhang Q, Nunez-Cantu O, Cap AP. Mitochondrial damage-associated molecular patterns activate γδ T-cells. *Innate immunity*. 2014;20(3): 261–268.

94. Dunn J, Kartchner L, Maile R, Cairns B. Mitochondrial damage-associated molecular patterns exacerbate acute lung injury following burn. *Journal of immunology.* 2015;194(1 Supplement): 132.19–132.19.

95. Maile R, Jones S, Pan Y, Zhou H, Jaspers I, Peden DB, et al. Association between early airway damage-associated molecular patterns and subsequent bacterial infection in patients with inhalational and burn injury. *American journal of physiology. Lung cellular and molecular physiology*. 2015;308(9): L855–L860.

96. Delves PJ, Martin SJ, Burton DR, Roitt IM. *Roitt's Essential Immunology*. John Wiley & Sons; 2011. 1 p.

97. Alexander JW, Ogle CK, Stinnett JD, MacMillan BG. A sequential, prospective analysis of immunologic abnormalities and infection following severe thermal injury. *Annals of surgery*; 1978;188(6): 809–816.

98. Ogle CK, Alexander JW, Nagy H, Wood S, Palkert D, Carey M, et al. A long-term study and correlation of lymphocyte and neutrophil function in the patient with burns. *Journal of Burn Care & Rehabilitation*. 1990;11(2): 105–111.

99. Glenn D Warden ADMJBAPJ. Evaluation of Leukocyte Chemotaxis In Vitro in Thermally Injured Patients. *Journal of Clinical Investigation*.1974;54(4): 1001–1004.

100. Butler KL, Ambravaneswaran V, Agrawal N. Burn injury reduces neutrophil directional migration speed in microfluidic devices. *PLoS ONE*. 2010.

101. Kurihara T, Jones CN, Yu YM, Fischman AJ, Watada S. Resolvin D2 restores neutrophil directionality and improves survival after burns. *The FASEB Journal*. 2013.

102. Jones CN, Moore M, Dimisko L, Alexander A, Ibrahim A, Hassell BA, et al. Spontaneous Neutrophil Migration Patterns during Sepsis after Major Burns. *PLoS ONE*. [Online] 2014;9(12): e114509. Available from: doi:10.1371/journal.pone.0114509

103. Epstein FH, Weiss SJ. Tissue Destruction by Neutrophils. *New England Journal of Medicine*. 989;320(6): 365–376.

104. Male D, Brostoff J, Roth D, Roitt I. *Immunology*. Elsevier Health Sciences; 2012. 1 p.

105. Ernerudh J, Bakteman K, Steinwall I, Sjöberg F. Long-term immunosuppression in burned patients assessed by in vitro neutrophil oxidative burst (Phagoburst®). *Burns : journal of the International Society for Burn Injuries*. 2007.

106. Sachse C, Wolterink G, Pallua N. Neutrophil intracellular pH and phagocytosis after thermal trauma. *Clinica Chimica Acta*. 2000;295(1-2): 13–26.

107. Vindenes H, Bjerknes R. Activation Of Polymorphonuclear Neutrophilic Granulocytes Following Burn Injury: Alteration Of Fc-Receptor And Complement-Receptor Expression And Of Opsonophagocytosis. *Journal of Trauma- Injury, Infection, and Critical Care*. 1994;36(2): 161.

108. Johansson J, Sjögren F, Bodelsson M, Sjöberg F. Dynamics of leukocyte receptors after severe burns: An exploratory study. *Burns : journal of the International Society for Burn Injuries*. 2011;37(2): 227–233.

109. Köller M, Clasbrummel B, Kollig E, Hahn MP, Muhr G. Major injury induces increased production of interleukin-10 in human granulocyte fractions. *Langenbeck's Archives of Surgery*. 1998;383(6): 460–465.

110. Volenec FJ, Wood GW, Mani MM, Robinson DW, Humphrey LJ. Mononuclear Cell Analysis of Peripheral Blood from Burn Patients. *Journal of Trauma-Injury, Infection, and Critical Care*. 1979;19(2): 86.

111. Peterson V, Hansbrough J, Buerk C, Rundus C, Wallner S, Smith H, et al. Regulation of Granulopoiesis following Severe Thermal Injury. *Journal of*

Trauma- Injury, Infection, and Critical Care. 1983;23(1): 19.

112. Silva KD, Gamelli RL, Shankar R. Bone marrow stem cell and progenitor response to injury. *Wound repair and regeneration : official publication of the Wound Healing Society [and] the European Tissue Repair Society*. [Online] Blackwell Science, Ltd; 2001;9(6): 495–500. Available from: doi:10.1046/j.1524-475x.2001.00495.x

113. Altman LC, Klebanoff SJ, Curreri PW. Abnormalities of monocyte chemotaxis following thermal injury. *The Journal of surgical research*. 1977;22(6): 616–620.

114. Lloyd RS, Levick PL. Blood monocyte dysfunction following thermal injury. *Burns : journal of the International Society for Burn Injuries*. 1977;3(4): 245–252.

115. Wang G-Q, Zhang Y, Wu H-Q, Zhang W-W, Zhang J, Wang G-Y, et al. Reduction of CD47 on monocytes correlates with MODS in burn patients. *Burns : journal of the International Society for Burn Injuries*. 2011;37(1): 94–98.

116. Venet F, Tissot S, Debard A-L, Faudot C, Crampé C, Pachot A, et al. Decreased monocyte human leukocyte antigen-DR expression after severe burn injury: Correlation with severity and secondary septic shock. *Critical Care Medicine*. 2007;35(8): 1910–1917.

117. Yang H-M, Yu Y, Chai J-K, Hu S, Sheng Z-Y, Yao Y-M. Low HLA-DR expression on CD14+ monocytes of burn victims with sepsis, and the effect of carbachol in vitro. *Burns : journal of the International Society for Burn Injuries*. 2008;34(8): 1158–1162.

118. Xiu F, Stanojcic M, Wang V, Qi P, Jeschke MG. C-C Chemokine Receptor Type 2 Expression on Monocytes Before Sepsis Onset Is Higher Than That of Postsepsis in Septic Burned Patients: A New Predictor for Sepsis in Burned Injury. *Annals of surgery*. [Online] 2015;: 1. Available from: doi:10.1097/SLA.0000000000001531

119. Xiu F, Jeschke MG. Perturbed mononuclear phagocyte system in severely burned and septic patients. *Shock.* 2013;40(2): 81–88.

120. Paterson HM, Murphy TJ, Purcell EJ, Shelley O, Kriynovich SJ, Lien E, et al. Injury primes the innate immune system for enhanced Toll-like receptor reactivity. *Journal of immunology*. 2003;171(3): 1473–1483.

121. Cairns BA, Barnes CM, Mlot S, Meyer AA, Maile R. Toll-like receptor 2 and 4 ligation results in complex altered cytokine profiles early and late after burn injury. J Trauma. 2008 Apr;64(4):1069-77

123. Loose LD, Turinsky J. Macrophage dysfunction after burn injury. *Infection and immunity*. American Society for Microbiology; 1979;26(1): 157–162.

124. D'Arpa N, Accardo Palumbo A, Amato G, D'Amelio L, Pileri D, Cataldo V, et al. Circulating dendritic cells following burn. *Burns : journal of the International Society for Burn Injuries*. 2009;35(4): 513–518.

125. Williams KN, Szilagyi A, He L-K, Conrad P, Halerz M, Gamelli RL, et al. Dendritic cell depletion in burn patients is regulated by MafB expression. *Journal of burn care & research.* 2012;33(6): 747–758.

126. van den Berg LM, de Jong MAWP, Witte L de, Ulrich MMW, Geijtenbeek TBH. Burn injury suppresses human dermal dendritic cell and Langerhans cell function. *Cellular immunology*. 2011;268(1): 29–36.

127. Hiebert JM, McGough M, Rodeheaver G, Tobiasen J, Edgerton MT, Edlich RF. The influence of catabolism on immunocompetence in burned patients. *Surgery*. 1979;86(2): 242–247.

128. Carol L Miller CCB. Changes in Lymphocyte Activity after Thermal Injury: The Role Of Suppressor Cells. *Journal of Clinical Investigation*. 1979;63(2): 202–210.

129. Hultman C, Cairns B, Deserres S, Frelinger J, Meyer A. Early, complete burn wound excision partially restores cytotoxic T lymphocyte function. *Surgery*. 1995;118(2): 421–430.

130. Sjöberg T, Mzezewa S, Jönsson K, Salemark L. Immune response in burn patients in relation to HIV infection and sepsis. Burns. 2004 Nov;30(7):670-4.

131. Teodorczyk-Injeyan JA, Cembrzynska-Nowak M, Lalani S, Peters WJ, Mills GB. Immune deficiency following thermal trauma is associated with apoptotic cell death. *Journal of clinical immunology*. 1995;15(6): 318–328.

132. O'Sullivan ST, Lederer JA, Horgan AF, Chin DH, Mannick JA, Rodrick ML. Major injury leads to predominance of the T helper-2 lymphocyte phenotype and diminished interleukin-12 production associated with decreased resistance to infection. *Annals of surgery*. 1995;222(4): 482–92.

133. Ni Choileain N, MacConmara M, Zang Y, Murphy TJ, Mannick JA, Lederer JA. Enhanced regulatory T cell activity is an element of the host response to injury. *Journal of immunology*. 2006;176(1): 225–236.

134. Schlüter B, König W, Köller M, Erbs G, Müller FE. Differential regulation of T- and B-lymphocyte activation in severely burned patients. *The Journal of Trauma: Injury, Infection, and Critical Care*. 1991;31(2): 239–246.

135. Molloy RG, Nestor M, Collins KH, Holzheimer RG, Mannick JA, Rodrick ML. The humoral immune response after thermal injury: an experimental model. *Surgery*. 1994;115(3): 341–348.

136. Ishikawa K, Nishimura T, deSerres S, Meyer AA. The effects of transforming growth factor-beta neutralization on postburn humoral immunity. *The Journal*

of Trauma: Injury, Infection, and Critical Care. 2004;57(3): 529–536.

137. Barillo DJ, Goode R. Fire fatality study: demographics of fire victims. *Burns : journal of the International Society for Burn Injuries*. 1996;22(2): 85–88.

138. Pham TN, Kramer CB, Klein MB. Risk factors for the development of pneumonia in older adults with burn injury. *Journal of burn care & research.* 2010;31(1): 105–110.

139. Lundgren RS, Kramer CB, Rivara FP, Wang J, Heimbach DM, Gibran NS, et al. Influence of comorbidities and age on outcome following burn injury in older adults. *Journal of Burn Care & Research*. 2009;30(2): 307–314.

140. Masud D, Norton S, Smailes S, Shelley O, Philp B, Dziewulski P. The use of a frailty scoring system for burns in the elderly. *Burns : journal of the International Society for Burn Injuries*. 2013;39(1): 30–36.

141. Albornoz CR, Villegas J, Sylvester M, Peña V, Bravo I. Burns are more aggressive in the elderly: proportion of deep burn area/total burn area might have a role in mortality. *Burns : journal of the International Society for Burn Injuries*. 2011;37(6): 1058–1061.

142. Rani MM, Schwacha MGM. Aging and the pathogenic response to burn. *Aging and disease*. 2012;3(2): 171–180.

143. Hazeldine J, Lord JM. Innate immunesenescence: underlying mechanisms and clinical relevance. *Biogerontology*. 2014;16(2): 187–201.

144. Kovacs EJ, Grabowski KA, Duffner LA, Plackett TP, Gregory MS. Survival and cell mediated immunity after burn injury in aged mice. *Journal of the American Aging Association*. 2002;25(1): 3–9.

145. Kovacs EJ, Duffner LA, Plackett TP. Immunosuppression after injury in aged mice is associated with a TH1-TH2 shift, which can be restored by estrogen treatment. Mech Ageing Dev. 2004 Feb;125(2):121-3.

146. Cuthbertson DP. Post-shock metabolic response. *The Lancet*. Elsevier; 1942;239(6189): 433–437.

147. Wachtel TL, McCahan GR Jr., Monafo WW Jr. Fluid resuscitation in a porcine burn shock model. *Journal of Surgical Research*. 1977;23(6): 405–414.

148. Wolfe RR, Miller HI. Cardiovascular and metabolic responses during burn shock in the guinea pig. *The American journal of physiology*. 1976;231(3): 892–897.

149. Ferguson JL, Merrill GF, Miller HI, Spitzer JJ. Regional blood flow redistribution during early burn shock in the guinea pig. *Circulatory shock*. 1977;4(4): 317–326.

150. Ganrot K, Jacobsson S, Rothman U. Transcapillary Passage of Plasma Proteins in Experimental Burns. *Acta Physiologica Scandinavica*. 1974;91(4): 497–501.

151. Warden GD. Burn shock resuscitation. *World journal of surgery*. 1992;16(1): 16–23.

152. Wolfe RR, Miller HI. Burn shock in untreated and saline-resuscitated guinea pigs. Development of a model. *The Journal of surgical research*. 1976;21(4): 269–276.

153. Farkas LG, McCain WG, Birch JR, James J. The effects of four different chamber climates on oxygen consumption and healing of severely burned rats. *The Journal of Trauma: Injury, Infection, and Critical Care*. 1973;13(10): 911–916.

154. Wolfe RR. Review: acute versus chronic response to burn injury. *Circulatory shock*. 1981;8(1): 105–115.

155. Wilmore DW, Aulick LH. Metabolic changes in burned patients. *Surgical Clinics of NA*. 1978;58(6): 1173–1187.

156. Jeschke MG, Norbury WB, Finnerty CC, Mlcak RP, Kulp GA, Branski LK, et al. Age differences in inflammatory and hypermetabolic postburn responses. *Pediatrics*. 2008;121(3): 497–507.

157. Kraft R, Kulp GA, Herndon DN, Emdad F, Williams FN, Hawkins HK, et al. Is there a difference in clinical outcomes, inflammation, and hypermetabolism between scald and flame burn? *Pediatric Critical Care Medicine*. 2011;12(6): e275–e281.

158. Przkora R, Fram RY, Herndon DN, Suman OE, Mlcak RP. Influence of inhalation injury on energy expenditure in severely burned children. *Burns : journal of the International Society for Burn Injuries*. 2014;40(8): 1487–1491.

159. Norbury WB, Jeschke MG, Herndon DN. Metabolic changes following major burn injury: how to improve outcome. In: Vincent, JL (eds) *Yearbook of Intensive Care and Emergency Medicine,* vol 2006. Springer, Berlin, Heidelberg.

160. Garden OJ, Bradbury AW, Forsythe JLR, Parks RW. *Principles and Practice of Surgery*. Elsevier Health Sciences; 2012.

161. Baynes J, Dominiczak MH. *Medical Biochemistry*. Elsevier Health Sciences; 2014.

162. Goodall M, Stone C, Haynes BW. Urinary output of adrenaline and noradrenaline in severe thermal burns. *Annals of surgery*. 1957;145(4): 479–487.

163. Wilmore DW, Long JM, Mason AD, Skreen RW, Pruitt BA. Catecholamines: mediator of the hypermetabolic response to thermal injury. *Annals of surgery*. 1974;180(4): 653–669.

164. Wolfe RR, Durkot MJ. Evaluation of the role of the sympathetic nervous system in the response of substrate kinetics and oxidation to burn injury. *Circulatory shock*. 1982;9(4): 395–406.

165. Breitenstein E, Chioléro RL, Jéquier E, Dayer P, Krupp S, Schutz Y. Effects of beta-blockade on energy metabolism following burns. *Burns : journal of the International Society for Burn Injuries*. 1990;16(4): 259–264.

166. Arturson G. Metabolic changes and nutrition in children with severe burns. *Progress in pediatric surgery*. 1981;14: 81–109.

167. RR W, MJ D, MH W. Effect of thermal injury on energy metabolism, substrate kinetics, and hormonal concentrations. *Circulatory shock*. 1982;9(4): 383–394.

168. Wolfe RR, Herndon DN, Peters EJ, Jahoor F, Desai MH, Holland OB. Regulation of lipolysis in severely burned children. *Annals of surgery*. 1987;206(2): 214–221.

169. Herndon DN, Nguyen TT, Wolfe RR. Lipolysis in burned patients is stimulated by the β2-receptor for catecholamines. *Archives of Surgery*. 1994;129(12): 1301.

170. Tang Y, Shankar R, Gamboa M, Desai S, Gamelli RL, Jones SB. Norepinephrine modulates myelopoiesis after experimental thermal injury with sepsis. *Annals of surgery*. 2001;233(2): 266–275.

171. Cohen MJ, Shankar R, Stevenson J, Fernandez R, Gamelli RL, Jones SB. Bone marrow norepinephrine mediates development of functionally different macrophages after thermal injury and sepsis. *Annals of surgery*. 2004;240(1): 132–141.

172. Ben-Menachem E, Cooper DJ. Hormonal and metabolic response to trauma. *Anaesthesia & Intensive Care Medicine*. 2011;12(9): 409–411.

173. Wolfe RR, Durkot MJ, Allsop JR, Burke JF. Glucose metabolism in severely burned patients. *Metabolism: clinical and experimental*. 1979;28(10): 1031–1039.

174. Batstone GF, Alberti K, Hinks L, Smythe P, Laing JE. Metabolic studies in subjects following thermal injury, Intermediary metabolites, hormones and tissue oxygenation. *Burns : journal of the International Society for Burn Injuries*. 1976; 2(4)207-225

175. Khani S, Tayek JA. Cortisol increases gluconeogenesis in humans: its role in the metabolic syndrome. 2001;101(6): 739–747.

176. Shuck JM, Eaton P, Shuck LW, Wachtel TL, Schade DS. Dynamics of insulin and glucagon secretions in severely burned patients. *The Journal of Trauma: Injury, Infection, and Critical Care*. 1977;17(9): 706–713.

177. Marco J, Calle C, Román D, Díaz-Fierros M, Villanueva ML, Valverde I. Hyperglucagonism induced by glucocorticoid treatment in man. *New England Journal of Medicine*. 1973;288(3): 128–131.

178. Cunningham JJ, Hegarty MT, Meara PA, Burke JF. Measured and predicted calorie requirements of adults during recovery from severe burn trauma. *The American journal of clinical nutrition*. 1989;49(3): 404–408.

179. Khorram-Sefat R, Behrendt W, Heiden A, Hettich R. Long-term measurements of energy expenditure in severe burn injury. *World journal of surgery*. 1999;23(2): 115–122.

180. Soroff HS, Pearson, E, Artz CP. An estimation of nitrogen requirements for equilibrium in burned patients. *Surgery, Gynaecology and Obstetrics*. 1961; 112;159-172

181. Darmaun D, Matthews DE, Bier DM. Physiological hypercortisolemia increases proteolysis, glutamine, and alanine production. *The American journal of physiology*. 1988;255(3 Pt 1): E366–E373.

182. Kayali AG, Young VR, Goodman MN. Sensitivity of myofibrillar proteins to glucocorticoid-induced muscle proteolysis. *The American journal of physiology*. 1987;252(5 Pt 1): E621–E626.

183. May RC, Kelly RA, Mitch WE. Metabolic acidosis stimulates protein degradation in rat muscle by a glucocorticoid-dependent mechanism. *Journal of Clinical Investigation*. 1986;77(2): 614–621.

184. Batstone GF, Levick PL, Spurr E, Shakespeare PG, George SL, Ward CM. Changes in acute phase reactants and disturbances in metabolism after burn injury. *Burns, including thermal injury*. 1983;9(4): 234–239.

185. Peckett AJ, Wright DC, Riddell MC. The effects of glucocorticoids on adipose tissue lipid metabolism. *Metabolism: clinical and experimental*. 2011;60(11): 1500–1510.

186. Weinstein RS, Jilka RL, Parfitt AM, Manolagas SC. Inhibition of osteoblastogenesis and promotion of apoptosis of osteoblasts and osteocytes by glucocorticoids. Potential mechanisms of their deleterious effects on bone. *Journal of Clinical Investigation*. 1998;102(2): 274–282.

187. Calvano SE, Albert JD, Legaspi A, Organ BC, Tracey KJ, Lowry SF, et al. Comparison of numerical and phenotypic leukocyte changes during constant hydrocortisone infusion in normal humans with those in thermally injured patients. *Surgery, gynecology & obstetrics*. 1987;164(6): 509–520.

188. Mandell GL, Rubin W, Hook EW. The effect of an NADH oxidase inhibitor (hydrocortisone) on polymorphonuclear leukocyte bactericidal activity. *Journal of Clinical Investigation*. 1970;49(7): 1381–1388.

189. Rinehart JJ, Balcerzak SP, Sagone AL, LoBuglio AF. Effects of corticosteroids on human monocyte function. *Journal of Clinical Investigation*. [Online] American Society for Clinical Investigation; 1974;54(6): 1337–1343.

190. Butcher SK, Killampalli V, Lascelles D, Wang K, Alpar EK, Lord JM. Raised cortisol:DHEAS ratios in the elderly after injury: potential impact upon neutrophil function and immunity. *Aging Cell*. 2005;4(6): 319–324.

191. Dickerson RN, Gervasio JM, Riley ML, Murrell JE, Hickerson WL, Kudsk KA, et al. Accuracy of predictive methods to estimate resting energy expenditure of thermally-injured patients. *JPEN. Journal of parenteral and enteral nutrition*. 2002;26(1): 17–29.

192. Herndon DN, Tompkins RG. Support of the metabolic response to burn injury. *Lancet*. 2004;363(9424): 1895–1902.

193. Yu Y-M, Tompkins RG, Ryan CM, Young VR. The Metabolic Basis of the Increase in Energy Expenditure in Severely Burned Patients. *JPEN. Journal of parenteral and enteral nutrition*. 1999;23(3): 160–168.

194. Wolfe RR, Herndon DN, Jahoor F, Miyoshi H, Wolfe M. Effect of Severe Burn Injury on Substrate Cycling by Glucose and Fatty Acids. *New England Journal of Medicine*. 1987;317(7): 403–408.

195. Porter C, Herndon DN, Borsheim E, Chao T, Reidy PT, Borack MS, et al. Uncoupled skeletal muscle mitochondria contribute to hypermetabolism in severely burned adults. *AJP: Endocrinology and Metabolism*. 2014;307(5): E462–E467.

196. Gore DC, Chinkes D, Heggers J. Association of hyperglycemia with increased mortality after severe burn injury. *Journal of Trauma*. 2001.

197. Holm C, Hörbrand F, Mayr M, Donnersmarck von GH, Mühlbauer W. Acute hyperglycaemia following thermal injury: friend or foe? *Resuscitation*. 2004;60(1): 71–77.

198. Mowlavi A, Andrews K, Milner S, Herndon DN, Heggers JP. The effects of hyperglycemia on skin graft survival in the burn patient. *Annals of Plastic Surgery*. 2000;45(6): 629–632.

199. Demling RH, Seigne P. Metabolic management of patients with severe burns. *World journal of surgery*. 2000;24(6): 673–680.

200. Wolfe RR. Herman Award Lecture, 1996: relation of metabolic studies to clinical nutrition--the example of burn injury. *Am J Clin Nutr.* 1996 Nov;64(5):800-8

201. Wilmore DW, Aulick LH, Mason AD, Pruitt BA. Influence of the burn wound on local and systemic responses to injury. *Annals of surgery*. 1977;186(4): 444–458.

202. Cree MG, Fram RY, Herndon DN, Qian T, Angel C, Green JM, et al. Human mitochondrial oxidative capacity is acutely impaired after burn trauma. *American journal of surgery*. 2008;196(2): 234–239.

203. Gauglitz GG, Herndon DN, Kulp GA, Meyer WJ, Jeschke MG. Abnormal insulin sensitivity persists up to three years in pediatric patients post-burn. *The Journal of clinical endocrinology and metabolism*. 2009;94(5): 1656–1664.

204. Mulder AH, Tack CJ, Olthaar AJ, Smits P, Sweep FCGJ, Bosch RR. Adrenergic receptor stimulation attenuates insulin-stimulated glucose uptake in 3T3-L1 adipocytes by inhibiting GLUT4 translocation. *AJP: Endocrinology and Metabolism*. 2005;289(4): E627–E633.

205. Hunt DG, Ivy JL. Epinephrine inhibits insulin-stimulated muscle glucose transport. *Journal of applied physiology*. 2002;93(5): 1638–1643.

206. Cree MG, Zwetsloot JJ, Herndon DN, Qian T, Morio B, Fram R, et al. Insulin Sensitivity and Mitochondrial Function Are Improved in Children With Burn Injury During a Randomized Controlled Trial of Fenofibrate. *Annals of surgery*. 2007;245(2): 214–221.

207. Cree MG, Aarsland A, Herndon DN, Wolfe RR. Role of fat metabolism in burn trauma-induced skeletal muscle insulin resistance. *Critical Care Medicine*. 2007;35(9 Suppl): S476–S483.

208. Fan J, Li YH, Wojnar MM, Lang CH. Endotoxin-induced alterations in insulin-stimulated phosphorylation of insulin receptor, IRS-1, and MAP kinase in skeletal muscle. *Shock.* 1996;6(3): 164–170.

209. del Aguila LF, Claffey KP, Kirwan JP. TNF-alpha impairs insulin signaling and insulin stimulation of glucose uptake in C2C12 muscle cells. *The American journal of physiology*. 1999;276(5 Pt 1): E849–E855.

210. Sell H, Dietze-Schroeder D, Kaiser U, Eckel J. Monocyte chemotactic protein-1 is a potential player in the negative cross-talk between adipose tissue and skeletal muscle. *Endocrinology*. 2006;147(5): 2458–2467.

211. Cree MG, Wolfe RR. Postburn trauma insulin resistance and fat metabolism. *AJP: Endocrinology and Metabolism*. 2007;294(1): E1–E9.

212. Morio B, Irtun O, Herndon DN, Wolfe RR. Propranolol decreases splanchnic triacylglycerol storage in burn patients receiving a high-carbohydrate diet. *Annals of surgery*. 2002;236(2): 218–225.

213. Cree MG, Newcomer BR, Katsanos CS, Sheffield-Moore M, Chinkes D,

Aarsland A, et al. Intramuscular and liver triglycerides are increased in the elderly. *Journal of Clinical Endocrinology & Metabolism*. 2004;89(8): 3864–3871.

214. Barrow RE, Hawkins HK, Aarsland A, Cox R, Rosenblatt J, Barrow LN, et al. Identification of factors contributing to hepatomegaly in severely burned children. *Shock.* 2005;24(6): 523–528.

215. Cree MG, Newcomer BR, Herndon DN, Qian T, Sun D, Morio B, et al. PPAR-alpha agonism improves whole body and muscle mitochondrial fat oxidation, but does not alter intracellular fat concentrations in burn trauma children in a randomized controlled trial. *Nutrition & metabolism*. 2007;4(1): 9.

216. Barret JP, Jeschke MG, Herndon DN. Fatty infiltration of the liver in severely burned pediatric patients: autopsy findings and clinical implications. *The Journal of Trauma: Injury, Infection, and Critical Care*. 2001;51(4): 736–739.

217. Jeschke MG, Micak RP, Finnerty CC, Herndon DN. Changes in liver function and size after a severe thermal injury. Shock. 2007 Aug;28(2):172-7

218. Mittendorfer B, Jeschke MG, Wolf SE, Sidossis LS. Nutritional hepatic steatosis and mortality after burn injury in rats. *Clinical nutrition (Edinburgh, Scotland)*. 1998;17(6): 293–299.

219. Kraft R, Herndon DN, Finnerty CC, Hiyama Y, Jeschke MG. Association of postburn fatty acids and triglycerides with clinical outcome in severely burned children. *The Journal of clinical endocrinology and metabolism*. 2013;98(1): 314–321.

220. Cree MG, Zwetsloot JJ, Herndon DN, Newcomer BR, Fram RY, Angel C, et al. Insulin sensitivity is related to fat oxidation and protein kinase C activity in children with acute burn injury. *Journal of burn care & research.* 2008;29(4): 585–594.

221. Cree MG, Fram RY, Herndon DN, Qian T, Angel CA, Green JM, et al. Human mitochondrial oxidative capacity is acutely impaired following burn trauma. *The FASEB Journal*. FASEB; 2007;21(6): A839.

222. Krssak M, Petersen KF, Dresner A, DiPietro L, Vogel SM, Rothman DL, et al. Intramyocellular lipid concentrations are correlated with insulin sensitivity in humans: a 1H NMR spectroscopy study. *Diabetologia*. 1999;42(1): 113–116.

223. Virkamäki A, Korsheninnikova E, Seppälä-Lindroos A, Vehkavaara S, Goto T, Halavaara J, et al. Intramyocellular lipid is associated with resistance to in vivo insulin actions on glucose uptake, antilipolysis, and early insulin signaling pathways in human skeletal muscle. *Diabetes*. 2001;50(10): 2337–2343.

224. Perseghin G, Scifo P, De Cobelli F, Pagliato E, Battezzati A, Arcelloni C, et al. Intramyocellular triglyceride content is a determinant of in vivo insulin resistance in humans: a 1H-13C nuclear magnetic resonance spectroscopy

assessment in offspring of type 2 diabetic parents. *Diabetes*. 1999;48(8): 1600–1606.

225. Astrakas LG. Proton NMR spectroscopy shows lipids accumulate in skeletal muscle in response to burn trauma-induced apoptosis. *The FASEB Journal*. 2005;19(11): 1431–1440.

226. Muoio DM. Revisiting the connection between intramyocellular lipids and insulin resistance: a long and winding road. *Diabetologia*. 2012;55(10): 2551–2554.

227. Demling RH. Nutrition, anabolism, and the wound healing process: an overview. *Eplasty*. 2009;9: e9.

228. Porter C, Hurren NM, Herndon DN, Borsheim E. Whole body and skeletal muscle protein turnover in recovery from burns. *International Journal of Burns and Trauma*. 2013;3(1): 9–17.

229. Berg JM, Tymoczko JL, Stryer L. *Biochemistry*. W. H. Freeman; 2010.

230. Chang DW, DeSanti L, Demling RH. Anticatabolic And Anabolic Strategies In Critical Illness: A Review Of Current Treatment Modalities. *Shock.* 1998;10(3): 155.

231. Pereira C, Murphy K, Jeschke M, Herndon DN. Post burn muscle wasting and the effects of treatments. *The International Journal of Biochemistry & Cell Biology*. 2005;37(10): 1948–1961.

232. Rutan RL, Herndon DN. Growth delay in postburn pediatric patients. *Archives of Surgery*. 1990;125(3): 392–395.

233. Pereira CT, Barrow RE, Sterns AM, Hawkins HK, Kimbrough CW, Jeschke MG, et al. Age-dependent differences in survival after severe burns: a unicentric review of 1,674 patients and 179 autopsies over 15 years. *Journal of the American College of Surgeons*. 2006;202(3): 536–548.

234. Hart DW, Wolf SE, Chinkes DL, Gore DC, Mlcak RP, Beauford RB, et al. Determinants of skeletal muscle catabolism after severe burn. *Annals of surgery*. 2000;232(4): 455–465.

235. Biolo G, Fleming RYD, Maggi SP, Nguyen TT, Herndon DN, Wolfe RR. Inverse regulation of protein turnover and amino acid transport in skeletal muscle of hypercatabolic patients. *Journal of Clinical Endocrinology & Metabolism*. 2002;87(7): 3378–3384.

236. Gore DC, Chinkes DL, Wolf SE, Sanford AP, Herndon DN, Wolfe RR. Quantification of protein metabolism in vivo for skin, wound, and muscle in severe burn patients. *JPEN. Journal of parenteral and enteral nutrition*. 2006;30(4): 331–338.

237. Wolfe RR, Jahoor F, Herndon DN, Miyoshi H. Isotopic evaluation of the metabolism of pyruvate and related substrates in normal adult volunteers and severely burned children: effect of dichloroacetate and glucose infusion. *Surgery*. 1991;110(1): 54–67.

238. D'Asta F, Cianferotti L, Bhandari S, Sprini D, Rini GB, Brandi ML. The endocrine response to severe burn trauma. *Expert Review of Endocrinology & Metabolism*. 2014;9(1): 45–59.

239. Herndon DN, Hart DW, Wolf SE, Chinkes DL, Wolfe RR. Reversal of Catabolism by Beta-Blockade after Severe Burns. *New England Journal of Medicine*. 2001;345(17): 1223–1229.

240. Herndon DN, Rodriguez NA, Diaz EC, Hegde S, Jennings K, Mlcak RP, et al. Long-term propranolol use in severely burned pediatric patients: a randomized controlled study. *Annals of surgery*. 2012;256(3): 402–411.

241. Ali A, Herndon DN, Mamachen A, Hasan S, Andersen CR, Grogans R-J, et al. Propranolol attenuates hemorrhage and accelerates wound healing in severely burned adults. *Critical care.* 2015;19(1): 217.

242. Demling RH, DeSanti L. Oxandrolone, an anabolic steroid, significantly increases the rate of weight gain in the recovery phase after major burns. *The Journal of Trauma: Injury, Infection, and Critical Care*. 1997;43(1): 47–51.

243. Demling RH. Oxandrolone, an anabolic steroid, enhances the healing of a cutaneous wound in the rat. *Wound Repair and Regeneration*. 2000; 8(2):97-102

244. Porro LJ, Herndon DN, Rodriguez NA, Jennings K, Klein GL, Mlcak RP, et al. Five-Year Outcomes after Oxandrolone Administration in Severely Burned Children: A Randomized Clinical Trial of Safety and Efficacy. *ACS*. 2012;214(4): 489–502.

245. Sakurai Y, Aarsland A, Herndon DN, Chinkes DL, Pierre E, Nguyen TT, Patterson BW, Wolfe RR. Stimulation of muscle protein synthesis by long-term insulin infusion in severely burned patients. *Annals of Surgery.* 1995 Sep;222(3):283-94; 294-7

246. Gilpin DA, Barrow RE, Rutan RL, Broemeling L, Herndon DN. Recombinant human growth hormone accelerates wound healing in children with large cutaneous burns. *Annals of surgery*. 1994;220(1): 19–24.

247. Hart DW, Herndon DN, Klein G, Lee SB, Celis M, Mohan S, Chinkes DL, Wolf SE. Attenuation of posttraumatic muscle catabolism and osteopenia by long term growth hormone therapy. Ann Surg. 2001 Jun;233(6):827-34

248. Cioffi WG, Gore DC, Rue LW 3rd, Carrougher G, Guler HP, McManus WF, Pruitt BA Jr. Insulin-like growth factor-1 lowers protein oxidation in patients with thermal injury. Ann Surg. 1994 Sep;220(3):310-6

249. Herndon DN, Ramzy PI, DebRoy MA, Zheng M, Ferrando AA, Chinkes DL, et al. Muscle protein catabolism after severe burn: effects of IGF-1/IGFBP-3 treatment. *Annals of surgery*. 1999;229(5): 713–722.

250. Cree MG, Zwetsloot JJ, Herndon DN, Qian T, Morio B, Fram R, et al. Insulin sensitivity and mitochondrial function are improved in children with burn injury during a randomized controlled trial of fenofibrate. *Annals of surgery*. 2007;245(2): 214–221.

251. Jeschke MG, Williams FN, Finnerty CC, Rodriguez NA, Kulp GA, Ferrando A, et al. The effect of ketoconazole on post-burn inflammation, hypermetabolism and clinical outcomes. *PLoS ONE*. 2012;7(5): e35465.

252. Dunn WB, Broadhurst DI, Atherton HJ, Goodacre R, Griffin JL. Systems level studies of mammalian metabolomes: the roles of mass spectrometry and nuclear magnetic resonance spectroscopy. *Chemical Society Reviews*. 2010;40(1): 387.

253. Johnson CH, Patterson AD, Idle JR, Gonzalez FJ. Xenobiotic metabolomics: major impact on the metabolome. *Annual review of pharmacology and toxicology*. Annual Reviews; 2012;52(1): 37–56.

254. Lämmerhofer M, Weckwerth W. *Metabolomics in Practice*. John Wiley & Sons; 2013.

255. Lu W, Bennett BD, Rabinowitz JD. Analytical strategies for LC-MS-based targeted metabolomics. *Journal of chromatography. B, Analytical technologies in the biomedical and life sciences*. 2008;871(2): 236–242.

256. Park Y, Kim SB, Wang B, Blanco RA, Le N-A, Wu S, et al. Individual variation in macronutrient regulation measured by proton magnetic resonance spectroscopy of human plasma. *American journal of physiology.* 2009;297(1): R202–R209.

257. Wishart DS, Knox C, Guo AC, Eisner R, Young N, Gautam B, et al. HMDB: a knowledgebase for the human metabolome. *Nucleic acids research*. 2009;37: D603–D610.

258. Krishnan P, Kruger NJ, Ratcliffe RG. Metabolite fingerprinting and profiling in plants using NMR. *Journal of experimental botany*. 2005;56(410): 255–265.

259. Pauli GF, Jaki BU, Lankin DC. Quantitative 1H NMR: development and potential of a method for natural products analysis. *Journal of natural products*. 2005;68(1): 133–149.

260. Theodoridis GA, Gika HG, Want EJ, Wilson ID. Liquid chromatography–mass spectrometry based global metabolite profiling: A review. *Analytica Chimica Acta*. 2012;711: 7–16.

261. Gika HG, Theodoridis GA, Plumb RS, Wilson ID. Current practice of liquid

chromatography-mass spectrometry in metabolomics and metabonomics. *Journal of Pharmaceutical and Biomedical Analysis*. 2014;87: 12–25.

262. Allwood JW, Goodacre R. An introduction to liquid chromatography–mass spectrometry instrumentation applied in plant metabolomic analyses. *Phytochemical Analysis*. 2010; 21(1):33-47

263. Spagou K, Tsoukali H, Raikos N, Gika H, Wilson ID, Theodoridis G. Hydrophilic interaction chromatography coupled to MS for metabonomic/metabolomic studies. Lämmerhofer M (ed.) *Journal of Separation Science*. 2010;33(6-7): 716–727.

264. Horváth C, Nahum A, Frenz JH. High-performance displacement chromatography. *Journal of Chromatography A*. 1981;218: 365–393.

265. Nováková L, Solichová D, Solich P. Advantages of ultra performance liquid chromatography over high-performance liquid chromatography: Comparison of different analytical approaches during analysis of diclofenac gel. *Journal of Separation Science*. 2006;29(16): 2433–2443.

266. Dettmer K, Aronov PA, Hammock BD. Mass spectrometry-based metabolomics. Mass Spectrom Rev. 2007 Jan-Feb;26(1):51-78

267. Brown SC, Kruppa G, Dasseux JL. Metabolomics applications of FT-ICR mass spectrometry. *Mass spectrometry reviews*. 2005;24(2): 223–231.

268. Hu Q, Noll RJ, Li H, Makarov A, Hardman M, Graham Cooks R. The Orbitrap: a new mass spectrometer. *Journal of Mass Spectrometry*. 2005;40(4): 430–443.

269. Righi V, Andronesi O, Mintzopoulos D, Tzika AA. Molecular characterization and quantification using state of the art solid-state adiabatic TOBSY NMR in burn trauma. *International journal of molecular medicine*. 2009;24(6): 749–757.

270. Watanabe M, Sheriff S, Ramelot TA, Kadeer N, Cho J, Lewis KB, et al. NMR Based Metabonomics Study of DAG Treatment in a C2C12 Mouse Skeletal Muscle Cell Line Myotube Model of Burn-Injury. *International Journal of Peptide Research and Therapeutics*. 2011;17(4): 281–299.

271. Zhang Y, Cai B, Jiang H, Yan H, Yang H, Peng J, et al. Use of 1H-nuclear magnetic resonance to screen a set of biomarkers for monitoring metabolic disturbances in severe burn patients. *Critical care.* 2014;18(4): R159.

272. Liu X-R, Zheng X-F, Ji S-Z, Lv Y-H, Zheng D-Y, Xia Z-F, et al. Metabolomic analysis of thermally injured and/or septic rats. *Burns : journal of the International Society for Burn Injuries*. 2010;36(7): 992–998.

273. Fanos V, Caboni P, Corsello G, Stronati M, Gazzolo D, Noto A, et al. Urinary (1)H-NMR and GC-MS metabolomics predicts early and late onset neonatal

sepsis. *Early human development*. 2014;90 Suppl 1: S78–S83.

274. Mickiewicz B, Vogel HJ, Wong HR, Winston BW. Metabolomics as a Novel Approach for Early Diagnosis of Pediatric Septic Shock and Its Mortality. *American Journal of Respiratory and Critical Care Medicine*. 2013;187(9): 967–976.

275. Blaise BJ, Gouel-Chéron A, Floccard B, Monneret G, Allaouchiche B. Metabolic Phenotyping of Traumatized Patients Reveals a Susceptibility to Sepsis. *Analytical Chemistry*. 2013;85(22): 10850–10855.

276. Seymour CW, Yende S, Scott MJ, Pribis J, Mohney RP, Bell LN, et al. Metabolomics in pneumonia and sepsis: an analysis of the GenIMS cohort study. *Intensive care medicine*. 2013;39(8): 1423–1434.

277. Langley RJ, Tsalik EL, van Velkinburgh JC, Glickman SW, Rice BJ, Wang C, Chen B, Carin L, Suarez A, Mohney RP, Freeman DH, Wang M, You J, Wulff J, Thompson JW, Moseley MA, Reisinger S, Edmonds BT, Grinnell B, Nelson DR, Dinwiddie DL, Miller NA, Saunders CJ, Soden SS, Rogers AJ, Gazourian L, Fredenburgh LE, Massaro AF, Baron RM, Choi AM, Corey GR, Ginsburg GS, Cairns CB, Otero RM, Fowler VG Jr, Rivers EP, Woods CW, Kingsmore SF. An integrated clinico-metabolomic model improves prediction of death in sepsis. Sci Transl Med. 2013 Jul 24;5(195):195ra95. doi: 10.1126/scitranslmed.3005893

278. Langley RJ, Tipper JL, Bruse S, Baron RM, Tsalik EL, Huntley J, et al. Integrative 'Omic Analysis of Experimental Bacteremia Identifies a Metabolic Signature that Distinguishes Human Sepsis from SIRS. *American Journal of Respiratory and Critical Care Medicine*. 2014;190(4): 445–455.

279. Mickiewicz B, Duggan GE, Winston BW, Doig C, Kubes P, Vogel HJ. Metabolic Profiling of Serum Samples by 1H Nuclear Magnetic Resonance Spectroscopy as a Potential Diagnostic Approach for Septic Shock. *Critical Care Medicine*. 2014;42(5): 1140–1149.

280. Garcia-Simon M, Morales JM, Modesto-Alapont V, Gonzalez-Marrachelli V, Vento-Rehues R, Jorda-Miñana A, et al. Prognosis Biomarkers of Severe Sepsis and Septic Shock by 1H NMR Urine Metabolomics in the Intensive Care Unit. Bathen TF (ed.) *PLoS ONE*. Public Library of Science; 2015;10(11): e0140993.

281. Su L, Huang Y, Zhu Y, Xia L, Wang R, Xiao K, Wang H, Yan P, Wen B, Cao L, Meng N, Luan H, Liu C, Li X, Xie L. Discrimination of sepsis stage metabolic profiles with an LC/MS-MS-based metabolomics approach. BMJ Open Respir Res. 2014 Dec 10;1(1):e000056. doi: 10.1136/bmjresp-2014-000056

282. Ferrario M, Cambiaghi A, Brunelli L, Giordano S, Caironi P, Guatteri L, et al. Mortality prediction in patients with severe septic shock: a pilot study using a

target metabolomics approach. *Scientific reports*. [Online] Nature Publishing Group; 2016;6: 20391. Available from: doi:10.1038/srep20391

283. Jackson PC, Hardwicke J, Bamford A, Nightingale P, Wilson Y, Papini R, et al. Revised estimates of mortality from the Birmingham Burn Centre, 2001-2010: a continuing analysis over 65 years. *Annals of surgery*. 2014;259(5): 979–984.

284. Tompkins RG. Survival from burns in the new millennium: 70 years' experience from a single institution. *Annals of surgery*. 2015;261(2): 263–268.

285. Klein MB, Goverman J, Hayden DL, Fagan SP, McDonald-Smith GP, Alexander AK, et al. Benchmarking outcomes in the critically injured burn patient. *Annals of surgery*. 2014;259(5): 833–841.

286. Mann EA, Baun MM, Meininger JC, Wade CE. Comparison of mortality associated with sepsis in the burn, trauma, and general intensive care unit patient: a systematic review of the literature. *Shock.* 2012;37(1): 4–16.

287. United Nations. World Population Ageing 1950-2050. 2015, pages 1–3. Available from: http://www.un.org/en/development/desa/population/publications/pdf/ageing/WPA2015_Report.pdf (Accessed Jan. 2016)

288. Office for National Statistics: Population Ageing in the United Kingdom, its Constituent Countries and the European Union. 2012; 1–12. Available from: http://webarchive.nationalarchives.gov.uk/20160106100801/http://www.ons.gov.uk/ons/dcp171776_258607.pdf (Accessed January 2016)

289. Wong P, Choy VYC, Ng JSY, Yau TTL, Yip K-W, Burd A. Elderly burn prevention: A novel epidemiological approach. *Burns : journal of the International Society for Burn Injuries*. 2007;33(8): 995–1000.

290. Ho WS, Ying SY, Chan HH. A study of burn injuries in the elderly in a regional burn centre. *Burns : journal of the International Society for Burn Injuries*. 2001;27(4): 382–385.

291. Khadim MF, Rashid A, Fogarty B, Khan K. Mortality estimates in the elderly burn patients: The Northern Ireland experience. *Burns : journal of the International Society for Burn Injuries*. 2009;35(1): 107–113.

292. Lionelli GT, Pickus EJ, Beckum OK, DeCoursey RL, Korentager RA. A three decade analysis of factors affecting burn mortality in the elderly. *Burns : journal of the International Society for Burn Injuries*. 2005;31(8): 958–963.

293. Mahar P, Wasiak J, Bailey M, Cleland H. Clinical factors affecting mortality in elderly burn patients admitted to a burns service. *Burns : journal of the International Society for Burn Injuries*. 2008;34(5): 629–636.

294. Romanowski KS, Barsun A, Pamlieri TL, Greenhalgh DG, Sen S. Frailty

Score on Admission Predicts Outcomes in Elderly Burn Injury. *Journal of Burn Care & Research*. 2015;36(1): 1–6.

295. Roberts G, Lloyd M, Parker M, Martin R, Philp B, Shelley O, et al. The Baux score is dead. Long live the Baux score: A 27-year retrospective cohort study of mortality at a regional burns service. *The Journal of Trauma and Acute Care Surgery*. 2012;72(1): 251–256.

296. Asch MJ, Feldman RJ, Walker HL, Foley FD, Popp RL, Mason AD, et al. Systemic and pulmonary hemodynamic changes accompanying thermal injury. *Annals of surgery*. 1973;178(2): 218–221.

297. Harrison TS, Seaton JF, Feller I. Relationship of increased oxygen consumption to catecholamine excretion in thermal burns. *Annals of surgery*. 1967;165(2): 169–172.

298. Jahoor F, Herndon DN, Wolfe RR. Role of insulin and glucagon in the response of glucose and alanine kinetics in burn-injured patients. *Journal of Clinical Investigation*. 1986;78(3): 807–814.

299. Long CL, Schaffel N, Geiger JW, Schiller WR, Blakemore WS. Metabolic response to injury and illness: estimation of energy and protein needs from indirect calorimetry and nitrogen balance. *JPEN. Journal of parenteral and enteral nutrition*. 1979;3(6): 452–456.

300. Williams FN, Jeschke MG, Chinkes DL, Suman OE, Branski LK, Herndon DN. *Modulation of the hypermetabolic response to trauma: temperature, nutrition, and drugs.* Journal of the American College of Surgeons. 2009. pp. 489–502.

301. Klein MB, Silver G, Gamelli RL, Gibran NS, Herndon DN, Hunt JL, et al. Inflammation and the Host Response to Injury: An Overview of the Multicenter Study of the Genomic and Proteomic Response to Burn Injury. *Journal of Burn Care & Research*. 2006;27(4): 448–451.

302. Nicholson JK, Lindon JC. Systems biology: Metabonomics. *Nature*. 2008;455(7216): 1054–1056.

303. Park Y, Jones DP, Ziegler TR, Lee K, Kotha K, Yu T, et al. Metabolic effects of albumin therapy in acute lung injury measured by proton nuclear magnetic resonance spectroscopy of plasma: A pilot study*. *Critical Care Medicine*. 2011;39(10): 2308–2313.

304. Mutlak H, Zacharowski K. Metabolomics in acute lung injury: a new approach for monitoring therapeutic interventions. *Critical Care Medicine*. 2011;39(10): 2375–2376.

305. Rogers AJ, Matthay MA. Applying Metabolomics to Uncover Novel Biology in ARDS. *American journal of physiology. Lung cellular and molecular physiology*. [Online] 2014. Available from: doi:10.1152/ajplung.00376.2013

306. Schmerler D, Neugebauer S, Ludewig K, Bremer-Streck S, Brunkhorst FM, Kiehntopf M. Targeted metabolomics for discrimination of systemic inflammatory disorders in critically ill patients. *Journal of lipid research*. 2012;53(7): 1369–1375.

307. for the Alberta Sepsis Network, Mickiewicz B, Tam P, Jenne CN, Leger C, Wong J, et al. Integration of metabolic and inflammatory mediator profiles as a potential prognostic approach for septic shock in the intensive care unit. *Critical Care*. 2015;19(1): 1.

308. Rogers AJ, McGeachie M, Baron RM, Gazourian L, Haspel JA, Nakahira K, et al. Metabolomic derangements are associated with mortality in critically ill adult patients. Parikh SM (ed.) *PLoS ONE*. 2014;9(1): e87538.

309. Greenhalgh DG, Saffle JR, Holmes JH 4th, Gamelli RL, Palmieri TL, Horton JW, Tompkins RG, Traber DL, Mozingo DW, Deitch EA, Goodwin CW, Herndon DN, Gallagher JJ, Sanford AP, Jeng JC, Ahrenholz DH, Neely AN, O'Mara MS, Wolf SE, Purdue GF, Garner WL, Yowler CJ, Latenser BA; American Burn Association Consensus Conference on Burn Sepsis and Infection Group. American Burn Association consensus conference to define sepsis and infection in burns. J Burn Care Res. 2007 Nov-Dec;28(6):776-90

310. Gunther UL, Ludwig C, Ruterjans H. NMRLAB-Advanced NMR data processing in matlab. J Magn Reson. 2000 Aug;145(2):201-8

311. Ludwig C, Günther UL. MetaboLab--advanced NMR data processing and analysis for metabolomics. *BMC bioinformatics*. 2011;12(1): 366.

312. Savorani F, Tomasi G, Engelsen SB. icoshift: A versatile tool for the rapid alignment of 1D NMR spectra. *Journal of magnetic resonance.* 2010;202(2): 190–202.

313. Dieterle F, Ross A, Schlotterbeck G, Senn H. Probabilistic quotient normalization as robust method to account for dilution of complex biological mixtures. Application in 1H NMR metabonomics. *Analytical Chemistry*. 2006;78(13): 4281–4290.

314. Jackson JE. Principal components and factor analysis: part I-principal components. *Journal of Quality Technology*. 1980. 12(4):201-213

315. Eriksson L, Johansson E, Kettaneh-Wold N, Trygg J. *Multi-and Megavariate Data Analysis Part I: Basic Principles and Applications: Umetrics*. Umea; 2006.

316. Trygg, J. and Wold, S. (2002), Orthogonal projections to latent structures (O-PLS). J. Chemometrics, 16: 119–128. doi:10.1002/cem.695

317. Martens H, Naes T. *Assessment, validation and choice of calibration method*. Multivariate calibration; John Wiley & Sons, New York. 1989

318. Worley B, Powers R. Multivariate Analysis in Metabolomics. Bentham Science Publishers; 2013.

319. Matthiesen R, editor. *Bioinformatics Methods in Clinical Research*. [Online] Totowa, NJ: Humana Press; 2010. Available from: doi:10.1007/978-1-60327-194-3

320. Favilla S, Durante C, Vigni ML, Cocchi M. Assessing feature relevance in NPLS models by VIP. *Chemometrics and Intelligent Laboratory Systems*. 2013;129: 76–86.

321. Galindo Prieto B, Eriksson L, Trygg J. Variable influence on projection (VIP) for orthogonal projections to latent structures (OPLS). Åberg M (ed.) *Journal of Chemometrics*. 2014;28(8): 623–632.

322. Laffel L. Ketone bodies: a review of physiology, pathophysiology and application of monitoring to diabetes. *Diabetes/metabolism research and reviews*. 1999;15(6):412-26

323. Newman JC, Verdin E. Ketone bodies as signaling metabolites. Trends Endocrinol Metab. 2014 Jan;25(1):42-52. doi: 10.1016/j.tem.2013.09.002. Epub 2013 Oct 18

324. Wilmore DW. Alterations in protein, carbohydrate, and fat metabolism in injured and septic patients. *Journal of the American College of Nutrition*. 1983;2(1): 3–13.

325. Rousseau A-F, Losser M-R, Ichai C, Berger MM. ESPEN endorsed recommendations: nutritional therapy in major burns. *Clinical nutrition* 2013;32(4): 497–502.

326. Poggetti RS, Moore EE, Moore FA, Bensard DD, Parsons P, Anderson BO, et al. Gut and liver coordinated metabolic response following major torso injury. *The Journal of surgical research*. 1992;52(1): 27–33.

327. Dong YL, Sheng CY, Herndon DN, Waymack JP. Metabolic abnormalities of mitochondrial redox potential in postburn multiple system organ failure. Burns.1992 Aug;18(4):283-6

328. Taylor F, Levenson SM. Abnormal carbohydrate metabolism in human thermal burns. *New England Journal of Medicine.* 1944.231(13)437-445

329. Allison SP, Hinton P, Chamberlain MJ. Intravenous Glucose-Tolerance, Insulin, And Free-Fatty-Acid Levels In Burned Patients. *The Lancet*. 1968;292(7578): 1113–1116.

330. Demling RH, Seigne P. Metabolic Management of Patients with Severe Burns. *World journal of surgery*. 2000;24(6): 673–680.

331. Soeters MR, Soeters PB. The evolutionary benefit of insulin resistance.

Clinical nutrition. 2012;31(6): 1002–1007.

332. Wilmore DW, Goodwin CW, Aulick LH, Powanda MC, Mason AD, Pruitt BA, et al. Effect of injury and infection on visceral metabolism and circulation. *Annals of surgery*. 1980;192(4): 491–504.

333. Porter C, Tompkins RG, Finnerty CC, Sidossis LS, Suman OE, Herndon DN. The metabolic stress response to burn trauma: current understanding and therapies. *Lancet*. 2016;388(10052): 1417–1426.

334. Parry-Billings M, Calder PC, Newsholme EA, Evans J. Does glutamine contribute to immunosuppression after major burns? *The Lancet*. 1990.

335. Todd SR, Gonzalez EA, Turner K, Kozar RA. Update on postinjury nutrition. *Current opinion in critical care*. 2008;14(6): 690–695.

336. Pierre JF, Heneghan AF, Lawson CM, Wischmeyer PE, Kozar RA, Kudsk KA. Pharmaconutrition review: physiological mechanisms. *JPEN. Journal of parenteral and enteral nutrition*. 2013;37(5 Suppl): 51S–65S.

337. Mittendorfer B, Gore DC, Herndon DN, Wolfe RR. Accelerated Glutamine Synthesis in Critically Ill Patients Cannot Maintain Normal Intramuscular Free Glutamine Concentration. 1999. 23(5):243-252

338. Taya Y, Ota Y, Wilkinson AC, Kanazawa A, Watarai H, Kasai M, et al. Depleting dietary valine permits nonmyeloablative mouse hematopoietic stem cell transplantation. *Science* 2016;354(6316): 1145–1155.

339. Stinnett JD, Alexander JW, Watanabe C, MacMillan BG, Fischer JE, Morris MJ, et al. Plasma and skeletal muscle amino acids following severe burn injury in patients and experimental animals. *Annals of surgery*. 1982;195(1): 75–89.

340. Tredget EE, Shankowsky HA, Taerum TV, Moysa GL, Alton JD. The role of inhalation injury in burn trauma. A Canadian experience. *Annals of surgery*. 1990;212(6): 720–727.

341. Yardim-Akaydin S, Sepici A, Ozkan Y, Torun M, Simşek B, Sepici V. Oxidation of uric acid in rheumatoid arthritis: is allantoin a marker of oxidative stress? *Free radical research*. 2004;38(6): 623–628.

342. Yardim-Akaydin S, Sepici A, Ozkan Y, Simşek B, Sepici V. Evaluation of allantoin levels as a new marker of oxidative stress in Behçet's disease. *Scandinavian journal of rheumatology*. 2006;35(1): 61–64.

343. Landaas S. The formation of 2-hydroxybutyric acid in experimental animals. *Clinica Chimica Acta*. 1975. 58(1):23-32

344. Gall WE, Beebe K, Lawton KA, Adam K-P, Mitchell MW, Nakhle PJ, et al. α-Hydroxybutyrate Is an Early Biomarker of Insulin Resistance and Glucose

Intolerance in a Nondiabetic Population. Federici M (ed.) *PLoS ONE*. [Online] Public Library of Science; 2010;5(5): e10883. Available from: doi:10.1371/journal.pone.0010883

345. Padfield KE, Astrakas LG, Zhang Q, Gopalan S, Dai G, Mindrinos MN, et al. Burn injury causes mitochondrial dysfunction in skeletal muscle. *Proceedings of the National Academy of Sciences of the United States of America*. 2005;102(15): 5368–5373.

346. Khan N, Mupparaju SP, Mintzopoulos D, Kesarwani M, Righi V, Rahme LG, Swartz HM, Tzika AA. Burn trauma in skeletal muscle results in oxidative stress as assessed by in vivo electron paramagnetic resonance. Mol Med Rep. 2008;1(6):813-819

347. Barlow GB, Wilkinson AW. The effect of burns on the metabolism of tryptophan in children. *Clinica Chimica Acta*. 1972;41: 169–174.

348. Munn DH, Shafizadeh E, Attwood JT, Bondarev I, Pashine A, Mellor AL. Inhibition of T cell proliferation by macrophage tryptophan catabolism. *J ExpMed*. 1999 May 3;189(9):1363-72

349. Carlin JM, Borden EC, Sondel PM, Byrne GI. Interferon-induced indoleamine2,3-dioxygenase activity in human mononuclear phagocytes. J *Leukoc Biol.* 1989 Jan;45(1):29-34

350. Munn DH, Sharma MD, Lee JR, Jhaver KG, Johnson TS, Keskin DB, Marshall B, Chandler P, Antonia SJ, Burgess R, Slingluff CL Jr, Mellor AL. Potential regulatory function of human dendritic cells expressing indoleamine 2,3-dioxygenase. Science. 2002 Sep 13;297(5588):1867-70

351. Wang Y, Liu H, McKenzie G, Witting PK, Stasch J-P, Hahn M, et al. Kynurenine is an endothelium-derived relaxing factor produced during inflammation. *Nature medicine*. 2010;16(3): 279–285.

352. Changsirivathanathamrong D, Wang Y, Rajbhandari D, Maghzal GJ, Mak WM, Woolfe C, et al. Tryptophan metabolism to kynurenine is a potential novel contributor to hypotension in human sepsis. *Critical Care Medicine*. 2011;39(12): 2678–2683.

353. Darcy CJ, Davis JS, Woodberry T, McNeil YR, Stephens DP, Yeo TW, et al. An Observational Cohort Study of the Kynurenine to Tryptophan Ratio in Sepsis: Association with Impaired Immune and Microvascular Function. *PLoS ONE*. 2011;6(6): e21185.

354. Lögters TT, Laryea MD, Altrichter J, Sokolowski J, Cinatl J, Reipen J, et al. Increased Plasma Kynurenine Values And Kynurenine-Tryptophan Ratios After Major Trauma Are Early Indicators For The Development Of Sepsis. *Shock.* 2009;32(1): 29–34.

355. Li Y, Kilani RT, Rahmani-Neishaboor E, Jalili RB, Ghahary A.

Kynurenineincreases matrix metalloproteinase-1 and -3 expression in cultured dermal fibroblasts and improves scarring in vivo. J Invest Dermatol. 2014 Mar;134(3):643-650

356. Sentongo TA, Azzam R, Charrow J. Vitamin B12 Status, Methylmalonic Acidemia, and Bacterial Overgrowth in Short Bowel Syndrome. *Journal of Pediatric Gastroenterology and Nutrition*. 2009;48(4): 495–497.

357. Melo DR, Mirandola SR, Assunção NA, Castilho RF. Methylmalonate impairs mitochondrial respiration supported by NADH-linked substrates: involvement of mitochondrial glutamate metabolism. *Journal of Neuroscience Research*. 2012;90(6): 1190–1199.

358. Magnotti LJ, Deitch EA. Burns, Bacterial Translocation, Gut Barrier Function, and Failure. *Journal of Burn Care & Rehabilitation*. 2005;26(5): 383–391.

359. Scheppach W, Pomare EW, Elia M, Cummings JH. The contribution of the large intestine to blood acetate in man. *Clinical Science*. 1991;80(2): 177–182.

360. Mittendorfer B, Sidossis LS, Walser E, Chinkes DL, Wolfe RR. Regional acetate kinetics and oxidation in human volunteers. *AJP: Endocrinology and Metabolism*. American Physiological Society; 1998;274(6): E978–E983.

361. Pouteau E, Piloquet H, Maugeais P, Champ M, Dumon H, Nguyen P, et al. Kinetic aspects of acetate metabolism in healthy humans using [1-13C] acetate. *The American journal of physiology*. American Physiological Society; 1996;271(1 Pt 1): E58–E64.

362. Skutches CL, Holroyde CP, Myers RN, Paul P, Reichard GA. Plasma acetate turnover and oxidation. *Journal of Clinical Investigation*. 1979;64(3): 708–713.

363. Akanji AO, Humphreys S, Thursfield V, Hockaday TD. The relationship of plasma acetate with glucose and other blood intermediary metabolites in non-diabetic and diabetic subjects. *Clinica Chimica Acta*. 1989;185(1): 25–34.

364. Perry RJ, Peng L, Barry NA, Cline GW, Zhang D, Cardone RL, et al. Acetate mediates a microbiome-brain-β-cell axis to promote metabolic syndrome. *Nature*. 2016;534(7606): 213–217.

365. Dorokhov YL, Shindyapina AV, Sheshukova EV, Komarova TV. Metabolic methanol: molecular pathways and physiological roles. Physiol Rev. 2015 Apr;95(2):603-44

366. Lanza-Jacoby S, Rosato E, Braccia G, Tabares A. Altered ketone body metabolism during gram-negative sepsis in the rat. *Metabolism: clinical and experimental*. 1990;39(11): 1151–1157.

367. Harris RL, Frenkel RA, Cottam GL, Baxter CR. Lipid mobilization and metabolism after thermal trauma. *The Journal of Trauma: Injury, Infection,*

and Critical Care. 1982;22(3): 194–198.

368. Eaton S, Pierro A. Carnitine and Fatty Acid Oxidation in Sepsis. *Monatshefte für Chemie/Chemical Monthly*. [Online] Springer-Verlag; 2005;136(8): 1483–1492. Available from: doi:10.1007/s00706-005-0316-9

369. Famularo G, De Simone C, Martelli EA, Jirillo E. Carnitine and septic shock: a review. *Journal of Endotoxin Research*. 2016;2(2): 141–147.

370. Holecek M. Branched-chain amino acids and ammonia metabolism in liver disease: therapeutic implications. Nutrition. 2013 Oct;29(10):1186-91. doi:10.1016/j.nut.2013.01.022

371. Elia M, Carter A, Bacon S, Winearls CG, Smith R. Clinical usefulness of urinary 3-methylhistidine excretion in indicating muscle protein breakdown. *BMJ* 1981;282(6261): 351–354.

372. Liu X-R, Zheng X-F, Ji S-Z, Lv Y-H, Zheng D-Y, Xia Z-F, et al. Metabolomic analysis of thermally injured and/or septic rats. *Burns : journal of the International Society for Burn Injuries*. 2010;36(7): 992–998.

373. Khan N, Mupparaju SP, Mintzopoulos D, Kesarwani M, Righi V, Rahme LG, Swartz HM, Tzika AA. Burn trauma in skeletal muscle results in oxidative stress as assessed by in vivo electron paramagnetic resonance. Mol Med Rep. 2008;1(6):813-819

374. Righi V, Constantinou C, Mintzopoulos D, Khan N, Mupparaju SP, Rahme LG, et al. Mitochondria-targeted antioxidant promotes recovery of skeletal muscle mitochondrial function after burn trauma assessed by in vivo 31P nuclear magnetic resonance and electron paramagnetic resonance spectroscopy. *The FASEB Journal*. 2013;27(6): 2521–2530.

375. Parent BA, Seaton M, Sood RF, Gu H, Djukovic D, Raftery D, et al. Use of Metabolomics to Trend Recovery and Therapy After Injury in Critically Ill Trauma Patients. *JAMA surgery*. [Online] 2016;151(7): e160853. Available from: doi:10.1001/jamasurg.2016.0853

376. Dai D, Gao Y, Chen J, Huang Y, Zhang Z, Xu F. Time-resolved metabolomics analysis of individual differences during the early stage of lipopolysaccharide-treated rats. Sci Rep. 2016 Oct 3;6:34136. doi:10.1038/srep34136

377. Nathan C, Ding A. Nonresolving inflammation. *Cell*. 2010;140(6): 871–882.

378. Haas R, Smith J, Rocher-Ros V, Nadkarni S, Montero-Melendez T, D'Acquisto F, et al. Lactate Regulates Metabolic and Pro-inflammatory Circuits in Control of T Cell Migration and Effector Functions. Marrack P (ed.) *PLOS Biology*. [Online] Public Library of Science; 2015;13(7): e1002202. Available from: doi:10.1371/journal.pbio.1002202

379. Allard JP, Pichard C, Hoshino E, Stechison S, Fareholm L, Peters WJ, et al.

Validation of a new formula for calculating the energy requirements of burn patients. *JPEN. Journal of parenteral and enteral nutrition*. 1990;14(2): 115–118.

380. Harris JA, Benedict FG. A Biometric Study of Human Basal Metabolism. *Proceedings of the National Academy of Sciences of the United States of America*. 1918;4(12): 370–373.

381. Gehmlich K, Dodd MS, Allwood JW, Kelly M, Bellahcene M, Lad HV, et al. Changes in the cardiac metabolome caused by perhexiline treatment in a mouse model of hypertrophic cardiomyopathy. *Molecular bioSystems*. 2015;11(2): 564–573.

382. Smith CA, Want EJ, O'Maille G, Abagyan R, Siuzdak G. XCMS: processing mass spectrometry data for metabolite profiling using non-linear peak alignment, matching, and identification. Anal Chem. 2006 Feb 1;78(3):779-87

383. Dunn WB, Wilson ID, Nicholls AW, Broadhurst D. The importance of experimental design and QC samples in large-scale and MS-driven untargeted metabolomic studies of humans. *Bioanalysis*. 2012;4(18): 2249–2264.

384. Dunn WB, Broadhurst D, Begley P, Zelena E, Francis-McIntyre S, Anderson N, et al. Procedures for large-scale metabolic profiling of serum and plasma using gas chromatography and liquid chromatography coupled to mass spectrometry. *Nature Protocols*. 2011;6(7): 1060–1083.

385. Xia J, Psychogios N, Young N, Wishart DS. MetaboAnalyst: a web server for metabolomic data analysis and interpretation. *Nucleic acids research*. 2009;37: 652–660.

386. Sumner LW, Amberg A, Barrett D, Beale MH, Beger R, Daykin CA, et al. Proposed minimum reporting standards for chemical analysis Chemical Analysis Working Group (CAWG) Metabolomics Standards Initiative (MSI). *Metabolomics*. 2007;3(3): 211–221.

387. Xia J, Mandal R, Sinelnikov IV, Broadhurst D, Wishart DS. MetaboAnalyst 2.0--a comprehensive server for metabolomic data analysis. *Nucleic acids research*. [Online] 2012;40(Web Server issue): W127–W133. Available from: doi:10.1093/nar/gks374

388. Xia J, Sinelnikov IV, Han B, Wishart DS. MetaboAnalyst 3.0--making metabolomics more meaningful. *Nucleic acids research*. 2015;43(W1): 251–257.

389. Yang R, Chiang N, Oh SF, Serhan CN. *Metabolomics-Lipidomics of Eicosanoids and Docosanoids Generated by Phagocytes*. [Online] Hoboken, NJ, USA: John Wiley & Sons, Inc; 2011. 128366 p. Available from: doi:10.1002/0471142735.im1426s95

390. Gottschlich MM, Alexander JW. Fat kinetics and recommended dietary intake in burns. *JPEN. Journal of parenteral and enteral nutrition*. 1987;11(1): 80–85.

391. Cetinkale O, Yazici Z. Early postburn fatty acid profile in burn patients. *Burns : journal of the International Society for Burn Injuries*. 1997;23(5): 392–399.

392. Pratt VC, Tredget EE, Clandinin MT, Field CJ. Fatty acid content of plasma lipids and erythrocyte phospholipids are altered following burn injury. *Lipids*. 2001;36(7): 675–682.

393. Qi P, Abdullahi A, Stanojcic M, Patsouris D, Jeschke MG. Lipidomic analysis enables prediction of clinical outcomes in burn patients. Sci Rep. 2016 Dec 16;6:38707. doi: 10.1038/srep38707

394. Prelack K, Dwyer J, Yu Y-M, Sheridan RL, Tompkins RG. Urinary Urea Nitrogen is Imprecise as a Predictor of Protein Balance in Burned Children. *Journal of the American Dietetic Association*. 1997;97(5): 489–495.

395. Lephart ED, Baxter CR, Parker CR. Effect of burn trauma on adrenal and testicular steroid hormone production. *Journal of Clinical Endocrinology & Metabolism*. 1987;64(4): 842–848.

396. Radford DJ, Wang K, McNelis JC, Taylor AE, Hechenberger G, Hofmann J, et al. Dehydroepiandrosterone sulfate directly activates protein kinase C-beta to increase human neutrophil superoxide generation. *Molecular endocrinology.* 2010;24(4): 813–821.

397. Banta S, Yokoyama T, Berthiaume F, Yarmush ML. Effects of Dehydroepiandrosterone Administration on Rat Hepatic Metabolism Following Thermal Injury. *Journal of Surgical Research*. 2005;127(2): 93–105.

398. Gianotti L, ALEXANDER JW, Fukushima R, Pyles T. Steroid Therapy Can Modulate Gut Barrier Function, Host Defense, and Survival in Thermally Injured Mice. *Journal of Surgical Research*. 1996;62(1): 53–58.

399. Araneo BA, Shelby J, Li GZ, Ku W, Daynes RA. Administration of dehydroepiandrosterone to burned mice preserves normal immunologic competence. *Arch Surg.* 1993 Mar;128(3):318-25

400. Araneo BA, Ryu S-Y, Barton S, Daynes RA. Dehydroepiandrosterone Reduces Progressive Dermal Ischemia Caused by Thermal Injury. *Journal of Surgical Research*. 1995;59(2): 250–262.

401. Dennis EA, Norris PC. Eicosanoid storm in infection and inflammation. *Nature Reviews Immunology*. 2015;15(8): 511–523.

402. Köller M, König W, Brom J, Raulf M, Gross-Weege W, Erbs G, et al. Generation of leukotrienes from human polymorphonuclear granulocytes of severely burned patients. *The Journal of Trauma: Injury, Infection, and*

Critical Care. 1988;28(6): 733–740.

403. Brom J, Köller M, Schönfeld W, Knöller J, Erbs G, Müller FE, et al. Decreased expression of leukotriene B4 receptor sites on polymorphonuclear granulocytes of severely burned patients. *Prostaglandins, leukotrienes, and essential fatty acids*. 1988;34(3): 153–159.

404. Damtew B, Marino JA, Fratianne RB, Spagnuolo PJ. Neutrophil lipoxygenase metabolism and adhesive function following acute thermal injury. *The Journal of laboratory and clinical medicine*. 1993;121(2): 328–336.

405. Hampson P, Dinsdale RJ, Wearn CM, Bamford AL, Bishop JRB, Hazeldine J, Moiemen NS, Harrison P, Lord JM. Neutrophil Dysfunction, Immature Granulocytes, and Cell-free DNA are Early Biomarkers of Sepsis in Burn-injured Patients: A Prospective Observational Cohort Study. Ann Surg. 2017 Jun;265(6):1241-1249

406. Miller-Graziano CL, Fink M, Wu JY, Szabó G, Kodys K. Mechanisms of altered monocyte prostaglandin E2 production in severely injured patients. *Archives of Surgery*. 1988;123(3): 293–299.

407. Fukushima R, Alexander JW, Wu JZ, Mao JX, Szczur K, Stephens AM, et al. Time course of production of cytokines and prostaglandin E2 by macrophages isolated after thermal injury and bacterial translocation. *Circulatory shock*. 1994;42(3): 154–162.

408. Brückner UB, Pfetsch H, Kinzl L, Bock KH, Gebhard F. [Prognostic importance of preclinically evaluated biochemical mediators in polytrauma]. *Zentralblatt fur Chirurgie*. 1999;124(4): 303–310.

409. Fullerton JN, O'Brien AJ, Gilroy DW. Lipid mediators in immune dysfunction after severe inflammation. *Trends in Immunology*. 2014;35(1): 12–21.

410. Bohr S, Patel SJ, Sarin D, Irimia D, Yarmush ML, Berthiaume F. Resolvin D2 prevents secondary thrombosis and necrosis in a mouse burn wound model. *Wound repair and regeneration.* 2013;21(1): 35–43.

411. Inoue Y, Yu Y-M, Kurihara T, Vasilyev A, Ibrahim A, Oklu R, et al. Kidney and Liver Injuries After Major Burns in Rats Are Prevented by Resolvin D2. *Critical Care Medicine*. 2016;44(5): 241–252.

412. Csontos C, Foldi V, Pálinkas L, Bogar L, Röth E, Weber G, et al. Time course of pro- and anti-inflammatory cytokine levels in patients with burns--prognostic value of interleukin-10. *Burns : journal of the International Society for Burn Injuries*. 2010;36(4): 483–494.

413. la Fuente De M, Garrido JJ, Arahuetes RM, Hernanz A. Stimulation of phagocytic function in mouse macrophages by neurotensin and neuromedin N. *Journal of neuroimmunology*. 1993;42(1): 97–104.

414. Garrido JJ, Arahuetes RM, Hernanz A, la Fuente De M. Modulation by neurotensin and neuromedin N of adherence and chemotaxis capacity of murine lymphocytes. *Regulatory peptides*. 1992;41(1): 27–37.

415. Malendowicz LK, Nussdorfer GG, Markowska A, Nowak KW, Torlinski L. Effects of neuromedin-N on the pituitary-adrenocortical axis of dexamethasone-suppressed rats. *Neuropeptides*. 1993;24(1): 1–4.

416. Betteridge DJ. What is oxidative stress? *Metabolism*. 2000. Feb;49(2 Suppl1):3-8

417. Slater TF, Cheeseman KH, Davies MJ, Proudfoot K, Xin W. Free radical mechanisms in relation to tissue injury. Proc Nutr Soc. 1987 Feb;46(1):1-12

418. Horton JW, White DJ. Role of xanthine oxidase and leukocytes in postburn cardiac dysfunction. *ACS*. 1995;181(2): 129–137.

419. Hippenstiel S, Krüll M, Ikemann A, Risau W, Clauss M, Suttorp N. VEGF induces hyperpermeability by a direct action on endothelial cells. Am J Physiol. 1998 May;274(5 Pt 1):L678-84

420. Chance B, Sies H, Boveris A. Hydroperoxide metabolism in mammalian organs. Physiol Rev. 1979 Jul;59(3):527-605

421. Horton JW. Free radicals and lipid peroxidation mediated injury in burn trauma: the role of antioxidant therapy. *Toxicology*. 2003;189(1-2): 75–88.

422. LaLonde C, Nayak U, Hennigan J, Demling R. Plasma Catalase and Glutathione Levels Are Decreased in Response to Inhalation Injury. *Journal of Burn Care & Research*. 1997;18(6): 515.

423. Endoh Y, Kawakami M, Orringer EP, Peterson HD, Meyer AA. Causes and Time Course of Acute Hemolysis After Burn Injury in the Rat. *Journal of Burn Care & Research*. 1992;13(2): 203.

424. LAWRENCE C, ATAC B. Hematologic changes in massive burn injury. *Critical Care Medicine*. 1992;20(9): 1284.

425. Hatherill JR, Till GO, Bruner LH, Ward PA. Thermal injury, intravascular hemolysis, and toxic oxygen products. *Journal of Clinical Investigation*. 1986;78(3): 629–636.

426. Wong C-H, Song C, Heng K-S, Kee IHC, Tien S-L, Kumarasinghe P, et al. Plasma Free Hemoglobin: A Novel Diagnostic Test for Assessment of the Depth of Burn Injury. *Plastic and Reconstructive Surgery*. 2006;117(4): 1206–1213.

427. Balla J, Vercellotti GM, Jeney V, Yachie A, Varga Z, Jacob HS, Eaton J, Balla G. Heme, heme oxygenase, and ferritin: how the vascular endothelium survives (and dies) in an iron-rich environment. Antioxid Redox Signal. 2007

Dec;9(12):2119-37

428. Abraham NG, Kappas A. Pharmacological and clinical aspects of heme oxygenase. *Pharmacological reviews*. 2008;60(1): 79–127.

429. Nguyen TT, Cox CS, Traber DL, Gasser H, Redl H, Schlag G, et al. Free radical activity and loss of plasma antioxidants, vitamin E, and sulfhydryl groups in patients with burns: the 1993 Moyer Award. *Journal of Burn Care & Rehabilitation*. 1993;14(6): 602–609.

430. Traber MG, Leonard SW, Traber DL, Traber LD, Gallagher J, Bobe G, et al. α-Tocopherol adipose tissue stores are depleted after burn injury in pediatric patients. *American Journal of Clinical Nutrition*. 2010;92(6): 1378–1384.

431. Hofmann AF. The continuing importance of bile acids in liver and intestinal disease. *Archives of internal medicine*. 1999;159(22): 2647–2658.

432. Chiang JYL. *Bile Acid Metabolism and Signaling*. [Online] Hoboken, NJ, USA: John Wiley & Sons, Inc; 2013. Available from: doi:10.1002/cphy.c120023

433. Gérard P. Metabolism of cholesterol and bile acids by the gut microbiota.*Pathogens.* 2013 Dec 30;3(1):14-24. doi: 10.3390/pathogens3010014

434. Jeschke MG. The hepatic response to thermal injury: is the liver important for postburn outcomes? *Molecular Medicine*. 2009;15(9-10): 337–351.

435. Linares HA. A report of 115 consecutive autopsies in burned children: 1966–1980. *Burns : journal of the International Society for Burn Injuries*.1982;8(4): 263–270.

436. Bolder U, Ton-Nu HT, Schteingart CD, Frick E, Hofmann AF. Hepatocyte transport of bile acids and organic anions in endotoxemic rats: impaired uptake and secretion. *Gastroenterology*. 1997;112(1): 214–225.

437. Vanwijngaerden Y-M, Wauters J, Langouche L, Vander Perre S, Liddle C, Coulter S, et al. Critical illness evokes elevated circulating bile acids related to altered hepatic transporter and nuclear receptor expression. *Hepatology*. 2011;54(5): 1741–1752.

438. Vemula M, Berthiaume F, Jayaraman A, Yarmush ML. Expression profiling analysis of the metabolic and inflammatory changes following burn injury in rats. *Physiological genomics*. 2004;18(1): 87–98.

439. Deitch EA. Bacterial Translocation of the Gut Flora. *Journal of Trauma, Injury, Infection, and Critical Care*. 1990;30:184-189

440. Maejima K, Deitch EA, Berg RD. Bacterial translocation from the gastrointestinal tracts of rats receiving thermal injury. *Infection and immunity*. American Society for Microbiology; 1984;43(1): 6–10.

441. Herndon DN, Zeigler ST. Bacterial translocation after thermal injury. *Critical Care Medicine*. 1993;21(2): S50.

442. Deitch EA, Xu D, Kaise VL. Role of the gut in the development of injury- and shock induced SIRS and MODS: the gut-lymph hypothesis, a review. *Front Biosci.* 2006 Jan 1;11:520-8

443. Lee J-H, Lee J. Indole as an intercellular signal in microbial communities. *FEMS microbiology reviews*. 2010;34(4): 426–444.

444. Herrmann KM. The Shikimate Pathway: Early Steps in the Biosynthesis of Aromatic Compounds. *The Plant cell*. 1995;7(7): 907–919.

445. Saiki K, Mogi T, Ogura K, Anraku Y. In vitro heme O synthesis by the cyoE gene product from Escherichia coli. *The Journal of biological chemistry*. American Society for Biochemistry and Molecular Biology; 1993;268(35): 26041–26044.

446. Holick MF. Vitamin D Deficiency. *New England Journal of Medicine*; 2007;357(3): 266–281.

447. Gottschlich MM, Mayes T, Khoury J, Warden GD. Hypovitaminosis D in acutely injured pediatric burn patients. *Journal of the American Dietetic Association*. 2004;104(6): 931–941.

448. Blay B, Thomas S, Coffey R, Jones L, Murphy CV. Low Vitamin D Level on Admission for Burn Injury Is Associated With Increased Length of Stay. *Journal of burn care & research.* 2017;38(1): 8–13.

449. Mickiewicz B, Thompson GC, Blackwood J, Jenne CN, Winston BW, Vogel HJ, et al. Development of metabolic and inflammatory mediator biomarker phenotyping for early diagnosis and triage of pediatric sepsis. *Critical care* 2015;19(1): 320.

450. Kauppi AM, Edin A, Ziegler I, Mölling P, Sjöstedt A, Gylfe Å, et al. Metabolites in Blood for Prediction of Bacteremic Sepsis in the Emergency Room. Yende S (ed.) *PLoS ONE*. [Online] Public Library of Science; 2016;11(1): e0147670. Available from: doi:10.1371/journal.pone.0147670

451. Seymour CW, Yende S, Scott MJ, Pribis J, Mohney RP, Bell LN, Chen YF, Zuckerbraun BS, Bigbee WL, Yealy DM, Weissfeld L, Kellum JA, Angus DC. Metabolomics in pneumonia and sepsis: an analysis of the GenIMS cohort study. *Intensive Care Med*. 2013 Aug;39(8):1423-34

452. Blaise BJ, Gouel-Chéron A, Floccard B, Monneret G, Allaouchiche B. Metabolic phenotyping of traumatized patients reveals a susceptibility to sepsis. *Anal Chem.* 2013 Nov 19;85(22):10850-5

453. Wearn C, Hardwicke J, Kitsios A, Siddons V, Nightingale P, Moiemen N. Outcomes of burns in the elderly: revised estimates from the Birmingham

Burn Centre. *Burns : journal of the International Society for Burn Injuries*. 2015;41(6): 1161–1168.

454. Stylianou N, Buchan I, Dunn KW. A model of British in-hospital mortality among burns patients. *Burns : journal of the International Society for Burn Injuries*. 2014;40(7): 1316–1321.

455. Quirinia A, Viidik A. The influence of age on the healing of normal and ischemic incisional skin wounds. Mech Ageing Dev. 1991 May;58(2-3):221-32

456. Bartlett DB, Firth CM, Phillips AC, Moss P, Baylis D, Syddall H, et al. The age-related increase in low-grade systemic inflammation (Inflammaging) is not driven by cytomegalovirus infection. *Aging Cell*. 2012;11(5): 912–915.

457. Kovacs EJ, Plackett TP, Witte PL. Estrogen replacement, aging, and cell-mediated immunity after injury. *Journal of Leukocyte Biology*. 2004;76(1): 36–41.

458. Butcher SK, Killampalli V, Chahal H, Alpar EK, Lord JM. Effect of age on susceptibility to post-traumatic infection in the elderly. *Biochemical Society Transactions*. 2003;31(2): 449–451.

459. Hazeldine J, Lord JM, Hampson P. Immunesenescence and inflammaging: A contributory factor in the poor outcome of the geriatric trauma patient. *Ageing research reviews*. 2015;24(Pt B): 349–357.

460. Vanzant EL, Hilton RE, López CM, Zhang J, Ungaro RF, Gentile LF, et al. Advanced age is associated with worsened outcomes and a unique genomic response in severely injured patients with hemorrhagic shock. *Critical care* 2015;19(1): 77.

461. Barzilai N, Huffman DM, Muzumdar RH, Bartke A. The Critical Role of Metabolic Pathways in Aging. *Diabetes*. 2012;61(6): 1315–1322.

462. Stinnett JD, Alexander JW, Watanabe C, MacMillan BG, Fischer JE, Morris MJ, et al. Plasma and skeletal muscle amino acids following severe burn injury in patients and experimental animals. *Annals of surgery*. 1982;195(1): 75–89.

463. Jahoor F, Desai M, Herndon DN, Wolfe RR. Dynamics of the protein metabolic response to burn injury. *Metabolism: clinical and experimental*. 1988;37(4): 330–337.

464. Evans WJ, Paolisso G, Abbatecola AM, Corsonello A, Bustacchini S, Strollo F, et al. Frailty and muscle metabolism dysregulation in the elderly. *Biogerontology*. 2010;11(5): 527–536.

465. Jeschke MG, Patsouris D, Stanojcic M, Abdullahi A, Rehou S, Pinto R, et al. Pathophysiologic Response to Burns in the Elderly. *EBioMedicine*. 2015;2(10): 1536–1548.

466. Jeschke MG, Kulp GA, Kraft R, Finnerty CC, Mlcak R, Lee JO, et al. Intensive Insulin Therapy in Severely Burned Pediatric Patients: A Prospective Randomized Trial. *American Journal of Respiratory and Critical Care Medicine*. 2010;182(3): 351–359.

467. Tarnow P, Jönsson A, Rimbäck G, Cassuto J. Increased dermal perfusion after skin burn injury by d-myo-inositol-1,2,6-trisphosphate. *Burns : journal of the International Society for Burn Injuries*. 1996;22(5): 363–368.

468. Engelke UFH, Tangerman A, Willemsen MAAP, Moskau D, Loss S, Mudd SH, et al. Dimethyl sulfone in human cerebrospinal fluid and blood plasma confirmed by one-dimensional 1H and two-dimensional 1H-13C NMR. *NMR in Biomedicine*. 2005;18(5): 331–336.

469. Szendroedi J, Yoshimura T, Phielix E, Koliaki C, Marcucci M, Zhang D, et al. Role of diacylglycerol activation of PKCθ in lipid-induced muscle insulin resistance in humans. *Proceedings of the National Academy of Sciences*. 2014;111(26): 9597–9602.

470. Zeden JP, Fusch G, Holtfreter B, Schefold JC, Reinke P, Domanska G, et al. Excessive tryptophan catabolism along the kynurenine pathway precedes ongoing sepsis in critically ill patients. *Anaesthesia and intensive care*. 2010;38(2): 307–316.

471. Barlow GB, Wilkinson AW. Plasma pyridoxal phosphate levels and tryptophan metabolism in children with burns and scalds. *Clinica Chimica Acta*. 1975;64(1): 79–82.

472. Cohen MJ, Serkova NJ, Wiener-Kronish J, Pittet J-F, Niemann CU. 1H-NMR-based metabolic signatures of clinical outcomes in trauma patients--beyond lactate and base deficit. *Journal of Trauma*. 2010;69(1): 31–40.

473. Fritsche KL. The science of fatty acids and inflammation. *Advances in Nutrition: An International Review Journal*. 2015;6(3): 293–301.

474. Orr SK, Butler KL, Hayden D, Tompkins RG, Serhan CN, Irimia D. Gene Expression of Proresolving Lipid Mediator Pathways Is Associated With Clinical Outcomes in Trauma Patients. *Critical Care Medicine*. 2015;43(12): 2642–2650.

475. Seymour CW, Liu VX, Iwashyna TJ, Brunkhorst FM, Rea TD, Scherag A, et al. Assessment of Clinical Criteria for Sepsis: For the Third International Consensus Definitions for Sepsis and Septic Shock (Sepsis-3). *JAMA: The Journal of the American Medical Association*. 2016;315(8): 762–774.

476. Nicholson JK, Everett JR, Lindon JC. Longitudinal pharmacometabonomics for predicting patient responses to therapy: drug metabolism, toxicity and efficacy. *Expert opinion on drug metabolism & toxicology*. 2012;8(2): 135–139.

477. Opal SM, Dellinger RP, Vincent J-L, Masur H, Angus DC. The next generation of sepsis clinical trial designs: what is next after the demise of recombinant human activated protein C?. *Critical Care Medicine*. 2014;42(7): 1714–1721.

478. Marshall JC. Why have clinical trials in sepsis failed? *Trends in molecular medicine*. 2014;20(4): 195–203.